The role of phytohormones and light signalling in the guard cell CO_2 response

Kishwar Jahan Shethi

A thesis submitted in partial fulfilment of the requirements for the degree of
Doctor of Philosophy

The University of Sheffield
School of Biosciences
Plants, Photosynthesis and Soil

July 2023

In loving memories of my parents....

Declaration

I, Kishwar Jahan Shethi, declare that this thesis has been composed entirely by myself unless otherwise referenced in the text. I confirm that this thesis has not been submitted for any other degree. All quotations have been distinguished by quotation marks and the sources acknowledged.

Acknowledgement

First and foremost, I would like to express my deepest appreciation and heartfelt thanks to my supervisor Dr Stuart Casson who has been a continuous support even before the start of my PhD journey. His phenomenal mentorship, constant guidance, and belief in my abilities significantly influenced my academic progression over the last few years. In addition, to support in academia and research, his supports were invaluable personally considering my caring responsibility. His positive gesture and smiling face was driving force to make my PhD journey less stressfull.

I am also profoundly grateful to my co-supervisor Professor Julie Gray for all her supports, cooperation, and valuable suggestions during the development of this work. My PhD journey has faced many ups and downs considering the unprecedented Covid-19 pandemic and most importantly the demise of my parents. And both my supervisors, Dr Stuart Casson and Professor Julie Gray played immense role to uphold me with their gracious presence and cheerful spirits.

I would like to acknowledge my scholarship awarding body Bangabandhu Overseas Scholarship, University of Dhaka for funding this research and providing financial support without which I could not be able to pursue my dream. I am also obliged to the Faculty of Science, University of Sheffield for their financial support towards my tuition fees to ease my journey.

I was fortunate to have wonderful people from the Casson group, Dr. Nicholas Zoulias, Dr. Natalia Hurtado and Julian Adams who always offered help and support whenever in need. I would also like to thank all the past and current members in the C33 lab group who have been integral part of my PhD experience through sharing their experience and ideas. Also, thanks to all the friends I made in Sheffield for their love and encouragement.

I am also thankful to my PhD advisors, Professor Matt Johnson and Dr. Lynda Partridge for their advice and guidance. My gratitude to collaborators Dr. Veronika Turečková and Dana Tarkowska from Palacky University and Institute of Experimental Botany of the Czech Republic for their help with mass spectrometry analysis. I would

also like to thank all the staff in Annex for the technical support with the plant growth chambers.

My special thanks to my siblings Rahnuma Jahan and Tanvir Ishraque for being my strength. Though they are younger than I am, they took care of my every responsibility back in Bangladesh and provide me with mental support being my stress reliever. They were always by my side through thick and thin.

I would like to take this opportunity to express my gratitude to Professor Rakha Hari Sarker, University of Dhaka who has instigated my research interest in plants, and being my first mentor holds a special place. I would also like to acknowledge Professor Parveen Rashid, University of Dhaka for her nurture and advice since 2015. Also thankful to Professor Md. Imdadul Hoque for his support in my academic career.

I am especially indebted to my husband Mohammad Robel Hossen Patwary to make this PhD journey a lifetime experience. The last four years taught us many lessons and strengthen our relationship since my husband and I started our journey to pursue PhD at the same time. I cannot deny the truth, that sometimes he was a pain but again it's his love, care and support that made my PhD journey memorable. I am also fortunate to have Wasit Ahnaf Patwary being such a sensible and loving son throughout this time. And delighted that now Wasit can recognise stomata!

Finally, I would like to remember my father whom I lost at the beginning of my PhD and my mother whom I lost just three months before. Without their sacrifice, hard work and incentive I would not be able to come so far. "My Lord, have mercy upon them (Parents) as they brought me up when I was small."

Last but not the least, I am thankful to the Almighty Allah for giving me the knowledge and strength to complete my journey.

Abstract

Stomata are formed by a pair of specialized guard cells surrounding a central pore to regulate plant carbon-water relations via changes in aperture. Stomatal aperture is regulated by internal and external cues including CO_2 concentrations [CO_2], light, hormones such as abscisic acid (ABA). Though ABA and CO_2 pathways are shown to converge to induce stomatal closure the exact mechanism is unknown. In addition, the photoreceptor phyB is known to regulate stomatal responses to elevated (E) [CO_2]. The present study aims to determine the role of phytohormones and photoreceptor phyB to mediate stomatal closure in response to E[CO_2]. Here, we propose that CO_2 acts though the ABA antagonist, gibberellins (GAs) and ABA:GA homeostasis modulates stomatal responses to E[CO_2]. In *Arabidopsis thaliana*, using both GA and GA biosynthesis inhibitor treatments alongside genetic tools it was demonstrated that GA can modulate stomatal responses to E[CO_2] in both isolated epidermis and whole leaves. A definitive role for negative regulators of GA responses, DELLA proteins was not established, and GAs did not act via ROS signaling. Absolute measurement of ABA and GAs suggests reduction in GAs and not ABA are critical to fine-tune the E[CO_2]-mediated stomatal closure. In Arabidopsis, hypersensitivity of *phyB-9* to E[CO_2] could be rescued by GA treatments. *phyB-9* has reduced levels of active GA compared to Col-0 but increased levels of the conjugated form of ABA, ABA-GE. Perturbations in ABA:GA homeostasis are responsible for the *phyB* E[CO_2] phenotype as sensitivity is rescued by genetically reducing ABA levels. The photoreceptor phyB also regulates stomatal responses to E[CO_2] in rice. E[CO_2] showed no effect on photosynthetic parameters and had a variable effect on tiller number and flag leaf measurements and ultimately did not increase rice yield. *OsphyB* mutants had significant reductions in yield irrespective of [CO_2], demonstrating its critical role in plant growth and development.

List of Abbreviations

A[CO_2]=Ambient CO_2 concentration (400-450ppm)

ABA= Abscisic acid

ABA-GE= Abscisic acid glucose ester

BL= Blue light

DMZ=Daminozide

E[CO_2]= 1000ppm of CO_2 concentration

e[CO_2]= Any elevation in CO_2 concentration from ambient.

F[CO_2]= [CO_2] free air

GA= Gibberellins

GA_3= Gibberellic acid

GC= Guard Cell

GCL= Guard Cell length

g_s = stomatal conductance; a measure of the ease with which gases are exchanged through stomata.

Hyg= Hygromycin

IRGA= Infra-red gas analyzer

MS media= Murashige and Skoog plant growth media

PBZ= Paclobutrazol

PCR= Polymerase Chain Reaction

PHYB = the apoprotein

PHYB = the gene encoding PHYB.

phyB = the photoreceptor with protein and chromophore.

phyB-9 = the mutant allele of PHYB.

PM= Plasma membrane

qRT-PCR= Quantitative Reverse Transcription PCR

RL= red light

ROS= Reactive oxygen species

SC= Stomatal complex

SCs= Subsidiary cells

SD= Stomatal density

WUE= Water use efficiency; ratio of water used in plant metabolism to water lost via transpiration.

$\Delta^{13}C$= Carbon isotope discrimination; the ratio of ^{12}C and ^{13}C in plant tissue.

Table of Contents

Chapter 1. Introduction

1.1 Global atmospheric [CO_2] elevation and plant responses

The global population is predicted to rise from a current population of 8 billion to 10 billion by the year 2050; a change that will require a significant increase in world food production and improvements in food systems (UN DESA, 2022). Meeting these demands is further complicated by predicted changes in climate, which render the target of increasing food production as a challenge. Multiple interactive factors including increasing greenhouse gases, rising temperatures, changing precipitation patterns, drought and salinity stress are likely to impact plant physiology and crop productivity (Makowski et al., 2020; Teng et al., 2023). Among these factors, the rapid increase in atmospheric carbon dioxide concentrations (a[CO_2]) is considered to have profound effects on agricultural production and food quality (Ziska, 2008; Taub, 2010; Gamage et al., 2018). Over the last 2 million years, the current global increases in a[CO_2] are unparalleled and 2022 saw a new high record of 417.06 parts per million (ppm) (NOAA, 2022; IPCC, 2023). As a parallel activity to the standard IPCC AR4 climate report the Coupled Climate-Carbon Cycle Model Intercomparison Project (C^4MIP) was initiated. C^4MIP projected that a[CO_2] could vary between 730 ppm to 1020 ppm by the end of 21st century. Compared with standard IPCC AR4 simulations, which considered a[CO_2] only (Meehl et al., 2005); the C^4MIP eleven climate models, with a representation of the land and ocean carbon cycle, performed simulations where the model was driven by an anthropogenic CO_2 emissions scenario between 1860 to 2100 (Meehl et al., 2007) (Figure 1.1). This elevation in CO_2 as a potential greenhouse gas is predicted to exacerbate global warming. Global temperatures have already risen 1.1ºC over the last ~140 years and this has initiated unprecedented changes to the Earth's climate (IPCC, 2023). In order to maintain or increase crop productivity in future warmer, drier and CO_2- enriched environments, a better understanding of how plants respond to e[CO_2] is required. a[CO_2] influences the primary physiological processes of land plants i.e. photosynthesis, respiration and water relations (Gamage et al., 2018). Stomata, the small pores on the surface of leaves, link these responses since they are the gateway for 95% of gas exchange between the plant and surrounding atmosphere (Keenan et al., 2013).

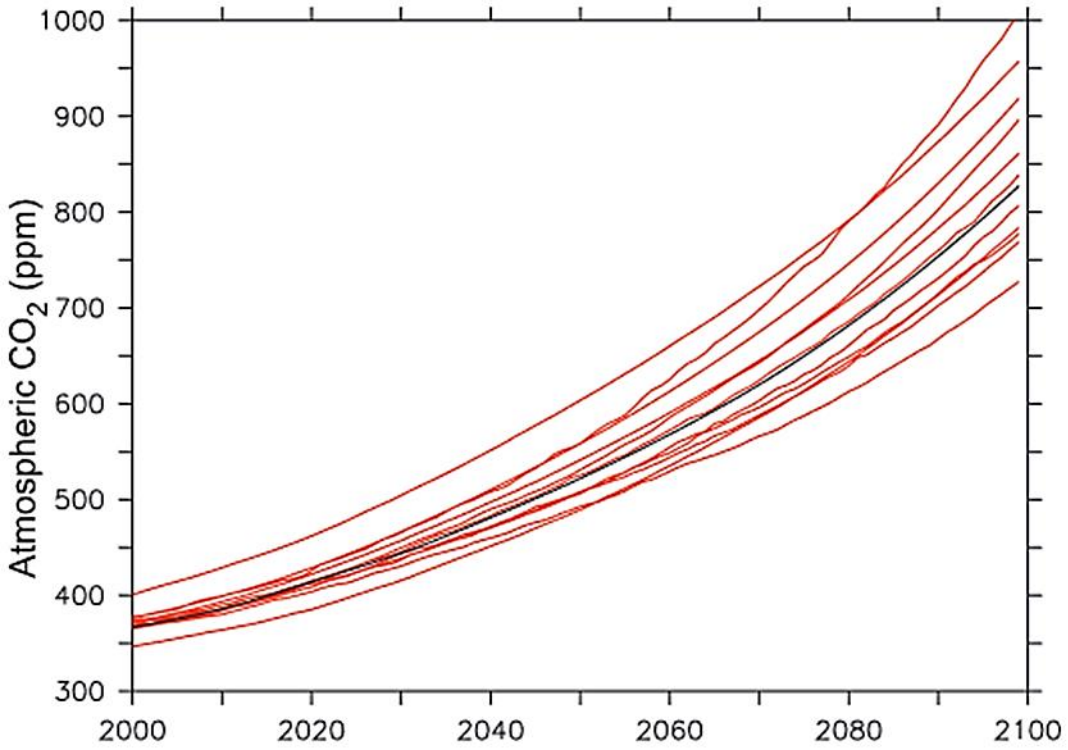

Figure 1.1 Increasing trend in global CO_2 concentration between 2000-2100. Atmospheric CO_2 concentration as simulated by the 11 C^4MIP models for the SRES A2 (IPCC Special Report on Emission Scenario A2) emission scenario (red) compared with the standard atmospheric CO_2 concentration used for many IPCC AR4 climate models (black) by 21st century. (Source Meehl et al. 2007, p. 790).

Stomata are found in the epidermis and consist of a pore surrounded by pair of guard cells (GCs). GC shape varies but they are primarily categorised as kidney shaped as in Arabidopsis or dumbbell shaped, as in grass species (Zeiger et al., 1987). Adjustment of stomatal aperture with the pore opening and closing is a dynamic response to varied internal and environmental signals which varies between and within species (reviewed in Matthews et al., 2020). In addition, stomatal density (number of stomata per unit of leaf area) as a developmental response, plays vital role to maintain optimum stomatal conductance (g_s) in plants related to their environment (Casson & Gray, 2008; Casson & Hetherington, 2010). Genetic pathway regulating stomatal development in leaves is well characterized, for the eudicot model *Arabidopsis thaliana* (Zoulias et al., 2018; Herrmann & Torii, 2021). The main difference between

the two stomatal adjustments is the scale of time since stomatal aperture can change in minutes, whereas changes in stomatal density are fixed during leaf development according to conditions experienced by the plant at the time (Jalakas et al., 2018).

In general, during the day-time stomatal opening is regulated to maintain optimum [CO_2] and trade off with water loss in the sub-stomatal chambers for continuous CO_2 assimilation (A). On the other hand, elevated [CO_2] (e[CO_2]) in the intercellular space of leaves (C_i) cause stomatal closure. The current trend of increasing a[CO_2] is therefore likely to impact on stomatal aperture (Zhang et al., 2018). In addition to aperture closure, an increase in a[CO_2] may lead to reductions in stomatal density in many species based on experiments with extant species and also from the analysis of fossil records (Woodward, 1987; McElwain & Chaloner, 1995; Chater et al., 2013 Engineer et al., 2016; Chater et al., 2017). The combined effect of smaller apertures and lower densities would be expected to negatively impact g_s and a recent study demonstrated g_s was reduced significantly by e[CO_2] changing on average by –8.3% per 100 ppm CO_2 increase (Liang et al., 2023). This may be advantageous where crops are being grown under water limited conditions due to reduced evapotranspiration (Leakey et al., 2009; Keenan et al., 2013; Sreeharsha et al., 2015). However, reduced evapotranspiration is reported to increase leaf heat stress (Long et al., 2004; Leakey et al., 2009; Long & Ort, 2010). This in combination with drought and rising temperature may negatively impact plant health, nutrient content, and food supply (Battisti & Naylor, 2009; Easlon & Bloom, 2013; Weigel, 2014; Wroblewitz et al., 2014). Thus, stomatal aperture regulation is crucial to maintain the trade-off between opening for optimum CO_2 uptake and closure to limit water loss in response to environmental stress. Therefore, the mechanisms that regulate stomatal aperture upon changes in [CO_2] are a potential target for crop improvement.

Several characteristics including rapid life cycle, prolific seed production, uncomplicated cultivation, a fully sequenced and annotated diploid genome, genetic resources with a significant number of gene knockout lines have made *Arabidopsis thaliana* a model organism in flowering plant research. Research revolving stomatal function and development is not any different. Therefore, much of our current knowledge and many of the findings presented during the study is based on Arabidopsis unless stated otherwise.

1.2 Stomatal aperture regulation

Active control of stomatal aperture is regulated by the surrounding two GCs. Stomatal opening and closure are mediated by changes in GC turgor that is determined by the transport of inorganic ions and organic metabolites across their plasma membrane (PM) and the subsequent movement of water (Keller et al. 1989; Schroeder & Hagiwara, 1989; Pandey et al., 2007; Kim et al., 2010; Kollist et al., 2014).

During stomatal opening, H^+-ATPase pumps out protons (H^+) from the GCs and this results in PM hyperpolarization leading to the uptake of potassium ions (K^+) via activate inward K^+ rectifying (K_{in}) channels, such as KAT1 (potassium channel in *Arabidopsis thaliana* 1), KAT2 (potassium channel in *Arabidopsis thaliana* 2), AKT1 (Arabidopsis thaliana K^+ transporter 1) and H^+/K^+ HAK-type symporters. Uptake of K^+ is counter-balanced by chloride (Cl^-) and nitrate ions (NO_3^-) taken up from the apoplast via nitrate transporters (NRT) and malate^{2-} production from starch breakdown and water transportation via aquaporins (AQP) (Assmann, 1993; Schroeder et al., 2001; Shimazaki et al., 2007; Daszkowska-Golec & Szarejko, 2013) . These help to generate enough GC turgor to keep the stomata open (Figure 1.2A). On the other hand, stomatal closure is driven by GC membrane depolarization via H^+-ATPase inhibition and activation of rapid type (R-type; QUAC1) and slow type (S-type; SLAC1) anion channels. In addition, release and/or uptake of Ca^{2+} from outside and/or the GC tonoplast depolarizes the GC membrane more. Such membrane depolarization drives efflux of K^+ via GC outward K^+ rectifying (K_{out}) channels (GORK) along with malate^{2-} and water extrusion from GCs to shrink and ultimately close over the stomatal pore (Figure 1.2B) (Blatt & Clint, 1989; Santelia & Lawson, 2016; Jezek & Blatt, 2017; Lemonnier & Lawson, 2023). In addition to ion exchange, cytoskeleton reorganization and metabolite production, the modulation of gene expression and the post-translational modifications regulate stomatal function (reviewed in Kim et al., 2010) .

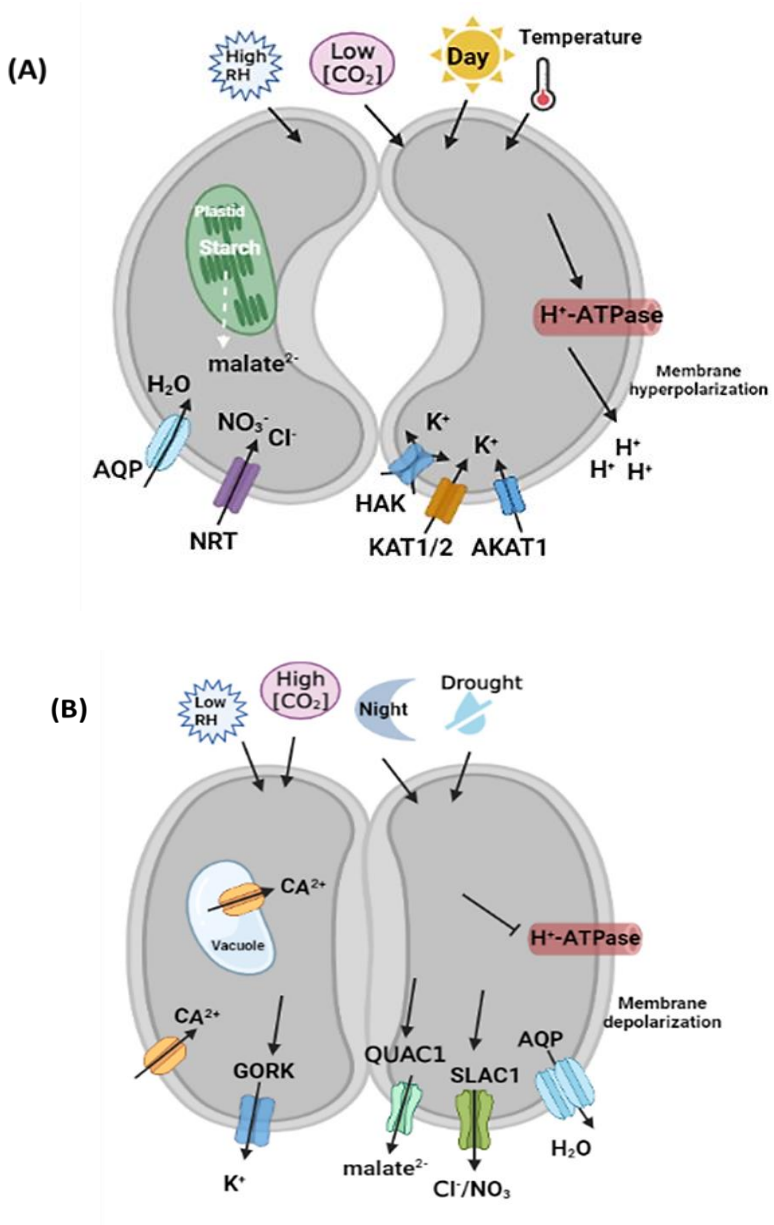

Figure 1.2 Stomatal function in response to various stimuli. (A) During stomatal opening H^+-ATPase pumps out H^+ and hyperpolarizes the GC membrane leading to K^+ uptake via activated K_{in} channels (KAT1, KAT2, AKT1) and HAK symporters. To counterbalance the ionic environment, anions including NO^{3-} and Cl^- enter the GC through NRT transporters while $malate^{2-}$ accumulates via starch breakdown. Thus, ions together with transported water via AQP generate enough turgor to swell the GC and keep the stomata open. **(B)** During stomatal closure, H^+-ATPase is inactivated while SLAC1 and QUAC1 anion channels are activated to facilitate ion efflux, resulting in membrane depolarization. At the same time, K_{out} channels like GORK are activated to efflux K^+ and AQP to release water. Thus, the GC turgor reduces and closes the stomata by shrinking themselves. Elevation of Ca^{2+} concentration inside GC via release from GC tonoplast and PM channels also helps in stomatal closure. Image "Created with Biorender.com".

Changes in the stomatal aperture can be directly linked to GC signalling responses to external as well as internal stimuli. Diverse signals including blue and red light, abscisic acid (ABA), [CO_2], drought, humidity, organic acids, and pathogens modulate stomatal apertures through intricate signal transduction networks (Israelsson et al., 2006; Hirayama & Shinozaki, 2007; MacRobbie & Kurup, 2007; Shimazaki et al., 2007; Underwood et al., 2007; Neill et al., 2008; Acharya & Assmann, 2009; Araújo et al., 2011). Research also showed that the endogenous circadian system regulates stomatal aperture (Salomé et al., 2002; Hubbard & Webb, 2011; Hassidim et al., 2017). In natural environments, stomata sense multiple signals simultaneously and respond to them in a hierarchical manner (Lawson & Morison, 2004; Lawson & Blatt, 2014; Lawson et al., 2010, 2018). Current data suggest that light intensity, a[CO_2] and endogenous plant hormones play prominent and interactive roles to modulate basal stomatal function. Therefore, to understand e[CO_2]-mediated stomatal closure response, recent updates and gaps on the molecular mechanisms of stomatal aperture control in relation to e[CO_2], hormones and light will be discussed in the following sections.

1.2.1 e[CO_2] mediated stomatal closure response

Through genetic analysis of the model plant *Arabidopsis thaliana*, different components specific to [CO_2]-induced stomatal closure have been identified. Activation of SLAC1 and R-/QUAC1 are critical for efflux of inorganic and organic ions to initiate stomatal closure (Schmidt et al., 1995; Pei et al., 1997; Geiger et al., 2009; Lee et al., 2009; Meyer et al., 2010; Sasaki et al., 2010; Xue et al., 2011; Dreyer et al., 2012). A group of kinases including OST1 (OPEN STOMATA 1), CDPKs (Ca^{2+}-dependent protein kinases) and GHR1 (GUARD CELL HYDROGEN PEROXIDE-RESISTANT 1) are reported to phosphorylate and activate SLAC1; whereas QUAC1 is known to be activated by OST1 only (Lee et al., 2009; Geiger et al., 2010, 2009; Brandt et al., 2012; Hua et al., 2012; Scherzer et al., 2012; Imes et al., 2013). Downstream of CO_2, mitogen activated protein kinases 4 and 12 (MPK4 and MPK12) are also suggested to function synergistically to regulate CO_2-induced stomatal function (Tõldsepp et al., 2018). A Raf-like protein kinase named HIGH LEAF TEMPERATURE1 (HT1) is predominantly expressed in GC and is a major negative

regulator of [CO_2] induced stomatal closure (Hashimoto et al., 2006). Other Raf-like protein kinases CONVERGENCE OF BLUE LIGHT AND CO_2 1 (CBC1) and CBC2 are also considered as negative regulators of high CO_2-induced stomatal closure and function in the same pathway as HT1 (Hiyama et al., 2017). Experiments have suggested that β-carbonic anhydrases (βCA1 and βCA4) in Arabidopsis GC enhance CO_2 catalysis into bicarbonate (HCO_3^-) and H^+ in the cytoplasm and are important intercellular messengers to mediate stomatal closure (Hu et al., 2010; Xue et al., 2011; Zhang, De-oliveira-Ceciliata et al., 2018). Plasma membrane intrinsic protein 2-1 (PIP2;1 aquaporin/AQP) interact with βCA1 and βCA4 to facilitate CO_2 influx and catalysis in GC (Wang et al., 2015). However, the primary CO_2/HCO_3^- sensor in GC to regulate early protein phosphorylation to initiate stomatal closure remain unidentified. MATE (MULTIDRUG AND TOXIC COMPOUND EXTRUSION)-like protein RHC1 (RESISTANT TO HIGH CARBON DIOXIDE 1) has been suggested as a bridge between βCAs and HT1 for HCO_3^- dependent activation of SLAC1 (Tian et al., 2015). Recently, MPK4 and MPK12 have been reported to interact with HT1 in response to e[CO_2]/ HCO_3^- to inhibit downstream HT1 and CBC1/2 and are suggested as the primary sensor of [CO_2] induced stomatal closure (Takahashi et al., 2022). The sequential events of stomatal closure under e[CO_2] studied so far has been illustrated in Figure 1.3.

e[CO_2] -induced reductions in g_s is the net result of two processes: the promotion of stomatal closure and the inhibition of stomatal opening (Assmann, 1993). Evidence has suggested that stomatal opening and closure responses are physiologically distinct and are not the inverse of each other (Assmann, 1993, 2000; He et al., 2018). In this context, a novel allele of the BIG locus named *CO_2 insensitive 1* (*cis1*) has been identified as a signaling component in the e[CO_2]-mediated stomatal response that distinguishes CO_2-mediated stomatal opening and closure. e[CO_2]-induced stomatal closure was impaired in *BIG* mutants compared to wild type behavior indicating that BIG is involved in e[CO_2]-induced stomatal closure. In contrast, e[CO_2]-induced inhibition of light induced stomatal opening is not compromised in *BIG* gene mutants demonstrating that BIG is not associated with e[CO_2]-mediated inhibition of stomatal opening (He et al., 2018). Therefore, e[CO_2]-induced stomatal closure study should be considered separate and independent of inhibition of stomatal opening in response to CO_2.

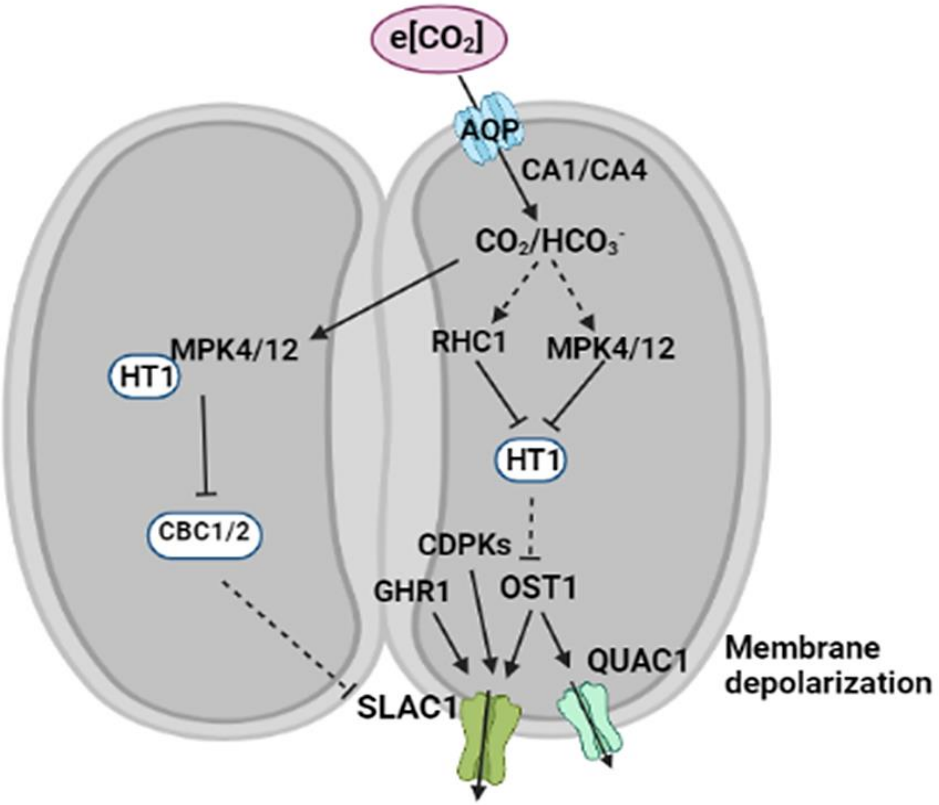

Figure 1.3 Regulation of stomatal closure in response to e[CO_2]. CO_2 enters GCs through AQPs where CA1/4 hydrolyses CO_2 into HCO_3^-. CO_2 and/or HCO_3^- acts on downstream kinases MPK4/12 and RHC1, which inactivate HT1, a negative regulator of e[CO_2]-induced stomatal closure. In the absence of HT1, OST1 is phosphorylated and activates anion channels SLAC1 and QUAC1. The kinases GHR1 and CDPKs are also able to activate the ion channels. In response to increases in CO_2/HCO_3^-, CBC1/2 is inactivated via the MPK4/12 and HT1 complex and thus activates SLAC1. SLAC1/QUAC1 drive membrane depolarization and results in stomatal closure. Negative regulators are shown within white oval shapes, line arrows are for direct positive regulation, bar lines for negative regulation, dashed arrows and dashed bar lines indicate hypothetical positive and negative regulation respectively. Image “Created with Biorender.com”.

1.2.2 Hormone mediated control of stomatal aperture

The interaction of multiple hormones determines stomatal aperture in a condition-specific manner (reviewed in Acharya and Assmann, 2009). Auxins and cytokinins are generally positive regulators of stomatal opening. On the contrary, ABA, jasmonates

(JAs), brassinosteroids (BRs) and salicylic acid (SA) are positive regulators of stomatal closure. Ethylene plays a dual regulatory role on stomatal apertures. Ethylene has been reported to cause stomatal closure via ethylene induced H_2O_2 synthesis in Arabidopsis leaves (Desikan et al. 2006). At the same time, ethylene has been reported to oppose stomatal closure in concert with other hormones. Ethylene overproducing mutant eto1-1 suppressed ABA-induced stomatal closure (Tanaka et al. 2005). Also, ethylene biosynthesis/signalling is required for cytokinins and auxins mediated suppression of ABA-induced stomatal closure (Tanaka et al. 2006). In case of gibberellins (GAs), little evidence of their association in GC function have been observed. So far, little work has been conducted regarding the role of gibberellins (GAs) on GC responses. These showed contradictory role as one reported GA had no effect on ABA-induced stomatal closure (Tanaka et al. 2006). Other group of research suggested that GA application promoted stomatal opening in *Vicia faba*, *Fritilaria imperalis* and *Commelina benghalensis* L. (Santakumari & Fletcher, 1987; Goring et al. 1990). Also, GA reported to regulate ABA-induced inhibition of stomatal opening in light (Goh et al. 2009).

Among the phytohormones, ABA is one of the important and known regulators of stomatal function due to its role in limiting stomatal aperture under drought. Evidence suggests that GC ABA and CO_2 signalling pathways converge during promotion of stomatal closure (Webb & Hetherington,1997).

1.2.2.1 ABA metabolism and transport in GC

ABA metabolism involving biosynthesis, catabolism, conjugation/deconjugation, and transportation are crucial to regulate the levels of bioactive ABA within plant cells. Many genes in ABA metabolism have been shown to be involved in stomatal responses (Merilo et al., 2013; Chater et al., 2015). ABA is synthesized mainly in the plastids and cytosol of vascular parenchyma cells and GC and involves several steps starting from zeaxanthin synthesized by the β-carotene pathway. In brief, ABA biosynthesis can be discussed in three steps. First, the carotenoid zeaxanthin is catalyzed to the all-*trans* violaxanthin in the chloroplast by zeaxanthin epoxidase (ZEP). Second, the intermediate violaxanthin is catalyzed to xanthoxin by nine-*cis* epoxycarotenoid dioxygenase (NCED) and transported from the chloroplast to the

cytoplasm. Third, xanthoxin is converted to abscisic aldehyde by short-chain dehydrogenase reductase (SDR/AtABA2) and oxidized to bioactive ABA by abscisic aldehyde oxidase (AAO) in the cytoplasm (Seo & Koshiba, 2002). ABA catabolism involves cytochrome P450 monooxygenase (CYP707As), which catalyse the formation of hydroxylated ABA i.e., phaseic acid (PA) and dihydro phaseic acid (DPA) (Ng et al., 2014; Sah et al., 2016). ABA and its catabolites can further be inactivated by ABA glucosyltransferase to form conjugated ABA-glucosyl ester (ABA-GE) (Ye et al., 2012; Sah et al., 2016). However, deconjugation of ABA-glucose by β-glucosidases (AtBG1 and AtBG2) release active ABA in the system (Burla et al., 2013). In addition, ABA transporters like ABCG22 in GC and ABCG25 in vascular tissue have been reported to allow ABA translocation (Kuromori et al., 2010). The main steps in ABA metabolism are shown in Figure 1.4.

Research indicates that GC can function as an ABA source since they are capable of autonomous ABA synthesis and efflux (Cornish & Zeevaart, 1986; Bauer et al., 2013; Zhang et al., 2014). ABC transporter genes ABCG40 and ABCG22 were reported to highly expressed in GC to maintain proper regulation of stomatal movements (Kang et al., 2010; Kuromori et al., 2011). Hydroxylation of ABA by CYP707A1 and ABA-glucosylating enzyme activities are also present in Arabidopsis GC (Okamoto et al., 2009; Dong et al., 2014; Liu et al., 2015).

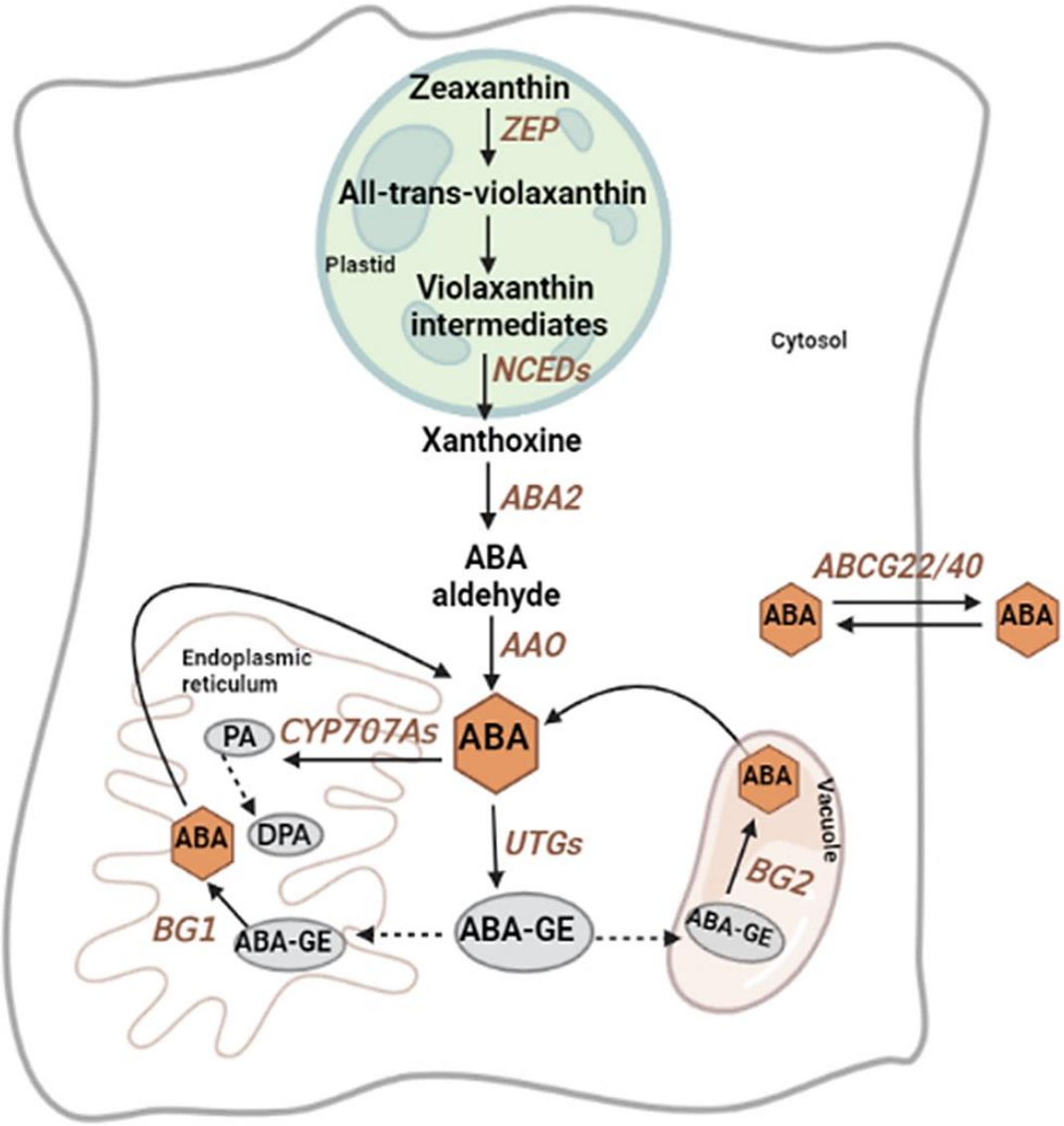

Figure 1.4 ABA metabolism involving biosynthesis, catabolism, conjugation-deconjugation and transport inside plant cells including GC. ABA is synthesized from zeaxanthin, a product of β-carotene pathway in a series of reactions inside plastid and cytosol. ABA is catabolized by CYP707As inside endoplasmic reticulum into PA and DPA. Besides, ABA can conjugate into ABA-GE by ABA glucosyltransferase inside the endoplasmic reticulum and vacuole and can be hydrolysed to ABA again by BG1/2. Delivery of ABA from source cell to GC is mediated by ABCG22/40 transporters. Enzymes involved in each step are shown in brown italic font. Line arrows indicate direct positive regulation, bar lines direct negative regulation, dashed arrows for possible positive regulation. Image “Created with Biorender.com”.

1.2.2.2 ABA signalling in GC

The PYR/PYL/RCAR (PYRABACTIN RESISTANCE/PYR1 LIKE/REGULATORY COMPONENT OF ABA RECEPTOR) family of proteins perceives intercellular ABA and this ligand-receptor complex inhibits type 2C protein phosphatases (PP2Cs), which allows the phosphorylation and activation of downstream Sucrose Non-fermenting 1-Related subfamily 2 protein Kinases (SnRK2s) (Fujita et al., 2009; Fujii & Zhu, 2009; Umezawa et al., 2009; Kim et al., 2010). SnRK2s are central regulators of ABA signalling in Arabidopsis and rice (Kobayashi et al., 2005). They are responsible for the activation of ABREs (ABA-responsive elements) binding factors (ABFs) and regulate transcription of several downstream ABA-responsive genes (Choi et al., 2000; Kim et al., 2002; Lopez-Molina et al., 2002). The participation of core ABA signalling is well established in ABA-mediated stomatal closure in GC via activation of OST1 (SnRK2.6). OST1 promotes stomatal closure by regulating SLAC1 and QUAC1 to drive PM depolarization and subsequent K^+ efflux via active GORK in presence of ABA (Kim et al., 2010; Hedrich, 2012; Roelfsema et al., 2012). CDPKs and GHR1 are also reported to activate SLAC1 in an ABA dependent manner during stomatal closure (Geiger et al., 2010; Hõrak et al., 2016). A simplified model of stomatal closure through activation of SLAC1 in the presence of ABA is presented on the following page (Figure 1.5). Like CO_2, the promotion of stomatal closure and the inhibition of stomatal opening in response to ABA are distinct from each other (Allen et al., 1999; Wang et al., 2001; Mishra et al., 2006). Because GCs are reported to synthesize ABA in a cell-autonomous way and receive ABA from the apoplast, a key question is which pathway is dominant in GC in response to various stimuli (Munemasa et al., 2015).

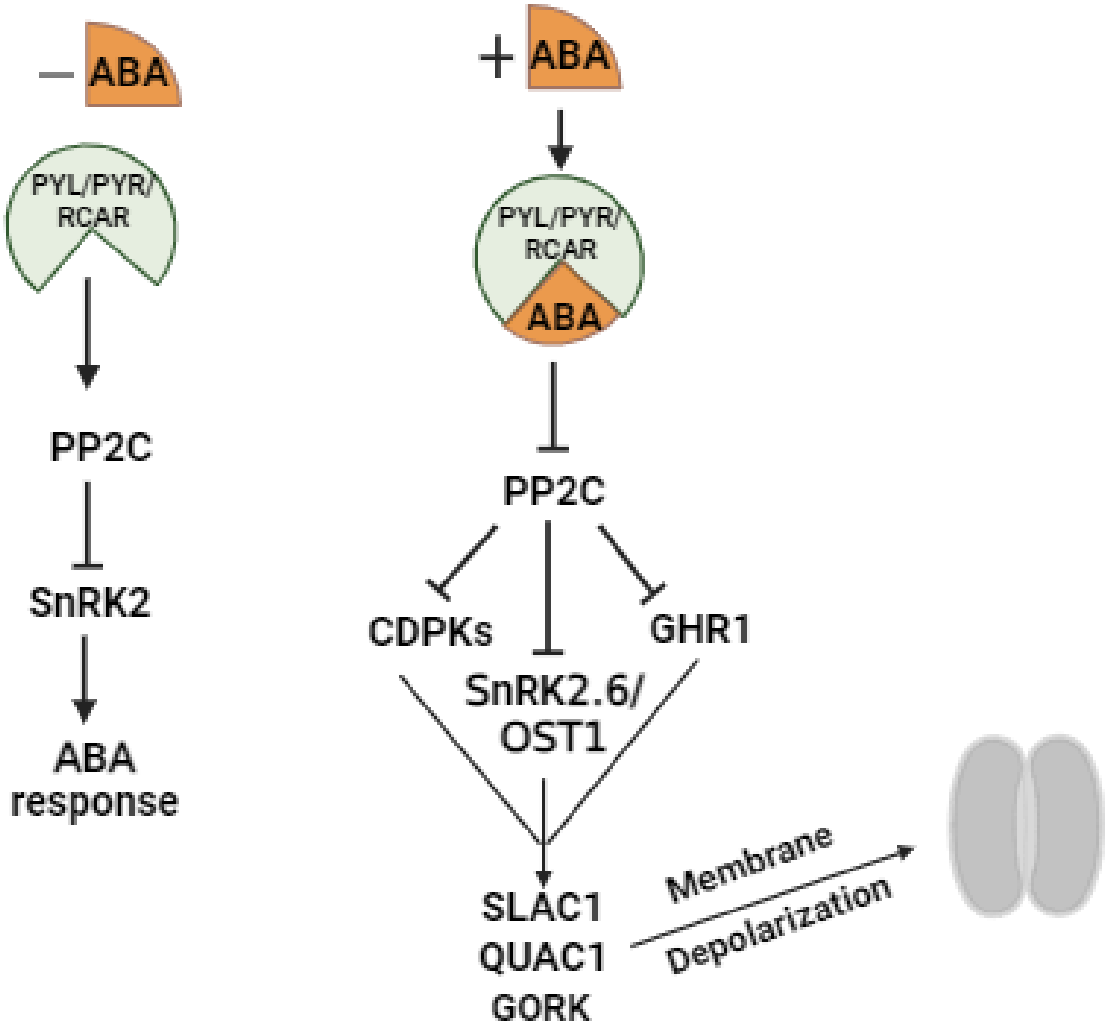

Figure 1.5 ABA signalling in GC closure response. (A) In absence of ABA, ABA receptors activate negative regulator of ABA signalling i.e., PP2Cs which further inactivate downstream SnRK2s, central regulators of ABA responses. **(B)** When ABA is present ABA receptors PYL/PYR/RCAR form a receptor-ligand complex and inactivate PP2Cs. This relieves suppression on downstream kinases like SnRK2.6/OST1, CDPKs and GHR1 allowing them to activate S-type and R-type channels like SLAC1 and QUAC1 and results in subsequent membrane hyperpolarization and stomatal closure. Line arrows indicates direct positive regulation and bar lines denotes negative regulation. Image “Created with Biorender.com”.

1.3 Interaction between e[CO_2] and ABA-mediated stomatal closure response

Since both the e[CO_2] and ABA induce stomatal closure it is plausible to have convergence between their signal transduction mechanism. Classical studies showed strong interactions between CO_2 sensing and ABA-mediated stomatal closure (Raschke, 1975; Leymarie, Lascève, et al., 1998; Leymarie, Vavasseur, et al., 1998; Leymarie et al., 1999). In Arabidopsis, dominant ABA-insensitive mutants *abi1-1* and *abi2-1* are reported to be defective in ABA signalling as well as in CO_2 responses in GC (Webb & Hetherington, 1997; Merilo et al., 2013). Phosphorylation via OST1 kinase to activate SLAC1, QUAC1 and K^+ channels are common between the e[CO_2] and ABA mediated stomatal closure (Negi et al., 2008; Vahisalu et al., 2008; Meyer et al., 2010; Xue et al., 2011). During ABA signalling ABI2 is reported to inhibit GHR1 dependent activation of SLAC1 while HT1 is suggested to negatively regulate GHR1 during e[CO_2]-mediated stomatal closure (Hõrak et al., 2016). Thus, GHR1 is a potential convergence between the two signals in GC. ABA insensitive mutant *growth controlled by ABA* (*gca2*) showed strong impairment in high CO_2-induced stomatal closing alongside no change in cytosolic Ca^{2+} transient rate (Young et al., 2006). Thus, provide potential involvement between the two GC closure responses to regulate downstream ion channels. A role of intercellular Ca^{2+} is evident from CO_2 and ABA responses in GC suggesting a common link between the pathways (Webb et al., 1996; Young et al., 2006; Xue et al., 2011). Thus, several downstream components have found to converge during ABA and CO_2 induced stomatal closure response (Figure 1.6). Several attempts were made to investigate involvement of ABA perception and signalling to e[CO_2]-mediated stomatal closure. In recent years, use of mutants in ABA receptors of the PYR/PYL/RCAR family showed their partial as well as complete involvement in CO_2-mediated closure (Chater et al., 2015; Dittrich et al., 2019). However, contrary to this data, analysis of SnRK2.6/OST1 kinase activity via Forster resonance energy transfer (FRET) biosensor determined no role of PYL4/5 towards the e[CO_2]-mediated stomatal closure (Zhang et al., 2020). In addition to signalling, components of ABA synthesis are required for a normal CO_2 response. Gas exchange measurements in ABA biosynthesis mutants *aba1*, *aba2-1, aba3* and *nced3nced5* reduced but did not abolish CO_2 responses as observed from several reports (Merilo

et al., 2013; Chater et al., 2015; Hsu et al., 2018). Additionally, ABA catabolism has been reported to be involved in e[CO_2]-mediated stomatal closure and reduced stomatal density response in Arabidopsis (Movahedi et al., 2021).

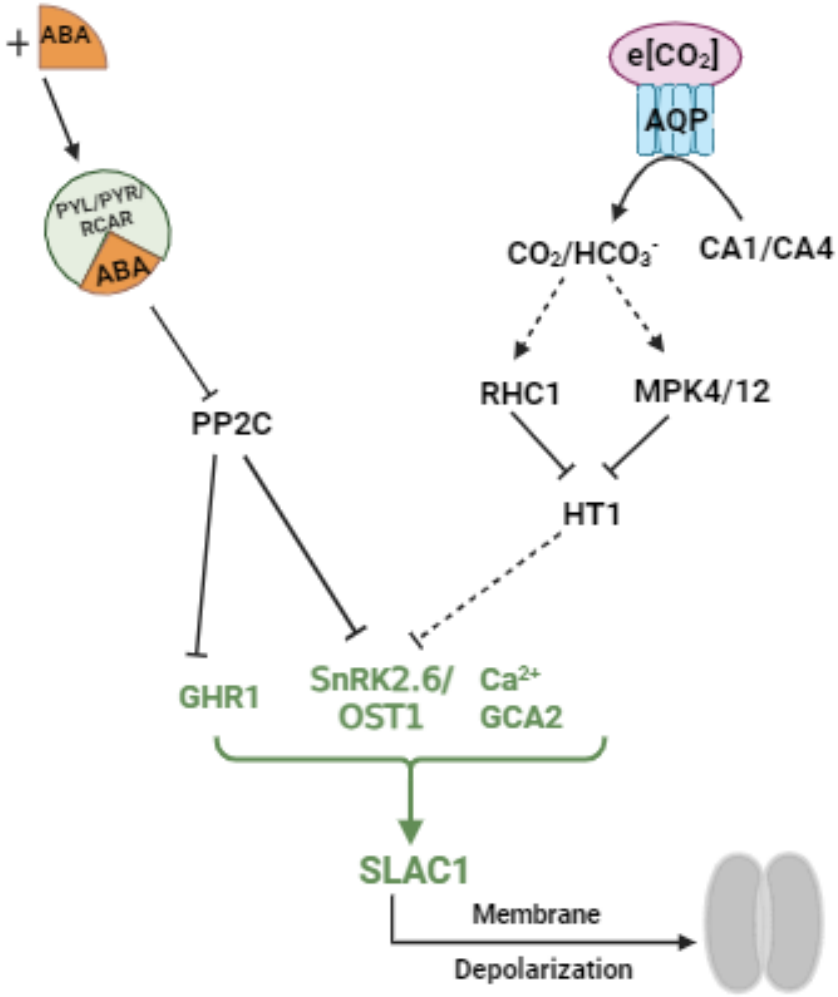

Figure 1.6 Regulatory steps and convergence points during ABA and CO_2 induced stomatal closure response. CO_2/HCO_3^- activate RHC1, MPK4 and MPK12, which in turn inactivate HT1 by phosphorylation. This is an important step since HT1 inhibits downstream components like OST1 essential for the activation of SLAC1. During ABA signalling, ABA binds to PYR/PYL/RCAR and this ligand-receptor complex inhibits PP2Cs to further inactivate/phosphorylate OST1 and GHR1 to activate downstream SLAC1. Also, GCA2 and Ca^{2+} are known to regulate SLAC1 between both the responses. Adopted and modified from (Hõrak et al., 2016; Jakobson et al., 2016). Line arrows for up regulation, barred lines for down regulation, dotted lines denote hypothetical regulation, green fonts to indicate common components between ABA and CO_2 induced stomatal closure response. Image "Created with Biorender.com".

Altogether these data indicate that either ABA perception and signalling is involved in GC sensitivity to e[CO_2] or an increase in [ABA] via biosynthesis in response to e[CO_2]. However, [ABA] has not been shown to change in response to e[CO_2] in leaves and in GC (Chater et al., 2015; Hsu et al., 2018). Therefore, although research indicates that e[CO_2]-mediated stomatal closure requires intact ABA metabolism and signalling pathways, none of the mechanisms appear to involve in any change in ABA levels. Thus, the exact involvement of ABA in e[CO_2]-mediated stomatal closure remains an interesting field to explore.

1.4 GA: potential factor of e[CO_2] and ABA-mediated signal transduction in GC

Hormonal regulation generally involves crosstalk and signal integration with either antagonistic and/or synergistic interactions. For example, auxin and BR mutually promote cell expansion (Nemhauser et al., 2004), while ABA and GA antagonistically regulate seed dormancy and germination (Kucera et al., 2005; Finkelstein et al., 2008). The antagonistic regulation of ABA and GA have been studied extensively in many developmental and stress responses in plants (reviewed in Liu & Hou, 2018). The endogenous levels of these hormones can be affected in opposite manners; for example, the GA deficient mutant *ga1-3* accumulates more ABA than WT and *aba2-2* ABA biosynthesis mutants have higher GA synthesis (Seo et al., 2006; Oh et al., 2007). In the context of stomatal aperture control, few studies have examined the role of GA, though it has been shown to modulate ABA-induced inhibition of stomatal opening in light (Göring et al., 1990; Goh et al., 2009). In addition, mutants that lack GA signalling responses have consistently increased basal stomatal aperture (Sukiran et al., 2020). However no previous studies have examined whether GA metabolism or signalling affects the GC e[CO_2]-mediated closure response. Considering the classical antagonism between ABA and GA signalling it might be predicted that e[CO_2] could negatively affect GC GA signalling. Therefore, an outstanding question to be addressed is whether GA signalling and metabolism antagonise GC ABA responses and adjust the overall hormonal response during e[CO_2]-mediated stomatal closure response (Hypothesis Figure 1.10). Much is known about GA metabolism and

signalling, and many genetic tools are available to examine GA responses as discussed in the following sections.

1.4.1 GA metabolism in plants

GAs are diterpene phytohormones abundantly found in higher plants and fungi though a few e.g. GA_1, GA_3, GA_4 and GA_7 are biologically active (Hedden & Phillips, 2000). In Arabidopsis, GAs are involved in seed germination, leaf and root growth, flowering in short-day conditions, anther, fruit and seed development (Sun, 2008). GA metabolism initiates from geranyl geranyl diphosphate (GGDP) in plastids. GGDP is catalysed by two terpene synthases (TPSs) *ent*-copalyl diphosphate synthase (CPS) and *ent*-kaurene synthase (KS) to form *ent*-kaurene which is the first committed intermediate in the GA pathway (Sun & Kamiya, 1997, 1994; Helliwell, Sullivan, et al., 2001). Then *ent*-kaurene is converted into GA_{12} via two cytochrome P450 monooxygenases (P450s). *ent*-kaurene oxidase (KO or CYP701A according to the P450 nomenclature) and *ent*-kaurenoic acid oxidase (KAO or CYP88A) form GA_{12} via stepwise oxidation in the outer membrane of plastids and in the endoplasmic reticulum respectively (Helliwell, Sullivan, et al., 2001; Nelson et al., 2004). The last step involves several oxidation reactions catalysed by 2-oxoglutarate-dependent dioxygenases (2ODDS) i.e., GA 20-oxidases (GA20ox) and 3-oxidases (GA3ox) by two parallel pathways in the cytoplasm (Spray et al., 1996; Itoh et al., 2001; Appleford et al., 2006). Both the pathways form various GA intermediates and bioactive GAs. The only difference between the pathways is that one produces non-13-hydroxylated GAs (e.g., GA_4 and GA_7) and the other contains 13-hydroxylated GAs (e.g., GA_1 and GA_3). A new bioactive GA named 16,17-dihydroGA12 16-α-ol (DHGA12) catalysed by a 2ODD known as GAS2 (GAIN-OF-FUNCTION IN ABA-MODULATED SEED GERMINATION) was also reported recently in Arabidopsis and maize (Liu et al., 2019). Enzymes involved in the early stages of GA synthesis i.e., CPS, KS and KO are each encoded by single gene in Arabidopsis whereas KAO has two genes (Koornneef & van der Veen, 1980; Helliwell, Chandler, et al., 2001). On the contrary, GA20ox and GA3ox are each encoded by small gene family of five and four members respectively and each of them show tissue specific expression pattern (Thomas et al., 1999; Mitchum et al., 2006). Level of active GAs in any system are not only dependent on synthesis

but also on deactivation. The major GA catabolism is regulated by 2β-hydroxylation, which is catalysed by a class of 2ODDs, GA 2-oxidases (GA2ox) and can inactivate both bioactive GAs and their precursors (Thomas et al., 1999; Schomburg et al., 2003). Therefore, these group of enzymes remain active in the late stage of GA synthesis and are encoded by multigene family of seven members in Arabidopsis (Rieu et al., 2008). Other deactivation mechanisms involve 16 α,17-epoxidation of non-13-hydroxylated GAs and methylation of active GAs in Arabidopsis by GA methyltransferases (GAMT1 and GAMT2) (Zhu et al., 2006; Varbanova et al., 2007). Generalised steps involve in GA metabolism is presented in Figure 1.7.

1.4.2 GA perception and signalling in plants

Since GAs are hydrophobic carboxylic acids, they may travel across PM as a protonated acid by passive diffusion (Hooley et al. 1992). Thus, plants might have both membrane-bound and cytosolic soluble GA receptors (Gilory & Jones 1994; Park et al. 2005). Recent studies have demonstrated that GA signal is perceived by the GA receptor GIBBERELLIN INSENSITIVE DWARF (GID1), a soluble protein localized to both cytoplasm and nucleus (Sun, 2008). There are three GID1 orthologs in Arabidopsis with some overlapping functions (Nakajima et al., 2006). GA binding to the receptor forms a GA–GID1 complex to activate the downstream signalling pathway. Binding of GA to GID1 results in a conformational change to promote its interaction with DELLA proteins, the master repressors of GA responses (Harberd et al., 2009; Sun, 2010). DELLAs are a subset of nuclear transcriptional regulators of the GRAS family proteins and Arabidopsis contains 5 DELLAs: REPRESSOR OF ga1-3 (RGA), GA-INSENSITIVE (GAI), RGA-LIKE1 (RGL1), RGL2 and RGL3. They display overlapping as well as also some distinct functions in repressing GA responses (Dill & Sun, 2001; King et al., 2001; Lee et al., 2002; Cheng et al., 2004; Tyler et al., 2004). The GA-GID1-DELLA complex enhances binding of SLEEPY (SLY1, a subunit of the SCF (SKP1, CULLIN, F-BOX) E3 ubiquitin ligase complex) to initiate degradation of DELLAs via the ubiquitin-proteasome pathway (reviewed in Sun, 2011). In addition to ubiquitination, proteolysis independent and SUMOylation (small ubiquitin-related modifier) have also been reported in regulations of DELLAs (Ariizumi et al., 2008; Conti et al., 2014).

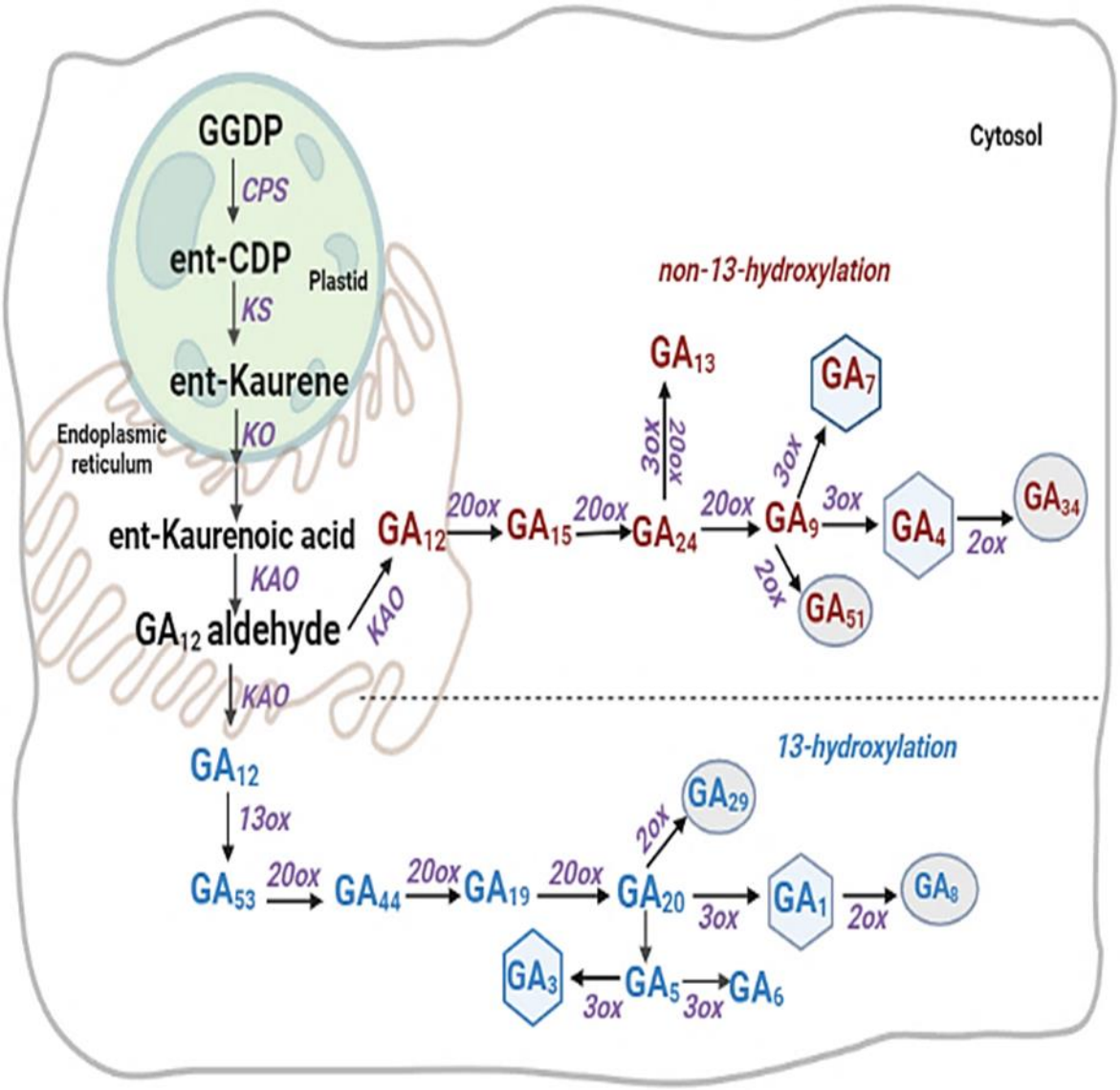

Figure 1.7 GA biosynthesis and catabolism in plants partitioned in three different organelles. Early steps occur in plastid where the first committed component of pathway, ent-Kaurene is formed from GGDP via CPS and KS. Then ent-Kaurene is oxidised stepwise to form GA_{12} by P450 monooxygenases in endoplasmic reticulum. In the third step, GA_{12} is moved to the cytoplasm and forms several GA intermediates and active GA by two parallel pathways. One pathway involves 13-hydroxylation reactions (shown with blue font) whereas other is non-13-hydroxylation (shown in red font). Both the pathways are catalysed by several GA20ox and GA3ox enzymes. Deactivation of GAs is also catalysed another class of 2ODDs, GA2ox. The pathway is adopted from Yamaguchi et al. 2008. The enzymes are shown in purple italic font. Active GAs from each pathway is shown within hexagon shape whereas inactive are shown in oval shape. Image "Created with Biorender.com".

Though DELLA-dependent GA signalling pathway is considered central to GA signal transduction, DELLA-independent GA signalling also exists e.g., GA-induced cytosolic Ca^{2+} increase in plant cells occurs via a DELLA-independent pathway (Okada et al., 2017). Also, a microarray study of DELLA-quadruple mutant in Arabidopsis showed some GA-regulated genes are not DELLA dependent (Cao et al., 2006). A generalised overview of GA signalling is shown in Figure 1.8.

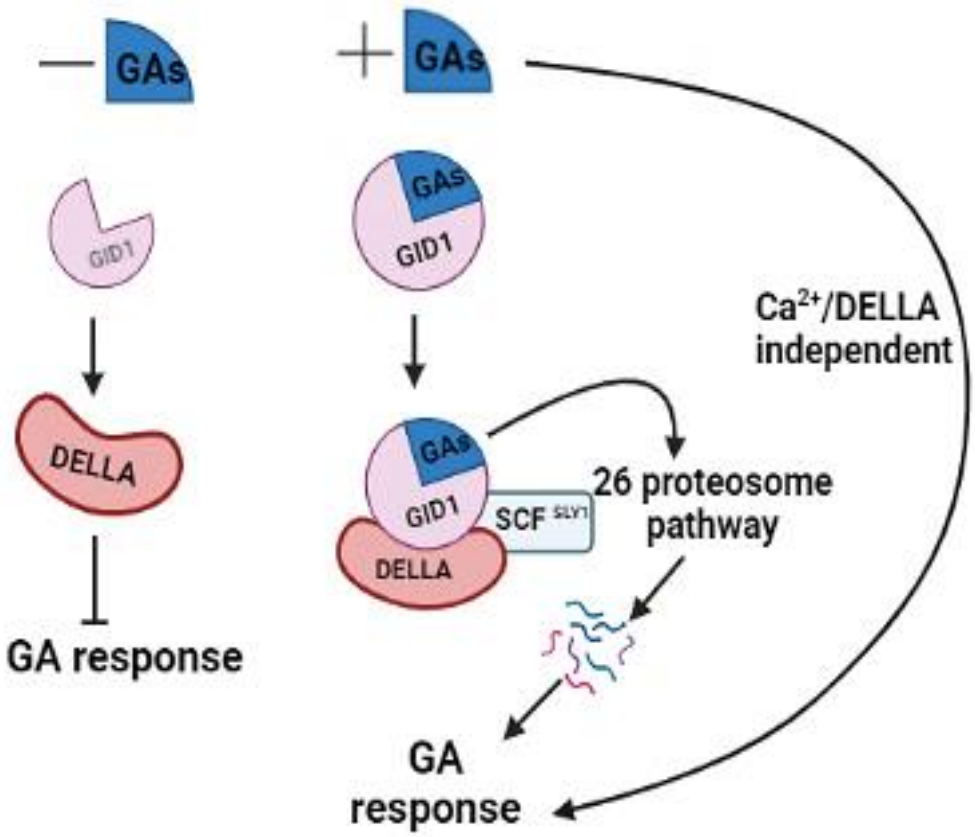

Figure 1.8 GA signalling components towards GA responses in plants. **(A)** In the absence of GA, GID1 receptor remains free and unable to act on DELLA proteins. Active DELLAs repress most of the GA responses. **(B)** In the presence of GA, GID1-GA complex can bind to the DELLA and cause conformational changes that enhance SCF^{SLY1} binding to the GID1-GA-DELLA complex. This then degrade DELLAs via 26-ubiquitin-proteosome pathway and release the negative pressure on any DELLA-dependent GA response. Line arrows for positive regulation and barred lines for negative regulation. Image "Created with Biorender.com".

1.5 Light mediated regulation of stomatal aperture

Stomata open in response to light to facilitate gas exchange to support photosynthesis. Light is one of the key external signals not only for photosynthesis but also for almost every aspect of a plant's physiology and development. To accurately determine light from their surrounding environment, plants have evolved five major classes of photoreceptors. Photoreceptors in Arabidopsis include: Phytochromes (phyA-E) perceive red/far-red light (600–750 nm); Cryptochromes (CRY1 and CRY2), Phototropins (PHOT1 and PHOT2), F-box containing Flavin binding proteins (e.g., ZEITLUPE, FKF1/LKP2) for blue/UV-A light (320–500 nm); and UVR8 for UV-B light (280–320 nm) (Bae & Choi, 2008). Stomatal aperture is regulated by diurnal changes in light quality and intensity as in general, stomata remain open under daylight and close at night in C3 and C4 species whereas CAM (crassulacean acid metabolism) species show the opposite response (Cockburn, 1983). Also, unpredictable changes in the quality of light throughout the day and stages of life impact stomatal dynamic response and diurnal behaviour (Matthews et al., 2020).

Stomatal opening responses to light is discussed under two distinct pathways: the red light (RL) or photosynthesis response and the GC-specific blue light (BL) response (Zeiger, 1983; Assmann & Shimazaki, 1999; Shimazaki et al., 2007; Doi et al., 2015; Inoue & Kinoshita, 2017). All the components required for BL induced stomatal opening response are reported to be localised in the GCs themselves with no direct involvement of photosynthesis or a mesophyll signal (Kinoshita & Shimazaki, 2001; Ueno et al., 2005; Hayashi et al., 2011; Ando & Kinoshita, 2018). However, recently two kinases, CONVERGENCE OF BLUE LIGHT AND CO_2 (CBC1 and CBC2), were identified as linking BL responses (via phototropins) to low [CO_2] found in the GC, suggesting an indirect involvement of photosynthesis (Hiyama et al., 2017). CBC1/CBC2 also negatively regulate stomatal opening through inactivating H^+-ATPase suggesting that they have dual roles in stomatal movement (Hayashi et al., 2020).

In response to BL, PHOT1 and PHOT2 undergo auto phosphorylation and initiate a downstream signalling cascade for stomatal opening (Kinoshita & Shimazaki, 2001; Christie, 2007; Shimazaki et al., 2007; Inoue & Kinoshita, 2017). BLUE LIGHT SIGNALLING 1 (BLUS1) is directly phosphorylated by the activated PHOTs (Takemiya

et al., 2013) and further activates PM H^+-ATPase in GCs via phosphorylation (Hayashi et al., 2011; Shimazaki et al., 2007). At the same time activated PHOTs phosphorylate CBC1/2 to inactivate downstream SLAC1 (Hiyama et al., 2017). These results in hyperpolarization of the membrane potential with simultaneous apoplast acidification and K^+ uptake through K_{in} channels directing stomatal opening (Kwak et al., 2001). In addition to PHOTs, CRY1 and CRY2 function additively to mediate BL induced stomatal opening. Both CRY and PHOT signalling pathways acts upstream of the COP1 (Constitutively Photomorphogenic 1)-SPA (SUPPRESSOR OF PHYA-105) E3 ligase complex. COP1-SPA is a master negative regulator of light signalling pathway and known to repress stomatal opening in darkness (Mao et al., 2005). COP1-SPA acts through ubiquitylation and targeted degradation of several positive light signalling factors including HY5 (LONG HYPOCOTYL 5), HYH (HY5-HOMOLOG), LAF1 (LONG AFTER FAR-RED LIGHT1), HFR1 (LONG HYPOCOTYL IN FAR-RED1) and others (Lau & Deng, 2012). In regard of stomatal aperture control, the downstream targets for COP1 degradation are not exactly known. However, reports on COP1 function to degrade microtubule function through the 26S proteasome pathway as well as its requirement for normal S-type anion channels activation indicate likely components of the stomatal closure mechanism (Khanna et al., 2014).

Unlike BL photoreceptors, RL response in GCs is not directly mediated by phytochromes. There are two opinions regarding RL induced stomatal response. Firstly, that the RL induced stomatal opening may result from GC responses to reduced Ci due to photosynthetic demand from both the mesophyll and GC chloroplasts (Roelfsema et al., 2002; Mott, 2009; Ando & Kinoshita, 2018). In addition, a component of the low CO_2 signalling network, HT1 regulates the RL-induced stomatal opening, providing further support for this Ci based hypothesis (Hashimoto et al., 2006; Matrosova et al., 2015). However, the second argument suggests that phytochromes are direct sensors of RL regardless of any change in Ci. Under constant Ci, g_s increased in response to RL questioning the sole role of Ci (Messinger et al., 2006; Lawson et al., 2008; Wang & Song, 2008). Furthermore, alteration of several enzymes associated with electron transport or the Calvin cycle leading to reduced photosynthetic rates demonstrated that stomata open in response to light regardless of the higher Ci values (Von Caemmerer et al., 2004; Baroli et al., 2008; Lawson et al., 2008). Several studies have suggested that an unidentified signal originating in the

mesophyll might potentially be sensed by GCs to drive stomatal responses (reviewed in Matthews et al., 2020).

phyB acts in concert with phyA, CRYs and PHOTs via MYB60, a R2R3-MYB gene of *Arabidopsis*, to regulate stomatal opening under white light (Wang et al., 2010; Chen et al., 2012). *phyBcop1* double mutant analysis revealed that phyB acts additively with COP1 to mediate stomatal aperture changes. In addition, stomata of the *pif3pif4* (PHYTOCHROME INTERACTING FACTORS) mutant opened wider than those of the wild type, suggesting that they may act downstream of phyB in regulating stomatal opening (Wang et al., 2010). In the absence of red light, blue light is very inefficient in inducing stomatal opening (Ogawa et al., 1978; Karlsson, 1986; Kinoshita et al., 2001; Mao et al., 2005). Also, an increase in g_s rate was reported when blue light was applied to a background of red light compared with red alone (Shimazaki et al., 2007). Thus, this indicates independent as well as synergistic behaviour of the two light signals towards stomatal aperture regulation. The common functional regulation between different photoreceptors involves inactivation of negative regulators of photomorphogenesis, including translocation of COP1 from the nucleus to the cytoplasm, destabilization of the COP1-SPA complexes and phosphorylation and subsequent degradation of PIFs. BL and RL signaling pathways converge on the phosphorylation and activation of PM H^+-ATPases, resulting in proton extrusion, K^+ uptake, water influx into GCs and consequent stomatal opening (reviewed in Matthews et al., 2020). A summary of these interactions is shown in a diagram (Figure 1.9).

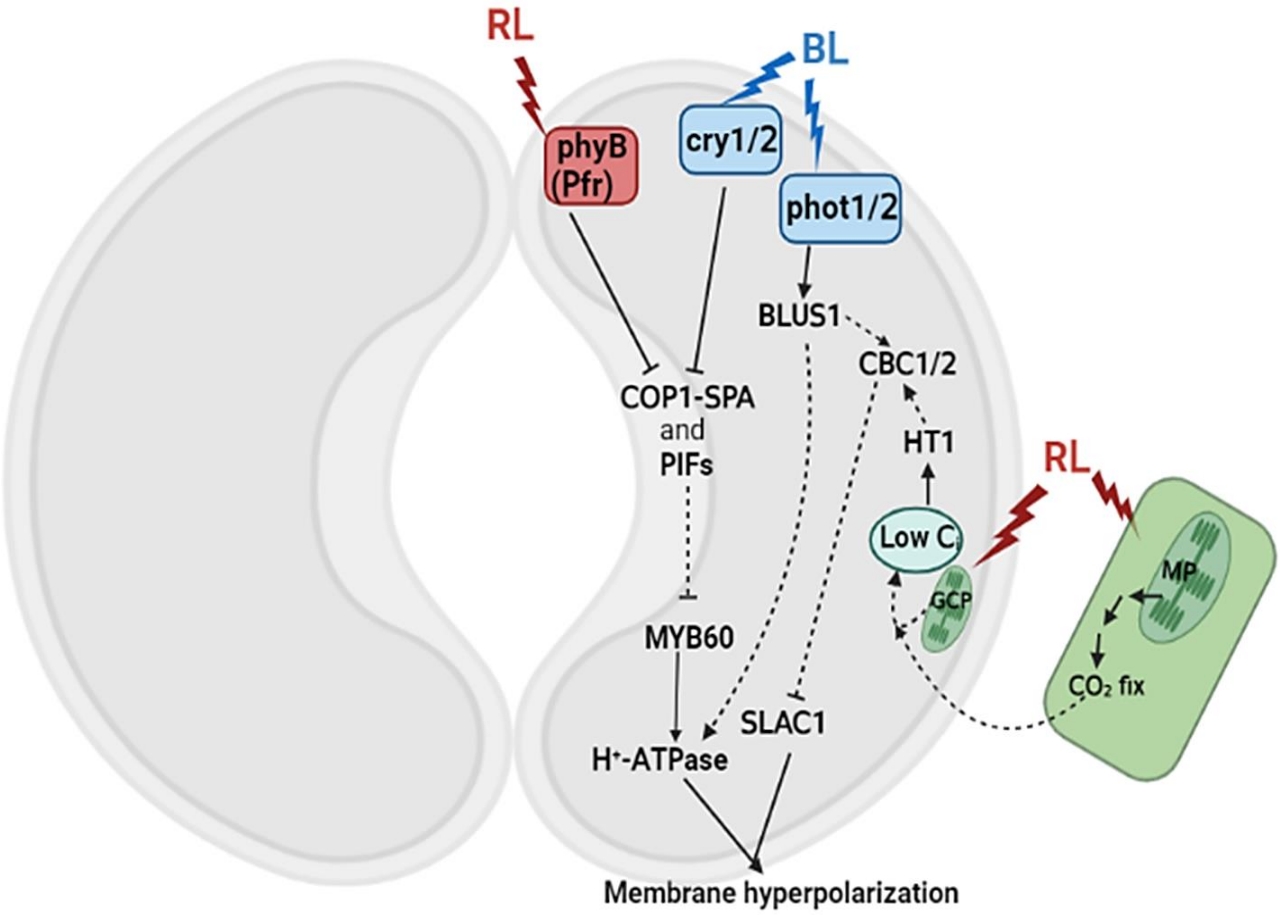

Figure 1.9 Light mediated regulation of stomatal opening response. Both RL and BL activated photoreceptors (phyB and CRYs) mediate stomatal function by inhibiting COP1-SPA and PIFs. These photomorphogenesis repressors may down regulate the transcription factor MYB60, which is required for stomatal movement regulation via H^+-ATPase activation. PHOTs regulate aperture via BLUS1 and CBC1/2 to activate and inactivate ion channels respectively. Additionally, RL induced photosynthesis results in a reduction in leaf [CO_2] leading to activation of HT1, which activates CBC1/2 to inactivate SLAC1. Line arrows are for direct positive regulation, bar lines for negative regulation, dashed arrows and dashed bar lines indicate positive and negative regulation respectively. Here GCP=guard cell protoplast, MP=mesophyll protoplast. Image "Created with Biorender.com".

1.6 Role of phyB, hormones and CO_2 in stomatal aperture responses

Among the phytochromes, phyB acts as the key photoreceptor for photomorphogenesis responses under high light (Casal et al., 2014). phyB appeared to be the most abundant phytochrome in seedlings grown at constant light as observed from immunoblotting where the ratio of PHYA, PHYB, PHYC, PHYD and PHYE was 5:40:15:15:25 (Sharrock & Clack, 2002). Studies showed that phyB is dominant in both the local and light-mediated systematic control of stomata development (Boccalandro et al., 2009; Casson et al., 2009; Casson & Hetherington, 2010). The role of phyB in response to RL mediated stomatal opening has already discussed in section 1.5 (Figure 1.9). *phyB* mutants were found to have increased ABA levels but conversely, *phyB* stomatal sensitivity to exogenous ABA was diminished compared to WT controls suggesting a role for phyB in regulating ABA responses (González et al., 2012). Recently, the interaction between OST1 and phyB provided evidence of crosstalk between ABA and phyB to negatively regulate RL induced stomatal opening response (Li et al., 2021). Light regulation of GA and ABA homeostasis during seed germination is broadly studied (Casal & Sánchez, 1998; Seo et al., 2009). For instance, light activated phyB inhibits expression of the MYB transcription factors *REVEILLE1/2*, which are the negative regulators of the GA biosynthesis gene *GA3ox2*; this relieves repression on GA biosynthesis and promotes germination (Jiang et al., 2016). Light activated phyB is also reported to either positively or negatively regulate GA metabolism at later stages of development such as hypocotyl growth and petiole elongation (Achard et al., 2007; De Lucas et al., 2008; Küpers et al., 2023). There is also evidence on a role of GA to modulate ABA-induced inhibition of stomatal opening in light (Göring et al., 1990; Goh et al., 2009).

It has been well established that low C_i stimulates stomatal opening, while high C_i induces stomatal closure (Mott, 1988; Mott, 1990). In this case, CBC1/2 is a good example of convergence between blue light and CO_2 signalling pathways likewise the dual functions of [CO_2], i.e., low [CO_2] promotes stomatal opening while high [CO_2] inhibits stomatal opening (Yang et al., 2020). Though a change in the C_i might act as a mesophyll-to-GC transmissible signal for RL-mediated stomatal behaviour, no signalling component converging the two stimuli downstream to phyB has reported.

Investigation involving interaction between phyB and phytohormones specifically ABA and GA towards e[CO_2]-mediated stomatal response might provide new insight to better handle stomatal physiology and crop production.

1.7 Involvement of rice phyB towards e[CO_2]-mediated response

Cereal grasses provide most of the global nutrition and rice fed more people than any other important cereal crops like wheat, barley, and maize (Mohapatra & Sahu, 2022). Global rice consumption is estimated to increase from 480 million tons in 2014 to nearly 550 million tons in 2030 (Yuan et al., 2021). Therefore, better rice yield is crucial to ensure food security and climate change is likely to be a constraining factor based on experimental and modelled projections of rice production (Peng et al., 2004; Krishnan et al., 2007; Wassmann, Jagadish, Heuer, et al., 2009; Wassmann, Jagadish, Sumfleth, et al., 2009). e[CO_2] and increases in temperature are two key determinants of climate change that have opposing effects on rice growth and performance (Muehe et al., 2019). Consequently, water scarcity is posing a greater threat to rice yield as rice cultivation is primarily based on irrigated lowland rice systems in warm and temperate regions of Asia, Africa, and Latin America (Rao et al., 2017). Existing literature evidences a complex effect of e[CO_2] towards rice production. For example, meta-analyses based on free air CO_2 enrichment (FACE) platforms denote increasing [CO_2] and temperature accompanied by low N supply are likely to deteriorate rice production and varied with cultivars (Lv et al., 2020; Hu et al., 2022).

As a grass species, rice features dumbbell-shaped GCs flanked by two paracytic subsidiary cells (SCs) arranged in parallel rows within epidermal cell files and exhibit more efficient and faster stomatal regulation compared to kidney shaped GCs (Merilo et al., 2014; McAusland et al., 2016; Haworth et al., 2018). In rice, faster stomatal movement is associated with the reciprocal responses of GCs and SCs during stomatal opening and closing response, a reduced ratio of internal volume to surface area due to dumbbell shape and, variable GC wall thickness and composition compared to their kidney-shaped counterparts (McKown & Bergmann, 2018) (Figure 1.10).

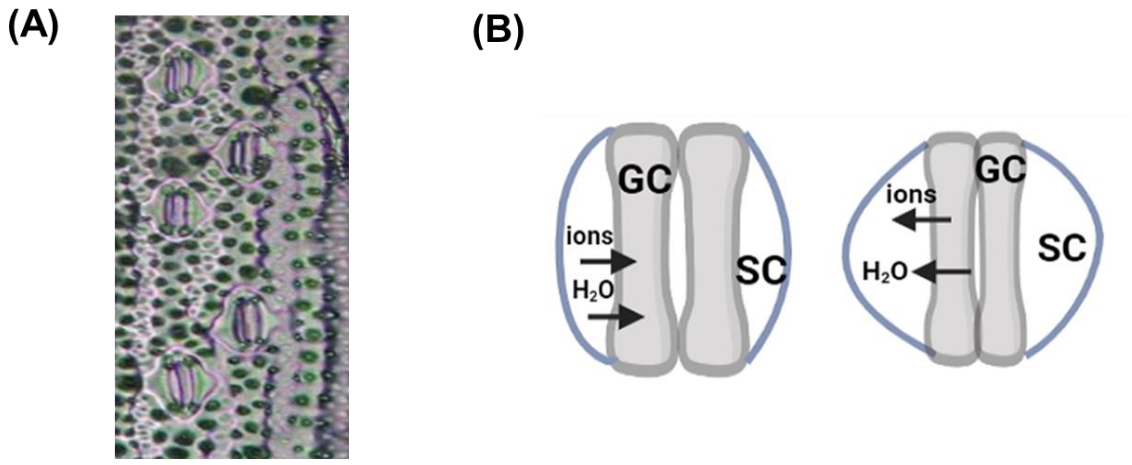

Figure 1.10 Rice stomata complex with pair of dumbbell shaped GCs surrounds by SCs. (A) Rice epidermal impression showing files containing stomatal complex**. (B)** During stomatal opening ions and water entered from SCs to increase turgor pressure. Stomatal closure involves efflux of ions and water from GC to adjacent SCs. Image "Created with Biorender.com".

Although stomatal morphology and patterning are different between Arabidopsis and rice, several components of the molecular pathway regulating stomatal development are common with some level of functional divergence (Liu et al., 2009; Raissig et al., 2016, 2017; Wu et al., 2019). Alteration of stomatal properties including stomatal density and aperture through genetic engineering have demonstrated improved drought tolerance and/or enhanced water-use efficiency in rice (WUE) (Huang et al., 2009; Hepworth et al., 2015; Hu et al., 2017; Li et al., 2017;Caine et al., 2019). Therefore, stomatal-based research in rice has potential to maintain and enhance rice productivity with current climate change scenarios.

Like Arabidopsis, rice phytochromes are the sole receptors for Red (R) and far-red light (FR) and mediate most of the photomorphogenic responses (Takano et al., 2009). The rice phytochrome gene family has three members, phyA, phyB, and phyC (Kay et al., 1989; Dehesh et al., 1991; Tahir et al. 1998; Basu et al., 2000). phyB is evolutionarily conserved with high protein sequence identity and mode of action between Arabidopsis and rice (Dehesh et al., 1991). Studies showed phyB-mediated

light signals modulate stomatal development in Arabidopsis (Boccalandro et al., 2009; Casson et al., 2009). However, phyB is reported not to regulate the expression of genes related to stomatal development in rice. At the same time, reduced leaf area and reduced transpiration because of lower stomatal density per unit leaf area in rice *phyB* showed improve drought tolerance (Liu et al., 2012). Thus, phyB renders an important role via stomatal manipulation towards rice production. However, their involvement towards e[CO_2]-mediated response remains unexplored.

1.8 Research aims and objectives

The primary aims of the project were:

(1) Investigate the role of gibberellins in regulating stomatal responses to e[CO_2].

(2) Investigate the role of phyB in regulating stomatal responses to e[CO_2].

To address the research aims the following objectives were outlined:

(1) Analyse stomatal aperture responses to changes in [CO_2] in the presence of GA and GA biosynthesis inhibitors.

(2) Take a genetic approach to dissect the role of GA in stomatal responses to [CO_2].

(3) Measure GA and ABA levels in leaves under different [CO_2].

(4) Examine the expression of key genes in hormone metabolism and signalling under different [CO_2].

(5) Analyse the response of phyB mutants in both Arabidopsis and rice under different [CO_2].

Collectively, this thesis is testing the hypothesis that [CO_2] in part acts through GA to modulate GC sensitivity to ABA (Figure 1.11).

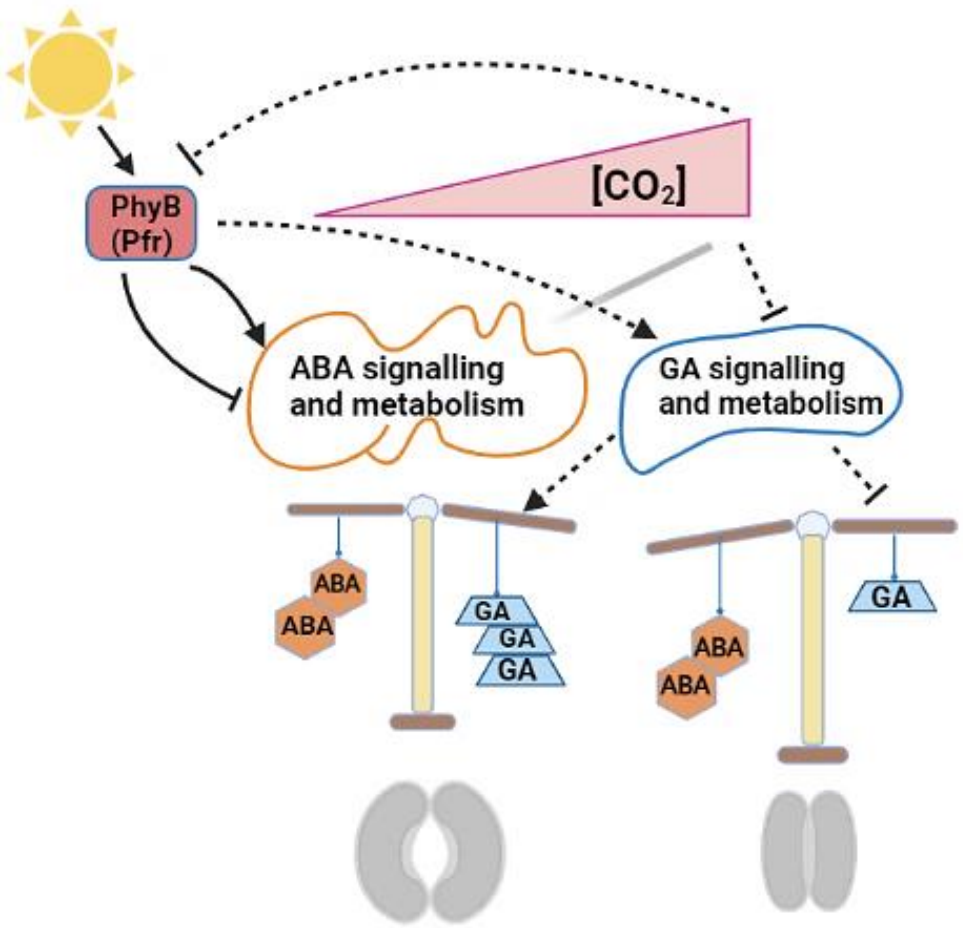

Figure 1.11 Conceptual events showing the hypotheses tested during the present study. e[CO_2] might regulate GA signalling and metabolism but not ABA directly and through changes in GA modulates GC sensitivity to ABA. At the same time, signals from light perceived by phyB may positively regulate GA signalling and metabolism while it has dual role on ABA metabolism during different stages of plant development. Thus, e[CO_2]-mediated stomatal closure might act via phyB dependent or independent way. Line arrows are for direct positive regulation, bar lines for negative regulation, dashed arrows and dashed bar lines indicate hypothetical positive and negative regulation respectively, fade line directs controversial involvement. Image "Created with Biorender.com".

Chapter 2. Materials and Methods

2.1 Materials

2.1.1 Plant materials

Arabidopsis and rice seed lines used to carry out different experiments during the project are presented in tables 2.1 and 2.2 respectively. Representative images of mature plants of each of the lines of Arabidopsis and rice are provided in supplementary (Supplementary 2.1 and 2.2).

2.1.2 General laboratory chemicals

All chemicals used during the present study were purchased from Sigma Aldrich or Fisher Scientific unless stated otherwise.

2.2 Plant growth conditions

2.2.1 Growth conditions for Arabidopsis

Depending on the experimental design, plants were grown and maintained in either tissue culture or compost. To grow and maintain Arabidopsis plants in compost, F2+Sand Levington®, Everris Professional compost was used. For both tissue culture and compost grown plants, seeds were stratified at 4°C for 2-3 days in the dark and then transferred to growth chambers Sanyo-Gallenkamp SGC970/P/PLL. Optimum plant growth conditions were: 11h photoperiod, relative humidity 65%, 22°C constant temperature and [CO_2] set as ambient ~450ppm with additive CO_2 (A[CO_2]). Light irradiance in the chambers was maintained at photosynthetically active radiation (PAR) 150±20 $\mu molm^{-2}s^{-1}$ and occasionally measured using a light meter (Apogee Model MQ-200 Quantum meter). High [CO_2] was achieved in one of the chambers using an additive [CO_2] injection to achieve 1000 ppm according to experimental requirements and noted as E[CO_2].

To carry out gene expression experiments plants were grown in the same chambers and same conditions as above. However, photoperiod length was 12h and temperature was set as 20/16°C (day/night)

Table 2.1 Arabidopsis seed lines used during the present study.

Name	Ecotype/Allele	Reference
Col-0	Columbia-0	Casson Laboratory stocks.
Ler	Landsberg erecta	Casson Laboratory stocks.
Ws-2	Wassilewskija	Casson Laboratory stocks.
pUBQ-XVE-GA20ox1-P2A-GA3ox1	Columbia-0	(Rizza et al. 2021)
ga2oxquintuple (ga2oxq)	Col-0/*ga2ox1-1*(WiscDsLox_333C08), *ga2ox2-1*(SALK_051749), *ga2ox3-1*(SALK_042818), *ga2ox4-1* (SALK_036923) and *ga2ox6-2* (SM_3_1859)	(Rieu et al., 2008)
dellaquintuple (dellaq)	Ler/ *gai-t6*, *rga-t2*, *rgl1-1*, *rgl2-1*, and *rgl3-4*	(Koini et al., 2009)
35STAP_RGAΔ17	Ler/TAP tagged RGAΔ17	(Feng et al., 2008)
35STAP_GAIΔ17	Ler/TAP tagged GAIΔ17	(Feng et al., 2008)
hpca1	Col-0/ SAIL_71_C11	(Wu et al., 2020)
phyB-9	Col-0/*phyB-9* (NASC_N6217)	(Reed et al., 1993)
***PHYBproPHYB:YFP* (*phyB*comp)**	*PHYBproPHYB:YFP* complemented in *phyB-9*	Unpublished and a gift from S. Casson.
phyB-9nced3nced5	Col-0/ *phyB-9* (NASC_N6217), *nced3-2* (GK_129B08), *nced5-2* (GK_328D05) and *nced5-3* (GK_380E07)	Present study
rve1	Col-0/reveille1 (SALK_025754C)	(Alonso et al., 2003)
rve2	Col-0/reveille2 (SALK_051842C)	(Alonso et al., 2003)
rve1rve2	Col-0/reveille1 (SALK_025754C), Col-0/reveille2 (SALK_051842C)	Present study.
RVE1OE	Col-0/ reveille1 (SALK_025754C)	Present study.
cca1lhy	Ws-2/*cca1-11*, Ws-2/*lhy-21*(NASC_N9862)	(Ding et al., 2007)

Seeds stocks were obtained from Eurasian Arabidopsis Stock Centre (Scholl et al., 2000) and accession number are indicated within first bracket.

Table 2.2 Rice seed lines used during the present study.

Name	Ecotype/Allele	Reference
NB	Nipponbare	Donated by Tinashe Mowdza.
OsphyB	*OsphyB-1*	(Takano et al., 2005)
OsphyB	*OsphyB-2*	(Takano et al., 2005)

2.2.2 Growth conditions for rice

Rice seeds were placed in sealed transparent magenta pots containing reversed osmosis (RO) water (water purified by reverse osmosis system) at ~1 cm level and were kept in a Sanyo growth chamber (12h photoperiod, day/night temperature 26°C/ 24°C, 200 $\mu molm^{-2}s^{-1}$ PAR) for germination. After 7 to 10 days seedlings were transferred to pots with soil saturated with water. Soil mix consisted of 71% sterilised Kettering loam (Boughton), 23.5% John Innes No. 3 compost, 5% sand and 0.5% Osmocote extract standard slow-release fertilizer (v/v). For all the rice experiments, plants were grown in 16 cm pots except the thermal imaging experiment where the plants were grown in pots of 12cm. After transplanting, plants were grown in controlled environment growth cabinets PGR15 Conviron (Controlled Environments Ltd, Winnipeg, MB, Canada) under optimal conditions for rice, unless stated otherwise. The optimum conditions for rice were: 12h photoperiod, irradiance set at 600 $\mu molm^{-2}s^{-1}$ PAR, relative humidity 60%, day/night temperature 30°C/24°C and [CO_2] set as ambient ~450ppm (A[CO_2]). Valoya NS1 broad spectrum LEDs with far-red diodes were used to maintain irradiance. Experiences from rice fields represented 100 and 700 $\mu mol\ m^{-2}\ s^{-1}$ 24 h as the low and high range of light intensities (De Datta, 1981; Huang et al. 2013). Therefore, 600 $\mu molm^{-2}s^{-1}$ PAR was used as optimum light intensity during the present study. High [CO_2] was achieved at 1000 ppm (E[CO_2]) in one of the chambers using an additive [CO_2] injection according to experimental requirements.

Plant pots were kept in trays with a constant supply of water to the pot base and were also watered from the top twice a week. From the 5th growth week, plants were fertilized in intervals of two weeks with Chempak High Nitrogen Feed No. 2. Flag leaves were considered for every measurement taken except for thermal imaging

experiment since they are photosynthetically more active than other leaves in mature rice plants (Adachi et al., 2017).

2.3 Genetic transformation

2.3.1 Generation of RVE1 overexpression line

Arabidopsis *RVE1* overexpression lines (*RVE1OE*) were developed through floral dip transformation (Bent, 2006) using Agrobacterium transformed with the binary vector pMDC32 containing a 35S::RVE1 construct using cDNA of *RVE1* (Weigel & Glazebrook, 2006). The cloned vector was kindly provided by Dr Nicholas Zoulias. Seeds from the T1 generation were selected on four combinations of GA_3 and hygromycin (selection marker, Hyg) since high expression of RVE1 affected the germination. The media combinations were as follows with ½ MS media: 50µM GA_3+25mg/ml Hyg; 50µM GA_3+50mg/ml Hyg; 100µM GA_3+25mg/ml Hyg and 100µM GA_3+50mg/ml Hyg. 12 lines were selected that appeared resistant across the 4 combinations of media (Supplementary 2.3) and T2 generation was developed from each of the 12 lines. Seeds from T2 generation was further screened on the following media based on their delayed germination percentage: ½ MS media, ½ MS media+100µM GA_3 and ½ MS media+100µM GA_3+25mg/ml hygromycin. Putative RVE1OE lines were isolated from their delayed germination response (Supplementary 2.4) and were further confirmed using higher gene expression compared to wild line via qPCR analysis (Supplementary 2.5).

2.3.2 Seed sterilisation

Seeds were always sterilised before growing them in tissue culture media. Seeds were dehydrated for 3-5 minutes at room-temperature in 70% ethanol. The 70% ethanol was then aspirated, and the seeds were then incubated in 1% sodium hydrochlorite and 0.1% Tween-20 for 20 minutes with agitation. Seeds were then washed five to six times with autoclaved RO H_2O inside a laminar flow hood.

2.3.3 Tissue culture media

To prepare ½ MS media 2.2 g/L MS media (Sigma AldrichI, M5519-50L) was added and mixed properly into 800ml RO H_2O. The pH of the solution was adjusted to 5.7 using 1M KOH and made the volume up to 1L. To solidify the media, Plant Agar (Duchefa Biochemie, 1100 g/cm^2, P1001) was added (1.2% w/v) into a Duran bottle containing the media. To sterilize, media was autoclaved at 121°C for 30 minutes. Where plant tissue culture media (here ½ MS media) was supplemented with hormones or chemicals, these were filter sterilized (0.2µm pore sized filter) and added to autoclaved media prior to pouring into petri dishes at the required concentrations.

2.4 Mutants generation

2.4.1 Generation of double mutant

To develop an *rve1rve2* double mutant, a cross was made between *rve1* as acceptor and *rve2* as donor (Table 2.1). Double mutants were identified by genotyping individual F2 seedlings for wild-type loci and T-DNA insertions within both genes (method discussed in section 2.5; supplementary 2.7).

2.4.2 Generation of triple mutant

To develop a triple mutant, *phyB-9* was crossed with the *nced3nced5* double mutant where the single mutant was the acceptor, and the double mutant was the donor. F2 progeny were first screene based on the *phyB-9* phenotype and then genotyped for T-DNA insertions within *NCED3* and *NCED5* (method discussed in section 2.5; supplementary 2.9). Putative *phyBnced3nced5* triple mutants were confirmed for the *phyB-9* mutation by Sanger sequencing.

2.5 Plant genotyping

Genotyping was carried out to confirm different mutant lines that were developed and used during the study on regular basis. The genotyping protocol used three sets of PCR primers; forward primer, reverse primer and T-DNA left border primer (LBa1).

Forward primer and reverse primer were specifically designed for the gene of interest whereas forward primer and LBa1 were used to identify TDNA insertion (Figure 2.1).

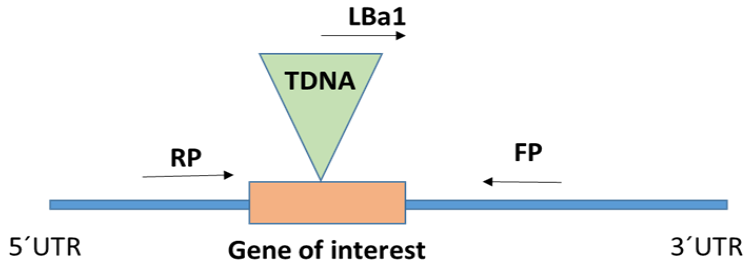

Figure 2.1 Genotyping protocol. Diagrammatic representation of genotyping protocol where forward primer = FR, reverse primer = RP, T-DNA left border primer = LBa1.

2.5.1 Genomic DNA extraction

A leaf disc (approximately 1 cm diameter) or several young seedlings were ground in 400 µl Edward's Extraction Buffer (200 mM Tris-HCl (pH 7.5), 250 mM NaCl, 25 mM EDTA, 0.5% SDS) using a micro pestle and centrifuged at 13500 rpm for 5-10 minutes. The supernatant was transferred to another 1.5 ml Eppendorf containing 400 µl of isopropanol (Fisher Scientific Laboratory Grade Propan-2-ol, 1067432) and the sample was mixed gently and centrifuged at 13500 rpm for 5-10 minutes to pellet nucleic acids. The supernatant was discarded without disturbing the pellet, re-centrifuged at 13500 rpm for 2 minutes and any remaining supernatant was aspirated. Then the pellet was air dried for 15 minutes and then reconstituted in 50 µl of sterile RO H_2O and swirled to mix and stored at -20°C (Edwards et al., 1991).

2.5.2 Polymerase Chain Reaction (PCR)

PCR has been adapted from ThermoScientific™ DreamTaq™ Green PCR master mix (2X) which is a ready-to-use solution containing DreamTaq DNA polymerase, optimized DreamTaq Green buffer, $MgCl_2$ and dNTPs. Each PCR reaction included autoclaved RO H_2O, forward and reverse primers (100µM stocks) and ThermoScientific™ DreamTaq™ Green PCR master mix (2X) as shown in Table 2.3.

Table 2.3 Components and volumes required for PCR analysis.

25µl Reaction (2X)	
Component	**Volume/Reaction (µl)**
Primer A (100pmol/µl)	0.5
Primer B (100pmol/µl)	0.5
Sterile H_2O	9.5
DreamTaq Green PCR Master Mix (2X)	12.5

23 µl of thus master mix was pipetted into each PCR tube (0.2 ml). 2 µl of template DNA was pipetted into each tube, mixed, and briefly centrifuged to spin down the contents and eliminate air bubbles. Samples were loaded into the thermal cycler using the set-up shown in table 2.4. Reaction volume was set to 25 µl for 35 cycles. Products were analyzed by agarose gel electrophoresis using a 1% agarose gel.

Table 2.4 Thermal profile, incubation temperature and times for PCR are listed below.

Conditions	**Step 1**	**Step 2**	**Step 3**	**Step 4**	**Step 5**	**Step 6**	**Step 7**
Temperature (°C)	95	95	55	72	Repeat Steps 2-4	72	12
Time	3 min	30 sec	30 sec	1 min	for 35 cycles	5 min	∞

2.5.3 Gel electrophoresis

DNA and PCR products were visualized using a GelDoc-It™ system using VisionWorks® LS analysis software (UVP LLC) following agarose gel electrophoresis. 1% Agarose (Sigma Agarose Gelpowder) was mixed with 1X TAE Buffer (1X TAE: 200 ml 50X TAE stock, 9.8 L RO H_2O). 50X TAE buffer was prepared as: 242 g Tris Base, 57.1 ml glacial acetic acid, and 100 ml 0.5 M EDTA adjust to 1 L with RO H_2O. The agarose powder was mixed into 1X TAE buffer and microwaved for 2 minutes to dissolve. Then the solution was kept for 5-10 minutes in room temperature to cool

down and 1 drop (~5ul) of ethidium bromide was added (10 mg/ml, Alfa Aesar), which act as a fluorescent indicator. The liquid solution was poured into a transparent gel tray fitted with a comb to create wells. The gel was submerged in 1X TAE buffer. Where required, 6X loading buffer (0.2% w/v bromophenol blue, 50% v/v glycerol) was added to samples up to a total volume to 10-15 µl and mixed well using pipette. Samples were loaded in to each well, as well as a DNA ladder (2.5 µl GeneRuler, DNA Ladder Mix ready-to-use 0.1 µg/L, 50 µg) to determine DNA fragment sizes. Gels were run at 120 V for 30 minutes using a BioRad mini sub-cell and power supply.

2.6 Gene expression analysis

2.6.1 RNA extraction and quantification

The protocol followed is in accordance with the Quick-RNA™ MiniPrep kit (Zymo Research, Cambridge Biosciences R1055a). RNA extraction also included a DNase treatment to remove contaminating genomic DNA. RNA concentrations were measured at 595 nm using the 'Nucleic Acid', 'RNA-40' option on the NANODROP-8000 Spectrophotometer V1.1 (ThermoScientific). RNase-free H_2O was used as a blank, 2 µl of blanking buffer and extracts were loaded on to the reading pin.

2.6.2 RNA visualization

To visualize extracted RNA quality 1% Agarose (Sigma Agarose Gelpowder) was mixed with 0.5X TBE Buffer (0.5X TBE: 20 ml 5X TBE stock, 800 ml RO H_2O). 5X TBE buffer was prepared as: 54 g of Tris base, 27.5 g boric acid and 20 mL of 0.5 M EDTA (pH 8.0) adjust to 1 L with RO H_2O. Instead of usual DNA loading dye TnTrack 6X loading dye was added to samples up to a total volume of 10-15 µl and mixed well before loading into individual wells. Other steps were like DNA gel electrophoresis as in 2.5.3 except that gels were run at 100V for 30 minutes.

2.6.3 cDNA Synthesis

For cDNA synthesis, a protocol was adapted from the Applied Biosystems High-Capacity cDNA Reverse Transcription Kit. The protocol was conducted using up to 2µg of total RNA per 20µl reaction and included an RNase inhibitor (RiboLock, Fisher

Scientific, 10859710). Using the table provided in the protocol manual, the volumes of each component needed to prepare the master mix were calculated in accordance the number of reactions. The concentration of individual RNA samples was equalized such that 10µl of RNA equalled 2µg (or equivalent, depending on experiments, Table 2.5).

Table 2.5 Table showing the components and volumes required for cDNA synthesis.

Component	Volume/Reaction (µl)
Individual RNA sample (e.g. 2 µg)	**10.0**
10X RT Buffer	2.0
25X dNTP Mix (100mM)	0.8
10X RT Random Primers	2.0
MultiScribe™ Reverse Transcriptase	1.0
RNase Inhibitor	0.5
Nuclease-free H_2O	3.7
Total per Reaction	20.0

The prepared 2X RT master mix was placed on ice and mixed gently. 10 µl of 2X RT master mix was pipetted into each well of the reaction plate or individual tube. 10 µl (2 µg) of RNA sample was pipetted in to each well and the reaction plate or tubes were then sealed. The plate was briefly centrifuged to spin down the contents to eliminate any air bubbles. To perform reverse transcription, the thermal cycler was programmed with the following thermal profile (Table 2.6). Reactions were loaded into the thermal cycler and the reaction sample volume was set to 20 µl.

Table 2.6 Table showing thermal profile, incubation temperature and times, for cDNA synthesis.

	Step 1	Step 2	Step 3	Step 4
Temperature (°C)	25	37	85	4
Time	10	120	5	∞

2.6.4 qPCR Analysis

For qPCR analysis 10 µl of the cDNA (2.1.0) was diluted to 5 µg/ml for qPCR. The following protocol was adapted from Thermo Scientific Maxima SYBR Green/ ROX qPCR Master Mix (K0221) (Table 2.7).

Table 2.7 Components and reaction volumes required for qPCR analysis.

Component	Volume/Reaction (µl)
2X SYBR Green qPCR Mix	10
Primer Mix	1
Autoclaved H_2O	1.2
cDNA	5
$MgCl_2$ solution (25mM)	2.8
Total	20

The components when combined give a single reaction volume of 20 µl. 'Primer mix' refers to combined forward and reverse primers used to target a specific gene sequence where each primer concentration was 7.5 pmol/µl and 1 µl of this primer mix was used per 20 µl reaction. The house-keeping gene ubiquitin (*UBC21*) was used as reference gene to standardize expression across samples as this gene is expressed uniformly across different treatments. Reactions were performed using a BIO-RAD CFX Connect Real-Time System with BIO-RAD CFX Manager 3.1 software using the profile shown in Table 2.8.

Table 2.8 Thermal profile, incubation temperature and times for qPCR analysis.

	Step 1	Step 2	Step 3	Step 4	Step 5	Step 6	Step 7
Temperature (°C)	95	95	57	72	Repeat steps 2-4	95	65
Time	2 min	15 sec	15 sec	20 sec	for 39 cycles	10 sec	5 sec

Relative expression of target genes in the different samples was calculated from *UBC21* normalized target signals using the ΔΔCT method (Livak & Schmittgen, 2001). Product specificity was verified by running a dissociation curve. The dissociation curve was viewed for the entire plate to check for anomalies and to determine relative fold

change in gene expression (2-ΔcT). Using excel software, the following layout (Table 2.9) was used to interpret qPCR data.

Table 2.9 Excel layout to interpret qPCR data to determine the rate of expression of a sample relative to a control.

Sample	Threshold	Ct Value	Δ	Average Δ	ΔΔ	minus	2Ln

Ct refers to the number of cycles required for the fluorescence signal to surpass background expression levels (threshold). Ct values are inversely proportional to the amount of target nucleic acid present within the same sample. Delta (Δ) is the sample Ct value for the target gene minus the control Ct value (*UBC21*). Average delta (average Δ) is used to find the mean value between biological and technical replicates. Delta delta (ΔΔ) normalizes expression relative to a chosen calibrator sample, which is then inverted to produce the opposite sign, either positive or negative. 2Ln (natural log) is used to establish gene expression of the test sample relative to the calibrator sample; zero relative expression is shown as 1.

2.7 Stomatal functions bioassay with [CO_2]

Plants were grown at optimum growth condition as stated in 2.2.1 for approximately 31-36 days post germination. The abaxial epidermis was removed following tape-peel method to observe the stomatal function (Lawrence et al., 2018). According to the tape-peel method, a mature, fully expanded single leaf was attached to two pieces of clear Scotch tape (Sigma) with one piece adhering to the abaxial side. Using the index finger and thumb on each hand, the two pieces of tape were gently peeled apart and the abaxial epidermal peel was immediately floated, cuticle-side up in resting buffer [10 mM MES (pH 6.2)] in a petri dish. Epidermal peels were transferred to fresh small Petri dishes (5 cm) containing opening buffer [50mM KCl, 10 mM MES/KOH (pH 6.2)] and sealed using micropore tape (3 M; St Paul, MN, USA). These were then incubated for 2 hours in the light (~150±20 µmol m^{-2} s^{-1}) whilst [CO_2] free air was bubbled into the opening buffer. CO_2-free air was achieved by passing ambient air through a soda lime trap to remove [CO_2] levels from ambient (450-500 ppm) to [CO_2] free air (25±10

ppm). Such treatment brought about normalized stomatal opening across all the peels. After 2 hours of [CO_2] free treatment, peels were treated by bubbling into the opening buffer for another 2 hours with either [CO_2] free air, 450-500 ppm CO_2 (ambient lab air) or 1000ppm CO_2 (Stout, 1988; Webb & Hetherington, 1997) supplied from a pressurized cylinder containing CO_2 in air (BOC, Special Gasses, UK). From now onwards, the three [CO_2] treatments i.e., [CO_2] free air, ambient [CO_2] and 1000ppm [CO_2] will be mentioned as F[CO_2], A[CO_2] and E[CO_2] respectively. Since promotion of closure was determined at A[CO_2] and E[CO_2] treatments started from F[CO_2] treated normalized samples, comparison always made between F[CO_2] and A[CO_2] or F[CO_2] and E[CO_2]. The temperature was maintained by having the dishes suspended in a water tank at ~20˚ C throughout the 4 hours of incubation period. Any chemicals and hormones used as treatments during the bioassay was applied from the second two hours unless otherwise is stated and always maintained with mock treatment. To avoid any potential diurnal rhythmic effects on stomatal aperture, experiments were always started at the same time of the day starting around 2-2.5 hours after the onset of the light period.

Tapes containing peels were then mounted onto slides and visualised within 10-15 minutes post treatment using a Brunel SP300F microscope. Images were taken using a MotiCam Pro 252B camera operated by Micro-Manager 1.4 software. Single images were taken using 40X objective. A single image of a calibration slide (1 division = 0.01 mm) under the same set-up was used to calibrate images for counting. The major steps involved in stomatal function bioassay showed in a simplified diagram (Figure 2.2A).

In each experiment, 3 abaxial epidermal peels per treatment were taken where each peel was isolated from single leaves from three separate plants. A minimum of 40 stomata were measured from 3 peels and experiments were repeated over 3 consecutive days to give a total number of 120 stomata measurement per treatment.

Width and length measurements were taken using the line tool in the ObjectJ plugin in ImageJ software version 1.8.0_322 (Figure 2.2B). Stomatal aperture area or pore area (P area) was calculated using aperture width (A_W) and aperture length (A_L) measurements as the following equation:

P area = π * (0.5 * A_W) * (0.5 * A_L).

GC area was measured by subtracting the aperture area from the stomatal complex area. Stomatal complex area (SC) was calculated using the following equation.

SC area = π * (0.5 * SC_w) * (0.5 * SC_L).

So, GC area is as follows-

GC area = (π * (0.5 * SC_w) * (0.5 * SC_L) - π * (0.5 * A_w) * (0.5 * A_L)).

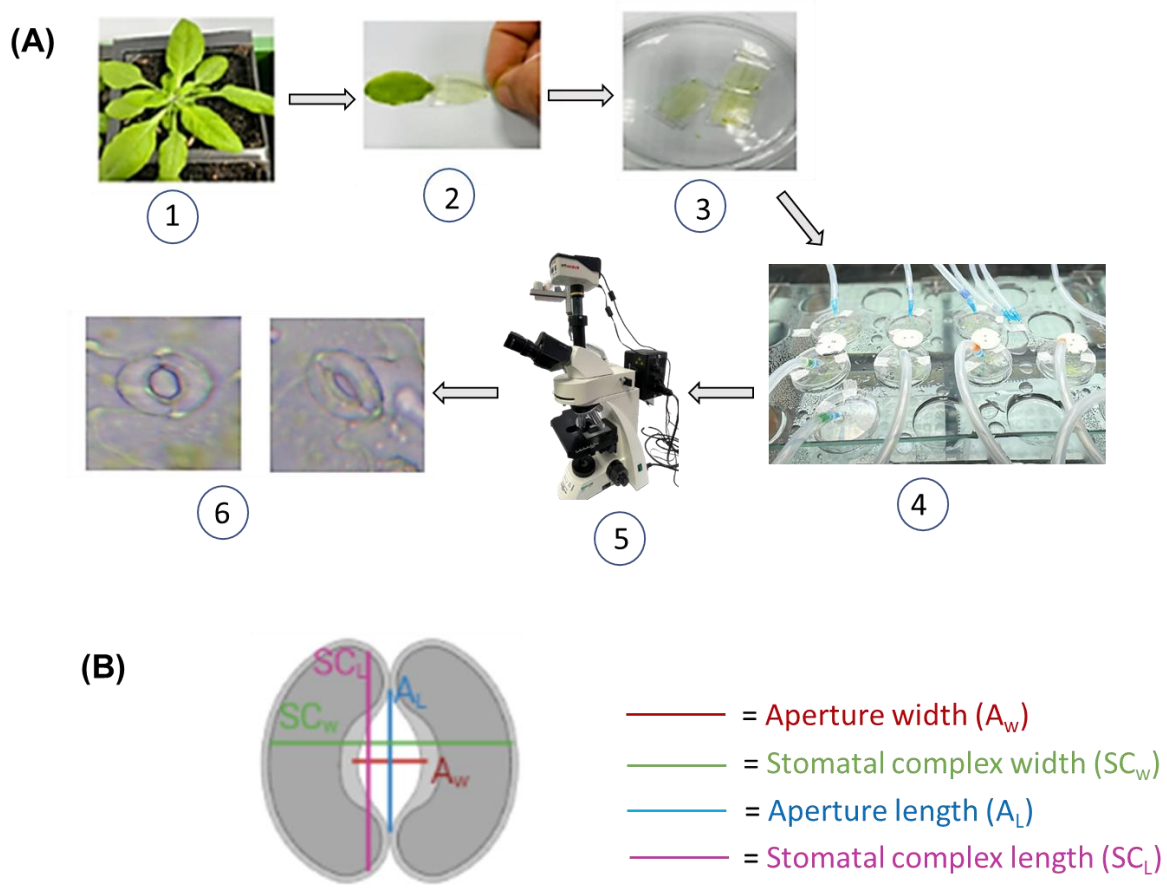

Figure 2.2 Stomatal functions bioassay. (A) Major steps in stomatal functions bioassay where (1) one mature leaf from each biological replicate was taken; (2) epidermal strip from abaxial surface was isolated using tape peel method, (3) collected in resting buffer followed by (4) incubation in opening buffer with treatment of interest inside the water tank. Then after 4 hours of treatment (5) using camera attached microscope (6) images were taken under 400X magnification. **(B)** Image of one representative stoma showing the line tool used in ImageJ to measure width and length of aperture and stomatal complex respectively. Image "Created with Biorender.com".

2.8 ROS (Reactive Oxygen Species) assay

To estimate ROS generation abaxial epidermal peels were prepared as described above in 2.7 and incubated in 50mM KCl, 10 mM MES/KOH (pH 6.2) at 20°C, in the light (~150±20 µmol $m^{-2}s^{-1}$) whilst being aerated with F[CO_2] air for 2h. They were then transferred to 50mM KCl, 10 mM MES/KOH (pH 6.15) at 22°C, PPD of ~150±20 µmol m^{-2} $s^{-1}$and either aerated with A[CO_2] CO_2 or E[CO_2] air for 2h. The epidermal peels were then loaded (by pipetting) with 25 µM (final concentration) H2DCF-DA (2',7'-dichlorodihydrofluorescein diacetate) (Invitrogen, UK) from a 25 mM stock in DMSO for 10 minutes in dark. They were then washed in 50mM KCl, 10 mM MES/KOH (pH 6.2) at 22°C for 10 min in the light (PPD 150 µmol m^{-2} s^{-1}) to remove excess H2DCF-DA and the fluorescence intensity (Ex/Em: ~492–495/517–527 nm) was measured using an Olympus BX51 fluorescence microscope and ImageJ software version 1.8.0_322. For ROS analysis, pixel intensities of forty stomatal areas (fluorescence zone of two guard cells) relative to their background intensities (an equivalent sized area beside the stoma) were measured per treatment in three separate replicated experiments (total stomatal number=120; n=3). Fluorescence intensities were normalised to those of controls. The method is adapted from published research (Chater et al., 2015).

2.9 Stomatal traits measurement

2.9.1 Stomatal impression

Stomatal densities from leaves were estimated by counting stomata from nail varnish impressions. The method of nail varnish impressions (WEYERS & JOHANSEN, 1985) was adapted to measure stomatal traits like stomatal density and guard cell length. Light, fast set vinyl polysiloxane impression material (ImpressPLUS Wash, Perfection Plus, UK) was applied to either abaxial or adaxial surface of mature and fully expanded leaves. Once the material was set, it was removed from the leaf surface, and a coat of transparent nail varnish was applied to the impression. After nail varnish set, a transparent piece of tape was laid on top of it being removed afterwards, carrying the nail varnish epidermal impression with it. The piece of tape was then affixed to a glass

slide and observed under microscope. A Brunel n300-M microscope equipped with a Prior ES10ZE Focus Controller and Moticam 5 camera operated using Micro-Manager 1.4 software was used to take files of Z-stack images. For Arabidopsis, five fields of view were taken from midrib to margin per impression and there were 3 replicates/impressions per plant line. For rice, five fields of view were taken from midrib to margin per impression and there were 2 impressions/replicates per flag leaf. At least two leaves were considered for each biological replicate.

2.9.2 Stomatal density and GC length measurements

For stomatal density measurement images were taken using 20X objective. Each Z-stack file was opened through ImageJ software, which was calibrated at the beginning of each counting session. The calibration image was used to set the scale option for counting, with 1296 pixels equating to 60 divisions on the calibration slide. 60 x 10 µm (0.01 mm) = 600 µm, which is the known distance value. The pixel aspect remained 0.1 and the unit of length was set to 'µm'. The scale option is used to establish a 400 x 400-pixel region of interest to begin the count. Stomata with a surface area 50% or more inside the region of interest were counted separately and stored using excel. The data was analysed by calculating the SD per condition or per control/mutant as follows:

Stomatal Density (SD) = total stomata/mm^2

To measure the GC length in rice, 40X objective was used and the scale adjustments were changed accordingly in ImageJ software version 1.8.0_322. GCL measured using the line tool on the software (Figure 2.3).

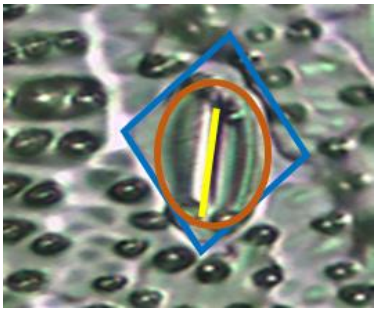

Figure 2.3 Rice stomatal complex from leaf impression. The yellow line is the length of GC measured (GCL), orange oval shape represents guard cells and the diamond shape is the rice stomatal complex encompasing subsidiary cells and guard cells.

2.10 Metabolites measurements

In collaboration with Veronika Turečková and Dana Tarkowska from Laboratory of Growth Regulators, Palacky University Olomouc & Institute of Experimental Botany AS CR, Czech Republic were measured different metabolites involved in ABA and GA biosynthesis pathways respectively. An image representative of one day of experiment involving either Col-0 or *phyB-9* is shown (Figure 2.4). Metabolites were measured from Col-0 and *phyB-9* fresh leaf discs treated the same way as described in [CO_2] functions bioassay (section 2.7). After the treatments, leaf discs were immediately collected in liquid nitrogen (LN_2) and fresh weight (FW) was measured. For analysis of ABA metabolites 60mg of FW/biological replicate was collected whereas, 15mg of FW/biological replicate was considered enough for GA metabolome analysis. The leaf discs were homogenized in Tissue Lyser with ceramic beads and stored in -80ºC for further analysis. This experiment was repeated for three days to generate the independent biological repeats, but each day also included separate samples. At least three technical replicates were considered to analyse each biological replicate. Measurements of ABA metabolites were conducted following published methods (Turečková et al., 2009). On the other hand, GA metabolites were measured according to another method adopted for GA analysis(Urbanová et al., 2013).

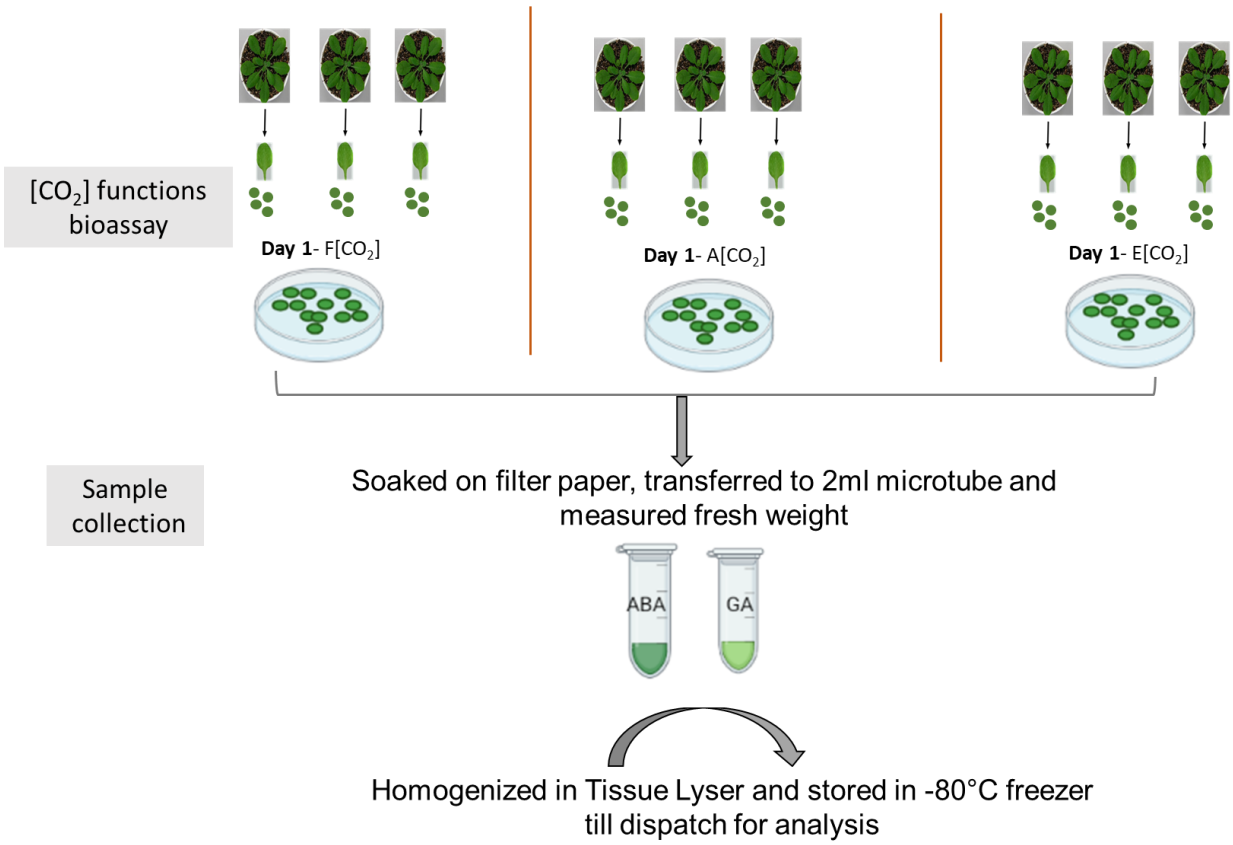

Figure 2.4 Leaf discs collection for metabolite analysis. Diagram showing steps to collect leaf discs samples either from Col-0 or *phyB-9* plants treated under [CO_2] functions bioassay. This is representative of one day among three separate days where each day is equivalent to one biological replicate. Leaf discs were collected from three different leaves of three individual plants. Image "Created with Biorender.com".

2.11 Thermal imaging

Thermal imaging analyses were conducted using an infrared (IR) thermal imaging camera FLIR T650SC (FLIR Systems Inc., Boston, MA, USA). The parameters were in default settings. The images were captured with 1-min intervals as time series.

Rice plants were grown as in 2.2.2 and plants between 35-41 days old post germination were transferred to [CO_2] treatment chamber one day before the experiment to acclimate. On the day of experiment the camera positioned in front of

the plants, at approximately 2 meters distance. The CO_2 treatment and timing were designed as follows:

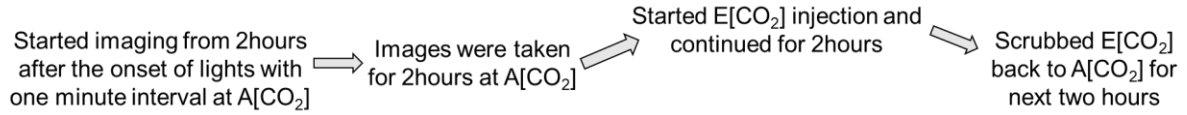

Therefore, a total 360 photos were generated at end of each day. However, first 60 images were not considered during analysis to discard any changes of chamber condition due to open door for setting up the camera. The running temperature during the image capture period and scheduled temperature were matched and found negligible difference (Supplementary 2.10). Total 5 days of imaging represented 5 biological replicates.

Images were analysed using the ResearchIR software (FLIR Systems, https://www.flir.com/). Total four regions of interest (ROIs) as spot measurements were defined on similar position of mature leaf. Average temperature of each replicate was estimated from those ROIs in the software (Figure 2.5). Data were collected from equivalent areas of mature leaves across treatments.

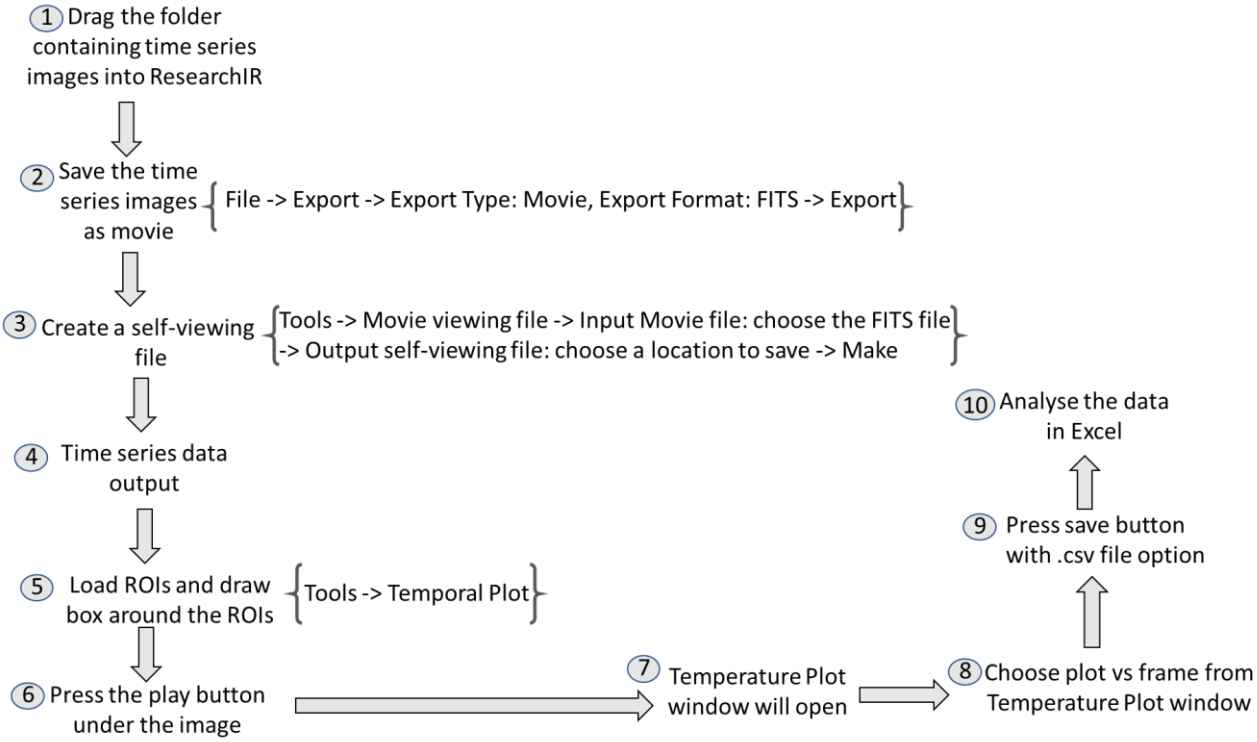

Figure 2.5 Major steps to analyse thermal images in ResearchIR. Functions to carry out under each step were shown within curly brackets.

2.12 Gas exchange analysis

Infrared gas analyser (IRGA; LI-6800 Portable Photosynthesis System, LI-COR Biosciences, Lincoln, NE, USA) coupled with a 6 cm^2 leaf chamber fluorometer (6800-01A, LI-COR Biosciences) was used to measure leaf stomatal conductance, net carbon assimilation and transpiration rates. Measurements were taken from fully expanded leaves of mature plants, starting at least 2 hours after the onset of the light period, and ceasing before the last three hours of the photoperiod. For Arabidopsis, leaf g_s responses to changing [CO_2] was measured by a method named petiole feeding (Ceciliato et al., 2019) with modification. The modified method is described in section 2.12.1.

For rice, measurements were taken from flag leaves under steady state condition as described in section 2.12.2.

To measure the g_s from either side of rice flag leaf (abaxial and adaxial) porometer (LI-6000 Portable Photosynthesis System, LI-COR Biosciences, Lincoln, NE, USA) was used and described in section 2.12.3.

2.12.1 Petiole feeding and whole leaf g_s analysis

Leaves from Arabidopsis plants grown at ambient conditions (described in section 2.2.1) aged 33-37 days post germination were taken. The petiole was first cut using a new razor blade and the cut surface of the petioles was immediately transferred to a petri dish filled with RO water. Petioles were cut a second time under water using a razor blade. The second cut under water was crucial for the petiole feeding technique and the followings steps are recommended:

(a) approximately one-third of the petiole should be cut but no more since longer petioles are better for the technique; (b) the razor blade should be positioned perpendicular to the petiole and at an oblique angle; (c) the cut should be made by gently moving the razor blade back and forth and not by pressing the blade against the petiole (Figure 2.6A 2) and (d) a plastic vial filled with RO H_2O and closed with plastic paraffin film (Parafilm M) should be prepared in advance. After the parafilm is

placed on the tube, one hole was made using fine tweezers to insert petiole. (e) After the second cut was made the petiole, with a droplet of water on its cut end, was immediately transferred to the plastic vial filled with RO water (Figure 2.6A 3). The droplet on the end of the petiole is essential to avoid xylem embolism.

Conditions for the leaf chamber were set as follows-

Air flow rate = 200 $\mu mols^{-1}$; air humidity = 60%; fan speed= 10000 rpm; temperature between leaf and block = 20ºC and light = 200 $\mu molm^{-2}s^{-1}$(10% blue light and 90% red light).

Leaves were placed inside the gas exchange chamber (Figure 2.6B) and equilibrated for 45–60 min at A[CO_2] (400ppm) to reach a stable stomatal conductance before the beginning of the experiments.

The settings of the time duration, [CO_2] and treatments depended on respective experiments. The treatments of interest (either GA_3 or PBZ) were always applied at the onset of the F[CO_2] in the system.

To determine the temporal response of g_s to E[CO_2], an analytical model derived from the model by Vialet-Chabrand et al., 2013 was used as described in McAusland et al., 2016. However, the model was adopted according to present experimental design and used to determine the maximum slope (Sl_{max}). Here, Sl_{max} was maximum rate of g_s closure to an increase in [CO_2] from 25 to 1000 ppm. The model described the temporal response of g_s using a time constant (k, min), an initial time lag (λ, min) and a steady-state g_s (G_{smax}, mmol m^{-2} s^{-1}) reached at given [CO_2]:

$$g_s = (G_{smax} - r_0)\, e^{-e(\lambda - t/k + 1)} + r_0 \qquad \text{Eqn. 1}$$

(t, time, where time 0 is the point at which [CO_2] was increased from 25 to 1000 ppm; r_0 (mmol m^{-2} s^{-1}), initial value of stomatal conductance before the change in [CO_2]). In this equation, the time constant k is a measure of the rapidity of response of g_s independent of the amplitude of variation in g_s (Eqn. 2).

A second parameter combining rapidity and amplitude of the response, the maximum slope (Sl_{max}), was used to describe the maximal slope of the g_s response to the step-change in [CO_2]:

$$Sl_{max} = k.(G - r_0)/e \qquad \text{Eqn. 2}$$

Parameter values were estimated using a Metropolis Hasting algorithm and a Bayesian model. The priors (*a priori* probability of the parameter values) used were uniform covering a large range of possible values and the initial values were chosen randomly. The initial values were chosen from observed values (± 10%) of both r_0 and G. For k, the range of values were selected from between 40 and 90 min, whilst λ values were between 6 and 25 min.

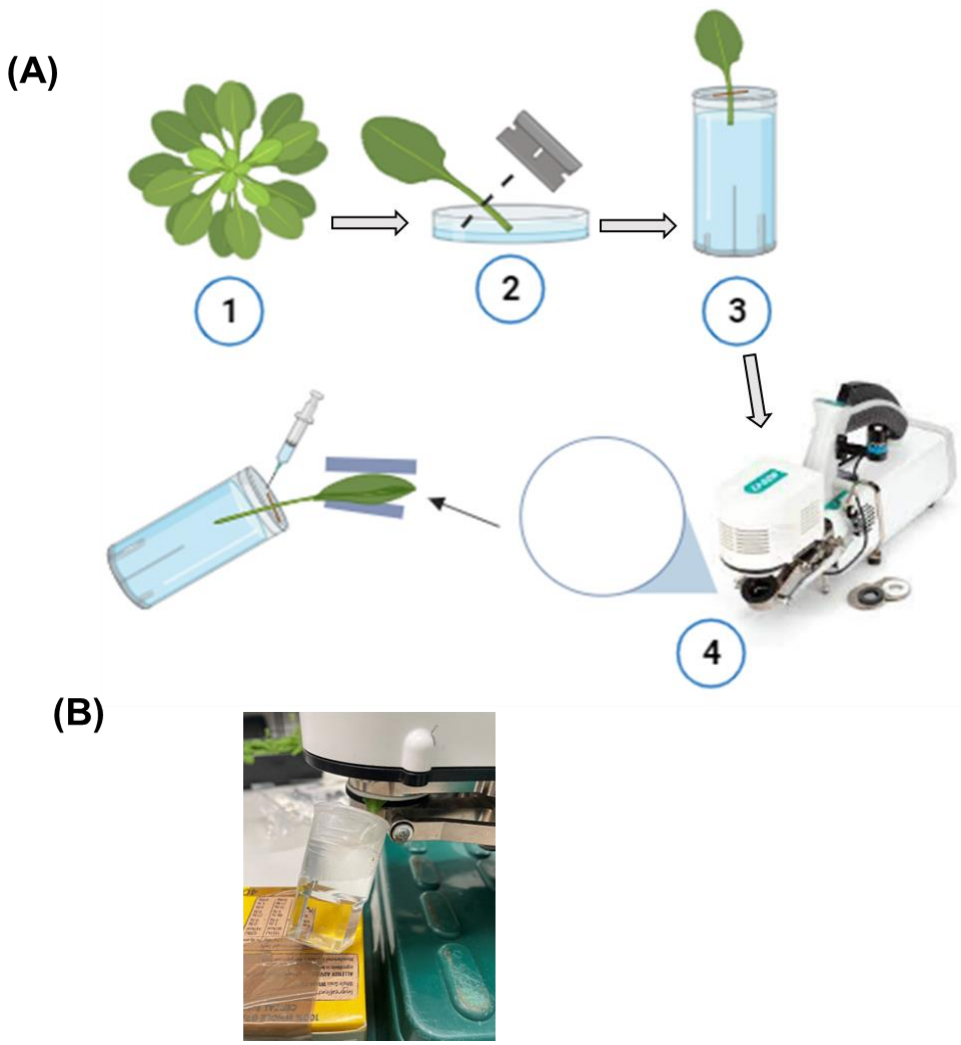

Figure 2.6 Petiole feeding and gas exchange analysis. (A) Schematic diagram showing major steps involved in petiole feeding experiment started from (1) choosing mature leaves from well-developed Arabidopsis; (2) cutting one third of the petiole submerged in RO H_2O; (3) RO H_2O filled vial holding cut petiole to avoid any xylem embolism and drying out and (4) IRGA and a zoom out view of the leaf inside the chamber of IRGA where [CO_2] and treatment of interests were applied. Image "Created with Biorender.com". **(B)** Representative image of RO H_2O filled vial holding leaf inside the IRGA chamber.

2.12.2 Steady-state measurements of rice

Steady state gas exchange measurements were conducted using fully mature rice flag leaves grown under two different [CO_2] chambers as described in section 2.2.2.

Leaf chamber conditions were controlled as follows:

Air flow rate = 400 $\mu mols^{-1}$; air humidity = 60%; fan speed= 10000 rpm; temperature between leaf and block = 30ºC and light = 600 $\mu molm^{-2}s^{-1}$ (10% blue light and 90% red light).

[CO_2] was set to 450 ppm for A[CO_2] grown plants and 1000 ppm for E[CO_2] grown plants. Flag leaf diameter was measured using a cm scale before each reading and set accordingly in the machine. After environmental condition were set in the leaf chamber, the leaf was clamped, and IRGAs were matched a few minutes later. The leaf was left to acclimate to the experimental conditions until stomatal conductance (g_s) and net carbon assimilation rates (A_n) were stable (~20-30 min). Then, measurements were logged for 5 minutes, every 30 seconds. g_s, A_n and transpiration (E) data were derived from csv file generated by the gas analyzer. A was divided by g_s to calculate intrinsic WUE (iWUE).

2.12.3 Porometer g_s measurements of rice

Porometer (LI-6000 Portable Photosynthesis System, LI-COR Biosciences, Lincoln, NE, USA) with a chamber aperture of 0.75cm was used to determine the g_s from abaxial and adaxial surface of rice flag leaf separately. Rice plants were grown under A[CO_2] and E[CO_2] conditions as described in 2.2.2 and measurements were taken inside the chamber to less interrupt their respective growth conditions. In addition, all the measurement were taken 2-2.5 hours after the onset of the light period and completed within midday. Measurements were collected using the LI-600 App (https://www.licor.com/env/support/LI-600/software.html).

2.13 Chlorophyll fluorescence

Photosystem II (PSII) dark and light-adapted chlorophyll fluorescence were investigated using a FluorPen (FP100, Photon Systems Instruments, Brno, CzechRepublic). Measurements were taken from the middle blade of fully expanded flag leaves. For dark-adapted quantum yield measurements (Fv/Fm), data was collected by adapting the leaves in dark for more than ½ an hour with leaf clips. On the other hand, light-adapted measurements (Fv'/Fm') were conducted ~5h into the light period.

2.14 Carbon isotope discrimination

Rice Plants were grown in conditions described in section 2.2.2 with two [CO_2] treatments named A[CO_2] and E[CO_2]. Leaf sections of 2 cm from two different flag leaves were taken from 6 biological replicates per treatment per genotype. The leaf sections were dried at 60ºC for 3 to 4 days and ground to a powder. X4 reference air samples were also collected from the respective growth chambers. 1-2 mg of each sample was added to foil cups and combusted at 1800º C, sample components were then separated via Gas Chromatograph and subjected to a ANCA GSL 20-20 Mass Spectrometer (Sercon PDZ Europa) magnetic field to ionize and separate ^{13}C and ^{12}C. Carbon isotope ratios were obtained in δ-notation and calculated according to (Masle et al., 2005).

$\delta = R/R_{standard} - 1$

R refers to the isotope ratio of the plant sample and R standard is the isotope ratio of the VPDB standard. The $\delta^{13}C$ values were converted to $\Delta^{13}C$ using,

$\Delta^{13}C = (\delta a - \delta p)/(1+ \delta p)$

δ a refers to the $\delta^{13}C$ of atmospheric [CO_2] from the reference sample and δ p is the $\delta^{13}C$ of the plant material.

2.15 Chlorophyll concentration assay

Chlorophyll concentration can be used to help explain the difference in photosynthetic ability between compared plants and expressed in mass or molar terms as a rate of reaction due of their fundamental role in photosynthesis. Chlorophyll concentration assay was conducted following a developed technique (Porra, 2002) . According to the technique, 0.1gm of rice flag leaf tissue (70-73 days old) was collected in 1.0 ml dH_20 and ground in 1ml of dH_2O using a pestle and mortar keeping on ice. Then 200 ul of homogenized sample pipetted into a labelled 2ml Eppendorf tube containing 800ul of 80% acetone and vortexed to mix properly. The mixture then spinned at 14000 rpm in bench-top centrifuge for 3 minutes and poured whole sample into quartz cuvette. The absorption reading of the acetone suspension was taken in the spectrophotometer at 750, 663 and 646 nm and calculated the concentration of chlorophyll and chlorophyll a/b ratio as follows.

First the absorption at 646 and 663 for the background at 750 was corrected as follows:

$$\mathbf{A_{646}^* = A_{646} - A_{750}}$$

$$\mathbf{A_{663}^* = A_{663} - A_{750}}$$

Then the following equations for the concentrations of chlorophylls a and b (ug/ml) was solved.

$$\mathbf{[Chl\ a] = 12.25A_{646}^* - 2.55\ A_{646}^*}$$

$$\mathbf{[Chl\ b] = 20.31A_{646}^* - 4.91\ A_{663}^*}$$

2.16 Yield measurements of rice

To determine the growth and yield of rice genotypes under two different [CO_2] conditions several phenotypic measurements were taken.

2.16.1 Tiller number

The tillering stage starts as soon as the seedling is self-supporting and generally finishes at panicle initiation. Therefore, total tiller numbers from each of the rice plants were counted when panicle initiation was completed at around 66 days post germination.

2.16.2 Flag leaf length and leaf area

Flag leaf length was measured from fully expanded and mature flag leaves using a cm scale. To determine the flag leaf area picture of each leaf measured was captured with the help of digital camera. Then the images were analysed using ImageJ software version 1.8.0_322 (Ahmad et al., 2015).

2.16.3 Panicle weight

Total panicle weight per plant was estimated by weighing all the panicles including seeded and seedless when they have dried completely. Then the panicles were separated as seedless and seeded panicles to weigh them as separate parameter. A portable balance was used to do all the measurements.

2.16.4 Seed weight

Seed weight was estimated by counting 100 seeds per plant, removing their husks manually and weighing on a portable balance.

2.17 Statistical analysis

All statistical analyses were performed using Graph Pad Prism version 9. ANOVA was used to test for differences between genotypes and interaction effects between factors, when appropriate. If significant differences were found, the analysis of

variance was followed by either multiple comparisons Tukey post-hoc test or Šídák's multiple comparison tests. Significant P values were denoted with asterisk. For box-and- whiskers plot the box always extends from the 25th to 75th percentiles and the line in the middle of the box is plotted at the median. The whiskers were created as minimum to maximum where the whiskers go down to the smallest value and up to the largest. Individual data points were drawn instead of box- and- whiskers plot when n≤12 and mean±SD also shown on graphs with the data points.

2.18 Primer sequences

A list of forward and reverse primers used for PCR and qRT-PCR of transgenes (Table 2.10). All primers were synthesised by Sigma Aldrich.

Table 2.10 Lists of primers.

Primer name	Primer type	Sequence
025754 RVE1 For.	PCR	TGTATTCACACAGGTTGCTCG
025754 RVE1 Rev.	PCR	CCGTATCATCCACCGAACCAG
RVE2 For. 2nd	PCR	GCGATTTTGGTGTTAGCTCTG
RVE2 Rev. 2nd	PCR	GCTTCTTCTTGCCATCTTCAG
HPCA1 For.	PCR	GCCTCTTTGCTCCTGATCTTG
HPCA1 Rev.	PCR	GAAGAAGCATGTCAAGTCCAG
SALK LBa1	PCR	TGGTTCACGTAGTGGGCCATCG
nced3-2_LBP1	PCR	ATCAAAGGAGTGTATGTGCGC
nced3-2_RP1	PCR	CTGGCTCTTCCCAAGCGTTC
nced5-2_RP2	PCR	CTGGTCATCACCTATTCGACG
nced5-2_LBP1	PCR	CGATCACTACAACCTCGTCTG
PhyBWtFor2	PCR	CTATGTGCTTGGTTGGTTCTAC
PhyBWtRev1	PCR	CCATGATACTGGGACTCTGTG
AtUBC21Fr	qPCR	GAATGCTTGGAGTCCTGCTTG
AtUBC21Rv	qPCR	CTCAGGATGAGCCATCAATGC
GA3ox1qFor	qPCR	CAGCTCATACCGACTCCACC
GA3ox1qRev	qPCR	CGGTGACCCAACCAAGATCA
GA3ox2qFor	qPCR	TCGGTGACTTGCTCCACATT
GA3ox2qRev	qPCR	CCCCACAGGTAAGCCATTGA
GA2ox1qFor	qPCR	AGAAAACCCAAGTCGCAGGT
GA2ox1qRev	qPCR	TACTCAACCCAACCCACGTC
GAIqFor	qPCR	ACTCGTTGGAAGGTGTACCG
GAIqRev	qPCR	ATGACGCTCAACTCGGTCAG
RVE1qFor	qPCR	TGGACAGATGAAGAGCACAAG
RVE1qRev	qPCR	CCCCACATGTTCTTCTATTCG
RVE2qFor	qPCR	AACGATGAAACAGAAGTGG
RVE2qRev	qPCR	TGTTCATCTCAGTCACCGAC

Chapter 3. Role of gibberellins in regulating stomatal aperture responses to elevated [CO_2]

3.1 Introduction

GCs integrate myriad of signals from external and internal sources and their interactions cause change in their turgor to maintain an optimal stomatal aperture. Two of the best-studied signals that regulate stomatal aperture are [CO_2] and the phytohormone ABA, which both promote stomatal closure in a concentration dependent manner. Experimental evidence suggests that GCs ABA and [CO_2] signalling pathways converged while promoting stomatal closure (Webb & Hetherington, 1997; Chater et al., 2015; Dittrich et al., 2019; Movahedi et al., 2021). However, although [CO_2] responses require the capacity for ABA biosynthesis and catabolism, there is no evidence of changes in ABA levels in GCs following changes in [CO_2]. It is hypothesised that [CO_2] has a role in sensitising GCs to ABA without altering ABA levels (Chater et al., 2015; Hsu et al., 2018). Members of the PYR/PYL/RCAR receptor family perceive ABA and the quadruple receptor mutants *pyr1/pyl4/pyl5/pyl8* and sextuple receptor mutants *pyr1/pyl1/pyl2/pyl4/pyl5/pyl8* showed reduced CO_2 responsiveness compared with wild type (Merilo et al., 2015; Hsu et al., 2018) and PYL4 and PYL5 were found essential in the stomatal response to increased [CO_2] (Dittrich et al., 2019). However, there are studies opposing the role of ABA receptors towards [CO_2]-induced promotion of stomatal closure (Hsu et al., 2018; Zhang et al., 2020). Due to such controversy on the involvement of ABA receptors, how [CO_2] influences GC sensitivity to ABA remains an open question.

Antagonism between hormones is a common concept in the field of hormone signalling pathway to maintain cellular homeostasis. For example, glucagon and insulin have antagonistic effects on each other where glucagon increases the sugar levels in blood and insulin decreases the sugar levels. Calcitonin and parathyroid hormones (PTH) are another example of antagonistic hormones as they have diametrically opposite functions in order to maintain Ca^{2+} levels in the blood. In plant systems, there are numerous examples of hormonal antagonism. For example, antagonism between auxin and cytokinin in shoot/root growth regulation (reviewed in Kurepa & Smalle, 2022); GAs can act as antagonists to ABA in many plants physiological and developmental processes (Reviewed in Liu & Hou, 2018). GA has also been reported to have a role in GCs aperture control. For example, GAs was reported not to affect ABA-induced stomatal closure (Tanaka et al., 2006), whereas other studies reported

that GAs could modulate ABA-induced inhibition of light responsive stomatal opening (Göring et al., 1990; Goh et al., 2009) . To maintain basal stomatal aperture, the GA receptor GID1 and the downstream DELLA transcription factors are reported to have a possible role (Sukiran et al., 2020). It is possible that [CO_2] could affect GA pathway that negatively regulates ABA signalling. The focus has therefore been on whether GAs influence basal GCs function or responses to ABA and studies have not determined whether GA can influence GCs responses to changes in [CO_2].

3.1.2 Objectives

In this chapter, I investigate the role of GAs in regulating stomatal closure in response to e[CO_2]. I hypothesise that [CO_2] sensitises GCs to ABA by targeting changes in GA metabolism or signalling. Therefore, it is the balance between GAs and ABA, as opposed to ABA concentration alone, that modulates GCs responses to high [CO_2] (Figure 3.1). The following objectives are proposed to test this hypothesis:

1. Investigate whether changing GA metabolism affects GCs response to [CO_2].
2. Determine whether [CO_2] regulates GA or ABA metabolism.

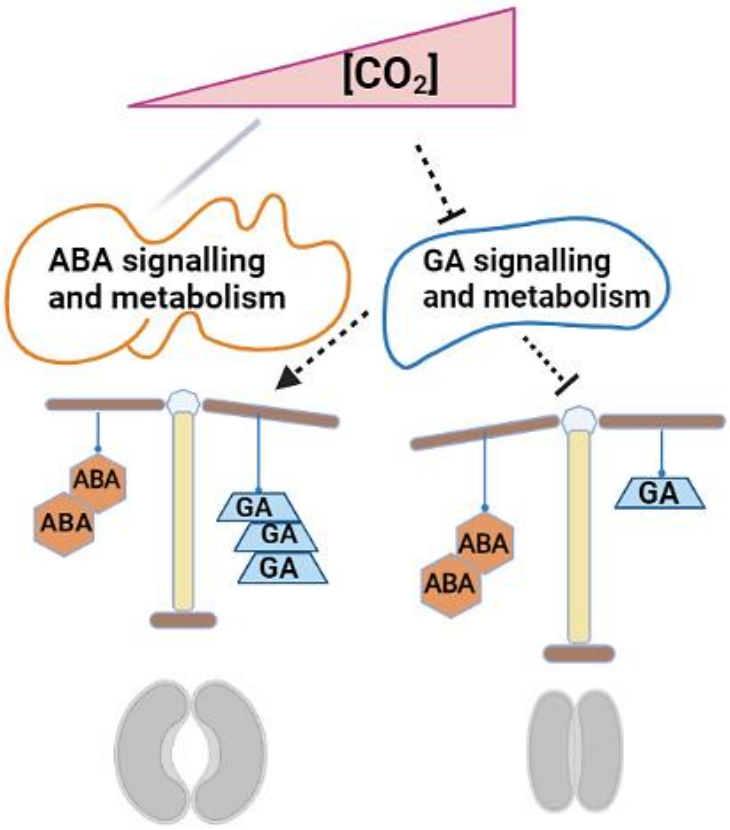

Figure 3.1 [CO_2] may sensitise guard cell responses to ABA by targeting GA signalling and metabolism. CO_2 promotion of stomatal closure is not driven by measurable changes in GCs ABA levels. To sensitise GCs to ABA, we propose that [CO_2] regulates changes in GA signalling or metabolism. Therefore, a homeostasis exists between ABA and GA where GA reduces with the elevation of [CO_2], and ABA remains unchanged. Dotted arrow indicates hypothesised positive regulation, dotted bar lines indicate negative regulation, and the faded gray line indicates regulation with contested data (Chater et al. 2015; Hsu et al. 2018; Dittrich et al. 2019, Zhang et al. 2020).

3.2 Gibberellins antagonise stomatal closure at elevated [CO_2]

To test the hypothesis that GAs have role in regulating stomatal closure in response to [CO_2] elevation, primary attempt was made to conduct stomatal bioassay using gibberellic acid (GA_3). Among the biologically active GAs (GA_1, GA_3, GA_4 and GA_7) GA_3 was chosen as it is readily available and widely used in GA experiments (McAinsh et al., 1996). Existing research on stomatal movement responses demonstrated a wide

range of exogenous GA_3 application with 50 µM in *Vicia faba* and *Fritallaria imperalis;* 0.1-10 µM to block ABA-induced inhibition of stomatal opening and 100µM to fine tune basal stomatal aperture in Arabidopsis (Fischer et al. 1990; Goh et al. 2009; Sukiran et al., 2020). Though not directly involve in stomatal response study, the application of different ranges of GA_3 has been reported to mitigate environmental stresses like salt and heavy metals from different plant species (Reviewed in Niharika et al., 2021). In addition, 50-100 µM of GA_3 has been reported to regulate fruit shape, size and senecence of different horticultural crops (Zhang et al. 2023).

Therefore, an initial experiment of stomatal functions bioassay (methods described in 2.7) was performed with a range of GA_3 concentrations (10µM, 50µM, 100µM and 200µM) to determine if there is any effect of GA on stomatal responses to changing [CO_2] (Figure 3.2). Comparisons between samples were made with the CO_2-free (F[CO_2]) control for each GA_3 treatment since peels were normalised under F[CO_2] before being exposed to treatments. As expected from previous studies, increasing [CO_2] from CO_2-free condition (F[CO_2]) to ambient [CO_2] (A[CO_2]) and from F[CO_2] to 1000ppm CO_2 (E[CO_2]) lead to significant reductions in stomatal pore aperture with mock-treated (0.1% ethanol) samples (Chater et al. 2015; Movahedi et al, 2021). Across all of the GA_3 concentrations used, [CO_2] was still observed to promote stomatal closure (Figure 3.2). However, closure at E[CO_2] was partially inhibited in a GA_3 concentration dependent manner, an effect that was not so significant at A[CO_2]. This can be more clearly evidenced by comparing stomatal apertures with the treated GA_3 along the mock at F[CO_2], A[CO_2] or E[CO_2] seperately (Figure 3.3A-C) or following normalisation to the relevant F[CO_2] (Figure 3.3D-F). Collectively this data shows that GA_3 can antagonise stomatal closure in response to E[CO_2] (Figures 3.2 and 3.3).

Of the tested GA_3 concentrations, GA_3 in the range of 50-200µM was sufficient to inhibit E[CO_2]-mediated stomatal closure. This range is consistent with previous studies, for example where the exogenous application of 100µM GA_3 was able to mitigate salt and heavy metals stress (Gangwar et al., 2011; Ali et al., 2015; Saleem et al., 2015; Xu et al., 2016; Wang et al., 2019). In addition, research to understand GA signalling and biosynthesis use of 100µM of GA_3 has been reported (Silverstone et al., 2001; Wen & Chang 2002; Rieu et al., 2008). Also, 100µM of GA_3 has been

demonstrated to study role of GAs in basal stomatal aperture regulation in Arabidopsis (Sukiran et al., 2020).

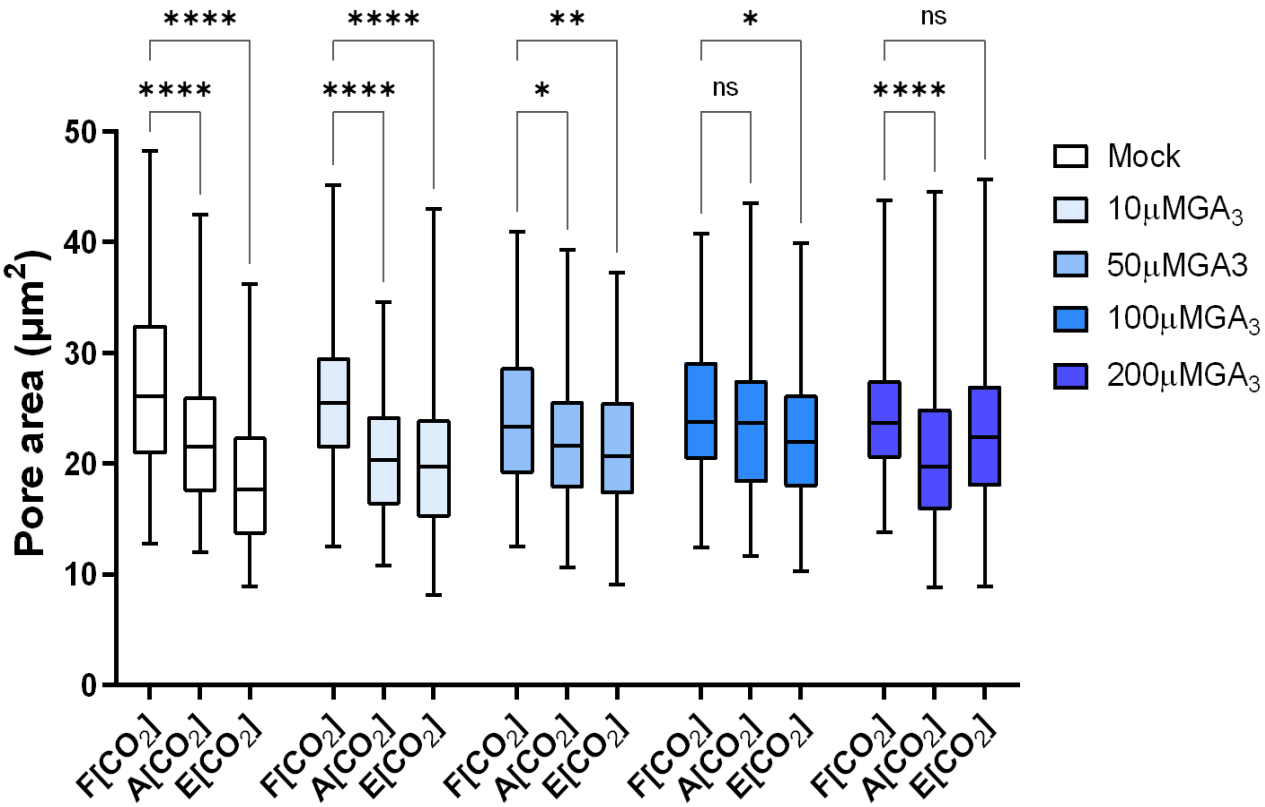

Figure 3.2 Effect of different concentrations of GA_3 on stomatal closure at different $[CO_2]$. Epidermal peels from Col-0 mature leaves were incubated in opening buffer at F[CO_2] air with four different GA_3 concentrations or a mock treatment of 0.1% ethanol, before application of A[CO_2] or E[CO_2]. Boxplots denote stomatal pore area extends from the 25th to 75th percentiles and the line in the middle of the box showed the median of observed pore area. The whiskers indicate the maximum and minimum pore area measured. Total stomata measured n=120. The statistical analysis was conducted using one-way ANOVA to compare between F[CO_2] and A[CO_2] or E[CO_2] treatments using Tukey's multiple comparison tests where *P < 0.05, **P < 0.01, ****P < 0.0001 and P ≥ 0.05 was nonsignificant (ns).

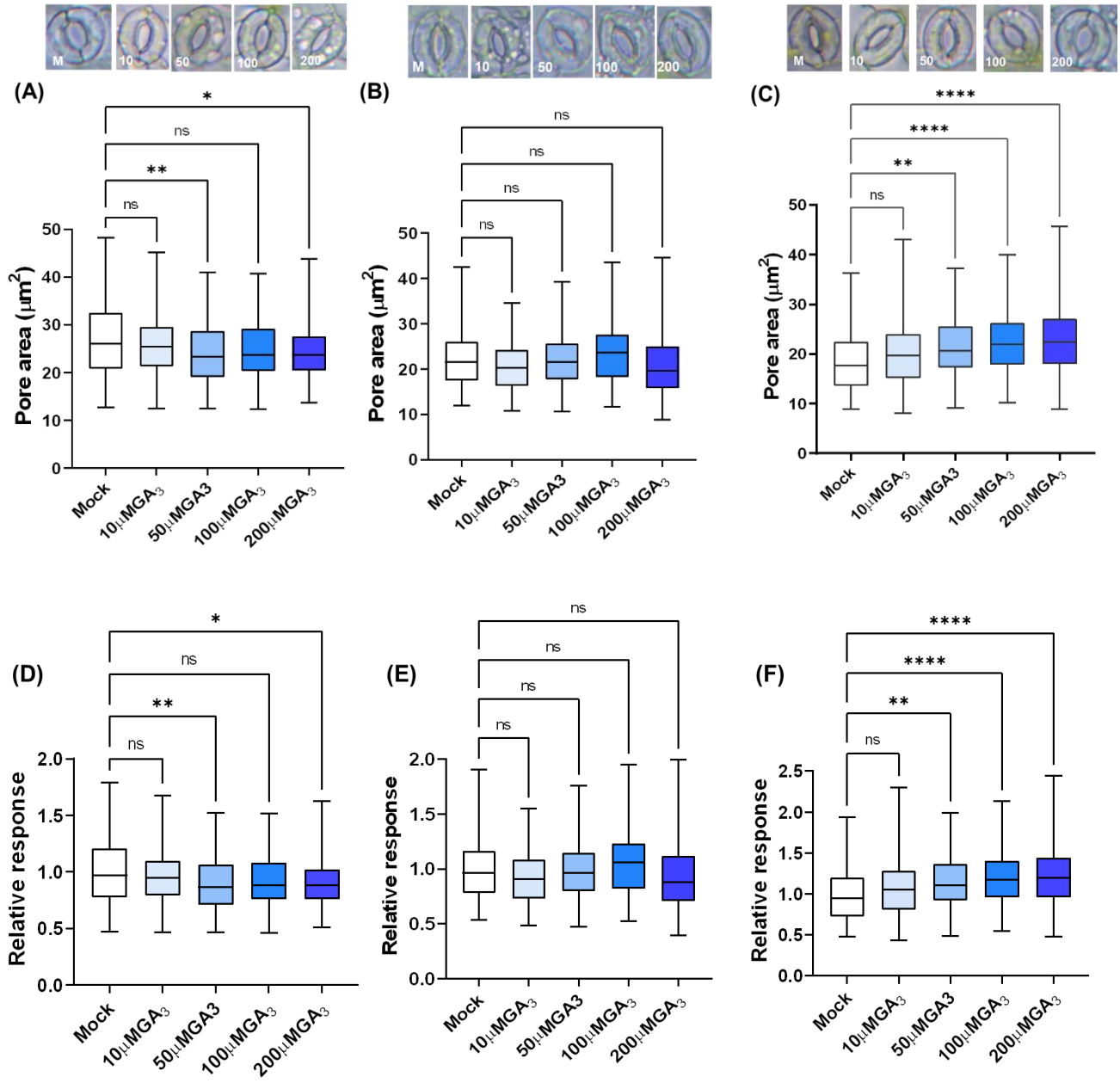

Figure 3.3 Comparison of different concentrations of GA_3 on stomatal closure at different [CO_2]. **(A)** The data same as figure 3.2 but here comparison was made between the mock and each of the four GA_3 treatments at [FCO_2], **(B)** at A[CO_2] and **(C)** at E[CO_2]. **(D)** Relative response of mock and four GA_3 treatments in proportion to their respective response at F[CO_2] using the same data as figure 3.2 at [FCO_2], **(E)** at A[CO_2] and **(F)** at E[CO_2]. Total stomata measured n=120. The statistical analysis was conducted using one-way ANOVA to compare between mock and the four GA_3 concentrations using Tukey's multiple comparison tests where *P < 0.05, **P < 0.01, ****P < 0.0001 and P ≥ 0.05 was nonsignificant (ns). Letter M=mock and numbers 10, 50, 100 and 200 denote concentrations of GA_3 on image panels at top of (A), (B) and (C).

To confirm the ability of GA_3 to inhibit CO_2-induced stomatal closure, a separate stomatal bioassay experiment was performed to test the effect of 100µM GA_3 under three [CO_2]. This experiment supported the results of the initial experiment, and demonstrated that 100µM GA_3 negatively affects the E[CO_2]-mediated stomatal closure (Figure 3.4A and B). Therefore the concentration of 100µM was utilised for future experiments. Since GA_3 is a weak acid, it dissociates fewer protons despite higher concentration compared to strong acid. Therefore, higher concentration like 100µM does not change the pH of the system significantly.

In Arabidopsis, the bioactive form of GAs is GA_4 (Sun et al., 2008). Therefore, a separate experiment was performed to determine whether GA_4, alongside GA_3, alters GCs responses to changing [CO_2] or not. Like GA_3, 100µM of GA_4 inhibited the E[CO_2]-mediated stomatal closure response (Figure 3.4C and D).

Exogenous application of commercially available GA, GA_3 and bioactive GA, GA_4 demonstrated that GAs can inhibit E[CO_2]-mediated promotion of stomatal closure. To analyse the impact of changes in endogenous GA content on [CO_2]-induced promotion of stomatal closure a transgenic line that allows estradiol-inducible GA biosynthesis was utilised. The pUBQ-XVE-GA20ox1-P2A-GA3ox1 line enables simultaneous expression of AtGA20ox1 and AtGA3ox1 following induction by β-estradiol and has been shown to increase endogenous GA levels (Rizza et al. 2021). A stomatal bioassay was performed using the pUBQ-XVE-GA20ox1-P2A-GA3ox1 line under three [CO_2] conditions (F[CO_2], A [CO_2] and E[CO_2]) with both mock (0.1% ethanol) and β-estradiol (5µM) treatments. The leaves were sprayed with same concentration of β-estradiol day before the experiment. As with exogenous GA application, an increase in endogenous GA inhibited E[CO_2]-mediated stomatal closure (Figure 3.5A and B).

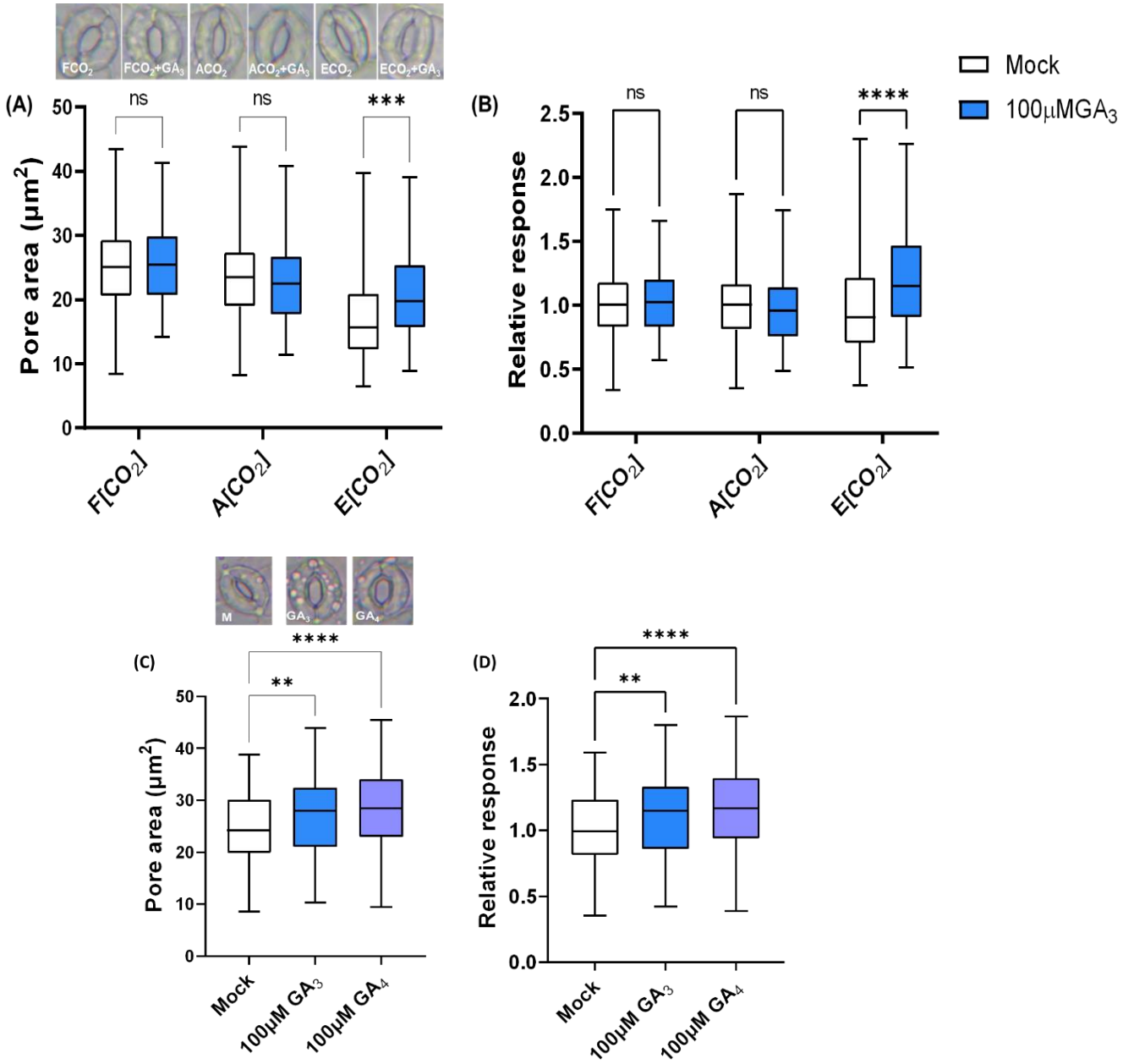

Figure 3.4 Effect of exogenously applied GAs on stomatal closure response at different [CO_2]. **(A)** Epidermal peels were incubated in F[CO_2] air with 100µM GA_3 alongside the mock before the application of A[CO_2] and E[CO_2]. **(B)** Relative response of 100µM GA_3 treated samples in proportion to their responses at respective [CO_2] using the same data as (A). **(C)** The experimental method was the same as (A) but used 100µM of GA_3 and GA_4 seperatly under E[CO_2] treatment. **(D)** Relative response of 100µM GA_3 and 100µM GA_4 treatment response in proportion to mock treated response. Number of stomata measured n=120. Statistical analysis was conducted using two-way ANOVA for (A), (B) and one-way ANOVA for (C) and (D) with Šídák's multiple comparison tests where *P < 0.05, **P < 0.01, ***P < 0.001, ****P < 0.0001 and P ≥ 0.05 was nonsignificant (ns).

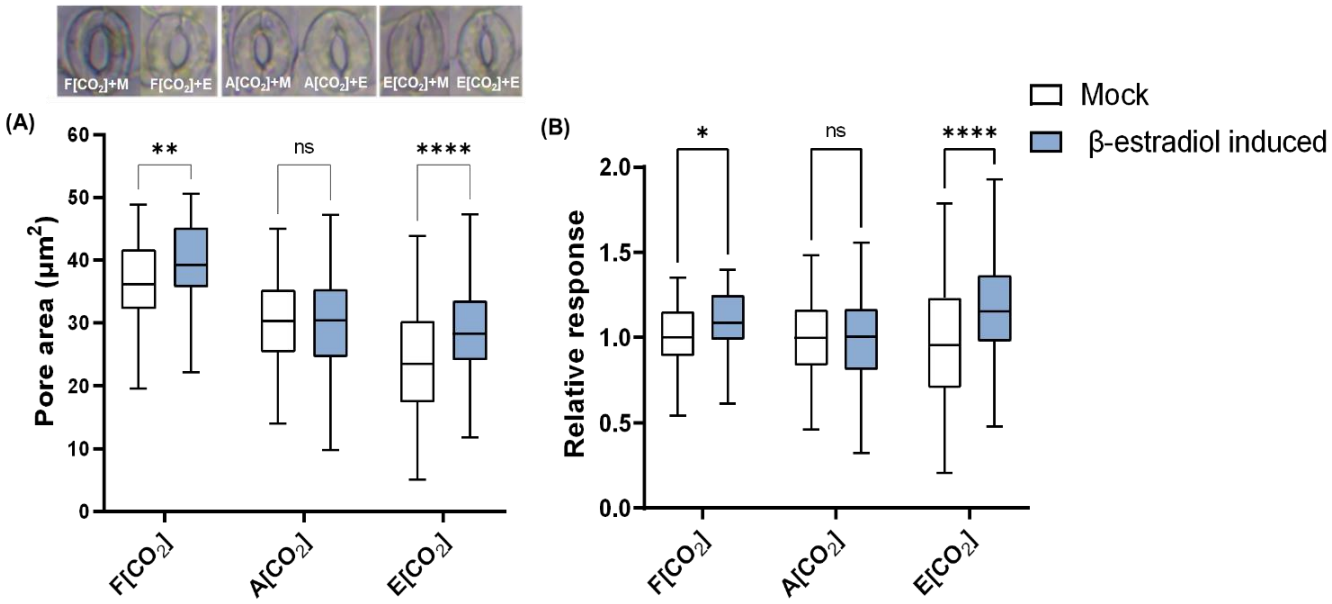

Figure 3.5 Effect of endogenously atered GAs on stomatal closure at different [CO_2]. **(A)** Epidermal peels from pUBQ-XVE-GA20ox1-P2A-GA3ox1 mature leaves were incubated in F[CO_2] air with 1μM β-estradiol alongside the mock (0.1% ethanol) for 2 hours before the application of A[CO_2] and E[CO_2] and measured the pore area. **(B)** Relative response of β-estradiol treated response in proportion to their mock response at F[CO_2], A[CO_2] and E[CO_2]. Here, n=120 stomata. Statistical analysis was conducted using two-way ANOVA with Šídák's multiple comparison tests where *P < 0.05, **P < 0.01, ***P < 0.001, ****P < 0.0001 and P ≥ 0.05 was nonsignificant (ns). Letter M for mock and E for β-estradiol induced on image panel at top of (A).

3.3 Inhibitors of gibberellin biosynthesis promote stomatal closure

Since the application of GA was found to inhibit the E[CO_2]-mediated stomatal closure response, I next investigated whether inhibiting the biosynthesis of GA pharmacologically changes sensitivity to different [CO_2]. There are several inhibitors of GA biosynthesis and their site of interaction with GA biosynthesis pathways has been determined by using cell-free enzyme systems and fungal or plant cell culture (Hedden, 1990; Rademacher, 2000). Figure 3.6A shows the three significant steps of GA biosynthesis and the sites of action of the inhibitors paclobutrazol (PBZ) and

daminozide (DMZ), which were utilised to test the effect of GA inhibitors on stomatal responses to [CO_2]. PBZ blocks the formation of ent-kaurenoic acid from ent-kaurene but can also inhibit sterol biosynthesis (Sugavanam, 1984; Hedden & Graebet, 1985; Burden et al., 1987). Therefore, an additional GA biosynthesis inhibitor, DMZ, was included as it inhibits the hydroxylation at late stages of GA biosynthesis which are specific for active GAs production (Rademacher, 2000, 2017).

For the stomatal bioassay experiment, PBZ and DMZ were used with a concentration of 1µM and 10µM respectively in consistent with the existing literature (Wen & Chang, 2002; Pateli et al., 2004; Rieu, Ruiz-Rivero et al, 2008; Feng et al, 2008; Band, 2012). In stomatal bioassays, both PBZ and DMZ were applied during the application of [CO_2] treatments and found to promote stomatal closure under F[CO_2] and A[CO_2] treatments. At E[CO_2], the addition of PBZ resulted in a further significant reduction of pore area, whereas there was no additive effect of DMZ application at E[CO_2] (Figure 3.6B and C). Given that exogenous and endogenous GA can suppress E[CO_2]-mediated promotion of stomatal closure and GA biosynthesis inhibitors strongly enhance stomatal closure both in the presence and absence of CO_2, it is concluded that GAs have the potential to regulate stomatal aperture response towards change in different [CO_2].

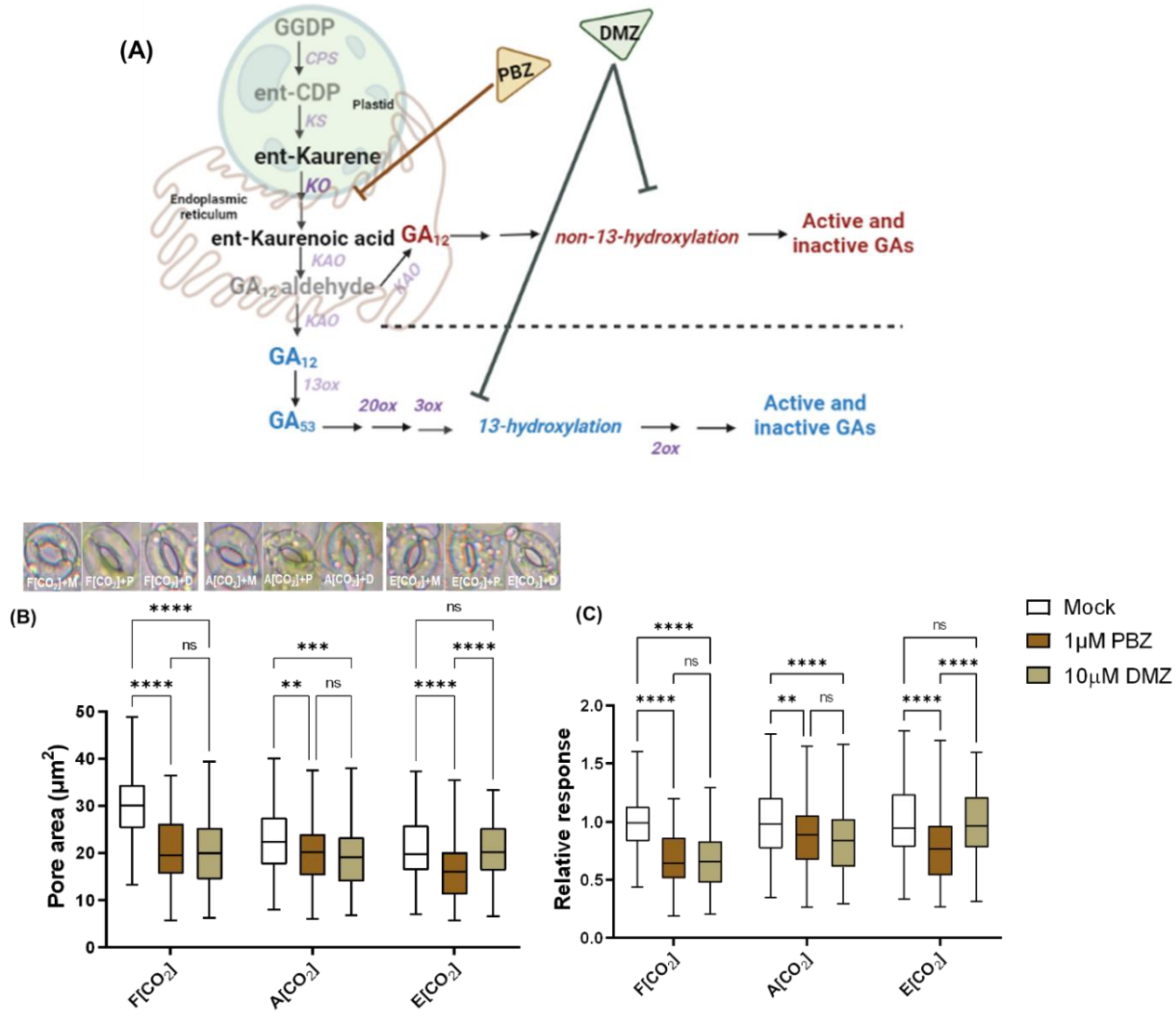

Figure 3.6 Effect of inhibitors of GA biosynthesis on stomatal closure at different [CO_2]. (A) The 3 main steps of GA biosynthesis leading to biologically active GAs and points of inhibition by PBZ and DMZ (adapted from Rademacher, 2017) **(B)** Pore area measurements from isolated epidermal peels of Col-0 mature leaves following application of 1μM PBZ and 10μM of DMZ at F[CO_2], A[CO_2] and E[CO_2] compared to mock treatment (0.1% ethanol). **(C)** Relative response of 1μM PBZ and 10μM DMZ treatment in proportion to their respective mock treatment at three different [CO_2] using the same data as (B). Number of stomata measured n=120. Statistical analysis was conducted using two-way ANOVA to compare [CO_2] and inhibitors of GA biosynthesis with Tukey's multiple comparison tests where **P < 0.01, ***P < 0.001, ****P < 0.0001 and P ≥ 0.05 was nonsignificant (ns). Letters M=mock, P=PBZ and D=DMZ on image panel at top of (B).

3.4 GA_3 antagonises ABA-mediated stomatal closure

CO_2 and ABA signalling pathways converge to promote stomatal closure, but it has been reported that changes in [CO_2] do not cause changes in leaf or GCs ABA levels (Chater et al. 2015; Hsu et al. 2018). This has led to the hypothesis that CO_2 acts by altering GCs sensitivity to ABA (Chater et al. 2015; Hsu et al. 2018; Dittrich et al. 2019). As data from present study has shown that GA can modulate responses to E[CO_2], I hypothesise that rather than changes in ABA, the elevation of [CO_2] could alter sensitivity to ABA by inhibiting GA biosynthesis or signalling. If this is the case, we might also expect GA to counter the promotion of stomatal closure by exogenous ABA. Therefore, a bioassay was designed where epidermal peels were treated under F[CO_2] conditions that promote opening (Material and Methods 2.7) and 100µM of GA_3 was applied in combination with either 0.2µM or 1µM ABA. Current-ejection method revealed that local ABA concentation of 0.2µM triggered stomatal closure (Huang et al. 2019). The 1µM concentation was used as this was also reported to induce stomatal closure (Ha et al. 2018; Chen et al. 2020).

As expected, ABA promoted stomata closure with each of the concentrations. However, it was observed that GA_3 could partially negate the closure effect of ABA on the stomatal aperture, which is significant with 1µM ABA (Figure 3.7A and B). Therefore, GA_3 is able to, at least partially, inhibit ABA-induced stomatal closure despite their sugnificant difference in concentrations. In general researches showed lower concentrations of endogenous GAs compared to ABA.

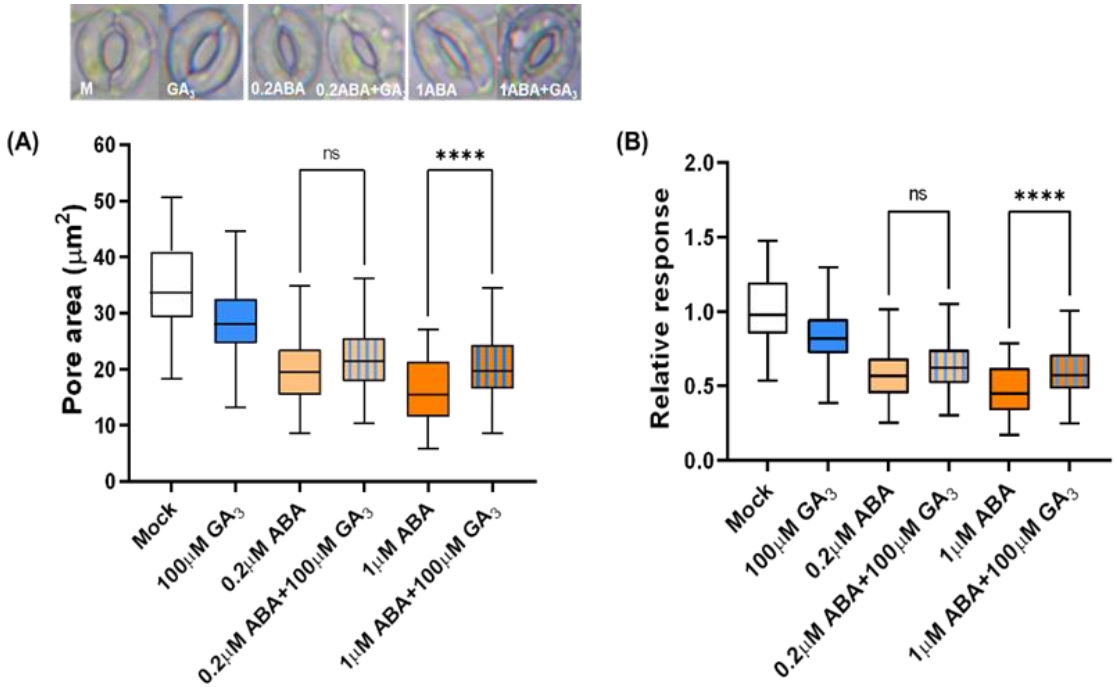

Figure 3.7 Combined effect of ABA and GA_3 on stomatal response under F[CO_2]. **(A)** Epidermal peels from Col-0 leaves were incubated for 2 hours under [FCO_2] before treatment with mock (0.1% ethanol), ABA, GA_3 or ABA and GA_3 for a further 2 hours. **(B)** Relative response of applied hormone treatments in proportion to the mock treatment using the same data as (A). Here, n=120 stomata. Statistical analysis was conducted using one-way ANOVA to compare the [ABA] response alone to the combined response of [GA_3] and the respective [ABA] with Tukey's multiple comparison tests where ****P < 0.0001 and P ≥ 0.05 was nonsignificant (ns).

3.5 A genetic analysis of the role of GA metabolism and signalling genes in guard cell [CO_2] responses

To further examine the role of GA metabolism and signalling in regulating GC responses to [CO_2], various mutants in GA metabolism and signalling were analysed. The amount of bioactive GAs in any system can be affected by their synthesis and deactivation rates. From the GA biosynthesis pathway (Figure 1.6), we know that the third step of GA biosynthesis is vital to maintain the level of GAs in response to both endogenous and environmental cues. This step is regulated by three small gene

families that code for 2-oxoglutarate-dependent-dioxygenases (2-ODDs). They are the GA 20-oxidases (GA20ox) that cleave C-20 to generate C-19 GAs, GA 3-oxidases (GA3ox) that form the bioactive GAs by 3β-hydroxylation and GA 2-oxidases (GA2ox) that deactivate bioactive GAs or their C-19 and C-20 precursors by 2β-hydroxylation (Hedden, 2020). Therefore, mutants in the GA20ox and GA3ox, are expected to produce less GA and mutants of GA2ox are expected to have more GA than wild type.

Stomatal bioassay experiments (described in section 3.2) show that GA counteracts E[CO_2]-mediated stomatal closure. It was therefore hypothesised that using mutants in GA2ox genes, which contain more GA, should mimic these experiments where exogenous GA was used. In Arabidopsis the GA2 oxidases are encoded by a small gene family of 7 genes. To observe the role of the GA2ox during stomatal closure response induced by elevation of [CO_2], a quintuple mutant of GA2ox (*ga2ox1 ga2ox2 ga2ox3 ga2ox4 ga2ox6*; *ga2oxq*) was used; this line has been demonstrated to contain more active GA than wild-type plants (Rieu et al., 2008). During the stomatal bioassay, as seen previously Col-0 stomatal closure was significant at both A[CO_2] and E[CO_2] compared to the F[CO_2] control. The *ga2oxq* stomata showed insensitivity towards A[CO_2] and whilst significant, the response to E[CO_2] was reduced compared to that of Col-0 (Figure 3.8A). The aperture of the *ga2oxq* mutant under F[CO_2] was smaller than that of Col-0 so to account for this difference, the proportional closing response was calculated relative to the aperture at F[CO_2] for the respective treatments (Figure 3.8B). This shows that accumulation of GA made the stomata insensitive to both A[CO_2] and E[CO_2]. To determine whether this smaller aperture at F[CO_2] was the result of smaller GCs in the *ga2oxq* mutant, GC area measurements were taken for Col-0 and *ga2oxq* across three different [CO_2]. These measurements show that the GCs of the mutant had a similar area as Col-0, indicating that there might be a potential defect in stomatal opening in the mutant and not a direct effect of GC area (Figure 3.8C). Therefore, this experiment further supports our hypothesis that GAs can inhibit E[CO_2]-mediated stomatal closure response.

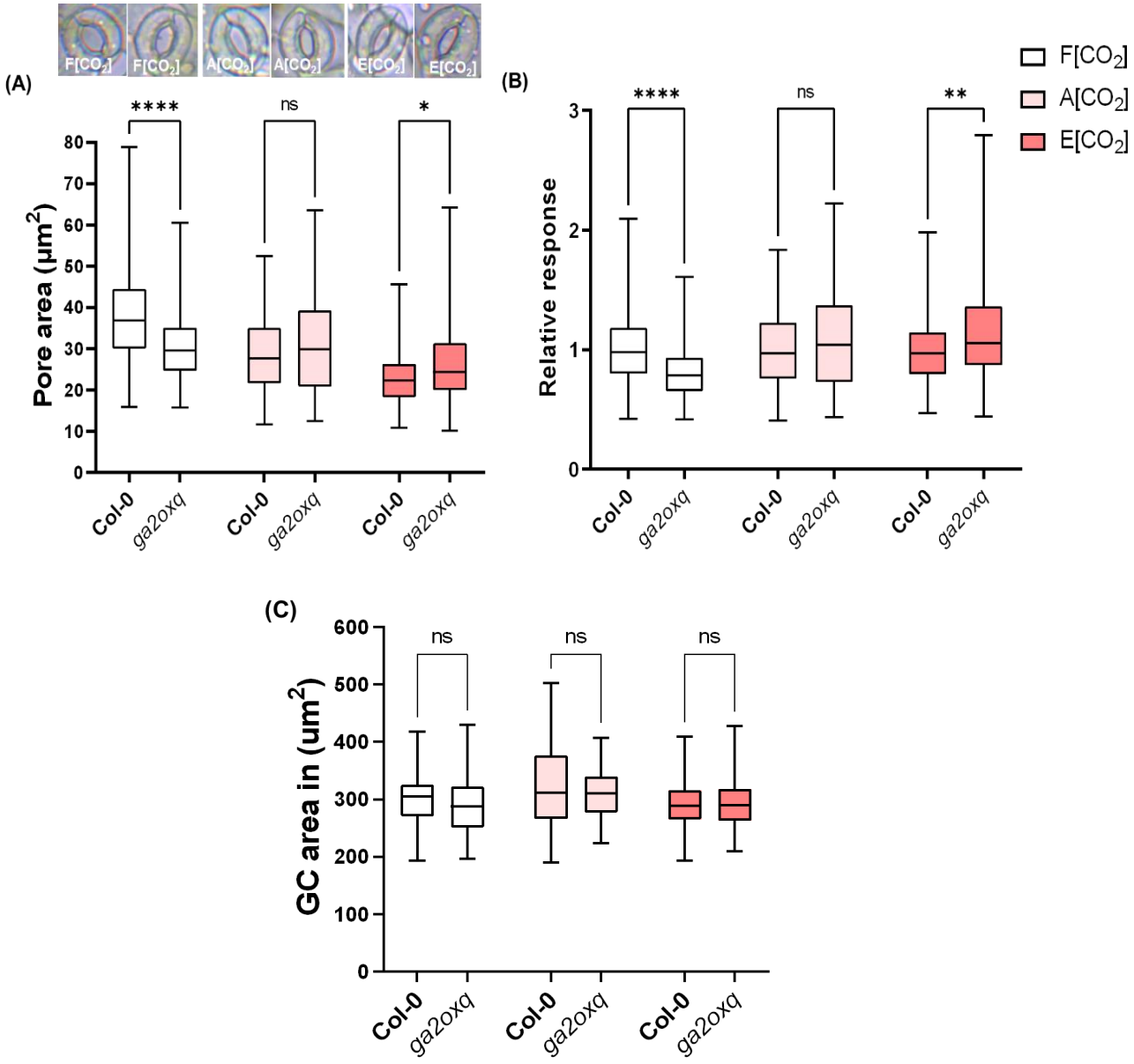

Figure 3.8 Involvement of GA catabolism genes towards E[CO_2]-mediated stomatal closure response. (A) Epidermal peels from mature leaves of Col-0 and *ga2oxq* incubated in opeing buffer under F[CO_2] for 2 hours followed by incubation with A [CO_2] and E[CO_2] for another 2 hours to measure pore area. **(B)** Relative response of both Col-0 and *ga2oxq* in proportion to their respective response at F[CO_2] using the same data as (A). **(C)** GC area of both Col-0 and *ga2oxq* under three [CO_2] conditions. Stomata measured n=120. Statistical analysis was conducted using two-way ANOVA with Šídák's multiple comparison tests where the significant difference between genotypes was *P < 0.05, ** P < 0.01, **** P < 0.0001 and P ≥ 0.05 was non-significant (ns).

As DELLAs are known negative regulators of GA signalling (Hauvermale et al., 2012; Locascio et al., 2013), I next investigated whether they are required for E[CO_2]-mediated stomatal closure. For this, a quintuple mutant of all the five DELLA genes (*dellaq*) (Koini et al., 2009) was tested using the stomatal bioassay system.

dellaq stomata did close in responses to both F[CO_2] to A[CO_2] and F[CO_2] to E[CO_2] treatments (Figure 3.9A). Whilst small differences were observed, particularly at F[CO_2], these were not significant and this could be seen more clearly when the proportional response (relative to F[CO_2]) was examined (Figure 3.9B). GC area measurements of the above-studied stomata at F[CO_2] and A[CO_2] were similar between the genotypes indicating that the difference in stomata closure was not mediated by a difference in GC size (Figure 3.9C). However, the GC area of *dellaq* was significantly smaller than Ler at E[CO_2].

In addition, stomatal bioassays were conducted using stabilized mutant lines of two of the DELLAs, 35STAP_RGAΔ17 and 35STAP_GAIΔ17(Feng et al., 2008). These lines have more of these respective DELLAs as opposed to *dellaq* and if DELLAs do regulate responses to changes in [CO_2], would be hypothesised to be hypersensitive to [CO_2] elevation. The 35STAP_RGAΔ17 line appeared relatively insensitive to changes in [CO2], with no significant closure response whereas the 35STAP_GAIΔ17 responded similarly to the Ler control (Figure 3.10A and B). GC area measurements showed negligible changes with the treatments of [CO_2] across the studied genotypes denoting there is no direct effect of GC area on aperture measurement (Figure 3.10C).

Together, this data indicates that the ability of GA to regulate stomatal responses to [CO_2] is not fully dependent on DELLA activity. However, the stabilised DELLA and in particular that of the 35STAP_RGAΔ17 line suggest that perhaps it is not the presence or absence of the DELLAs that is important for responses to [CO_2] but rather, the ability to be able to degrade them. GA is perceived by GA receptor GID1, a soluble protein localized to both cytoplasm and nucleus. The GA-GID1 complex enhances interaction between GID1 and DELLA by transcriptional reprogramming. In general, specific ubiquitin E3 ligase complex (SCF $^{SLY1/GID2}$) is required to recruit DELLA for polyubiquitination and subsequent degradation by 26S proteosome (reviewed in Sun et al. 2011).

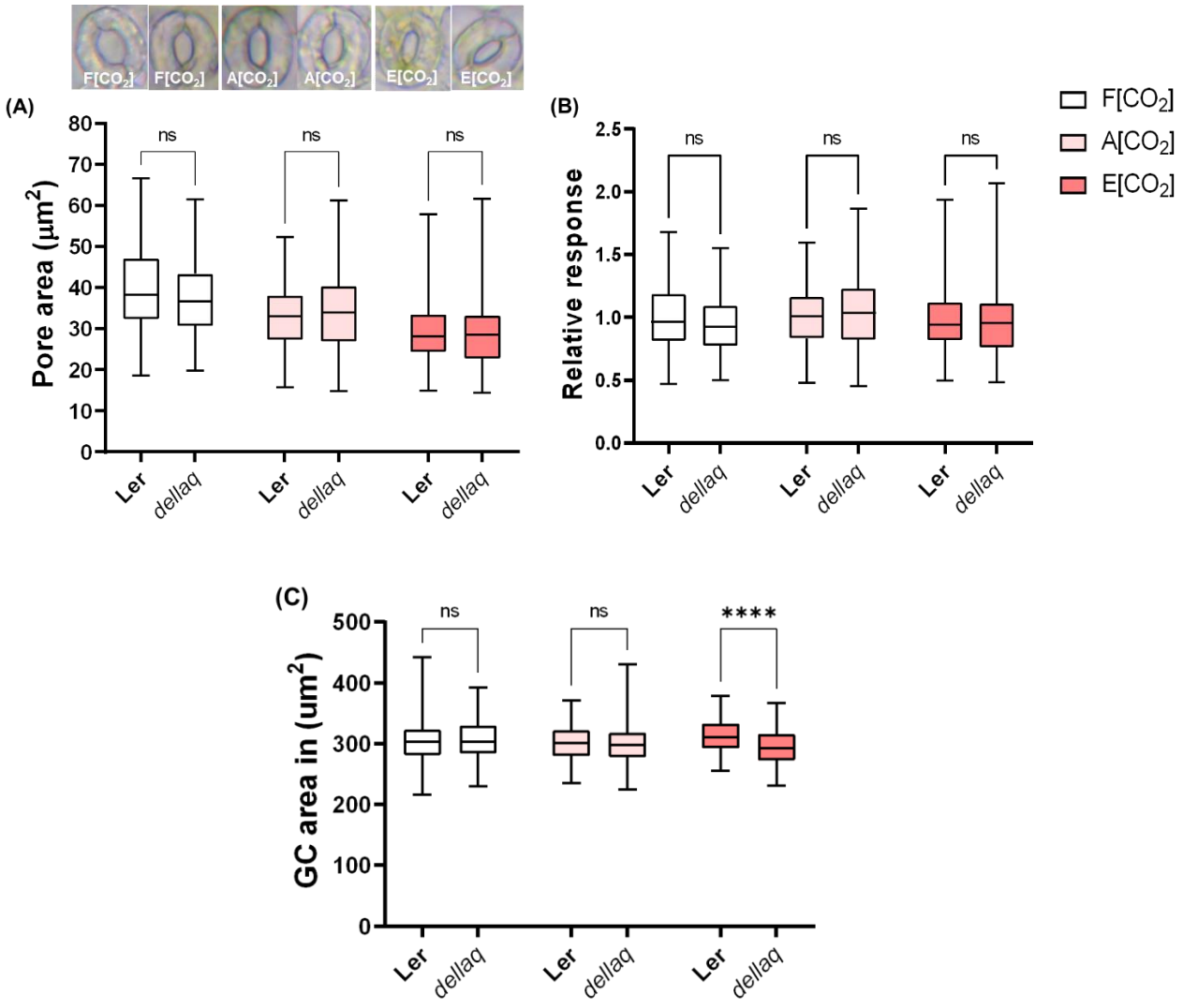

Figure 3.9 Analysis of the stomatal aperture response of the *dellaq* mutant towards elevation in [CO_2]. (A) Epidermal peels from mature leaves of Ler and *dellaq* incubated in opeing buffer under F[CO_2] for 2 hours followed by incubation with A [CO_2] and E[CO_2] for another 2 hours to measure pore are. **(B)** The relative response of both Ler and *dellaq* in proportion to their respective response at F[CO_2] using the same data as (A). **(C)** GC area of both Ler and *dellaq* under three [CO_2] conditions. Here n=120 stomata. Statistical analysis was conducted using two-way ANOVA with Šídák's multiple comparison tests where the significant difference between genotypes was ****P < 0.0001 and P ≥ 0.05 was non-significant (ns).

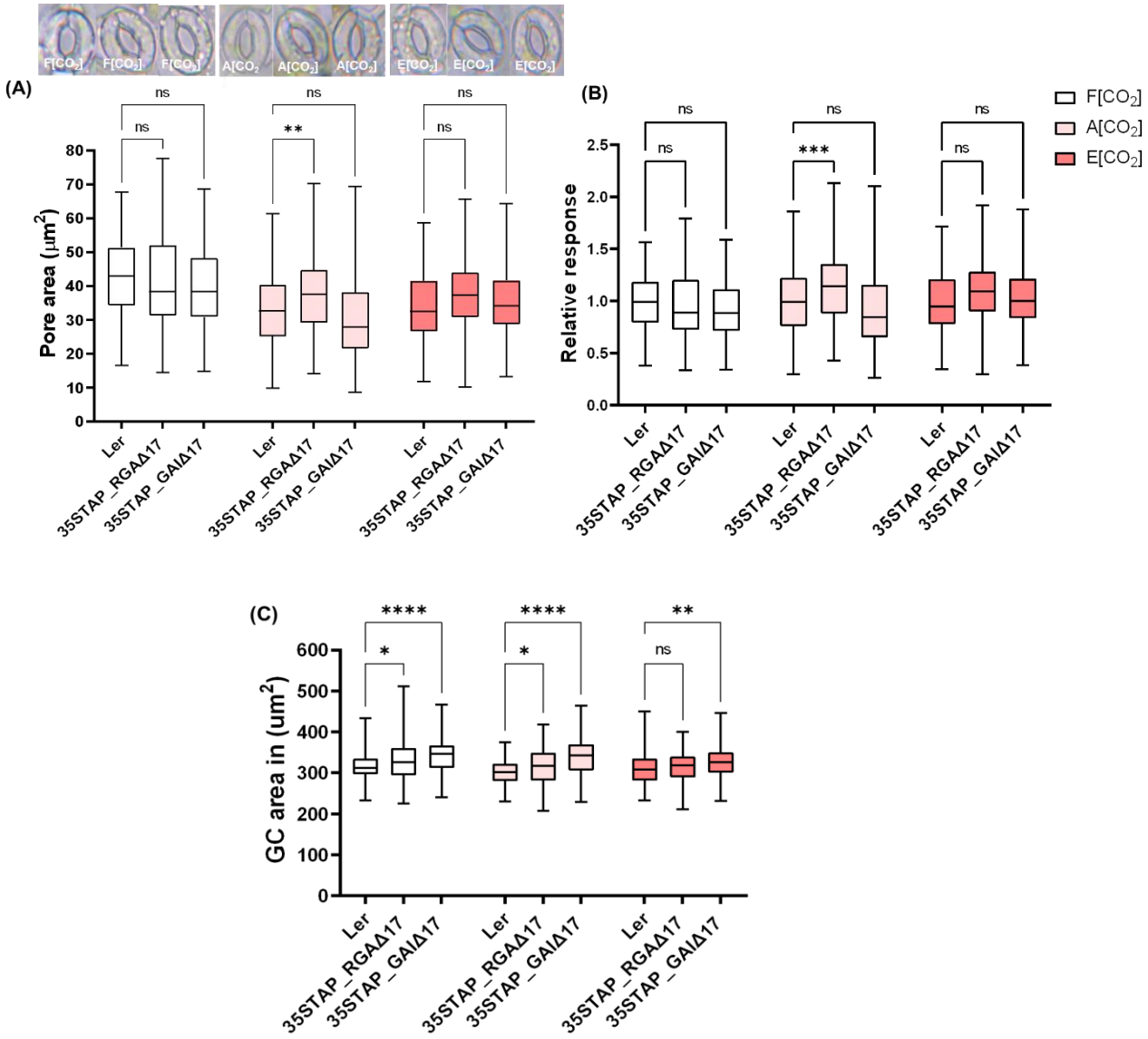

Figure 3.10 Stomata function response of DELLA stabilized mutant lines towards elevation of [CO_2]. **(A)** Pore area measurement from Ler and DELLA stabilized mutant lines *35STAP_RGAΔ17 and 35STAP_GAIΔ17* in response to F[CO_2] , A[CO_2] and E[CO_2]. **(B)** The relative response of the above mentioned lines in proportion to their respective response at F[CO_2] using the data from (A). **(C)** GC area of the studied lines under three different [CO_2]. Total number of stomata measuredn=120. Statistical analysis was conducted using two-way ANOVA with Šídák's multiple comparison tests where the significant difference between genotypes was *P < 0.05, **P < 0.01, ***P < 0.001 and ****P < 0.0001 and P ≥ 0.05 was non-significant (ns).

3.6 GA and GA inhibitors do not alter guard cell reactive oxygen species (ROS) production in response to E[CO_2] treatment

ROS have been demonstrated to be both generated and required for stomatal responses to both ABA and CO_2, as well as other stomatal responses (Kolla et al. 2007; Murata et al. 2015; Chater et al. 2015; Ehonen et al. 2019). Since I hypothesised that GA negatively regulates the ABA pathway to modulate stomatal closure in response to E[CO_2], I investigated whether GA alters ROS production.

ROS can be quantified using the fluorescent ROS indicator H_2DCFDA and therefore, a stomatal bioassay was performed to determine whether GA treatment inhibits CO_2-induced ROS production. Epidermal peels were incubated under F[CO_2] conditions before treatment under three [CO_2] (F, A, E) treatments in the presence of either mock (0.1% ethanol) or 100µM GA_3. These treatments were then followed by a ROS assay where the epidermal peels were stained with H_2DCFDA and GC fluorescence was quantified; an increase in fluorescence is associated with an increase in ROS production. The result demonstrated an increase in ROS production from F[CO_2] to A[CO_2] and E[CO_2], which aligns with previous reports (Chater et al., 2015) (Figure 3.11A). Interestingly, under F[CO_2] and A[CO_2] conditions, GA_3 treatment caused an increase in ROS production compared to respective mock treatments. ROS production under E[CO_2] was the same with both mock and GA_3 treatment (Figure 3.11A). To further clarify the relationship between GA and ROS in GCs, this experiment was repeated in the presence of 1µM PBZ, which had previously been shown to promote stomatal closure (Figure 3.6B). With 1µM of PBZ, ROS production increased under F[CO_2]. Under A[CO_2], ROS production was similar between PBZ and mock-treated samples. Conversely, at E[CO_2], ROS production was reduced compared to the mock (Figure 3.11B). Collectively, these data indicate that GA_3 does not inhibit CO_2 promotion of GC closure by regulating ROS production. Although there is clear evidence for the involvement of ROS in regulating stomatal aperture, it is not well understood how the ROS signals are sensed in the GC apoplast. Apoplastic ROS production initiates the activation of plasma membrane Ca^{2+} channels, leading to an increase in $[Ca^{2+}]_{cyt}$ levels (Ehonen et al., 2019). Very recently, a leucine-rich-repeat receptor kinase (LRR-RK) hydrogen-peroxide-induced Ca^{2+} (HPCA1) was found to be

responsible for extracellular H_2O_2 (eH_2O_2) mediated Ca^{2+} signalling. This has been identified as a cell-surface sensor for eH_2O_2 in plants and reported to mediate H_2O_2-induced activation of Ca^{2+} channels in GCs and is required for stomatal closure in response to ABA (Wu et al., 2020). However, no studies have investigated whether HPCA1 is required for [CO_2] promotion of closure or not. To test this, Col-0 and a *hpca1* mutant were studied using the bioassay system and after incubation under F[CO_2] conditions, treated with either F[CO_2], A[CO_2] or E[CO_2]. This analysis indicated *hpca1* stomata was not as responsive as Col-0 at E[CO_2] denoting involvement of HPCA1 in [CO_2] mediated stomatal closure, from both pore area and relative response data (Figure 3.12A and B). The GC area measurement showed no significant change with Col-0 at A[CO_2] and E[CO_2] treatments (Figure 3.12C), indicating that the GC area did not affect aperture measurement.

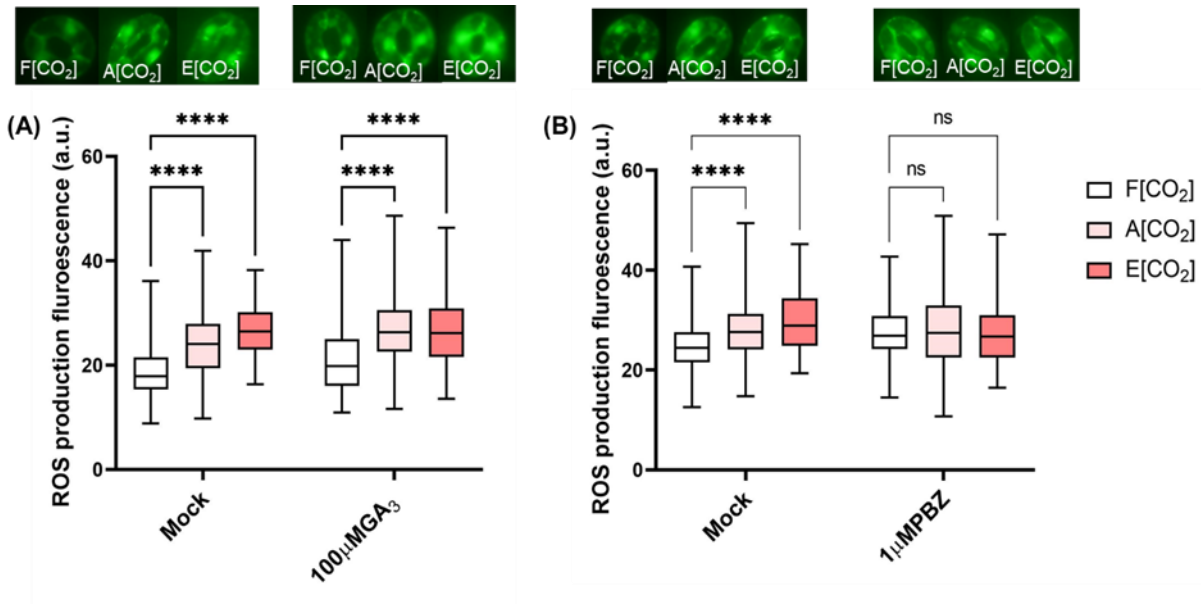

Figure 3.11 ROS assay with GA and inhibitor of GA under three concentrations of CO_2. (A) Epidermal peels from mature leaf of Col-0 incubated under F[CO_2] for 2 hours followed by mock (0.1% ethanol) and 100µM GA_3 application at F[CO_2], A[CO_2] and E[CO_2] for additional 2 hours. Then the epidermal peels were stained with H_2DCFDA and GC fluorescence was determined. **(B)** Experiment similar to (A) except 1µM PBZ was applied instead of GA_3. Fluorescent images of stomata on the top panel were representative of each treatment. Here n=110-120. Statistical analysis was conducted using ANOVA with Tukey's multiple comparison tests where the significant difference among treatments was ****P < 0.0001 and P ≥ 0.05 was non-significant (ns).

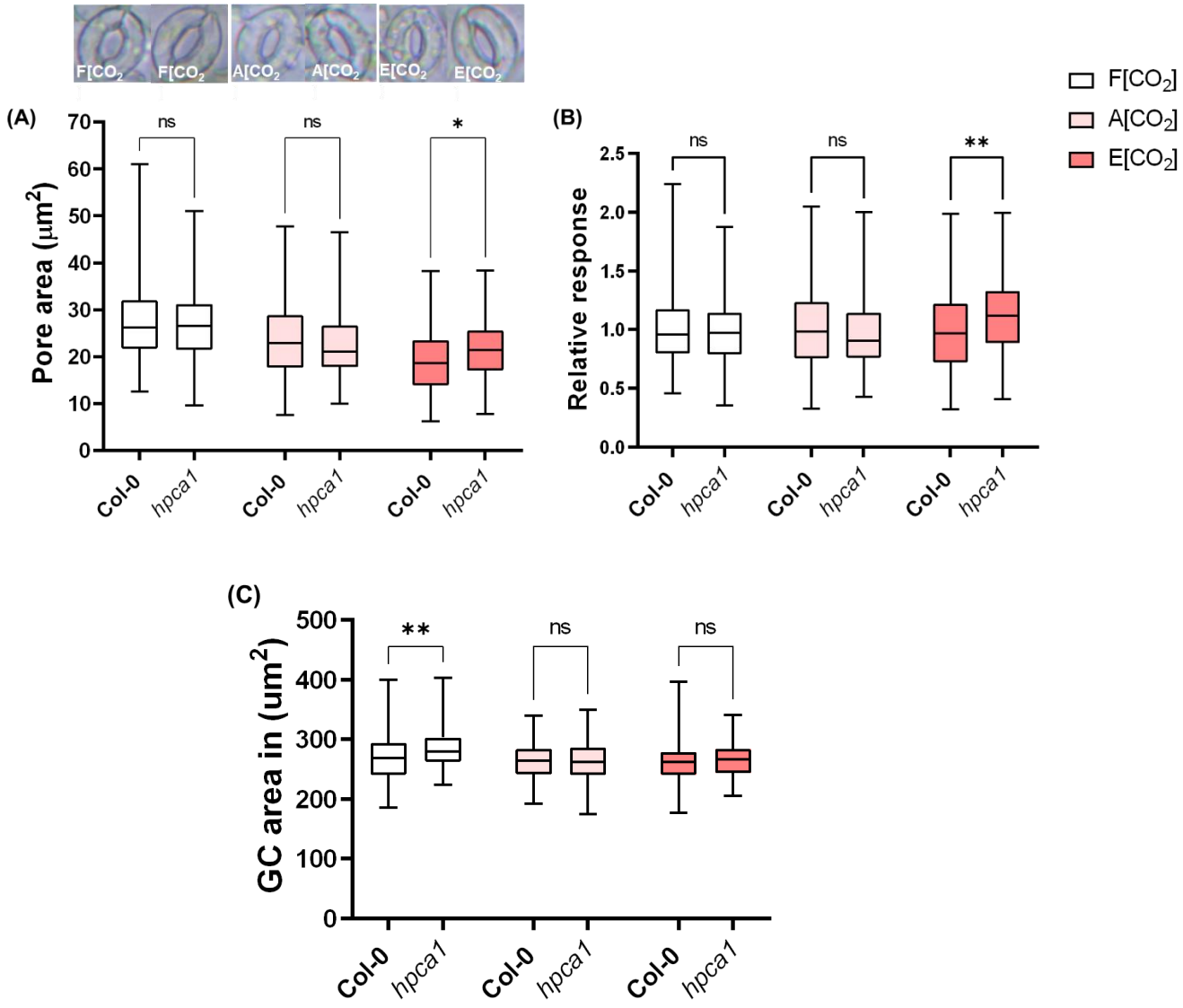

Figure 3.12 Stomata function response of Col-0 and *hpca1* towards elevation of [CO_2]. **(A)** Pore area measurement from Col-0 and *hpca1* treated at F[CO_2] , A[CO_2] and E[CO_2] following 2 hours of incubation at F[CO_2]. **(B)** The relative response from the above mentioned lines in proportion to their respective response at F[CO_2] using the data from (A). **(C)** GC area of the studied lines under three [CO_2]. Number of stomata measured n=120. Statistical analysis was conducted using two-way ANOVA with Šídák's multiple comparison tests where *P < 0.05, **P < 0.01 and P ≥ 0.05 was non-significant (ns).

3.7 Gibberellic acid and paclobutrazol have opposite effects on whole-leaf gas exchange responses to [CO_2]

Study of stomatal physiology using isolated epidermis helps us understand GC-specific stomatal responses devoid of any contribution by underlying mesophyll cells. Analysis of whole leaf responses and experiments where peels are laid back onto mesophyll cells or grafted or separated suggest that there are mesophyll signals that influence GC response (Lee 2006; Mott et al., 2008; Sibbernsen & Mott, 2010; Fujita et al., 2013). However, despite several mesophyll signals having been proposed, there is still some debate as to the absolute identity of the mesophyll signals involved and whether different signals are generated for different responses (Santelia & Lawson 2016, Lawson et al. 2018). Studies demonstrated a correlation of stomatal conductance (g_s) with the rates of mesophyll photosynthesis under different conditions (Wong et al., 1979; Farquhar & Wong, 1984; Mansfield et al., 1990; Buckley et al., 2003).

To determine whether GA affects whole leaf stomatal responses to changes in [CO_2], GA_3 and PBZ were petiole-fed through the transpiration stream with leaf gas exchange measured using an IRGA system (Ceciliato et al., 2019 and section 2.12.1). Excised leaves were initially fed with RO H_2O (pH 6.0-6.5) and g_s was monitored until a steady state level was achieved inside the gas exchange chamber; this usually required ~45 mins to 1 hour at 450 ppm [CO_2]. The steady-state stomatal conductance was then recorded for a further 10 min before the [CO_2] was reduced to 25ppm to promote stomatal opening. Mock (0.1% ethanol) or treatment (100µM GA_3 or 1µM PBZ) was injected into the transpiration stream at the start of the 25ppm [CO_2] phase for 30 minutes and this was followed by the addition of 1000ppm [CO_2] for 1 hour to promote stomatal closure (Figure 3.13A). As observed with stomatal bioassay experiments (described in section 3.2), 100µM of GA_3 was found to increase the g_s under 1000ppm of [CO_2] compared to mock fed leaves 10 mins after the start of the 1000ppm [CO_2] treatment and remained elevated above that of the mock treatment for the duration of the 1000ppm [CO_2] treatment. Though 100µM of GA_3 was applied at the beginning of 25ppm of [CO_2] treatment, the g_s remained lower compared to the mock, indicating GA_3 has a negative effect on high [CO_2] mediated stomatal closure only. When the [CO_2] was shifted again to 25ppm from 1000ppm, the g_s remained higher than mock

for 20 mins and then started to lower down again, indicating that the role of GAs is specific to E[CO_2] (Figure 3.13B).

To complement the stomatal function bioassay described in section 3.3, I next investigated the impact of petiole feeding with 1µM PBZ using this whole leaf gas exchange system. Here, the plants were sprayed with 1µM PBZ the night before the experiment and everything else were same as GA_3 feeding experiment, such that PBZ was also then petiole fed at the start of the 25ppm CO_2 treatment. Since GA biosynthesis Since GA biosynthesis has been reported to occur during the night time, PBZ was sprayed night before the experiment (Prasetyaningrum et al. 2021). PBZ has been observed to reduce the g_s across all the [CO_2] treatments compared to the mock-fed leaves, which is opposite to the response observed with effect as GA_3 treatment (Figure 3.13D).

To determine the speed of stomatal closure with mock and GA_3 feeding, the maximum slope (SI_{max}) was calculated between 40 to 90 minutes (50 minutes of 1000ppm [CO_2] incubation). SI_{max} was calculated from the dynamic sigmoidal model (Vialet-Chabrand et al., 2013) (details in section 2.12.1). The SI_{max} is higher in mock-fed stomata than those treated with 100µM GA_3 stomata (Figure 3.13C), clearly denoting a slower closure in the presence of GA_3. However, similar measurements from PBZ-fed samples showed non-significant SI_{max} values compared to the mock (Figure 3.13E). Though this indicates a similar closure speed for both mock and PBZ-treated stomata at 1000ppm [CO_2], the g_s values (Figure 3.13D) showed a positive effect of PBZ towards stomatal closure.

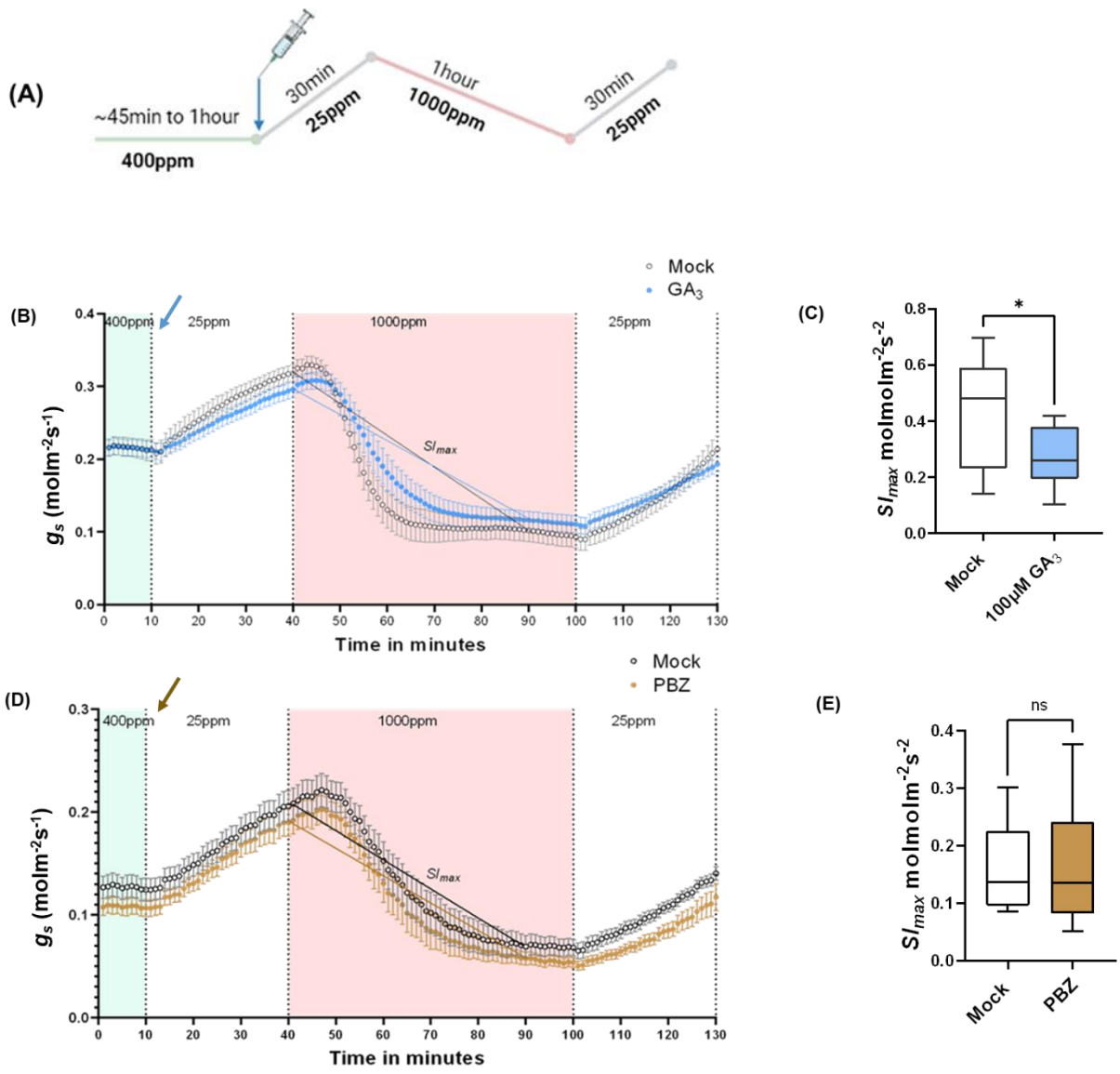

Figure 3.13 Effects of GA_3 and PBZ on whole leaf gas exchange responses to [CO_2]. (A) Schematic diagram to show the IRGA programme set for specified time and [CO_2]. Mock (0.1% ethanol) and 100μM GA_3 or 1μM PBZ was injected into the transpiration stream of the examined leaf petiole at the beginning of the 25ppm [CO_2] phase. **(B)** g_s value changes with time in response to [CO_2] changes with mock or 100μM GA_3 feeding. **(C)** SI_{max} data derived from the fitted dynamic sigmoidal model measured from both mock and GA_3 treated samples during 50 minutes of 1000ppm [CO_2] injection. **(D)** Same as (B) but with the addition of 1μM PBZ. **(E)** same as (C) but for PBZ-treated samples. For (B) and (D), statistical analysis was conducted with the average of different leaf samples (n=10) and their standard error of the mean (SEM). Student's t-test was conducted for SI_{max} where *P < 0.05 and P ≥ 0.05 was nonsignificant (ns) from (C) and (E), respectively. Arrows at the top of (B) and (D) indicated the addition of GA_3 and PBZ.

3.8 Differential expression of GA signalling and metabolism genes in response to E[CO_2]

The experimental data from stomatal function bioassay and whole leaf gas exchange measurements have demonstrated that GAs modulate GC responses to E[CO_2]. The amount of bioactive GAs in any system can be affected by their synthesis and deactivation. To determine whether changes in [CO_2] affect the expression of genes involved in GA metabolism or signalling, a qRT-PCR analysis was performed on leaf tissue exposed to different [CO_2]. Col-0 were grown in compost at A[CO_2] to the same age as would be used for bioassays (30 to 31 days old post germination). They were then subjected to either ambient or elevated [CO_2] treatments (450ppm and 1000ppm respectively) for 2 hours, 6 hours and 24 hours.

Genes involved in GA catabolism (*RVE1*, *RVE2*, *GA2ox1*) showed increased expression after 6 hours of E[CO_2] treatment relative to the A[CO_2] control. *RVE1* was also consistently upregulated at 2h and 24h, with *RVE2* and *GA2ox* expression varying across these timepoints. In contrast, the general trend for genes involved in GA synthesis or signalling showed reduced expression across these timepoints, though *GA3ox1* and *GA3ox2* expression was increased under 6h E[CO_2] (Figure 3.14). Collectively, the general trend was for an increase in the expression of catabolism genes and repression on expression of synthesis and signalling indicates an increment of [CO_2] impacts GA metabolism and signalling pathways.

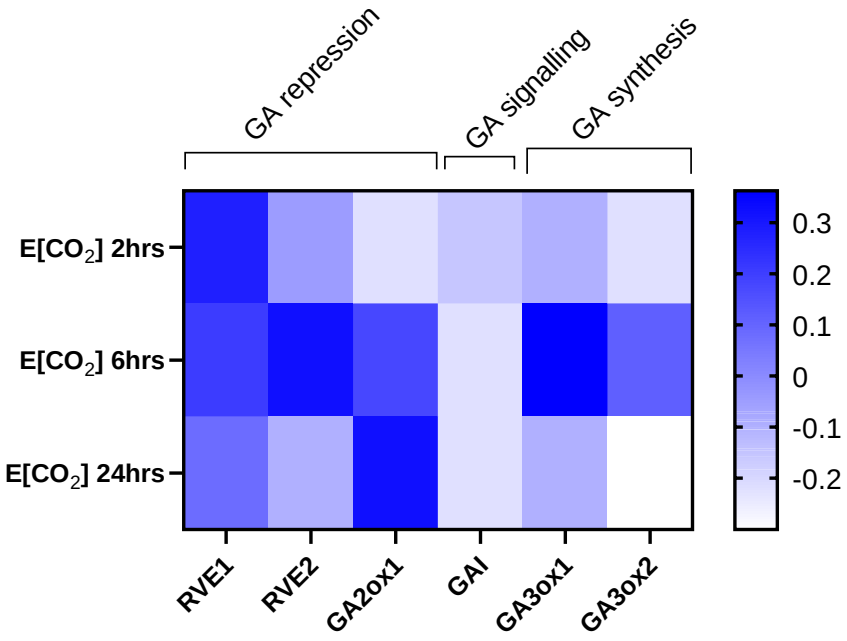

Figure 3.14 Effect of E[CO_2] under three time periods on genes regulating GA catabolism or synthesis. Heatmap showing differential expression of some representative genes in GA catabolism and synthesis after the transfer of plants from ambient (A) [CO_2] (~450ppm) to elevated (E) [CO_2] treatment (1000ppm) for three different periods from mature leaf tissue of Col-0 where the number of replicates n=3. An expression value of 0 (derived from log10 values of normalised A[CO_2] treated samples) was used as a baseline to demonstrate the upper and lower expression of genes according to the colour scale gradient.

3.9 Leaf ABA and GAs content changes at E[CO_2]

The gene expression analysis indicates that changes in [CO_2] can influence the expression of genes involved in GA metabolism and signalling. To determine more directly whether changes in [CO_2] can influence GA content of the leaf, a mass spectrometry approach was taken with analysis performed on leaf discs treated in the bioassay system with different [CO_2]. Given that I have hypothesised that CO_2 enhances sensitivity to ABA by modulating GA levels, ABA content was also analysed. Material was collected at University of Sheffield and analysis was done in collaboration with the Laboratory of Growth Regulators, Palacky University and the Institute of Experimental Botany, Czech Republic. It should be noted that as with bioassays, the

experimental design means that comparisons are only appropriate between F[CO_2] and A[CO_2] or F[CO_2] and E[CO_2] (we cannot compare A[CO_2] to E[CO_2]).

Data shown in figure 3.15B indicated a decrease in ABA levels when [CO_2] increased from F[CO_2] to A[CO_2]. There was no significant difference in ABA between F[CO_2] and E[CO_2], though the trend was still for a reduction in ABA following an increase in [CO_2]. ABA glucose ester (ABA-GE) is an ABA storage or transport form accumulating in the vacuole and apoplast (Dietz et al., 2000). Conjugation of ABA into ABA-GE can inactivate ABA and thereby lower the cellular ABA level therefore contributing to the homeostatic regulation of cellular ABA levels (Dong & Hwang, 2014). Similar to ABA, ABA-GE did not change with the elevation of [CO_2] compared to F[CO_2]. Interestingly, ABA-GE was comparatively higher than ABA content at A[CO_2] and E[CO_2] treatments but not at F[CO_2] (Figure 3.15C) .

In parallel with the ABA measurements, an analysis of GA metabolism was performed (Figure 3.16A-D). Figure 3.16B showed measurements of non-13-hydroxylated gibberellins starting from non-13-hydroxylation pathway intermediates GA_{24} and G_9 to active GA_4 and inactive GAs (GA_{51} and GA_{34}). Although there is a non-significant change in active GA_4 between F[CO_2] and A[CO_2] and between F[CO_2] and E[CO_2]; pathway intermediate GA_9 and inactive GA_{51} decreased significantly with [CO_2] elevation from F[CO_2] to A[CO_2] and from F[CO_2] to E[CO_2] respectively. Thus, indicates potential involvement of GA metabolism towards [CO_2] mediated stomatal closure.

On the other hand, simultaneously occurring 13 -hydroxylation pathway to produce the active and inactive form of GAs showed significant decrease in active GA_1 to pose stomatal closure in response to E[CO_2]. However, the GA intermediates (GA_{19} and GA_{20}) as well as inactive GAs (GA_{29} and GA_8) remained indifferent with [CO_2] elevation (Figure 3.16D) and thus did not direct any point of action.

In summary, the ABA and ABA-GE measurements indicate a negligible change in their content with the elevation of [CO_2] consistent with previous findings (Chater et al., 2015; Hsu et al., 2018). On the contrary, there is a significant change in the amount of active GA_1 (but not GA_4) and some intermediates, indicating that E[CO_2] does modulate GA content.

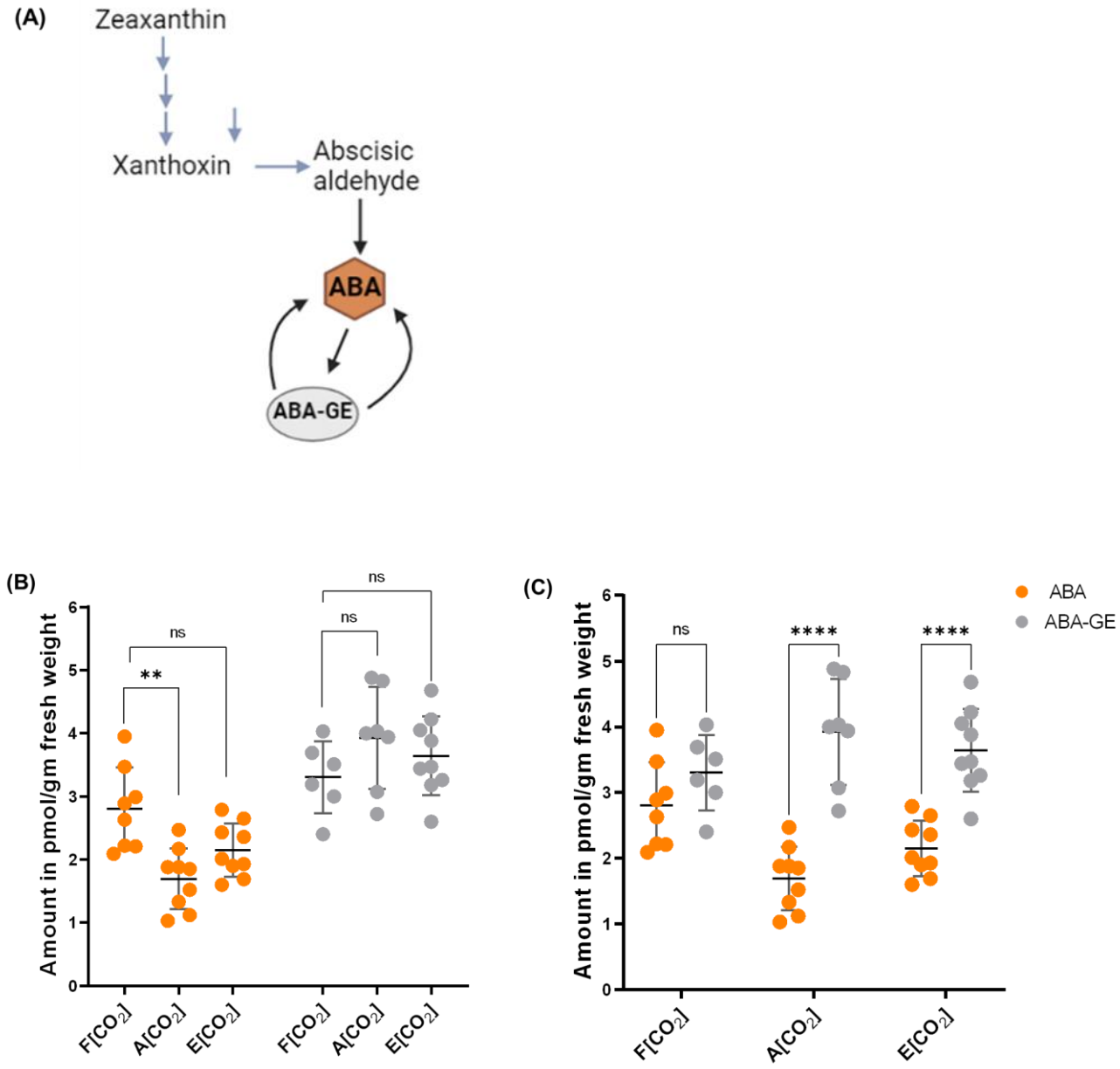

Figure 3.15 ABA and ABA-GE measurements from mature leaf tissue at three different [CO_2]. **(A)** A simplified diagram shows the generalized steps in ABA metabolism where measured components are shown in hexagon shape with bold font (adopted from Dong & Hwang 2014). **(B)** Amount of ABA and ABA-GE measured through UPLC–ESI-MS/MS from mature leaf discs treated with different [CO_2] in line with stomatal bioassay experiments. **(C)** Comparison made between ABA and ABA-GE at each [CO_2] derived from the same data as (B). The number of biological replicates was three/sample, and technical replicates were 3 from each biological replicate. Statistical analysis was conducted using two-way ANOVA with Tukey's multiple comparison tests where the significant difference among means with SD was **< 0.01, ****P < 0.0001 and P ≥ 0.05 was non-significant (ns).

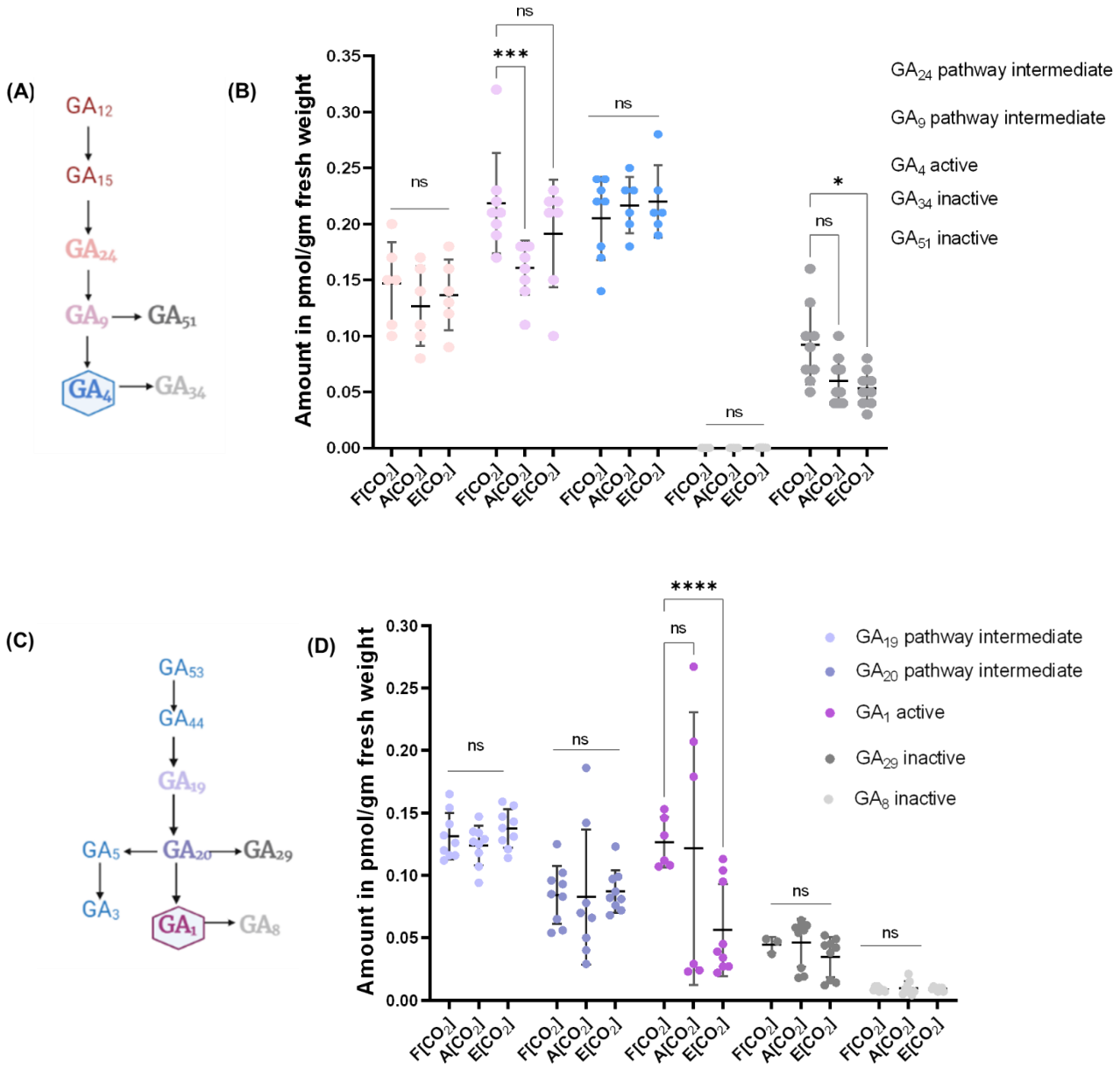

Figure 3.16 Measurement of GAs and their intermediate and inactive forms from mature leaf tissue at three different [CO_2]. **(A)** Steps in the non-13-hydroxylation pathway where bold fonts indicate the measured components and their **(B)** amounts from fresh mature leaf tissue treated with F[CO_2], A[CO_2] and E[CO_2] in a way similar to bioassay experiments using UPLC–ESI-MS/MS. **(C)** Stages in the 13-hydroxylation pathway where measured components are shown with bold fonts and **(D)** their amounts measured through UPLC–ESI-MS/MS from mature leaf disc treated with different [CO_2] in line with stomatal bioassay experiments. The number of biological replicates was three/sample, and technical replicates were three from each biological replicate. Statistical analysis was conducted using two-way ANOVA with Tukey's multiple comparison tests where the significant difference among means with SD was *P < 0.05, ***P < 0.001, ****P < 0.0001 and when P ≥ 0.05 was non-significant (ns). Active GAs shown within a hexagonal shape and other measured GA forms with bold font.

3.10 An analysis of GA metabolism and signalling genes in guard cells

The stages of GA biosynthesis are separated into distinct subcellular compartments starting from plastids to the endoplasmic reticulum and ultimately, the cytoplasm. Additionally, early, and later steps in GA biosynthetic pathway occur in distinct cell types at different stages of plant growth and development. For example, *GA3ox1* is expressed in almost all stages of development whereas *GA3ox2* is primarily expressed in germinating seeds and vegetative tissues (Mitchum et al., 2006). Similarly, components in GA signalling show overlapping as well as distinct functions to repress GA response. For example, *RGA* and *GAI* transcripts are ubiquitous in all tissues whereas, *RGL1/2/3* are present in germinating seeds and/or glowers and siliques (Tyler et al., 2004). Therefore, such subcellular compartmentalization and intercellular separation provide another layer of complexity in GA regulated response in plants.

Stomatal function bioassays involving PBZ application indicate that direct changes in GCs GA metabolism are sufficient to modulate stomatal responses to [CO_2] (section 3.3 and Figure 3.6B). At the same time, IRGA analysis through petiole feeding with GA_3 showed GA can negate E[CO_2]-mediated stomatal closure which suggest that GCs can receive GA from the transpiration stream (section 3.7 Figure 3.13B). This does not rule out that this GA is not taken up by GCs but does open the possibility that other cells can contribute. The Arabidopsis eFP Browser database and data form RNA extracted from the epidermis of 5-week-old Col-0 in which GC were the only living cells, was used to identify which genes in GA signalling and metabolism are putatively expressed in GCs (Winter et al., 2007; Pandey et al., 2010). It's important to remember that there are differences in methodologies to describe gene expression and the level of expression of a gene differed from tissue to tissue.

Table 3.1 List of genes in GA metabolism pathway with different expression levels.

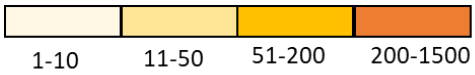

Pathways	Function	Gene name	Locus	GC expression
GA biosynthesis	Terpene synthase	*CPS/GA1*	AT4G02780	
		KS/GA2	AT1G79460	
	Cytochrome P450 monooxygenases	*ATKO1/CYP701A3 /GA3*	AT5G25900	
		KAO/CYP88A3	AT1G05160	
		KAO2 /CYP88A4	AT2G32440	
	2-oxoglutarate-dependent dioxygenases (2ODDs)	*GA20ox1*	AT4G25420	
		GA20ox2	AT5G51810	
		GA20ox3	AT5G07200	
		GA20ox4	AT1G60980	
		GA20ox5	AT1G44090	
		GA3ox1	AT1G15550	
		GA3ox2	AT1G80340	
		GA3ox3	AT4G21690	
		GA3ox4	AT1G80330	
GA catabolism	2-oxoglutarate-dependent dioxygenases (2ODDs)	*GA2ox1*	AT1G78440	
		GA2ox2	AT1G30040	
		GA2ox3	AT2G34555	
		GA2ox4	AT1G47990	
		GA2ox6	AT1G02400	
		GA2ox7	AT1G50960	
		GA2ox8	AT4G21200	
		GA2ox9	AT5G58660	
		GA2ox10	AT3G47190	No data on eFP
GA deactivation	Methyltransferase	*GMAT1*	AT4G26420	No data on eFP
		GMAT2	AT5G56300	
	Cytochrome P450 monooxygenases	*ELA1/CYP714A1*	AT5G24910	
		ELA2/CYP714A2	AT5G24900	
	Fe dependent 2-oxoglutarate-dependent dioxygenases	*GAS2*	AT2G36690	
GA signalling	GA receptors	*GID1A*	AT3G05120	
		GID1B	AT3G63010	
		GID1C	AT5G27320	
	DELLA, GA signalling repressor	*GAI/RGA2*	AT1G14920	
		RGA	AT2G01570	
		RGL1	AT1G66350	
		RGL2	AT3G03450	
		RGL3	AT5G17490	
	OGT, GA signalling repressor	*SPY*	AT3G11540	
	F-box protein	*SLY1*	AT2G17980	
		SLY2/SNZ/SNE	AT5G48170	

The difference in the expression gradient made it difficult to decide what constitutes an appropriate cutoff value to determine whether a gene is actually expressed in the system. For example, the *GA2ox1* expression value was 3.34 whereas for *GA2ox2* and *GA2ox8*, the respective values were 16.55 and 96.49, which is still relatively low. Therefore, a colour gradient scale was set ranging from 1-1500 as determined from gene expression values on the Arabidopsis eFP Browser. Almost every known gene from GA metabolism and signalling was putatively expressed in GC but with varying levels (Table 3.1).

3.11 Discussion

ABA is well studied as a positive regulator of stomatal closure in response to diverse biotic and abiotic stresses (Assmann, 1993; Schroeder et al., 2001); CO_2 responses are altered in plants with differences in ABA levels and so a base level of ABA and ABA signalling has also been shown to be required in high [CO_2]-mediated stomatal closure (Chater et al., 2015; Dittrich et al., 2019). There is also evidence that CO_2 itself sensitises stomata to ABA however, changes in [CO_2] do not causes any change in GC ABA levels and there is controversy as to whether [CO_2] acts via the PYR/RCAR family of ABA receptors to sensitise GCs to ABA (Hsu et al., 2018; Dittrich et al. 2019; Zhang et al., 2020). In this study, an alternative hypothesis has been considered and that rather than ABA, [CO_2] acts on an antagonist of ABA to enhance sensitivity to this ABA response. Although GAs is a known antagonist to ABA action for plant developmental events, e.g., seed germination and dormancy, root growth, flower initiation, shade response and to abiotic stress regulation (Liu & Hou, 2018; Shu et al., 2018; Vishal & Kumar, 2018); there are few studies that have examined the role of this hormone in GC function. GA application enhanced stomatal opening transiently in *Vicia faba* and *Fritillaria imperialis* (Fischer et al., 1990) and in *Commelina benghalensis* L. under darkness (Santakumari & Fletcher, 1987; Göring et al., 1990). In contrast, GA-deficient tomato plants under water stress and Arabidopsis with 10µM of exogenous GA treatment showed no effect on stomatal apertures (Cramer et al., 1995; Tanaka et al., 2006). GA_3 at a concentration ≤0.1µM has been reported to reduce ABA-induced inhibition of stomatal opening in the light in Arabidopsis leaves (Goh et al., 2009). Whilst not focused on CO_2 responses, this data supports the

hypothesis that the homeostatic balance between ABA and GA can regulate stomatal aperture. Also, GA_3 was reported to increase basal stomatal apertures in a DELLA and GID dependent manner (Sukiran et al., 2020). Determination of the optimum GA concentration is critical as the GA concentration in a plant is generally connected with its growth and development through crosstalk among different hormonal signalling pathways (Nemhauser et al., 2006).

Therefore, an initial bioassay experiment was conducted to evaluate the effect of different concentrations of GA_3 (50-100µM) on stomatal aperture responses to [CO_2] and 100µM GA_3 was found to significantly inhibit E[CO_2]-mediated stomatal closure response (Figure 3.4A). Though not directly involve in stomatal response study, the application of 100µM GA_3 from different plant species has been reported to mitigate environmental stresses like salt and heavy metals as well as in GA metabolism research (Silverstone et al., 2001; Wen & Chang 2002; Rieu et al., 2008; Ali et al., 2015; Saleem et al., 2015; Xu et al., 2016; Wang et al., 2019). Based on present findings and concentrations used in the literature, 100µM GA_3 was therefore chosen for subsequent experiments. Whilst 100µM GA_3 may seem excessive, even with the recent development of GA biosensors (Rizza et al., 2021), cellular GA levels have not been determined. Furthermore, the uptake capacity of guard cells for GA_3 is not known and this is also not the bioactive form in Arabidopsis. GA_4, which is one of the main bioactive forms (Talon et al., 1990), did elicit the same response as GA_3 (Figure 3.4C) and it would be interesting to determine whether GCs show enhanced sensitivity to GA_4 over GA_3. The concentrations used in this study are comparable with those used in a number of studies investigating the action of GA and involving exogenous GA application. The concentration of GA used is not significantly outside that expected within some cells as determined by the GPS GA biosensor developed by the lab of Alexander Jones (Rizza et al. 2021 - 18uM GA_4 is predicted for some cells). This same paper also highlights this issue of differential cell permeability to GA, so whilst endogenous levels may be lower than those that are exogenously applied (and potentially only 5x), there is always the question of how efficiently exogenously applied hormones are taken up by the target cells and tissue. When considering mass spec data (Figure 3.16), it must also be appreciated that the quantity is comparative to fresh weight, much of which will be apoplastic water and cell wall material and so result in a significantly lower concentration than may be found in cells themselves.

Addition to exogenous application of GA, transgenic manipulation of GA levels was also shown to inhibit E[CO_2] promotion of stomatal closure. Whilst still not an absolute demonstration of an *in vivo* role of GA in this response, the use of the β-estradiol inducible pUBQ-XVE-GA20ox1-P2A-GA3ox1 line (Rizza et al., 2021), demonstrates that endogenous GA levels also have the potential to modulate E[CO_2] responses (Figure 3.5). Finally, inhibitors of GA biosynthesis (namely, PBZ and DMZ) showed positive effects towards E[CO_2]-mediated stomatal closure (Figure 3.6B).

Mutants in the GA metabolism and signalling also added to our understanding of participation of GA regulation in E[CO_2]-mediated stomatal closure. GA biosynthesis is a complex procedure completed in three different organelles of plant tissue involving terpene synthases (TPSs), cytochrome P450 monooxygenases (P450s) and groups of 2-oxoglutarate-dependent dioxygenases (2ODDs). Maintenance of effective regulation of bioactive GAs deactivation is also crucial, and this is mediated primarily by a class of 2ODDS, GA 2-oxidases (GA2oxs) (Yamaguchi, 2008). *ga2oxq* has been reported to produce more GAs and elongated hypocotyls (Rieu et al., 2008) in Arabidopsis, and overexpression resulted in lower GAs in rice and Arabidopsis associated with dwarf phenotypes (Schomburg et al., 2003; Lo et al., 2008). Further, upregulation of *GA2ox* genes by different stresses indicates a dynamic change of GA metabolism (Li et al., 2019). Here, a *ga2oxq* mutant was shown to be insensitive to E[CO_2]-mediated stomatal closure (Figure 3.8), suggesting that the ability to breakdown active GAs is required in order for GCs to respond to E[CO_2]. Stomatal density showed no change between *ga2oxq* and Col-0 (Supplementary 2.11) indicating the mutation does not affect stomatal number.

Bioactive GAs in plants are also maintained through feedback and forward regulation of GA metabolism (Hedden & Phillips, 2000; Olszewski et al., 2002). GA signalling components required for this homeostatic regulation are the GID1 receptors, DELLA proteins and the F-box protein SLEEPY1 (SLY1) (Sun & Gubler, 2004; Ueguchi-Tanaka et al., 2007) DELLAS are well-known repressors of many GA-dependent plant responses (Achard & Genschik, 2009). However, GA-induced increase in $[Ca^{2+}]_{cyt}$ were observed in transgenic plants expressing a mutated degradation-resistant version of RGA (RGAD17) and in the *della* quintuple mutant, suggesting the presence of a DELLA-independent pathway in Arabidopsis (Okada et al., 2017). In tobacco, Ca^{2+}-dependent protein kinases (NtCDPK1) was found to be phosphorylated in

response to GAs in plants and auto phosphorylated *in vitro* (Ishida et al., 2008; Ito et al., 2014, 2017), again suggestive of a DELLA-independent pathway. This is relevant because the bioassay data indicates that, unlike with the *ga2oxq* mutant, stomata of the *dellaq* mutant are still responsive to E[CO_2] mediated stomatal response (Figure 3.9). However, analysis of the stabilised DELLA lines, in particular 35TAP_RGAΔ17 (Feng et al., 2008) found that these were relatively insensitive to E[CO_2] (Figure 3.10). This provides evidence both for and against DELLA requirements for responses to E[CO_2]. Further data from the Casson lab has recently shown that *sleepy* mutants are also relatively insensitive to [CO_2] (data not shown) and this may indicate that it is the stability of the DELLAs that is important for responses to [CO_2], rather than their absence. Stomatal density count showed no change between Ler and *dellaq* though the stable lines had significantly higher count (Supplementary 2.12 and 2.13 respectively). However, stomatal index measurements would be required to clarify whether stomatal development is affected or not.

ROS are known to be required for GC ABA-responses and are also produced during bicarbonate-induced stomatal closure (Pei et al., 2000; Zhang et al., 2001; Kwak et al., 2003; Kolla et al., 2007). They are also reported to be involved in cross-talk between ABA and high [CO_2]-mediated stomatal closure (Chater et al., 2015; Ehonen et al., 2019). Moreover, GA has been reported to modulate ROS levels in regulating cell growth, stress tolerance and seed germination (Fath et al., 2001; Schopfer et al., 2001; Achard et al., 2008; Li et al., 2018). Present data supports the existing literature with regards to the connection between ROS and E[CO_2]-mediated stomatal function. Though PBZ appeared to enhance ROS at F[CO_2] but did not change significantly with [CO_2] elevation. GA_3 appeared not to block the ROS production as expected with inhibition of closure in response to E[CO_2] (Figures 3.11A and B). This suggests GAs do not act via ROS regulation to negate E[CO_2]-mediated stomatal closure. The extracellular H_2O_2 (eH_2O_2) activated Ca^{2+} currents in GCs were reported to mediate stomatal closure induced by ABA in Arabidopsis (Pei et al., 2000). And eH_2O_2 sensor HPCA1 is required for such eH_2O_2 mediated increase of cytosolic [Ca^{2+}] during stomatal closure (Wu et al., 2020). Therefore, [CO_2] sensitivity of *hpca1* stomata could provide a regulatory cascade for E[CO_2] mediated stomata closure. Though not very straight forward, our data supported the involvement of HPCA1 in promoting stomatal closure responses to E[CO_2] (Figure 3.12A and B). Since HPCA1 is a sensor for

extracellularly produced H_2O_2 to initiate downstream Ca^{2+} signalling E[CO_2]-mediated stomatal closure is likely to work via Ca^{2+} dependent pathway. However, collectively the data here demonstrates that the ability of GA to antagonise E[CO_2]-mediated stomatal closure is likely to be ROS-independent, though a role in regulating Ca^{2+} signalling remains to be investigated. Stomatal density determined no change between Col-0 and *hpca1* (Supplementary 2.14) indicating that absence of HPCA1 do not affect stomatal number, though stomatal index measurements would be required to clarify whether stomatal development is affected.

With involvement of GAs in modulating E[CO_2]-mediated stomatal closure response in GCs, the next question arises about the source of GA. Does GA negatively regulate E[CO_2]-mediated stomatal closure in GC only or could it work in whole leaves? Therefore, an attempt was made to measure whole leaf g_s fed with either GA_3 or PBZ. Using this system, the g_s of wholes leaves fed with GA_3 showed a reduction in sensitivity to E[CO_2] (Figures 3.13B and C) and supports the potential for non-GC derived GA, though it does not exclude the possibility that this petiole fed GA_3 mediates it's effect by being taken up by GCs. However, no significant effect of PBZ was observed from the petiole feeding experiment (Figure 3.13D and E). The reasons might be that the g_s for the treated samples was already reduced due to PBZ treatment on the day before experiment. Interestingly, stomatal function bioassay with PBZ supports the role of GC GA as being important for responses to [CO_2]. Additionally, other stomatal function bioassays with GA application and alteration by using GA mutants support the involvement of GC derived GAs. Analysis of the expression pattern of GA metabolism genes in GC determine that though there is difference in gene expression levels, almost all the genes are expressed in GC (Table 3.1). Thus, it is plausible to conclude that GC derived GA is sufficient to modulate GC response to high [CO_2] but other tissues may also be involved. Existing literature also support the correlation between GC metabolism and mesophyll signals in stomatal responses under a range of different conditions for C_3 and CAM species (Wong et al., 1979; Farquhar & Wong, 1984; Mansfield et al., 1990; Buckley et al., 2003; Santos et al., 2021). Experimental data also that showed that isolated peels have altered responses to RL or [CO_2] compared to those reported for intact leaves (Lee & Bowling, 1992; Olsen & Junttila, 2002; Roelfsema et al., 2002; Mott et al. 2008).

Next, gene expression analysis of GA metabolism genes from mature leaf tissue provided insights into changing gene expression patterns in response to E[CO_2] (Section 3.8). Though direct correlation was not observed across different GA metabolism genes, a trend of upregulation of GA repressors with [CO_2] elevation was observed (Figure 3.14). However, the mRNA expression of GA metabolism and signalling genes reported to be negligibly affected by e[CO_2] in Arabidopsis (Ribeiro et al., 2012). Reasons might be the difference in [CO_2] i.e., 750ppm as opposed to 1000ppm used in this study alongside differences in growth conditions and GA_3 treatment.

Whilst transcriptional analysis can be informative, gene expression and metabolic pathways can be regulated by other mechanisms. According to the hypothesis the balance between ABA and GAs regulates E[CO_2]-mediated stomatal response. The amount of ABA remained unchanged at E[CO_2] treated leaf tissue compared to F[CO_2] samples (Figure 3.15 A and B), similar to existing researches that reported no change of ABA with elevation in [CO_2] (Chater et al., 2015; Hsu et al., 2018). Also, the inactive or storage form of ABA, i.e., ABA-GE, remained unaltered with an increase in [CO_2] (Figure 3.15 A and B), indicating no change in ABA and their conjugates in our experimental system. Measurement of GAs from both 13-hydroxylated and non-13-hydroxylated pathways was conducted (Figure 3.16 B and D). Though no significant change was found for 13-hydroxylated GA_4, a significant decrease was observed in pathway intermediate GA_9 when [CO_2] increased to the ambient level. And 13-hydroxylated active GA_1 significantly decreased at E[CO_2] samples compared to F[CO_2] samples. Both GA and ABA content have been shown to change in response to elevated [CO_2] (~800 mu mol mol^{-1}) in other plants species. For example, GAs have been reported to increase, whereas ABA decreased in *Gingko biloba*, rice and tall fescue connecting with photosynthesis and growth increment (Li et al., 2011; Yu et al., 2019; Qi et al., 2021). Interaction of phytohormones is known to modulate stomatal apertures like ABA, and jasmonic acid (JA) are known to act antagonistically in the RL-induced stomatal opening (Zhu et al., 2019), while ABA and JA act synergistically to trigger stomatal closure in response to elevated [CO_2] (Geng et al., 2016). This is the first report of the involvement of GAs, known antagonists to ABA, to alter E[CO_2]-mediated stomatal closure where their decrease sensitise the closure response of stomata without changing the ABA amount. The existing literature demonstrates an

interaction between carbon metabolism and GAs synthesis with a positive relation between GA synthesis and carbon metabolism during the nighttime (Paparelli et al., 2013; Prasetyaningrum et al., 2021). Increased GA at night may help stomata be less inhibited by increased Ci due to nighttime respiration and help stomata to open more on next morning. At the same time GA metabolism genes were reported to express variably across the day e.g., GA3ox1 was reduced at daytime (Prasetyaningrum et al., 2021). This might sensitise the stomata to remain more open at daytime in response to reduced Ci as result of photosynthetic efficiency. Thus, under varying carbon availability GAs has the relevance to modulate stomatal aperture and ultimately their growth.

3.11.1 Concluding Remarks

1. GAs inhibit E[CO_2]-mediated stomatal closure in the epidermis and the whole leaf system.
2. GA inhibition of E[CO_2]-mediated stomatal closure requires GA2ox genes and may be mediated by changes in expression of genes involved in GA metabolism.
3. GAs may act in a DELLA-independent pathway without ROS participation in the studied physiological response.
4. Active GA1 content is reduced under E[CO_2] with no change in ABA.

Chapter 4. A role for phyB in regulating stomatal aperture responses to elevated [CO_2]

4.1 Introduction

Regulation of the stomatal aperture is a complex process integrating an array of environmental cues, including light quantity and quality, [CO_2], temperature and vapour pressure deficit (VPD) (reviewed in Lemonnier & Lawson, 2023). For light, it has been determined that stomata open in response to both red and blue wavelengths, though blue light (BL) and red light (RL) responses have different fluence responses (Matthews et al. 2020). PHOTOTROPIN (PHOT) photoreceptors perceive BL to activate PM bound H^+-ATPase present in GCs, activating inwardly rectifying K^+ channels. The uptake of K^+ is accompanied by GCs accumulating both Cl^- and malate[2], which is believed to be generated by starch breakdown (Kinoshita et al., 2001; Shimazaki et al., 2007; Horrer et al., 2016; Santelia & Lawson, 2016). The BL response is independent of photosynthesis as it saturates at very low fluence rates incapable of driving net carbon assimilation for photosynthesis (Matthews et al., 2020). On the contrary, the RL response occurs at high fluence rates and is reported to be dependent on photosynthesis because it is abolished by treatment with the PSII inhibitor 3-(3,4-dichlorophenyl)-1,1-dimethylurea (DCMU) (Sharkey & Raschke, 1981; Schwartz & Zeiger, 1984; Tominaga et al., 2001; Olsen et al., 2002).

As well as RL driven photosynthetic responses, there is also evidence for the direct involvement of the red/far-red photoreceptor phyB in RL-mediated stomatal opening response (Wang et al., 2010). phyB was shown to act in concert with phyA and the BL receptors CRY and PHOT to regulate stomatal opening under white light, suggesting the presence of common components between the RL and BL signalling pathways (Wang et al., 2010; Chen et al., 2012). Collectively, this indicates roles for both photoreceptors and photosynthesis in light-mediated stomatal opening.

Inarguably stomatal response link and coordinate with mesophyll demand for CO_2, and higher irradiance positively regulates carbon assimilation rates and drives down the [CO_2] within the leaf. PHOT driven BL responses and stomatal responses to low [CO_2] have been shown to interact through two kinases, CONVERGENCE OF BLUE LIGHT AND CO_2 1 and 2, demonstrating links between photoreceptor and [CO_2] responses (CBC1/2; Hiyama et al., 2017). Interestingly, previous work from the Casson lab demonstrated that *phyB-9* mutants have a hypersensitive response towards E[CO_2]-

mediated stomatal closure, whilst plants overexpressing phyB (35SphyB) are less sensitive to this signal (Brown, 2018). Figure 4.1 shows the respective data as follows:

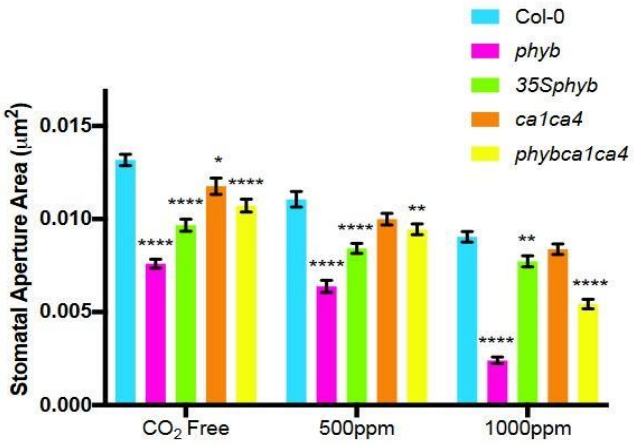

Figure 4.1 Stomatal aperture area of mature leaves for Col-0, *phyB*, 35SphyB, *ca1ca4* and *phyBca1ca4.* Plants were grown at 130 μmolm^{-2}s^{-1} light and 500 ppm CO_2. Epidermal peels of the plants were subjected to [CO_2] free air, 500ppm and 1000ppm. The bar graphs show the stomatal aperture area plotted against each [CO_2] treatment. Mean values are shown for each genotype (n = 120) with error bars indicating mean +/- SEM. Symbols indicate significant difference in aperture area compared with Col-0; one-way AVOVA with post-hoc Dunnett's test, (p*= ≤ 0.05, p**= ≤ 0.01, p***= ≤ 0.001, p****= ≤ 0.0001). (Adopted from Brown, 2018).

However, no distinct signalling components have been reported downstream of the RL perceiving phytochromes that regulate GC responses to [CO_2]. Findings from the previous chapter demonstrated that E[CO_2] can mediate changes in GA metabolism and propose that this enhances sensitivity to ABA to promote GC closure. Phytochromes are known to regulate ABA and GA in an opposite manner during seed germination (Dong et al., 2008; Hedden, 2020; Li et al., 2022; Sano & Marion-Poll, 2021). However, such regulation differs at different stages of plant life alongside to various external stimuli. For example, phyB can positively regulate ABA biosynthesis and signalling in shoots to synchronize shoot and root growth in response to unfavourable light exposure (Ha et al., 2018). phyB is also known to positively regulate both GA and auxin biosynthesis during hyponastic leaf movement (Küpers et al., 2023). However, light is also known to negatively regulate GA to stabilise DELLAs to

inhibit Arabidopsis hypocotyl growth (Achard et al., 2007). Thus, it is evident that phyB may regulate ABA and GA either positively or negatively in many physiological and developmental responses.

Therefore in this chapter, we hypothesise that phyB regulates ABA:GA homeostasis in GCs and changes to this homeostasis in *phyB* mutants leads to the hypersensitive response of *phyB* stomata to E[CO_2] (Figure 4.2).

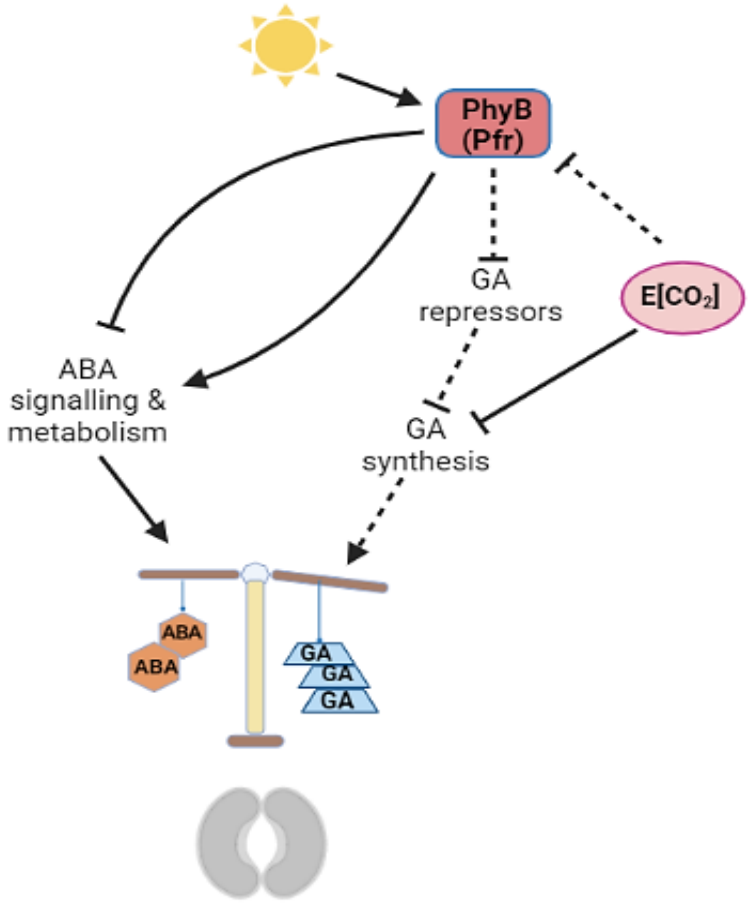

Figure 4.2 Conceptual events showing the stomatal closure involving light signals and hormonal regulation. The proposition states E[CO_2] either directly repress GA production during stomatal closure response or regulates phyB active form to down-regulate GA synthesis (this latter possibility is not directly tested in this work). Conversely, phyB may act via ABA to alter sensitivity to E[CO_2] but collectively the outcome is for a change in ABA: GA homeostasis, which may modulate GC sensitivity to E[CO_2]. Arrows for up-regulation, barred lines for down-regulation and dotted bar lines indicate hypothesised negative regulation. Image “Created with Biorender.com”.

4.1.2 Objectives

The following objectives put forward to test the hypothesis:

1. Investigate whether GA affects GC sensitivity of *phyB*-9 to E[CO_2].
2. Determine whether the hypersensitive closure response of *phyB-9* mutants to E[CO_2] is due to changes in ABA or GA metabolism.

4.2 Role of phyB in stomatal aperture response to E[CO_2]

The enhanced sensitivity of *phyB-9* mutant stomata to E[CO_2] (Brown, 2018), indicates that phyB is required for wild-type responses to E[CO_2]. This previous work had analysed the stomatal response to changes in [CO_2] for both *phyB* mutants and plants overexpressing phyB (35SphyB; data shown in Figure 4.1), which strongly support a role for phyB in stomatal responses to E[CO_2]. However, following the completion of this work, a second site mutation in the *VENOSA4* gene was identified in the *phyB-9* mutant that affects various leaf traits (Yoshida et al. 2018). Therefore, to further confirm the role of phyB in regulating stomatal responses to [CO_2], a [CO_2] response bioassay was performed on a transgenic line in which the *phyB-9* mutant was complemented with a *PHYBproPHYB:YFP* transgene (*phyB*$_{comp}$, unpublished line, Casson lab). Here, the *PHYB* cDNA was translationally linked to YFP and placed under the control of 2.1kb of upstream sequence. In this bioassay, the *phyB*comp line behaved like the wild-type under F[CO_2] and E[CO_2], though it had a slightly reduced pore area at A[CO_2]. By way of contrast, *phyB-9* mutants had reduced pore areas under all [CO_2] treatments (Fig. 4.3A). By normalising the response of each genotype to their F[CO_2] control, *phyB-9* mutants were observed to be relatively more sensitive to E[CO_2] compared to both Col-0 and the complemented line (Fig. 4.3B).

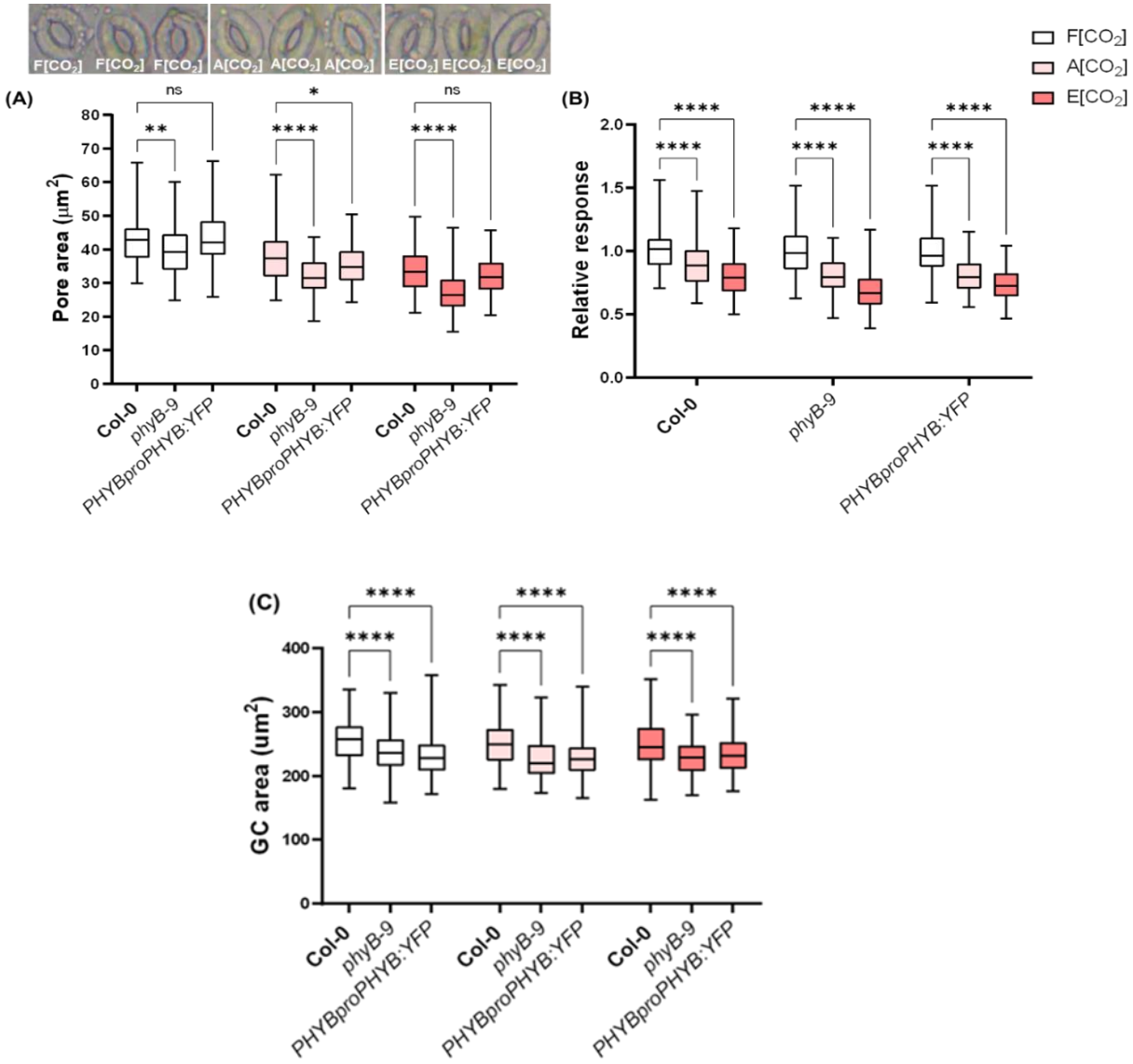

Figure 4.3 Stomatal function response of phytochromeB-9 complemented line in *phyB-9* mutant background towards the elevation of [CO_2]. (A) Epidermal peels from mature leaves of Col-0, *phyB-9* and the complemented *PHYBproPHYB:YFP* line were incubated in an opening buffer under F[CO_2] for 2 hours followed by incubation with A[CO_2] and E[CO_2] for another 2 hours to measure pore area. Pore areas from Col-0 were separately compared to *phyB-9* and the *phyB*comp line under three different [CO_2]. **(B)** CO_2 responsiveness of studied genotypes relative to their F[CO_2] treated samples derived from the same data as (A). **(C)** GC area of Col-0, *phyB-9* and *phyB*comp line under three [CO_2] conditions from the same stomata measured to analyse for data (A). Number of stomata measured n=120. Statistical analysis was conducted using two-way ANOVA with Tukey's multiple comparison tests, where comparisons were made between genotypes in (A) and (C) and between [CO_2] treatments in (B). The adjusted P values were *P < 0.05, **P < 0.01, ****P < 0.0001 and P ≥ 0.05 were non-significant (ns).

The GC area measurement showed that the *phyB-9* mutant and *phyB*comp line both had significantly smaller GC areas than Col-0 (Figure 4.3C). Whilst the *phyB*comp line rescued GC CO_2 responses, as determined by pore area measurements (Figure 4.3A), the GCs of this line were still smaller than those of the WT and not significantly different to those of the *phyB-9* mutant. This could be due to incomplete complementation of the mutant phenotype within this complementation line or may indicate that GC size itself is regulated by second site mutations within the phyB-9 line, which have been reported (Yoshida et al. 2018). It should be noted that GC pore area of 35SproPHYB plants were less sensitive to CO_2 (Brown, 2018), which collectively supports the role of phyB stomatal aperture responses to CO_2.

4.3 The hypersensitivity of *phyB-9* mutant stomata to E[CO_2] is rescued by GA treatment

There is evidence of coordinated regulation of light, GA and ABA signalling in plant developmental processes, and phyB is one of the significant regulators between ABA and GA homeostasis (Seo et al., 2006, 2009; Lau & Deng, 2010; Lee et al., 2012; Zhao et al., 2022). We already observed the involvement of phyB in stomatal physiology towards E[CO_2]-mediated closure response (Figure 4.3A), whilst the previous chapter demonstrated that GA inhibits E[CO_2]-mediated stomatal closure of Col-0 (Section 3.2). Therefore, it is relevant to investigate whether GA affects the hypersensitive stomatal closure response observed in *phyB-9*.

To analyse the impact of GA on *phyB-9* responses to [CO_2], the stomatal bioassay system was again utilised, as described in section 3.2 with peels incubated in the presence of mock treatment (0.1% ethanol) or 100µM GA_3. Use of different concentrations of GA3 (50-200 µM) in stomatal function bioassay demonstrated 100 µM as optimum for present study (Figures 3.2 and 3.3). As expected, the *phyB-9* pore area decreased with increasing [CO_2] in the presence of the mock treatment. Incubation in the presence of 100µM GA_3 resulted in a significant increase in pore area at E[CO_2] compared to the mock-treated samples. However, the same GA_3 treatment did not significantly change the pore area under both the F[CO_2] and A[CO_2] treatments (Figure 4.4A). The relative stomatal response of GA_3 treated samples

compared with their respective mock treatments at each [CO_2] condition was drawn using the same data as Figure 4.4A and confirms that GA_3 antagonises E[CO_2]-mediated stomatal closure response in *phyB-9* (Figure 4.4B). Pore area measurement from both lines were drawn on same graph to determine whether GA_3 application can reverse the hypersensitivity of *phyB-9* to that of Col-0. 100µM GA_3 inhibited E[CO_2]-mediated closure response in both lines (Figure 4.4C). Interestingly, *phyB* mutants treated with GA_3 had a similar pore aperture to E[CO_2] mock-treated Col-0 GCs but not to those also treated with GA_3. Therefore, it can be deduced that the effect of GA_3 is specific to E[CO_2] and, as was the case with Col-0, can partially inhibit the stomatal closure response. This data may also suggest that *phyB* has a reduced level of GA compared to Col-0 and this explains the rescue to mock and not GA_3 treated WT levels.

To determine whether the hypersensitivity of *phyB*-9 to E[CO_2] is due to changes in the expression of genes involved in GA metabolism and signalling, a qRT-PCR approach was taken. Since, the g_s of wholes leaves fed with GA_3 showed a reduction insensitivity to E[CO_2] in Col-0, qRT-PCR was performed alongside the analysis performed on Col-0 (Chapter 3, Fig. 3.14). Therefore, bioassay-aged *phyB-9* plants grown at A[CO_2] were transferred to E[CO_2] for 2 hours, 6 hours and 24 hours before RNA was extracted from mature leaves; samples were also taken from plants retained in the A[CO_2] conditions at these same times. The expression of several genes known to regulate GA metabolism was checked and compared with Col-0 samples. Representative of GA biosynthesis genes, *GA3ox1* and *GA3ox2* appeared to have lower expression compared to Col-0 at 6hours and 24hours treatment. GA catabolism gene *GA2ox1* also appeared to be less compared to Col-0. However, the expression of both *RVE1* and *RVE2*, which have been reported to repress expression of the GA biosynthesis gene *GA3ox2* during phyB-mediated seed dormancy and germination (Jiang et al., 2016), showed differential expression whilst the GA signalling gene *GAI* (one of the DELLAs) remained similar to Col-0 (Figure 4.5).

The gene expression analysis here does not provide strong evidence that the enhanced sensitivity of *phyB-9* stomata to E[CO_2] is driven by the regulation of these particular genes, though it is possible that it could affect other genes that regulate GA metabolism or signalling.

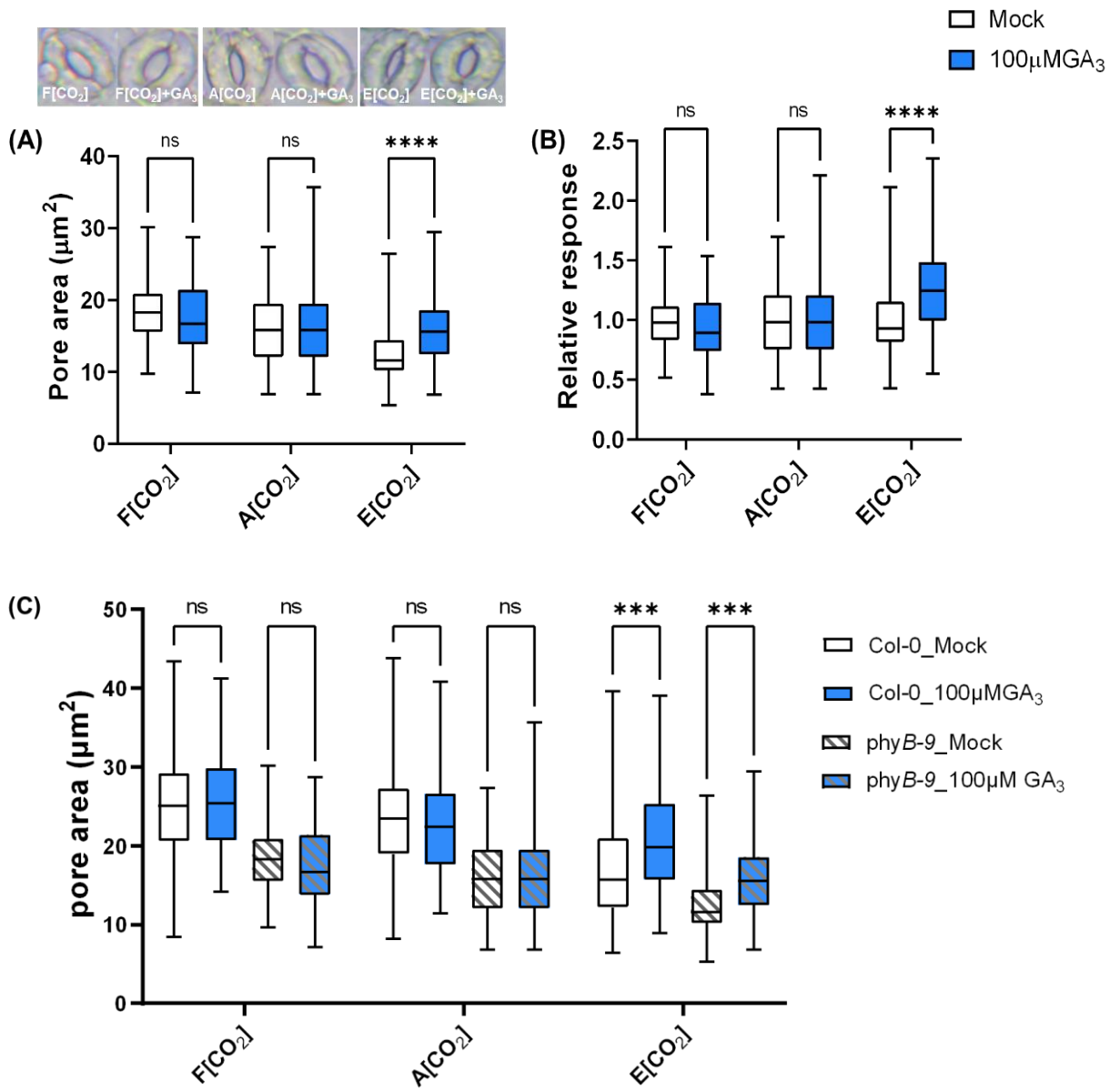

Figure 4.4 Effect of exogenously applied GA_3 on stomatal closure response at different $[CO_2]$. **(A)** Epidermal peels from *phyB-9* mature leaves were incubated in F[CO_2] air with mock treatment (0.1% ethanol) or 100µM GA_3 for 2 hours before the application of A[CO_2] and E[CO_2]. Pore area was measured 2 hours following the [CO_2] treatments. Pore area was measured and compared between the mock and GA_3 treatments at each of the [CO_2] condition. **(B)** Relative response of 100µM GA_3 treated samples in proportion to their respective mock treatment at each of the three different [CO_2] treatments using the same data as (A). **(C)** Pore area measurement of both Col-0 and *phyB-9* derived from same data as figure 3.2A and figure 4.4A and compared between the mock and GA_3 treatments at each of the [CO_2] conditions. Total number of stomata measured n=120. Statistical analysis was conducted using two-way ANOVA with Šídák's multiple comparison tests. The adjusted significant P value was ****P < 0.0001, and P ≥ 0.05 was non-significant (ns).

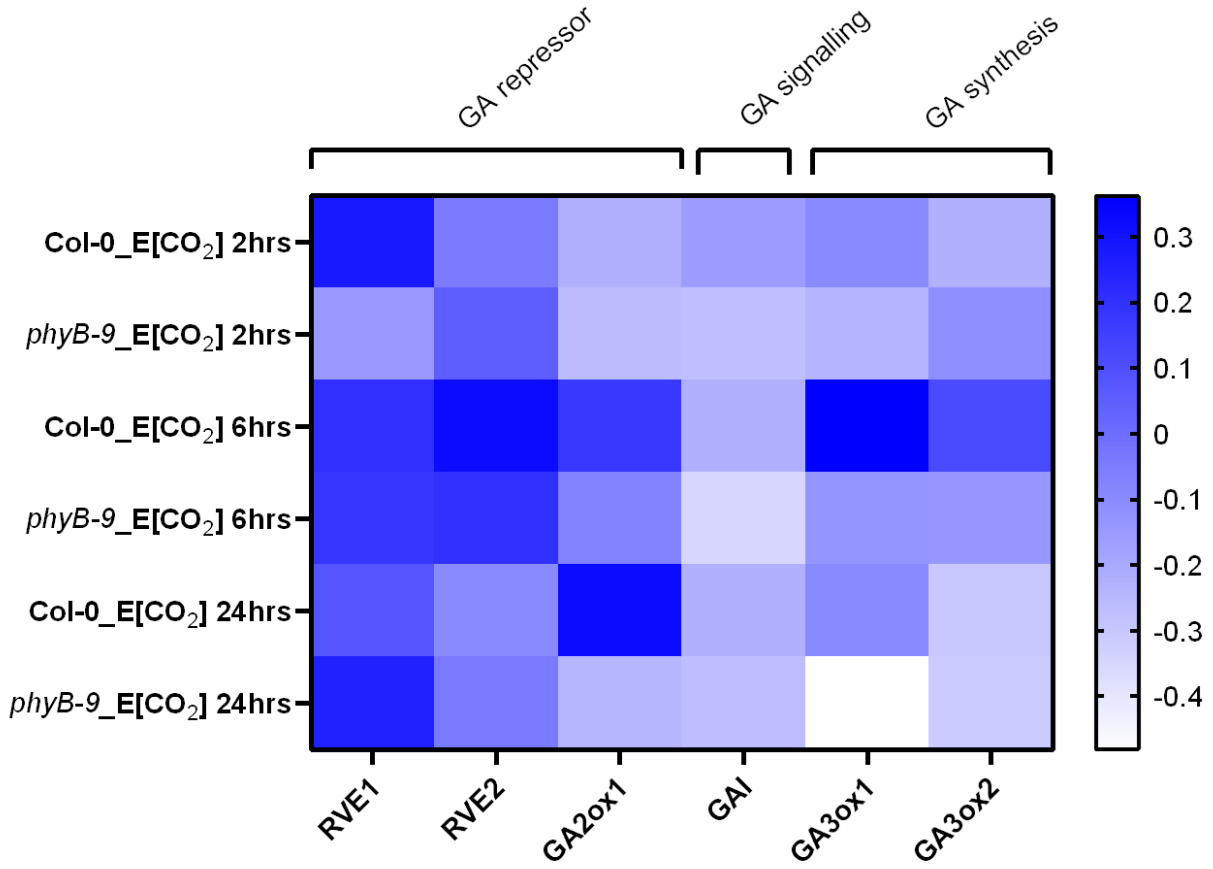

Figure 4.5 Effect of E[CO_2] under three time periods on genes involved in GA metabolism. Heatmap showing differential expression of representative genes in GA metabolism and signalling after the transfer of Col-0 and *phyB-9* plants from A[CO_2] to E[CO_2] treatment for three different periods. Gene expression of *phyB-9* was analysed relative to Col-0 expression at respective [CO_2] treatment. Here biological replicates n=3 and each has 3 technical replicates. An expression value of 0 (derived from log10 values of normalised A[CO_2] treated samples) was used as a baseline to demonstrate the upper and lower expression of genes according to the colour scale gradient.

4.4 phyB modulates leaf ABA and GAs contents in response to E[CO_2]

The previous section demonstrated that, as with the wild type, GAs can partially inhibit stomatal closure under E[CO_2] in *phyB-9* mutants. Whilst the gene expression analysis was not particularly informative, given phyB's known roles in regulating ABA: GA homeostasis (reviewed in Zhao et al., 2022), it remains possible that the hypersensitive phenotype of *phyB-9* mutants could be due to changes in ABA and/or GA metabolism (Figure 4.2). Therefore, ABA and GAs content was measured in mature leaf tissue of *phyB-9* through mass spectrometry analysis under three different [CO_2] treatments; the same analysis as was performed on Col-0 leaves (see section 3.9).

No significant change in the amount of ABA was observed in *phyB-9* leaf tissue under the different [CO_2] treatments and ABA levels were similar in *phyB-9* and Col-0 (see section 3.9). However, ABA-GE (the ABA storage or transport form) was found to decrease significantly at E[CO_2] compared to F[CO_2] treated samples in *phyB-9*. This raises the possibility that phyB may be involved in regulating ABA levels through conjugation under different [CO_2] (Dong & Hwang, 2014), though there was no reciprocal change in free ABA. Interestingly, a higher amount of absolute ABA-GE than ABA was visible across all the [CO_2] treatments (Figure 4.6B). Even the ABA-GE amount was considerably higher in *phyB-9* than Col-0 at F[CO_2] and A[CO_2], correlating with the involvement of ABA-GE towards smaller aperture of *phyB-9* (Fig. 4.3A). Thus, absolute amount of ABA-GE and its change under E[CO_2] suggests a potential involvement of conjugated ABA towards E[CO_2]-mediated hypersensitive closure response in *phyB-9*. Comparison of ABA amount between Col-0 and *phyB-9* determines no significant change whereas, ABA-GE was comparatively higher at the [CO_2] treatments in *phyB-9* (Figure 4.6C). Thus, ABA-GE is proved to be a potential factor rather than ABA between the lines to explain *phyB-9* hypersensitivity closure response compared to Col-0.

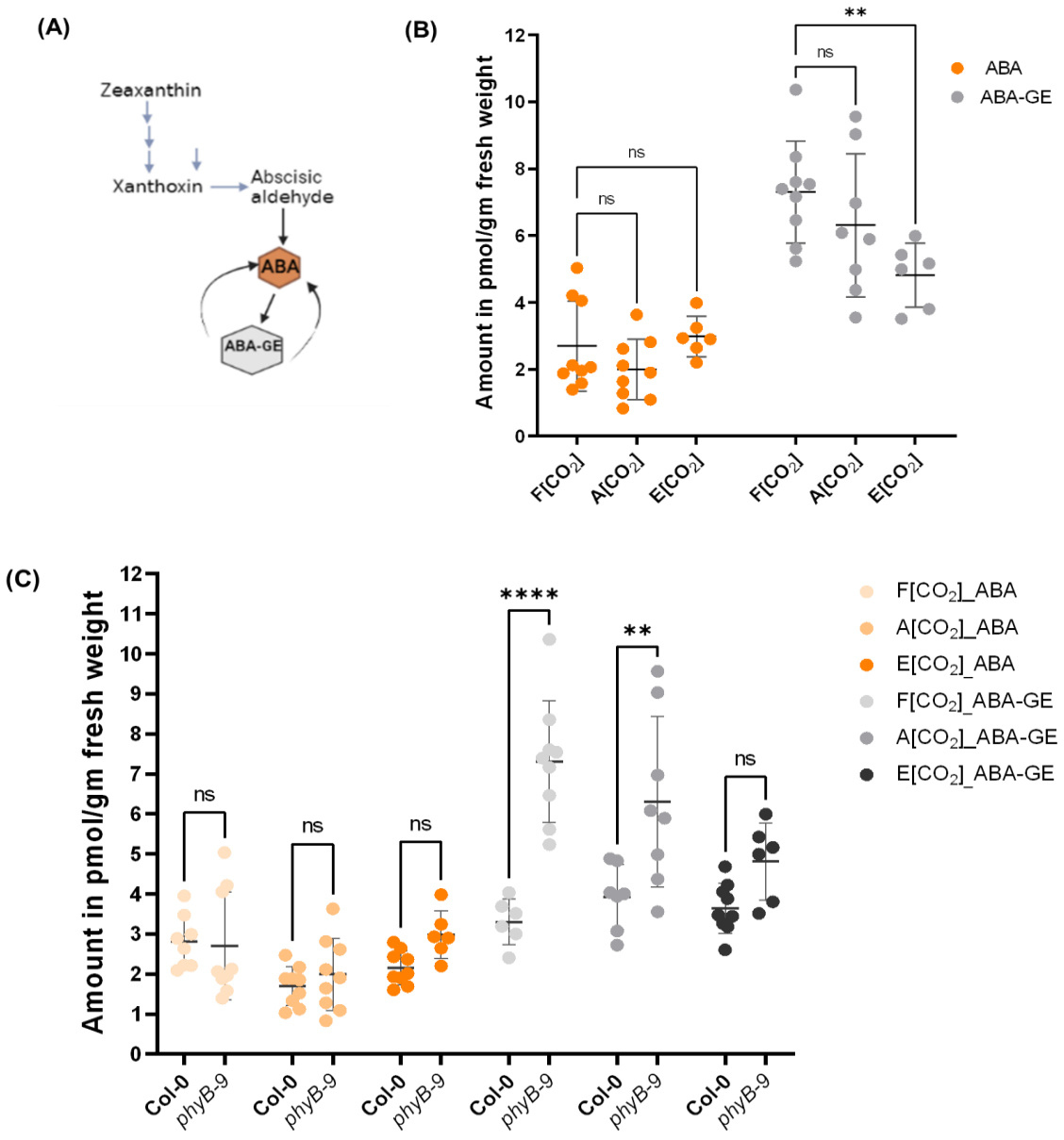

Figure 4.6 ABA and ABA-GE measurements from mature leaf tissue at three different [CO_2]. (A) A simplified diagram adopted from Dong & Hwang 2014 shows the steps in ABA metabolism where measured components are shown in hexagon shape with bold font. **(B)** ABA and ABA-GE content as measured through UPLC–ESI-MS/MS from mature leaf disc of *phyB-9* treated with different [CO_2] in line with stomatal bioassays. **(C)** Amount of ABA and ABA-GE from mature leaf disc of Col-0 and *phyB-9* treated with different [CO_2] similar to bioassay experiments using UPLC–ESI-MS/MS and comparison made between the genotypes at F[CO_2], A[CO_2] and E[CO_2]. The number of biological replicates was three/sample, and technical replicates were three from each biological replicate. Statistical analysis was conducted using two-way ANOVA with Tukey's multiple comparison tests. The adjusted significant P-value among means with SD was **P < 0.01, and P ≥ 0.05 was non-significant (ns).

As well as ABA, GAs was also measured. The non-13-hydroxylation pathway starting from GA_{12} occurs in the cytoplasm and a simple flow diagram is shown in Figure 4.7A. The content of the pathway intermediate GA_{24} did not change under the different [CO_2] treatments, but the intermediate GA_9, which is the direct precursor of active GA_4, shows a significant reduction at A[CO_2] and E[CO_2] compared to F[CO_2]. In line with the reduction in GA_9, active GA_4 also decreased with increasing [CO_2] (Figure 4.7B). This evidenced E[CO_2] lowered active GA with a potential point of action. However, the pathway's inactive GAs (GA_{34} and GA_{51}) remained the same with [CO_2] change.

In contrast to the non-13-hydroxylation pathway, all the measured pathway intermediates (GA_{19} and GA_{20}), active GA (GA_1) and inactive form of GA (GA_{29} and GA_8) during 13-hydroxylation pathway of GA biosynthesis (Figure 4.7C) showed no significant change with [CO_2] elevation (Figure 4.7D). Such observations indicate that in *phyB-9,* non-13-hydroxylated GAs might play a role towards high [CO_2]-mediated stomatal closure response. However, To further clarify the involvement of active GAs towards the hypersensitive closure of *phyB-9* in response to E[CO_2], the measured active GAs were compared between the wild-type and the mutant at each [CO_2] treatment (Figure 4.8). The data clearly indicate lower GAs in *phyB-9* compared to Col-0 and suggesting their role in sensitizing the *phyB-9* more towards E[CO_2]-mediated closure response. In particular, 13-hydroxylated GAs are already at a very low level in *phyB* mutants without E[CO_2] treatment and so this might suggest that phyB is required to maintain this pool and that this then impacts on the E[CO_2] regulation of non-13-hydroxylated GAs in *phyB* mutants.

Collectively, the measurements of active and inactive ABA and different forms of GAs indicate that higher ABA-GE and lower active GAs may be involved in *phyB-9* hypersensitivity to E[CO_2].

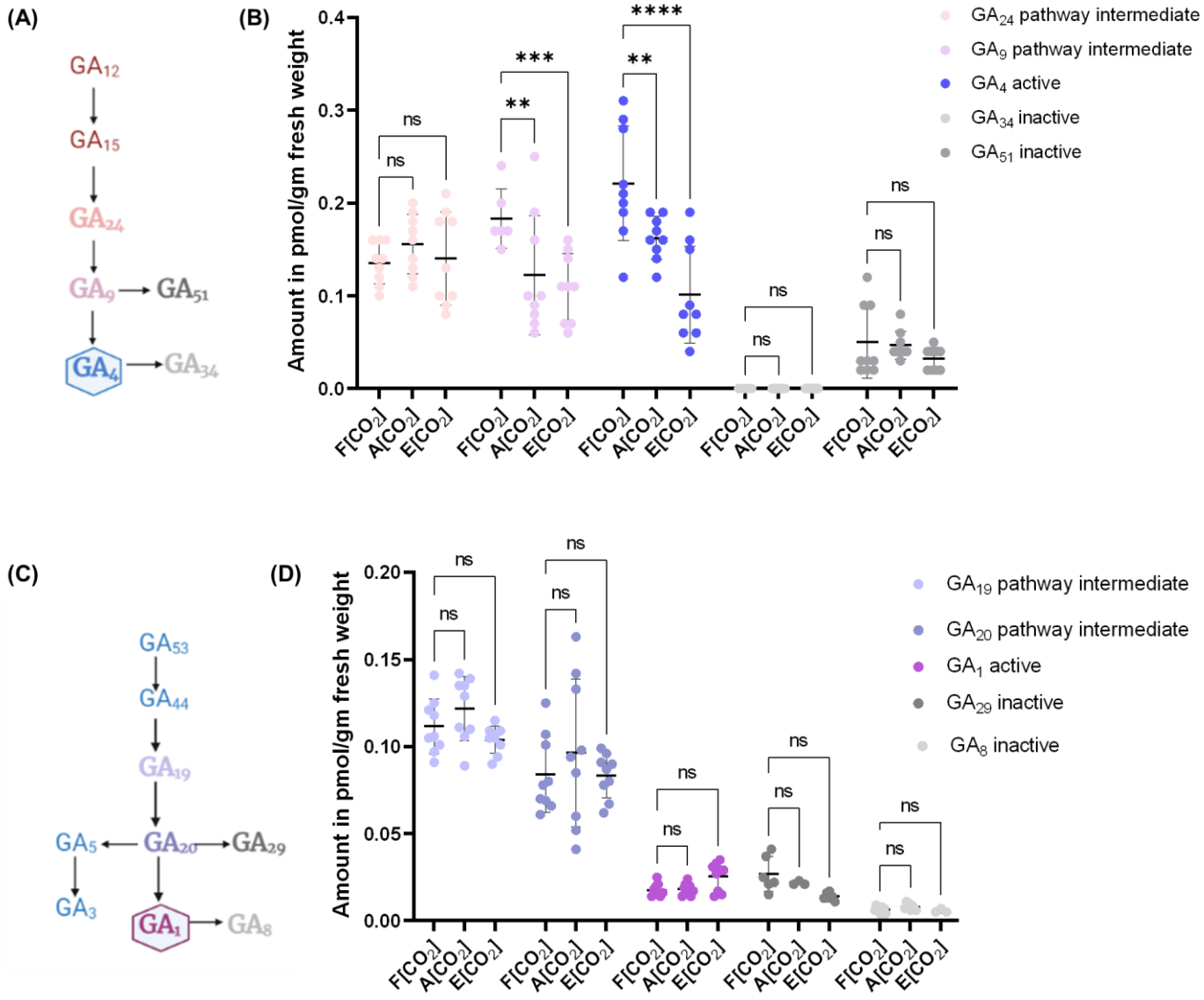

Figure 4.7 Measurement of GAs, their intermediate and inactive forms from mature leaf tissue of *phyB-9* at three different [CO_2]. (A) Steps in the non-13-hydroxylation pathway where bold fonts indicate the measured components and active GA are shown in a hexagon box, and their **(B)** amounts from fresh mature leaf tissue of *phyB-9* treated with F[CO_2], A[CO_2] and E[CO_2] in a way similar to bioassay experiments using UPLC–ESI-MS/MS. **(C)** Stages in the 13-hydroxylation pathway where measured components are shown with bold fonts and active GA inside hexagon box, and **(D)** their amounts measured through UPLC–ESI-MS/MS from mature leaf disc treated with different [CO_2] in line with stomatal bioassay experiments. The number of biological replicates was three/sample, and technical replicates were three from each biological replicate. Statistical analysis was conducted using two-way ANOVA with Tukey's multiple comparison tests. Adjusted P values among means with SD were ** $P \leq 0.01$, *** $P \leq 0.001$, **** $P < 0.0001$ and non-significant (ns) when $P \geq 0.05$.

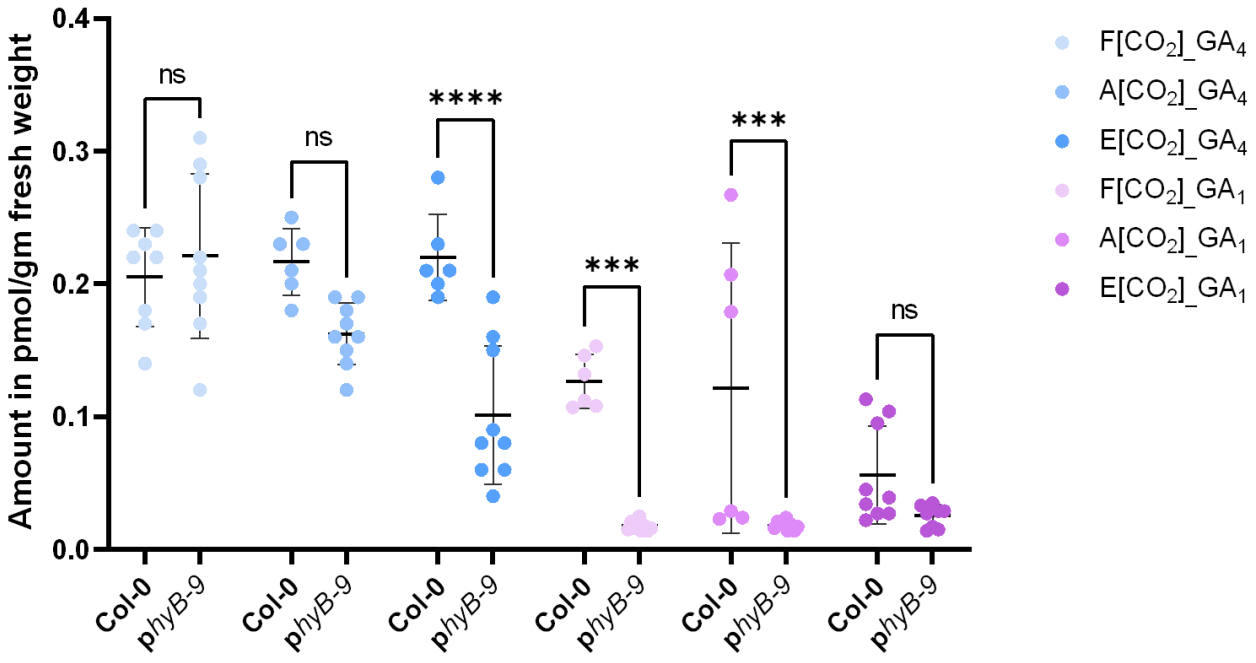

Figure 4.8 Comparison of active GAs between Col-0 and *phyB-9*. GA_4 and GA_1 measurements from Col-0 (section 3.9) and *phyB-9* (section 4.4) was compared at three tested [CO_2] conditions. The number of biological replicates was three/sample, and technical replicates were three from each biological replicate. Statistical analysis was conducted using two-way ANOVA with Tukey's multiple comparison tests. Adjusted P values among means with SD were ** $P \leq 0.01$, *** $P \leq 0.001$, **** $P < 0.0001$ and non-significant (ns) when $P \geq 0.05$.

4.5 Reduction in ABA biosynthesis rescues the phyB hypersensitive stomatal response to E[CO_2]

Findings from Casson lab and this project indicate the involvement of the RL photoreceptor phyB and the hormones ABA and GA in regulating stomatal closure in response to E[CO_2]. The mass spectrometry measurements indicate that *phyB* mutants have more ABA-GE compared to Col-0, though this doesn't appear to lead to comparative differences in free ABA. To determine whether the hypersensitive response of *phyB-9* stomata to E[CO_2] is linked to ABA metabolism, a genetic approach was taken to manipulate ABA levels in *phyB-9*. A *phyB nced3 nced5* triple

mutant was generated; NCED3 and NCED5 are rate limiting enzymes in ABA biosynthesis and it has previously been shown that *nced3 nced5* mutants are less responsive to E[CO_2] (Frey et al. 2012; Chater et al. 2015). Confirmation of the triple mutant *phyB-9 nced3 nced5* was conducted through genotyping of *nced3* and *nced5* followed by sequencing of the phyB locus (supplementary 2.8 and 2.9 respectively).

To determine whether altering ABA metabolism impacts on the *phyB-9* response to E[CO_2], a [CO_2] response bioassay was conducted using Col-0, *phyB-9*, *nced3nced5* and *phyB-9nced3nced5*. The bioassay system involving more than three lines was found to be limited to the experimental capacity, and therefore the [CO_2] treatments were split into two different sets of experiments. In the first set, the stomatal response of the tested four lines was carried out using F[CO_2] and A[CO_2] (Figure 4.8) and the second set involved stomatal function response at F[CO_2] and E[CO_2] (Figure 4.9).

The pore area of *phyB-9* and *nced3nced5* at F[CO_2] was significantly less than Col-0, whereas *phyB-9nced3nced5* had a similar pore area to Col-0. Following incubation at A[CO_2] *phyB-9* demonstrated a reduced aperture, as reported earlier (Brown, 2018 and in this report), whereas the *nced3nced5* mutant did not show any response to the A[CO_2] treatment, supporting previous data (Chater et al. 2015). The triple mutant *phyB-9nced3nced5* had both aperture and responses similar to that of Col-0 (Figure 4.8A). All the mutants, except for *nced3 nced5*, showed a closure response towards A[CO_2] when the same data was used to determine the proportional response to F[CO_2] (Figure 4.8B). Whilst aperture responses appeared similar to Col-0 for the triple mutant, measurements of GC area at both F[CO_2] and A[CO_2] showed a significantly lower GC area in *phyB-9* and *phyB-9nced3nced5* compared to Col-0 (Figure 4.8C).

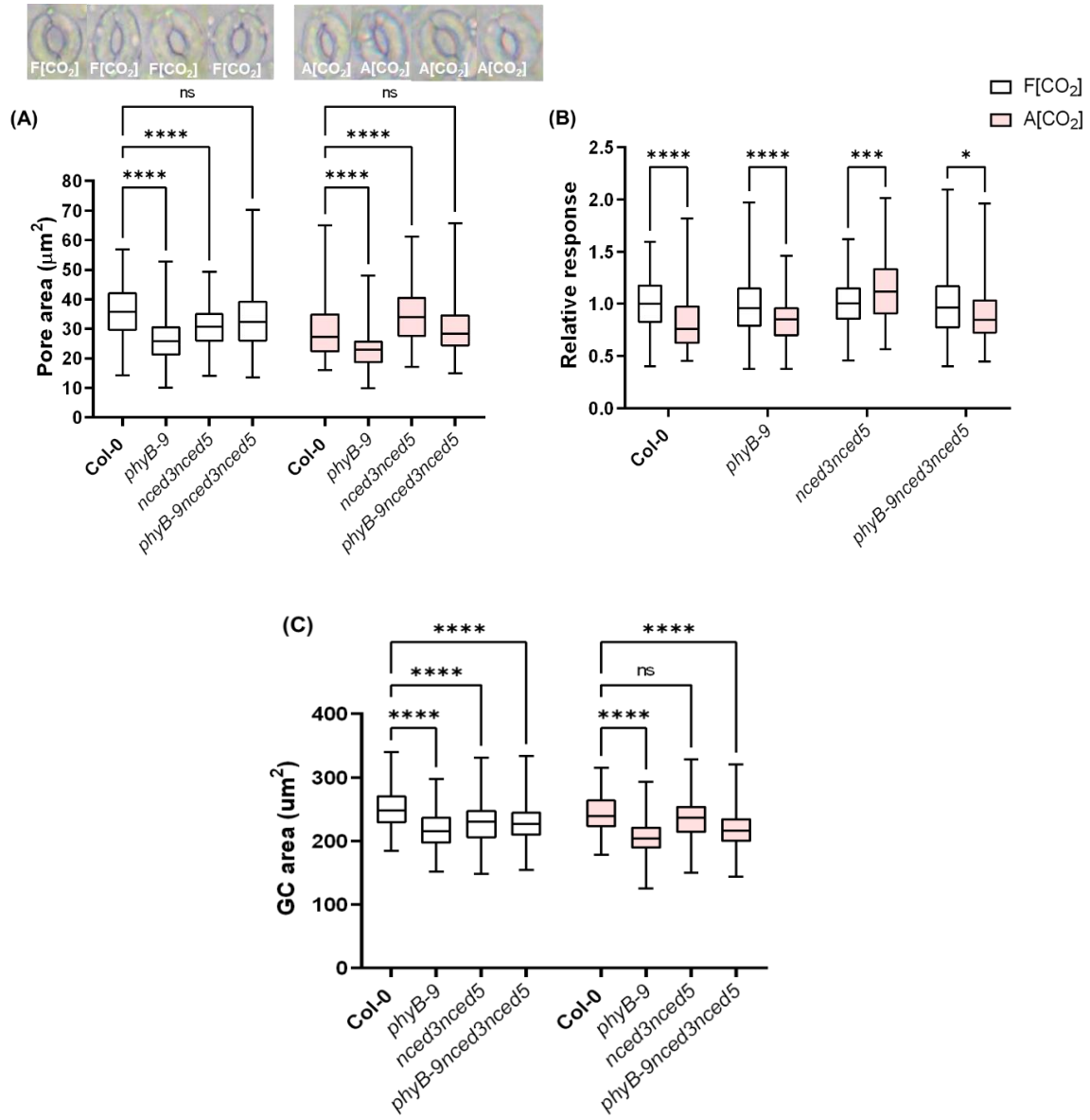

Figure 4.8 Involvement of phyB and ABA biosynthesis genes *NCED3* and *NCED5* towards stomatal function response at A[CO_2]. (A) Epidermal peels from mature leaves of Col-0, *phyB-9, nced3nced5* and *phyB-9nced3nced5* were incubated in an opening buffer under F[CO_2] for 2 hours followed by incubation with A[CO_2] for another 2 hours, before measuring pore area. Pore area measurements were separately compared between Col-0 and each mutant at F[CO_2] and A[CO_2]. **(B)** Response of each of the studied genotypes at A[CO_2] in proportion to their respective response at F[CO_2] was analysed using the data from (A). **(C)** GC area measurements and comparisons were made between the genotypes separately at F[CO_2] and A[CO_2]. Number of stomata measured n=120. Statistical analysis was conducted using two-way ANOVA with Tukey's multiple comparison tests for (A) and (C); and with Šídák's multiple comparison tests for (B) where adjusted P values were *P < 0.05, ***P < 0.001, ****P < 0.0001 and P ≥ 0.05 was non-significant (ns).

This experimental approach was then repeated to examine the stomatal response to F[CO_2] and E[CO_2], using the four lines mentioned above. *phyB-9* showed reduced aperture at F[CO_2] as well as hypersensitive response towards E[CO_2] as reported (Brown 2018 and in this report). As reported previously, *nced3nced5* mutants appeared relatively insensitive to E[CO_2] (Chater et al. 2015). In contrast, the triple mutant *phyB-9nced3nced5* demonstrated a similar pore area as Col-0 at both [CO_2] treatments indicating that the absence of ABA synthesis can overcome the hypersensitive closure response of *phyB-9* (Figure 4.9A). However, [CO_2] responsiveness had not been lost from *phyB-9nced3nced5.* Relative response data of each mutant line revealed how they responded at E[CO_2] proportional to their F[CO_2] response (Figure 4.9B). GC area measurements indicate their involvement towards aperture change in *phyB-9* but not in *nced3nced5* at both [CO_2] treatments (Figure 4.9C). Although GC area significantly reduced in *phyB-9nced3nced5* compared to Col-0 at E[CO_2], similar apertures between the lines (Figure 4.9A) indicate no effect of GC change on aperture response.

Overall, the two sets of experiments suggest that the hypersensitive response of stomatal closure towards E[CO_2] in *phyB-9* can be rescued by reducing ABA biosynthesis. And this was evident from the *phyB-9nced3nced5* triple mutant, which appeared to have a similar aperture change as Col-0 at A[CO_2] and E[CO_2]. However, the pore area phenotype of the respective parental lines and the triple mutant, do not support an epistatic interaction and instead suggest that phyB and NCED3/5 may act additively to regulate responses to E[CO_2].

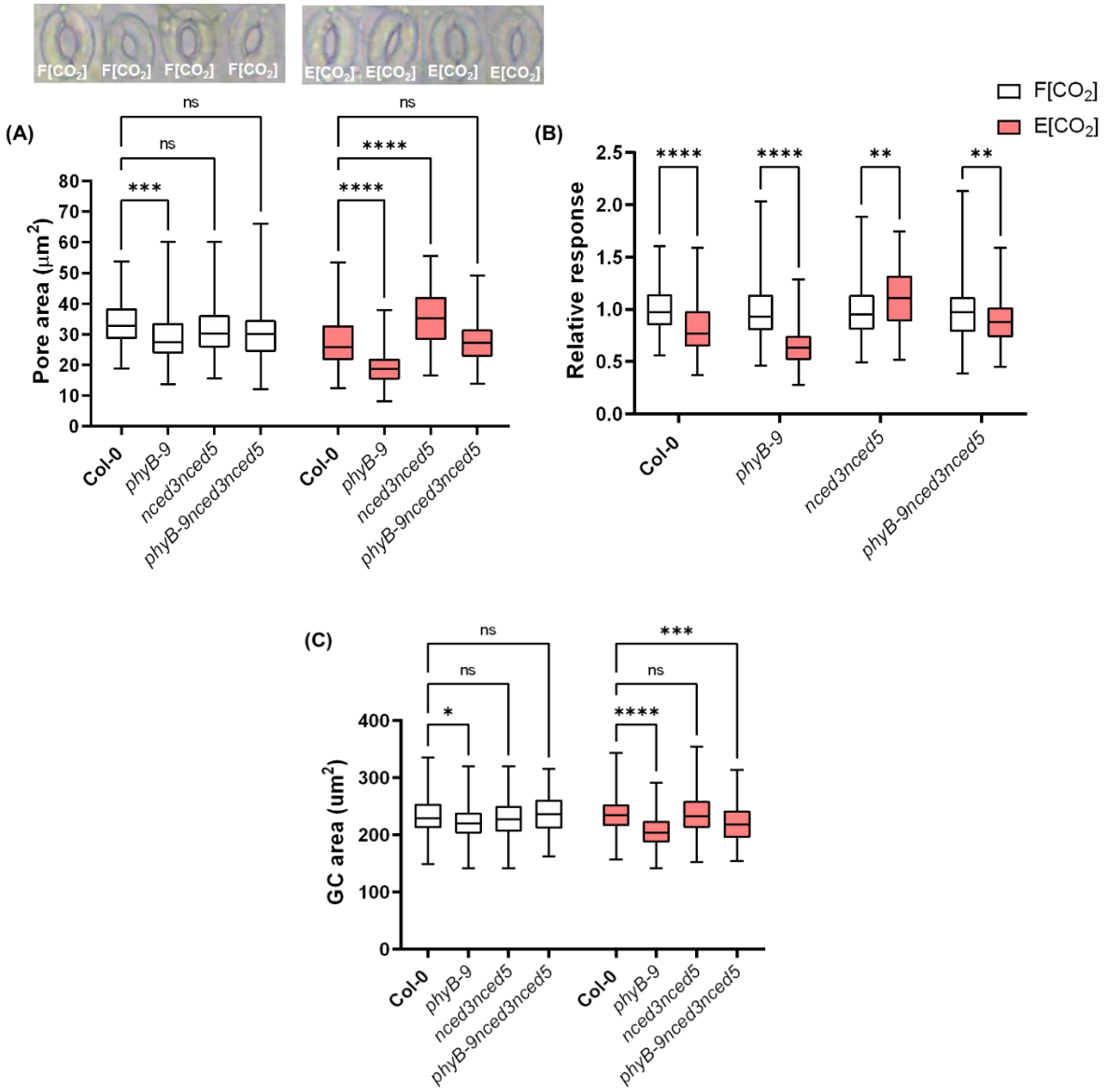

Figure 4.9 Involvement of phyB and ABA biosynthesis genes *NCED3* and *NCED5* towards stomatal function response at E[CO_2]. (A) Epidermal peels from mature leaves of Col-0, *phyB-9, nced3nced5* and *phyB-9nced3nced5* were incubated in an opening buffer under F[CO_2] for 2 hours followed by incubation with E[CO_2] for another 2 hours before measuring pore area. Pore area measurements were separately compared between Col-0 and each mutant at F[CO_2] and E[CO_2]. **(B)** Response of each of the studied genotypes at E[CO_2] in proportion to their respective response at F[CO_2] was analysed using the data from (A). **(C)** GC area measurements and comparisons were made between the genotypes separately at F[CO_2] and E[CO_2]. Here n=120. Statistical analysis was conducted using two-way ANOVA with Tukey's multiple comparison tests for (A) and (C); and with Šídák's multiple comparison tests for (B) where adjusted P values were *P < 0.05, **P < 0.001, ***P < 0.001, ****P < 0.0001 and P ≥ 0.05 was non-significant (ns).

4.6 REVEILLE genes modulate the stomatal response to E[CO_2]

RVE1 and RVE2 are MYB transcription factors that play a critical role in regulating GA biosynthesis in a phyB-dependent manner during primary seed dormancy and light-dependent germination (Finkelstein et al., 2008; Holdsworth et al., 2008; Graeber et al., 2012). So, the question is that whether phyB and RVE1/RVE2 interact to regulate GA metabolism functions in the mature plant to E[CO_2]-mediated stomatal closure response.

To determine the involvement of *RVE* genes, a [CO_2] response bioassay was conducted using Col-0, a single mutant of *RVE1* (*rve1*, Alonso et al. 2003) and a transgenic line overexpressing *RVE1* (*RVE1OE,* present study, Table 2.1). Prior to this bioassay, *RVE1* expression levels were analysed by qPCR in several *RVE1OE* lines to identify a candidate line for bioassays (Supplementary 2.5). Following the bioassay, it was evident that both the *rve1* mutant and *RVE1OE* line had significantly smaller pore areas than Col-0 at F[CO_2] (Figure 4.10A). Whilst the pore area of Col-0 was reduced at both A[CO_2] and E[CO_2] compared to the F[CO_2] control, both the *rve1* mutant or the *RVE1OE* line had reduced responses to the increase [CO_2] treatments, which was more clearly evident when the relative response at A-or-E[CO_2] to F[CO_2] was calculated (Figs. 4.10A-B). This collectively could suggest that both the mutant and OE line are relatively insensitive to [CO_2]. An analysis of GC area indicated that the GCs of the mutant are not different in size compared to Col-0, though those of the OE line are smaller (Figure 4.10c). Therefore, this suggests that in the case of the *rve1* mutant at least, GC size is not a contributor to the smaller pore areas and that the stomata are more closed under all treatments. Given that both the mutant and OE line had similar phenotypes and responses, this does not clearly define a role for RVE1 in [CO_2] responses.

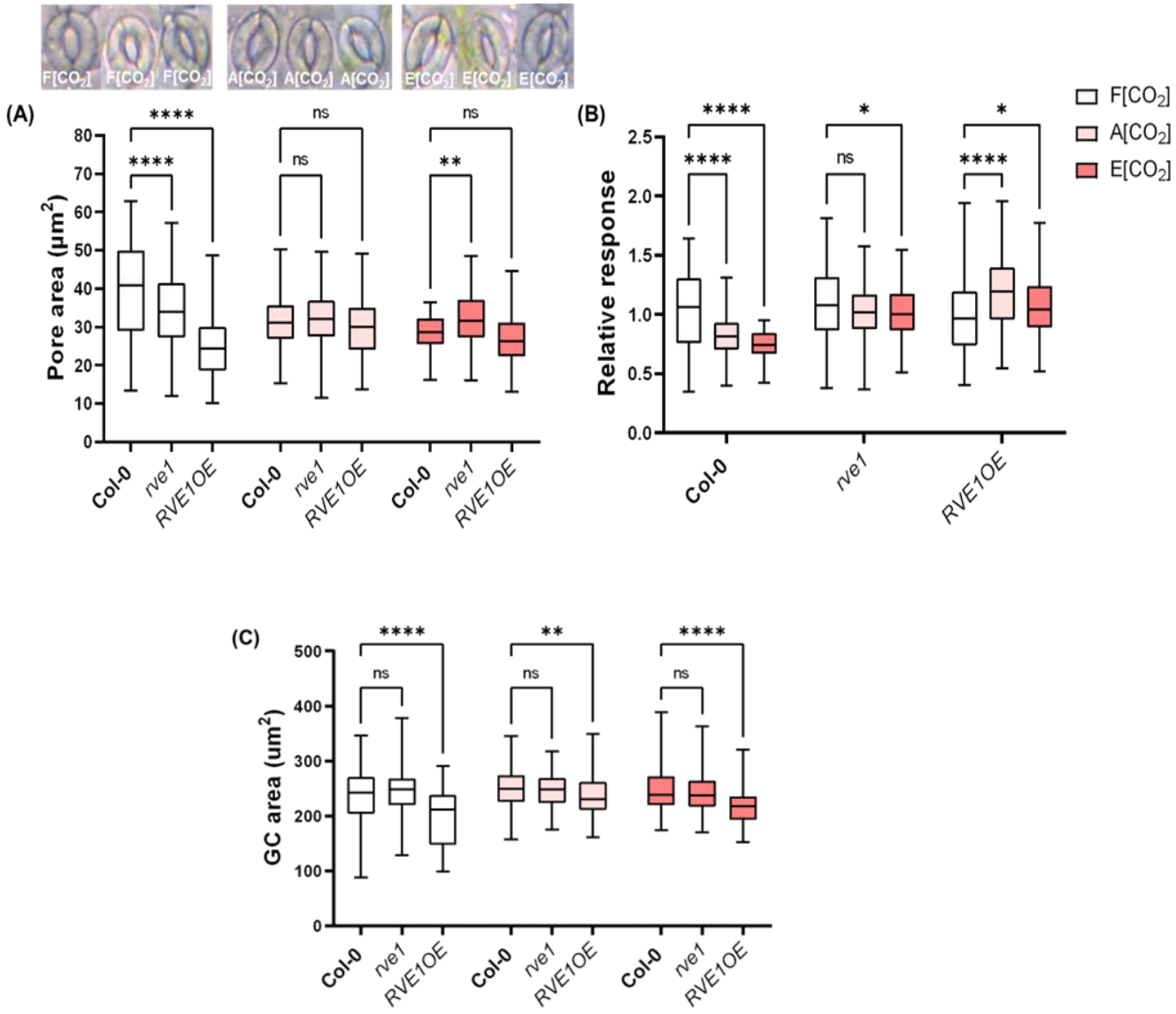

Figure 4.10 Involvement of RVE1 towards stomatal function response at different [CO_2]. **(A)** Epidermal peels from mature leaves of Col-0, *rve1* and *RVE1OE* were incubated in opening buffer under F[CO_2] for 2 hours, followed by incubation with A[CO_2] and E[CO_2] for another 2 hours prior to measuring pore area. Comparisons were made between Col-0 with *rve1* and *RVE1OE*, respectively, at each [CO_2] treatment. **(B)** Relative response of each of the studied genotypes at A[CO_2] and E[CO_2] in proportion to their respective response at F[CO_2] and analysed using the data from (A). (**C)** GC area measurements and comparison made between Col-0 with either *rve1* or *RVE1OE* at each [CO_2] condition. Number of stomata measured n=120. Statistical analysis was conducted using two-way ANOVA with Tukey's multiple comparison tests where adjusted P values are *P < 0.05, **P < 0.01, ****P > 0.0001 and P ≥ 0.05 was non-significant (ns).

RVE2 is the closest homolog of *RVE1* and reported additive with dual roles in controlling seed dormancy and germination (Zhang et al., 2007; Jiang et al., 2016). Therefore, another [CO_2] response bioassay was conducted using single mutants *rve1*, *rve2* (Alonso et al. 2003) and double mutant *rve1rve2* (present study, Table 2.1). As three lines was found to limit the experimental capacity the [CO_2] treatments were split into two sets of experiments as previously described (section 4.5). The first set described in Figure 4.11 involved the F[CO_2] and A[CO_2] treatments, while the second set involved the F[CO_2] and E[CO_2] treatments (Figure 4.12). Confirmation of the genotype of the *rve1rve2* line was achieved through T-DNA genotyping (Supplementary 2.7).

Pore area measurements of each studied mutant were compared with Col-0 at the two [CO_2] treatments. As seen previously, the pore area of the single *rve1* mutant was smaller than Col-0 under F[CO_2] conditions and this was also the case for the single *rve2* mutant but not for the *rve1rve2* double (Figure 4.11A). Col-0 showed a closure responses to the A[CO_2] treatment but this was less evident for the single mutant lines and yet the double mutant was determined to have a significant closure response (Figures 4.11A-B). GC area measurements indicated that the observed pore area changes are not clearly correlated with GC area (Figure 4.11C).

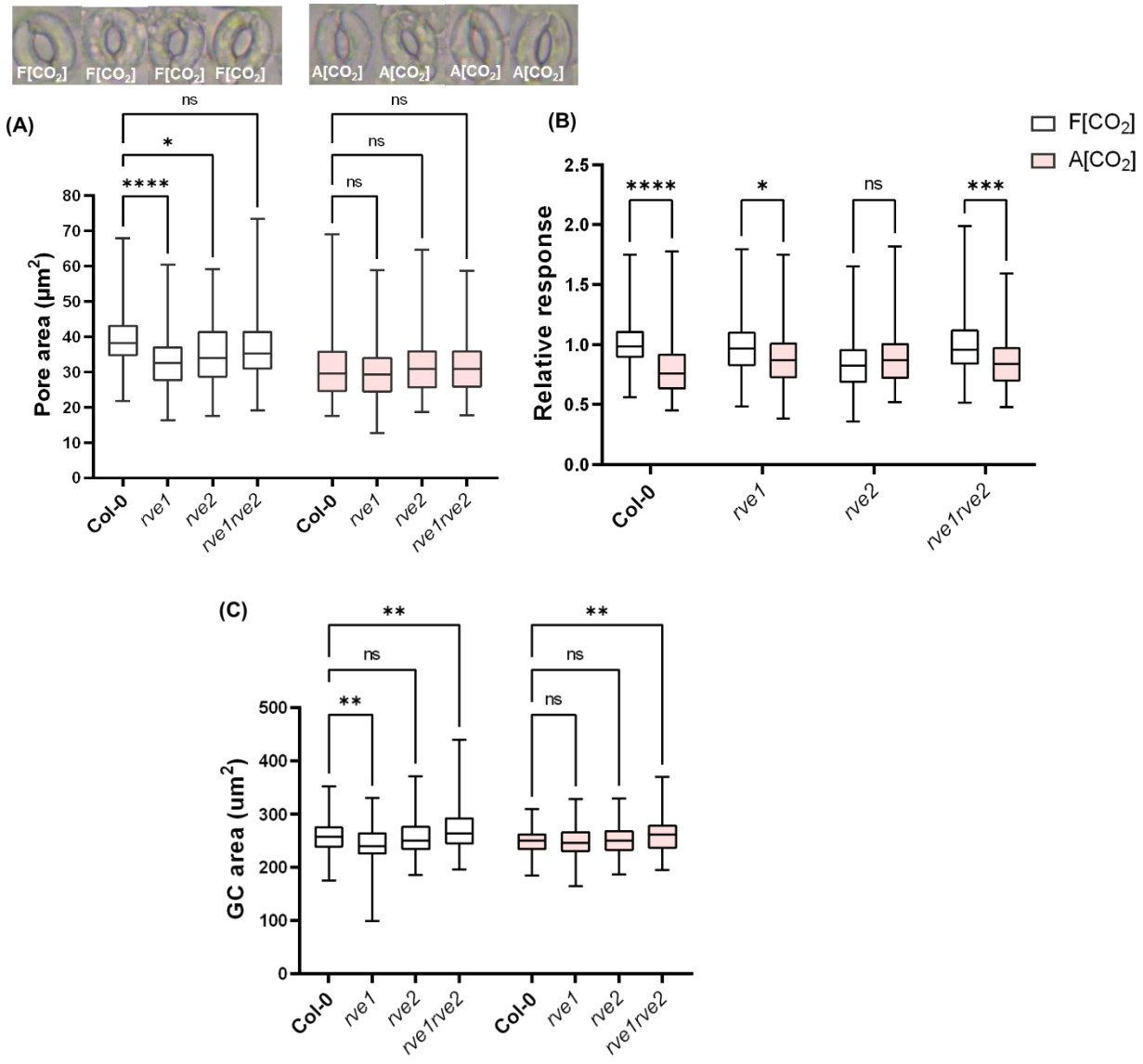

Figure 4.11 Involvement of RVE1 and RVE2 towards stomatal function response at A[CO_2]. **(A)** Epidermal peels from mature leaves of Col-0, *rve1*, *rve2* and *rve1rve2 were* incubated in an opening buffer under F[CO_2] for 2 hours, followed by incubation with A[CO_2] for another 2 hours before measuring pore area. Comparison made between Col-0 with the studied mutant lines at each [CO_2] treatment. **(B)** Relative response of each of the studied genotypes at F[CO_2] and A[CO_2] in proportion to their respective response at F[CO_2] and analysed using the same data as in (A). **(C)** GC area measurements and comparison made between Col-0 with each of the mutant lines at each [CO_2] condition. Number of stomata measured n=120. Statistical analysis was conducted using two-way ANOVA with Tukey's multiple comparison tests for (A) and (C) and two-way ANOVA with Šídák's multiple comparison tests for (B). Adjusted P values were *P < 0.05, **P < 0.01, ***P < 0.001, ****P > 0.0001, and P ≥ 0.05 was non-significant (ns).

The second set of experiments revealed more open stomata in *rve1*, *rve2* and *rve1rve2* compared to Col-0 at E[CO_2], suggesting an impaired closure response towards E[CO_2] (Figure 4.12A). There was no difference in pore area between the mutants with Col-0 at F[CO_2], which contrasts with the first set of experiments. The same data was utilised to determine the [CO_2] response of each genotype in proportion to their response at F[CO_2] and found all of them were responsive towards E[CO_2]-mediated closure, though the magnitude of the response was less in each of the mutants compared to Col-0 (Figure 4.12B). GC area measurements indicated pore area changes were independent of GC area with [CO_2] elevation for the mutants and wild line (Figure 4.12C).

Altogether, these data indicate RVE1 and RVE2 are involved in E[CO_2]-mediated stomatal closure response since the mutants showed significantly open stomata compared to Col-0 stomata. The relative responses data added more evidence by showing response dissimilar to Col-0 where the mutants had lower responsiveness towards E[CO_2].

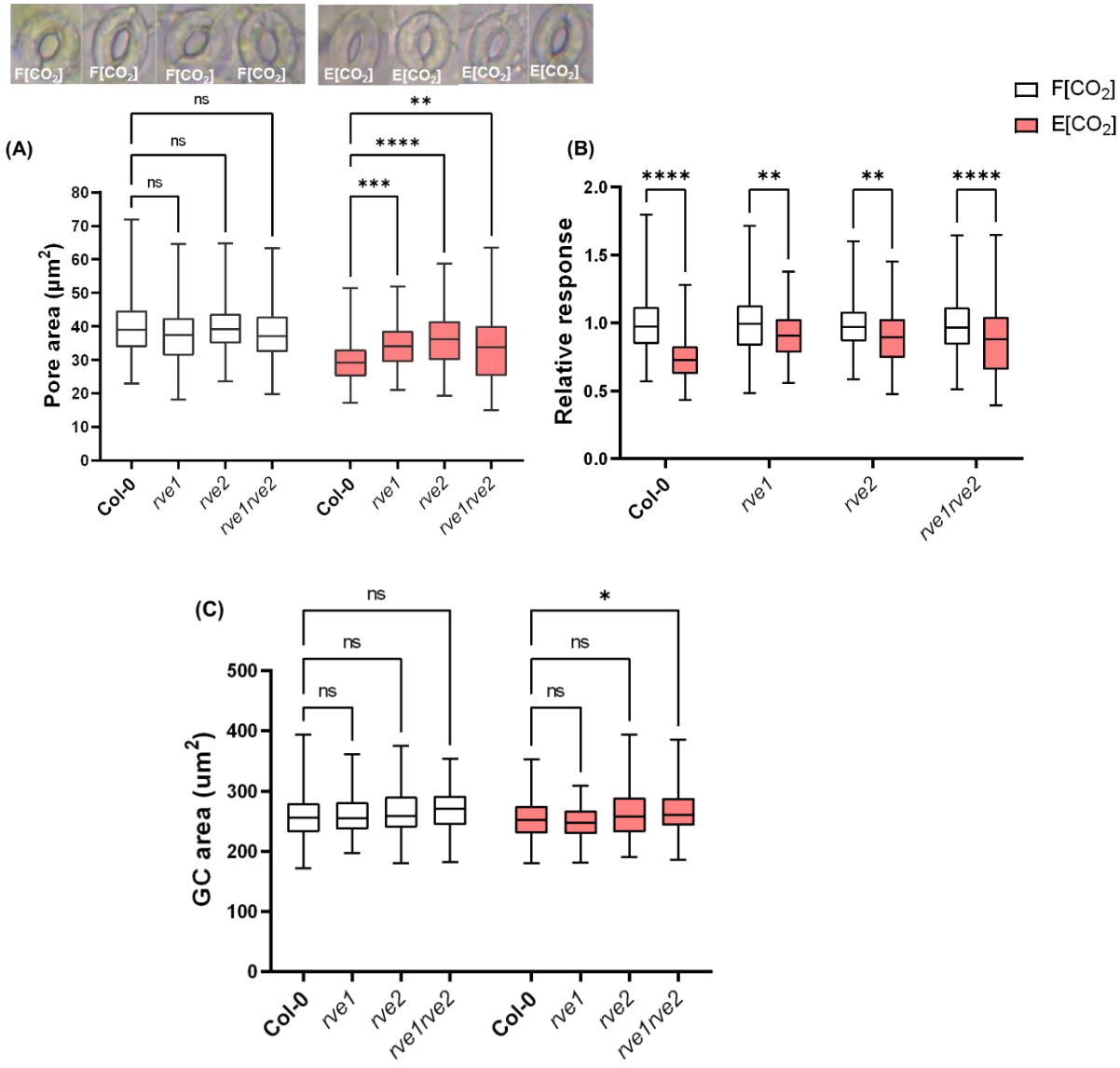

Figure 4.12 Involvement of RVE1 and RVE2 towards stomatal function response at E[CO_2]. (A) Epidermal peels from mature leaves of Col-0, *rve1*, *rve2* and *rve1rve2 were* incubated in an opening buffer under F[CO_2] for 2 hours, followed by incubation with E[CO_2] for another 2 hours prior to measuring pore area. Comparison made between Col-0 with the studied mutant lines at each [CO_2] treatment. **(B)** Relative response of each of the studied genotypes at F[CO_2] and E[CO_2] in proportion to their respective response at F[CO_2] and analysed using the same data as in (A). **(C)** GC area measurements and comparison made between Col-0 with each of the mutant lines at each [CO_2] condition. The number of stomata measured n=120. Statistical analysis was conducted using two-way ANOVA with Tukey's multiple comparison tests for (A) and (C) and two-way ANOVA with Šídák's multiple comparison tests for (B). Adjusted P values were *P < 0.05, **P < 0.01, ***P < 0.001, ****P > 0.0001, and P ≥ 0.05 was non-significant (ns).

4.7 Clock genes modulate stomatal response to E[CO_2]

Stomatal aperture responses are known to be regulated by the circadian clock (Webb, 2003; Kinoshita et al., 2011). The interaction of the circadian clock with stress signalling pathways integrates with internal and external stimuli to control growth, development, and stress response in plants (Sharma et al., 2022). However, whether the circadian clocks are integrating signals to mediate stomatal aperture in response to changes in [CO_2] has not been reported. CCA1 and LHY, which are MYB transcription factors, are two of the key transcription factors of the well-studied transcriptional-translation feedback loop to initiate and set the phase of clock-controlled rhythms in plants (Alabadí et al., 2001). The 8 members of the REVEILLE family, including RVE1 and RVE2, are closely related to CCA1 and LHY and collectively act in clock output pathways or, in the case of RVE8, regulates the expression of genes within central oscillator (reviewed in McClung, 2014). RVE1 is reported to be a direct target of CCA1 (Nagel et al., 2015) and of PRR5 and PRR7 (Liu et al., 2013; Nakamichi et al., 2012) the repressors of clock regulation, indicating the complicated nature of the circadian clock. Stomatal functions bioassay from previous section (section 4.6) revealed the potential involvement of RVE1 and RVE2 in regulating stomatal aperture responses to [CO_2]. Given that RVE1/2 are associated with regulating clock outputs, it was decided to investigate whether mutations in the core clock genes CCA and LHY also affect responses to [CO_2]. To do this, [CO_2] bioassays were performed on a double mutant *cca1lhy* in the Ws-2 background.

Under F[CO_2] conditions, the pore area of *cca1lhy* was greater than the Ws-2 control and this was observed under each of the [CO_2] treatments (Figure 4.13A). By normalising to the pore area under F[CO_2], it is evident that whilst the *cca1lhy* double mutant does respond to changes in [CO_2], as was found with *rve1* and *rev2*, the magnitude of the response is less than that of the control (Figure 4.13B). GC area was significantly lower in *cca1lhy* at F[CO_2] and A[CO_2] but similar to Ws-2 at E[CO_2] indicating that GC size alone cannot account for the differences in pore area under each [CO_2] (Figure 4.13C).

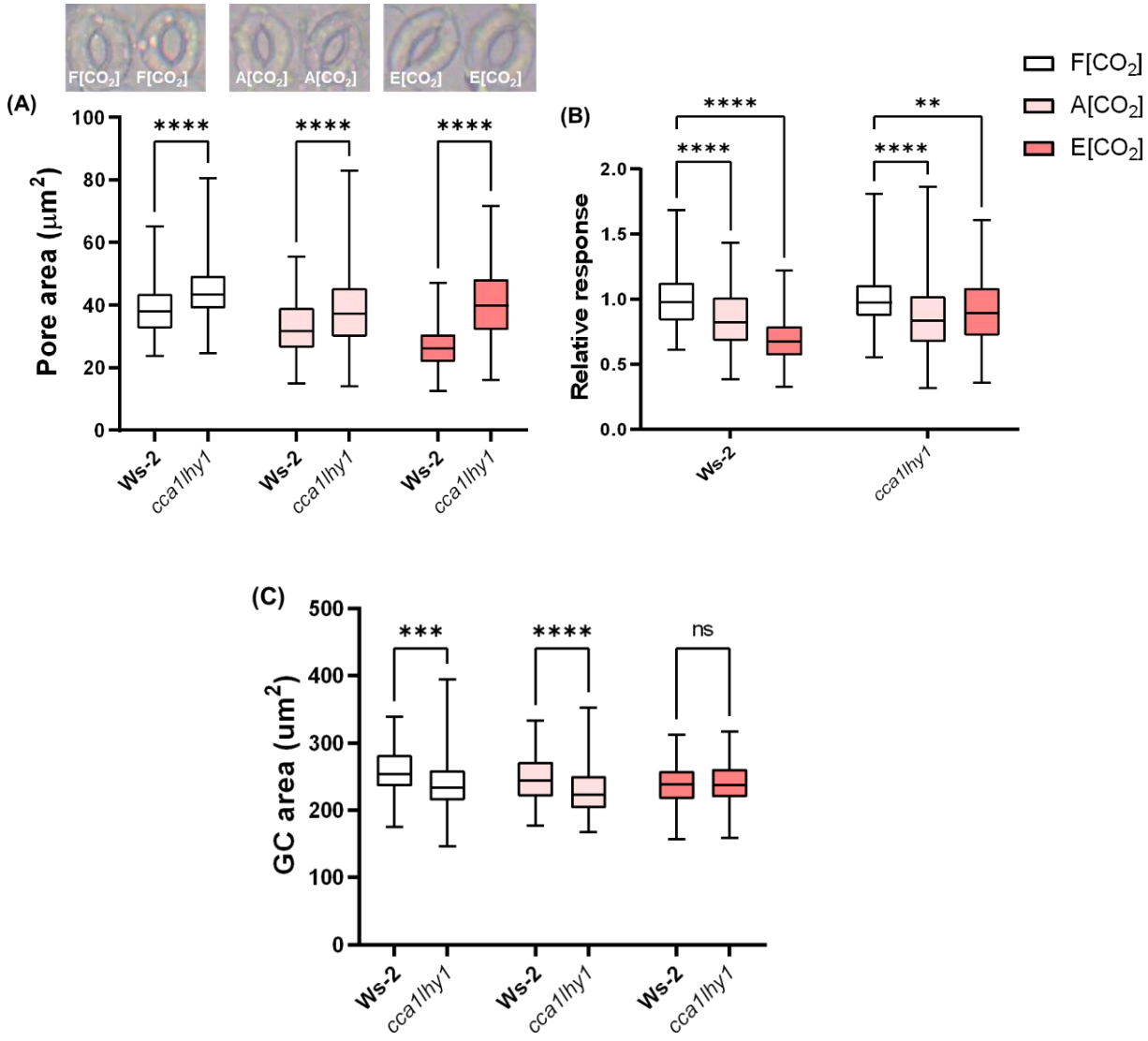

Figure 4.13 Involvement of CCA1 and LHY towards stomatal function response at E[CO_2]. **(A)** Epidermal peels from mature leaves of Ws-2 and *cca1lhy were* incubated in an opening buffer under F[CO_2] for 2 hours, followed by incubation with E[CO_2] for another 2 hours prior to measuring pore area. Comparison was made between Ws-2 with the studied mutant lines at each [CO_2] treatment. **(B)** Relative response of each of the studied genotypes at A[CO_2] and E[CO_2] in proportion to their respective response at F[CO_2] and analysed using the same data as in (A). **(C)** GC area measurements and comparison made between Ws-2 with each of the mutant lines at each [CO_2] condition. Number of stomata measured n=120. Statistical analysis was conducted using two-way ANOVA with Šídák's multiple comparison tests for (A) and (C) and two-way ANOVA with Tukey's multiple comparison tests for (B). Adjusted P values were *P < 0.05, **P < 0.01, ***P < 0.001, ****P > 0.0001, and P ≥ 0.05 was non-significant (ns).

4.8 Discussion

It had previously been determined that mutations in the photoreceptor phyB resulted in hypersensitive stomatal closure in response to E[CO_2] (Brown, 2018; Figure 4.3A). In this chapter, the aim was to investigate the mechanism involved in *phyB's* enhanced sensitivity to E[CO_2], with the main focus on determining whether this is due to changes in ABA:GA homeostasis. Given that the *phyB-9* allele had recently been determined to carry a second mutation that affects leaf and photosynthetic traits (Yoshida et al. 2018), it was first important to determine whether the E[CO_2] phenotype was specific to phyB. *phyB-9* bioassay experiments were repeated and the hypersensitivity to E[CO_2] was demonstrated to be due to phyB function as normal sensitivity to E[CO_2] was restored in a complementation line i.e., *PHYBproPHYB:YFP* (Figure 4.3A). Response data relative to F[CO_2] also supports this notion (Figure 4.3B). Additionally, the aperture change in response to E[CO_2] was found independent of GC area in the complementation line because stomatal closure response in the complementation line was indifferent to Col-0 despite of having similar GC area as *phyB* (Figure 4.3C). Now question arises on the regulation of such hypersensitive response.

phyB is known to regulate ABA and GA either positively or negatively at different stages of development as well as during stress responses. For example, phyB mediates antagonistic regulation of ABA and GA during seed germination while positively regulate ABA metabolism in shoots in response to adverse light exposure to light (Dong et al., 2008; Ha et al. 2018; Hedden, 2020; Sano & Marion-Poll, 2021; Li et al., 2022). GA is reported to be positively and negatively regulated by phyB during hyponastic leaf movement and hypocotyl growth respectively (Achard et al. 2007; Küpers et al., 2023). The previous result chapter points the involvement of GAs towards E[CO_2]-mediated stomatal closure in Col-0 (Chapter 3). Therefore, attempts were made to determine GAs for *phyB-9* hypersensitivity relative to Col-0.

The [CO_2] function bioassay using *phyB-9* in the presence of 100µM GA_3 experiment provided evidence of the involvement of GAs to negate [CO_2]-mediated stomatal closure as found in chapter 3 with Col-0 (Figure 4.4A and B). However, the hypersensitive closure response did not restore to similar level as Col-0 with 100µM GA_3 application, though it did restore the closure response to that of the E[CO_2] mock

treatment (Figure 4.4C). This result putatively supports *phyB* mutants have a reduced GA level compared to Col-0 and hence, indicates a quantitative ability of GA to negate E[CO_2] responses. The lower expression of some of the tested genes involved in GA metabolism (*GA3ox1* and *GA3ox2*) compared to Col-0 might direct their involvement in hypersensitivity of *phyB-9* (Figure 4.5). However, gene expression analysis of all the genes in GA metabolism would provide more insight. The current project revealed no change in ABA with [CO_2] elevation compared to F[CO_2] from mature leaf tissue of *phyB-9* (Figure 4.6B). Generally, higher levels of ABA have been reported in *phyB* mutants of Arabidopsis (González et al., 2012). However, the decrease in ABA-GE amount with [CO_2] elevation in *phyB-9* (Figure 4.6B) and the presence of a high amount of ABA-GE compared to Col-0 (Figure 4.6C) may contribute to the *phyB-9* hypersensitive response. ABA-GE has been proven to be a source of active ABA and is hydrolysed by the *Arabidopsis thaliana* beta-glucosidase1 (AtBG1) during water deficit, as evidenced by the impaired stomatal closure of *atbg1* in response to water stress. AtBG1-dependent regulation of ABA homeostasis and the phyB-mediated light signalling pathways were reported to act antagonistically in controlling stomatal development (Allen et al., 2019). Also, there is evidence for the accumulation of ABA-GE under moderate and severe heat stress (Jensen et al., 2023). At the same time, GA measurements from leaf tissue treated similarly as [CO_2] function bioassay showed a decrease in active GA, GA_4 and its immediate precursor GA_9 (Figure 4.7B). This directs evidence towards the hypothesis, i.e., the homeostatic balance of ABA: GA regulates stomatal movement upon [CO_2] changes (Figure 4.2) and phyB as one of the regulators of ABA: GA homeostasis for plant development and stress response (Seo et al., 2006, 2009; Lau & Deng, 2010; Lee et al., 2012) might sensitise E[CO_2]-mediated stomatal closure. Interestingly, GAs from the non-13-hydroxylation pathway showed change in *phyB-9* (Figure 4.7B) as compared with in Col-0. However, the levels of GA_1 were already significantly reduced in *phyB-9* compared to Col-0 and this may be a factor in *phyB* hypersensitivity (Figure 3.13). This might suggest that in WT plants, phyB has a role in regulating GA1 levels in response to [CO_2] and that in the absence of phyB, the GA_4 pathway is targeted. Collectively then, the lower GA_4 and GA_1 in *phyB-9* compared to Col-0 suggests their involvement towards sensitizing the *phyB-9* more to E[CO_2]-mediated stomatal closure (Figure 4.8). This indicates how GA biosynthesis differs in different species, organs and developmental stages reported in

existing works of literature (Kobayashi et al., 1989; Sponsel et al., 1997; Israelsson et al., 2004; Eriksson et al., 2006; Hirano et al., 2008).

Stomatal aperture response data from bioassays, as well as conductance measurements from infrared gas analysis in the ABA synthesis mutant *nced3nced5* at E[CO_2], suggest either a [CO_2]-induced increase in ABA is required to initiate stomatal closure or in presence of reduced ABA, the sensitivity of stomatal closure to E[CO_2] is reduced (Chater et al., 2015). Enhanced closure of *phyB-9* mutant found to be rescued in absences of ABA biosynthesis genes *NCED3* and *NCED5* by developing *phyB-9nced3nced5*. The triple mutant was found to have a similar aperture as Col-0 at both A[CO_2] and E[CO_2] as opposed to the enhanced closure observed in *phyB-9* (Figure 4.8A and 4.9A). During seed germination, phyB-mediated light signals inhibit ABA biosynthesis through modulation of SOMNUS, a CCH-type zinc finger protein (Dong et al., 2008) specifically expressed in seeds. In addition, PIFs (an essential component of light-mediated response) and ABA synthesis have been reported to modulate leaf hyponasty in response to a low red-to-far-red ratio (Michaud et al., 2023). Therefore, present findings support the role of ABA in mediating E[CO_2]-mediated closure via phyB, or at least phyB could sensitise the response. However, the E[CO_2]-mediated stomatal closure response in the *phyB-9nced3nced5* indicates an additive genetic response and suggests their action via alternative pathways as the triple mutant was sensitive to [CO_2] elevation (Figure 4.8B and 4.9B). Stomatal density measurements from Col-0, *phyB-9* and *nced3nced5* are consistent with existing findings (Chater et al. 2015; Brown, 2018). Stomatal density of *phyB-9nced3nced5* is similar as *nced3nced5* but significantly higher than Col-0 and *phyB-9* (Supplementary 2.15).

In the context of seed germination, RVE1 and RVE2 have essential roles in regulating ABA and GA signalling and levels and are in turn regulated by phyB (Jiang et al., 2016; Zhao et al., 2022). Therefore, there could be a regulatory point through which phyB influences plant responses to high [CO_2]. Analysis of [CO_2] functions bioassay using *rve1* showed more open stomata compared to Col-0 at E[CO_2] (Figures 4.10A and 4.12A), indicating that it may positively regulate E[CO_2]-mediated stomatal closure. However, *RVE1OE* did not support such a response (Figure 4.10A) and using more than one line might circumvent this limitation.

In addition to *rve1* alone, [CO_2] functions bioassay involving *rve2* and *rve1rve2* demonstrated their involvement towards E[CO_2]-mediated stomatal closure as they

had more open stomata compared to Col-0 (Figure 4.12A). It's important to note that though the mutants were responsive to [CO_2] elevation as Col-0, the magnitude of response is different from the wild as evidenced by their relative response data (Figures 4.10B, 4.11B and 4.12B). Data on stomatal density revealed no change between the mutants and Col-0 (Supplementary 2.16) indicating that these mutations do not affect stomatal number, though stomatal index measurements would be required to clarify whether stomatal development is affected. The RVE group of the MYB-related (1R-MYB) subfamily has 11 member proteins including RVE1-RVE8 and RVE7-like, CCA1 And LHY(Du et al., 2013). In addition to circadian clock regulation processes, they play diverse roles in plant development and stress response (Liu et al., 2023). Therefore, other family members may have an additive role towards E[CO_2]-mediated stomatal function.

Although the role of circadian rhythms in stomatal function is known (Hennessey et al., 1993; Mansfield & Heath, 1963; Mendes & Marenco, 2014), integration between high [CO_2] and circadian clock has not studied directly. The present study revealed partial participation of core circadian clock genes *CCA1* and it's close homolog *LHY* towards E[CO_2]-mediated stomatal closure (Figure 4.13 A and B). CCA1 and LHY appeared to be integral for stomatal development since the double mutant *cca1lhy* had significantly reduced density compared to Ws-2 (Supplementary 2.17).

4.8.1 Concluding Remarks

1. *phyB-9* is hypersensitive towards E[CO_2]-mediated stomatal closure response.
2. 100µM of GA_3 can negate E[CO_2]-mediated stomatal closure in *phyB-9*.
3. GA_4 lowers with [CO_2] elevation, whereas ABA remains unchanged.
4. *phyB* sensitivity to E[CO_2] is restored if ABA biosynthesis is blocked by mutating *NCED3* and *NCED5*.
5. Circadian clock-related genes, *RVE1* and *RVE2* as well as *CCA1* and *LHY* partially regulate E[CO_2]-mediated stomatal closure.

Chapter 5. Role of phyB in regulating rice responses to elevated [CO_2]

5.1 Introduction

As a staple food for more than half of the global population, rice is grown in more than 100 countries (Fukagawa and Ziska 2019). Rice grows either in lowland or highland with a high demand of water from irrigation and/or rain. At present approximate 75% of global rice cultivation is based on irrigated lowland rice systems in warm and temperate regions of Asia, Africa, and Latin America (Rao et al., 2017). The global increases in a[CO_2] levels and the resulting predicted changes in temperature are, as with many crops, likely to present significant challenges for rice production. Studies have shown that like many other plant species, rice also experiences reduced g_s in response to e[CO_2] levels (Morison, 1987; Drake et al., 1997; De Costa et al., 2003). In addition, the nutritional content of the rice grains including proteins, minerals, and vitamin B was reported to be reduced with increasing [CO_2] demonstrating the inverse relation between plant carbon accumulation and nitrogen content with e[CO_2] (Zhu et al., 2018; Senthil-Nathan, 2021). Therefore as an external stimulus, e[CO_2] affects rice in multiple ways.

The photoreceptor phyB plays a significant role in a variety of photomorphogenic processes in plants (Rausenberger et al., 2010; Pham et al., 2018). Phytochromes mediate photomorphogenic roles and reported to maintain crosstalk between phytochrome-mediated light signals and drought signalling pathways in diverse plants (Franklin & Quail, 2010). Five alleles of phyB mutants were isolated through ɣ-ray mutagenesis of rice seedlings where *OsphyB1* had an insertion and other four *OsphyB2*-*OsphyB5* had deletions of nucleotides in the PHYB genes (Takano et al. 2005). Two allelic mutants of rice phyB (*OsphyB1* and *OsphyB2*) exhibited reduced transpiration, significant reductions in stomatal density and improved drought resistance compared to wild varieties (Liu et al., 2012). Similar observations have been reported from *phyB* mutants in Arabidopsis (Casson et al. 2009; Boccalandro et al. 2009). More widely, rice *phyB* mutants showed reduced NH_4^+ uptake and resistance to sheath blight and saline–alkaline stress (Jung et al., 2023), whilst *phyAB* double mutants were shown to have defects in anther and pollen development (Sun et al., 2017).

Although studies have demonstrated the role of e[CO_2] and phyB in rice separately, no work has studied their combined effect on rice physiology and development. For

the first time, the present study identified stomatal and phytohormone responses of Arabidopsis *phyB* mutants towards E[CO_2] (chapter 4). phyB is evolutionarily conserved with high protein sequence identity and mode of action between Arabidopsis and rice (Dehesh et al., 1991). Therefore, given the phenotypic responses of Arabidopsis *phyB* mutants to E[CO_2], phenotypic and physiological responses of rice *phyB* mutants were analysed in response to E[CO_2] (1000ppm) compared to A[CO_2] (450ppm). For this, both the rice phyB mutants i.e. *OsphyB1* and *OsphyB2* were chosen and several experiments were conducted including short-term E[CO_2] exposure and long-term growth at E[CO_2]. To determine the interaction of E[CO_2] and phyB in rice, a number of stomatal and photosynthetic traits were measured, alongside measurements of yield.

5.1.2 Objectives

The following objectives were put forward to study the role of rice phyB towards E[CO_2]:

1. The physiological response of rice *phyB* mutants, *OsphyB1* and *OsphyB2* to E[CO_2].
2. The developmental response of rice *phyB* mutant, *OsphyB1* grown under E[CO_2] condition.

5.2 Thermal imaging demonstrates that *OsphyB* mutants are hypersensitive to short-term elevation in [CO_2]

The stomata of Arabidopsis *phyB-9* mutants demonstrated increased sensitivity towards E[CO_2], with their stomata closing more than controls (chapter 4, section 4.2). To determine whether rice *phyB* mutants behave normally towards elevation in [CO_2], a stomatal function bioassay was attempted. However, despite several attempts it was not possible to isolate rice epidermis and functional stomata and so, alternative methods were explored. As a primary approach, infrared thermal imaging was utilized.

This is an established alternative to examine stomatal conductance by measuring leaf temperature at a scale varying from leaf to canopy (Jones, 1999; Leinonen et al., 2006; Costa et al., 2013). Leaf surface temperature is a good proxy to determine leaf cooling and transpiration capacity and can be used to indirectly assay stomatal behaviour in a dynamic environment.

OsphyB1 and *OSphyB2* mutants are in the japonica rice cultivar Nipponbare (NB) and so this was used as the control (segregating non-transgenic) for all experiments. Infrared thermal imaging experiments revealed that both mutants had significantly higher leaf temperature at A[CO_2] compared to NB, suggesting that the mutants have significantly lower stomatal conductance (Figure 5.1A). To assess the dynamic response of the *OsphyB* mutants to an increase in [CO_2], thermal imaging was performed across a time series as the cabinet [CO_2] was increased from A[CO_2] to E[CO_2] (1000ppm) followed by a return to ambient conditions in the growth chamber (Figure 5.1B). In line with the initial analysis, the leaves of *OsphyB* mutants were consistently hotter than those of the NB control, with no observable difference between the two mutant alleles. Also, the result indicates that *OsphyB1* and *OSphyB2* were more responsive to the [CO_2] shift compared to NB, given that the magnitude of the leaf temperature changes was greater. For example, temperature difference before and after [CO_2] injection was 0.4ºC in NB whereas this was 0.95ºC and 0.90ºC in *OsphyB1* and *OSphyB2* respectively. Similarly, the mutants showed higher temperature difference than NB between E[CO_2] injection and when the treatment is stabilized back to the A[CO_2]. This suggests that the *OsphyB* stomata both closed and opened more to the increase and decrease in [CO_2], though other factors such as stomatal density and plant architecture may contribute to stress responses (Zhao et al. 2022). As there was not a significant difference observed between the two alleles in terms of temperature changes over time and shifts in [CO_2], further experiments were conducted only with *OsphyB1*.

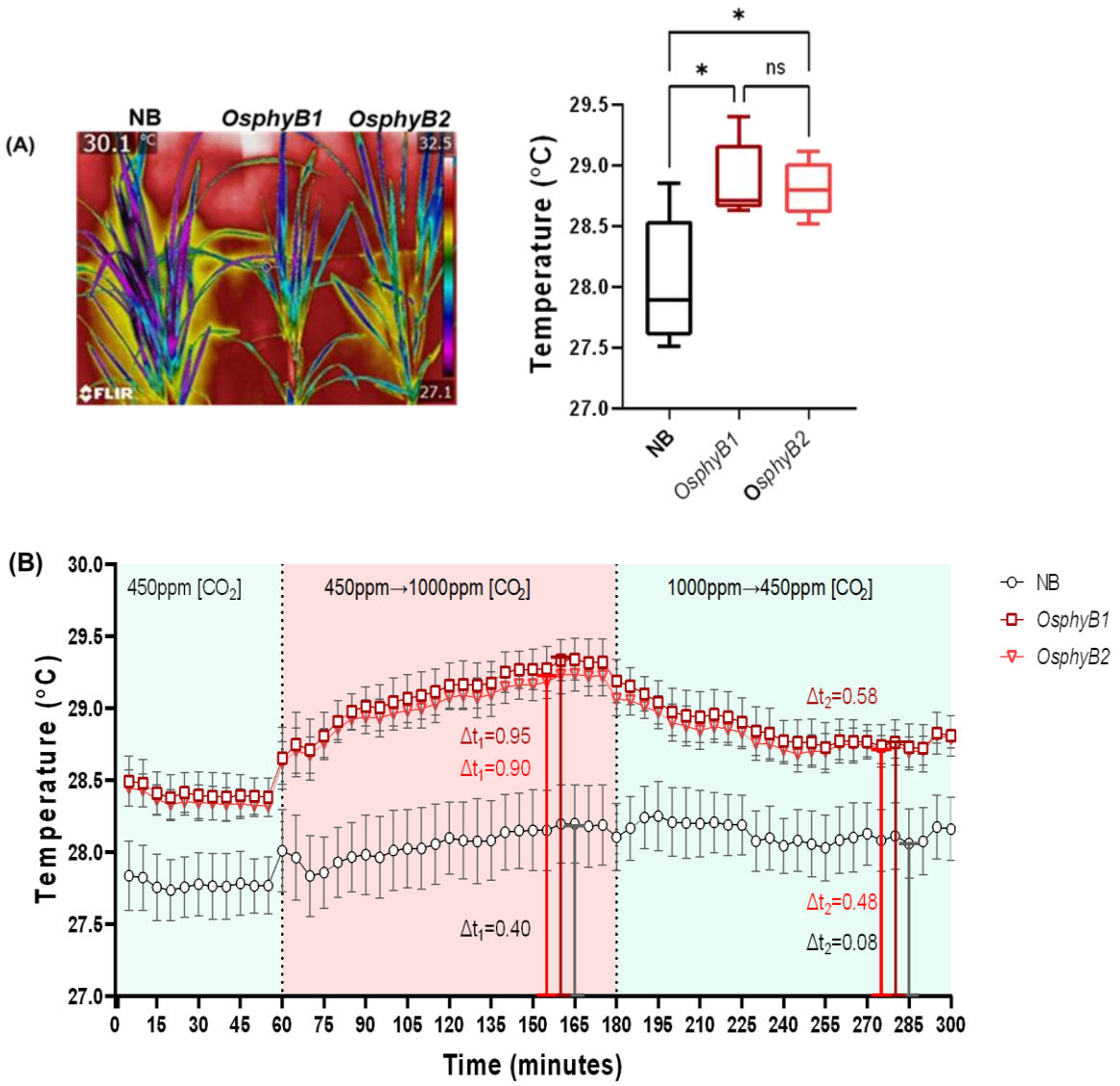

Figure 5.1 Leaf temperature measurement of *OsphyB* mutants and NB in response to changes in [CO_2]. (A) Representative infrared thermal images of NB, *OsphyB1,* and *OsphyB2* with temperature gradient scale alongside average temperature of the examined lines. Here, temperature measured for 300 minutes from 5 plants/line and did an avarage to determine temperature for respective genotypes. **(B)** Temperature measurements were taken every minute for 300 minutes where the first 60 minutes were at 450ppm [CO_2], followed by CO_2 injection to 1000ppm for 120 minutes before a CO_2 purge to return [CO_2] to 450ppm for a further 120 minutes. For visual clarity, data points are shown at 5 minute intervals instead of 1 minute. Δt_1 and Δt_2 denote temperature difference between 450ppm [CO_2] and after 1000ppm [CO_2] injection to 450ppm [CO_2] stabilization respectively. Measurements were taken at 45mins, 165 mins and 180 mins for the lines. Black font for NB and deep and light red for *OsphyB1,* and *OsphyB2* respectively. Plants were between 35-41 days old post germination and n=5 plants per line. Statistical analysis was conducted using two-way ANOVA with Tukey's multiple comparison tests with *P < 0.05 and P ≥ 0.05 non-significant (ns).

5.3 *OsphyB1* has altered stomatal responses to E[CO_2]

The previous section demonstrated that the magnitude of the response to a change in [CO_2] was greater in *OsphyB* mutants than the NB control. To observe whether OsphyB has a role in regulating long-term effects of growth under different [CO_2], on stomatal behaviour and related developmental traits, NB and *OsphyB1* were grown at either A[CO_2] or E[CO_2] (full conditions detailed in section 2.2.2). All measurements were taken from flag leaves, which make a significant contribution to rice yield and remain more active as they are the last to emerge on a mature flowering tiller (Sicher, 1993).

IRGA and porometer measurements were taken to provide information on both leaf gas exchange and photosynthetic performance under conditions matching cabinet growth chamber settings (sections 2.12.2 and 2.12.3 respectively). Unlike the IRGA, the porometer measures one surface of the leaf at a time, which allows for a comparison of the contribution of both abaxial (AB) and adaxial (AD) surface to leaf gas exchange as well as the combined total. Both IRGA (Figure 5.2A) and combined porometer measurements (Figure 5.2B) showed a good correlation in g_s measurement. In both A[CO_2] and E[CO_2], NB had a greater stomatal conductance (g_s) than the *OsphyB1* mutant, which correlates with the thermal imaging data (Figure 5.1B). A significant reduction in g_s was also observed at E[CO_2] for both NB and *OSphyB1* from IRGA and porometer respectively, which suggests that E[CO_2] supresses gas exchange in the long term though it is not clear whether this is specifically due to stomatal closure and/or changes in SD and GC size (Figure 5.2A and B). To investigate effect of stomatal anatomy towards g_s, SD and GCL measurements from AB and AD surfaces were combined and compared between the genotypes and [CO_2] treatments (methods described in section 2.9.2). SD was significantly lower in *OsphyB1* at both [CO_2] growth conditions compared to NB. Though statistically insignificant, a slight increase in SD was observed for both NB and *OsphyB1* when grown under E[CO_2] as compared to A[CO_2] (Figure 5.2C). There were no differences in GCL between the genotypes grown at A[CO_2] but growth under E[CO_2] led to significantly smaller GCL in NB whereas GCL remains unchanged in *OsphyB1* with [CO_2] elevation (Figure 5.2D). Whilst there are changes in SD and GCL

under E[CO_2], collectively, it seems more probable that the reduction in g_s observed at E[CO_2] is primarily driven by changes in stomatal pore aperture.

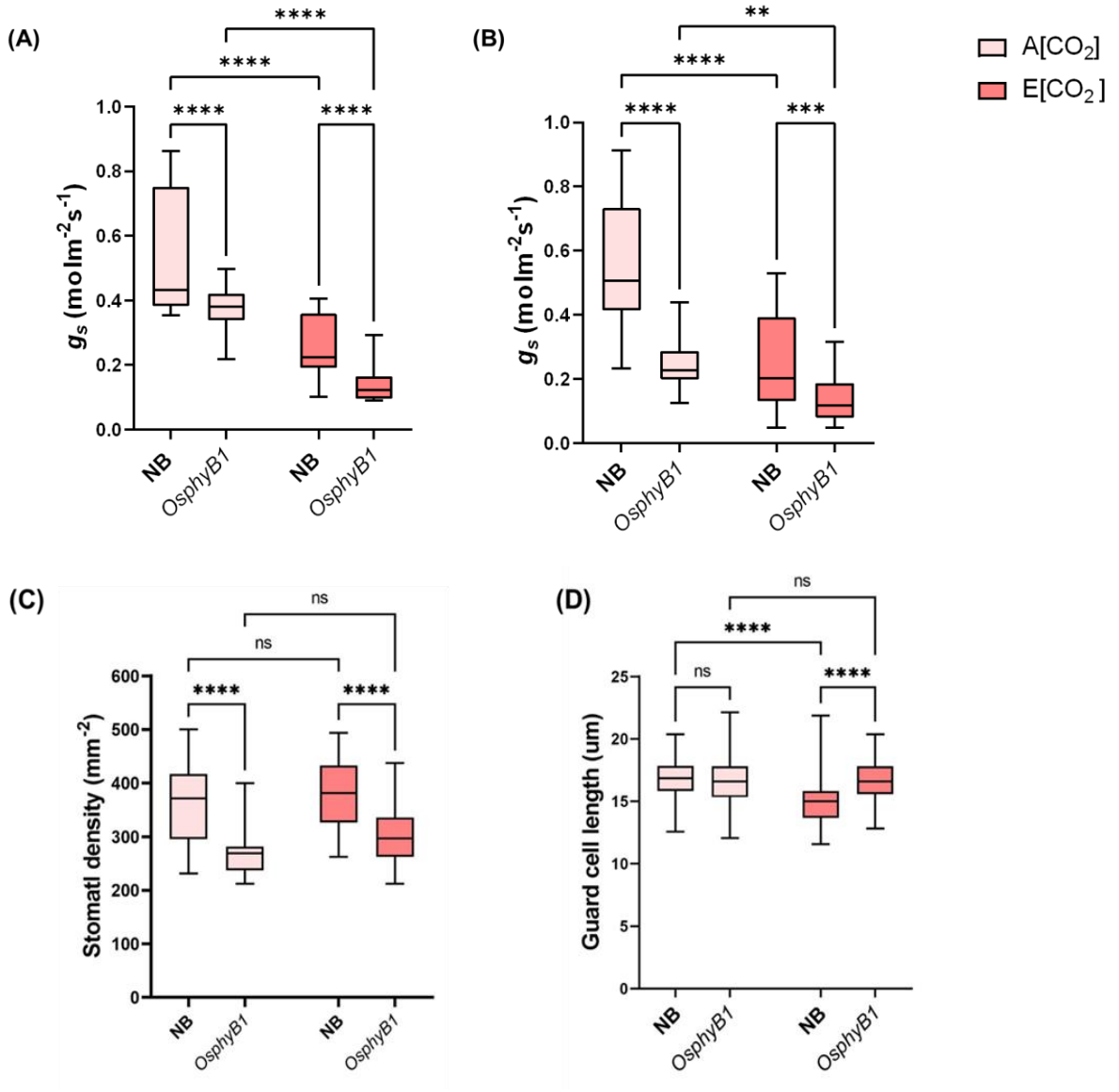

Figure 5.2 Total leaf stomatal conductance of NB and *OsphyB1* from flag leaves of plants grown under A[CO_2] and E[CO_2]. (A) g_s measurements using IRGA (LI-6800 Portable Photosynthesis System). **(B)** combined g_s of both AB and AD surfaces using a porometer (LI-600 Portable Photosynthesis System) **(C)** Combined SD measurement from AB and AD surfaces. **(D)** Combined GCL measurement from AB and AD surfaces. Plants were between 55-56 days old for (A), 60 days old for (C), and (D) whereas 70-73 days old for (B) post-germination. The biological replicates were n=6. Statistical analysis was conducted using two-way ANOVA with Tukey's multiple comparison tests where the difference between genotypes and [CO_2] treatments were significant with **P < 0.01, ***P < 0.001, ****P < 0.0001.

5.4 The stomatal conductance of the abaxial and adaxial surfaces responds differentially to E[CO_2]

Stomata on the AB and AD leaf surfaces of amphistomatous species have been reported to respond differently to external stimuli such as changes in light quantity and [CO_2] (Long et al., 1989; Mott & Peak, 2018; Wall et al., 2022). Porometer measurements were therefore taken to separately measure the g_s of both the AB and AD surfaces in the examined genotypes under different [CO_2] conditions. E[CO_2] promoted stomatal closure on both surfaces of NB and *OsphyB1* as evidenced by lower g_s measurements. However, the magnitude of response was different between the surfaces (Figure 5.3A). The AB surface of both NB and *OsphyB1* showed a greater magnitude of a response towards E[CO_2] compared to the AD surface. In the case of NB, the mean AB g_s at E[CO_2] was 41% that of the g_s at A[CO_2], whereas for the AD surface this was 67% and for *OsphyB* these were 31% and 48% respectively. When comparing NB to *OsphyB*, there was very little difference in g_s on the AB surface however, *OsphyB* had significantly lower g_s on the AD surface under both A[CO_2] and E[CO_2] (Figure 5.3A).

Significant differences in stomatal anatomy like SD and GCL on the AB and AD surfaces have been observed to be responsible for differences in g_s between species (*Phaseolus vulgaris* and wheat) and within species (wheat) (Wall et al., 2022). To determine the involvement of stomatal anatomy towards the differential g_s across the genotypes and with different [CO_2], SD, and GCL measured from both surfaces are presented separately (Figure 5.3B and C). For NB, the SD of the AD surface was consistently less than that of the AB surface but changes in [CO_2] did not alter the SD of either surface (Figure 5.3B). However, GCL was reduced under E[CO_2] on both surfaces to a similar extent. [CO_2] causes changes in GCL but the AB and AD surfaces have very similar measurements and hence for NB, there were no major surface specific differences in SD and GCL that could explain the surface differences in g_s (Figures 5.3A-C). For *OsphyB*, the SD was found to increase at E[CO_2] on the AB surface but there were no differences in GCL with changes in [CO_2] (Figure 5.3B-C). For the AD surface, neither SD or GCL showed a significant change with [CO_2]. Therefore, whilst changes in [CO_2] do drive some genotype and surface specific

differences in SD or GCL, these changes do not appear to account for the surface specific differences in g_s and implicate stomatal pore aperture as the possible driver.

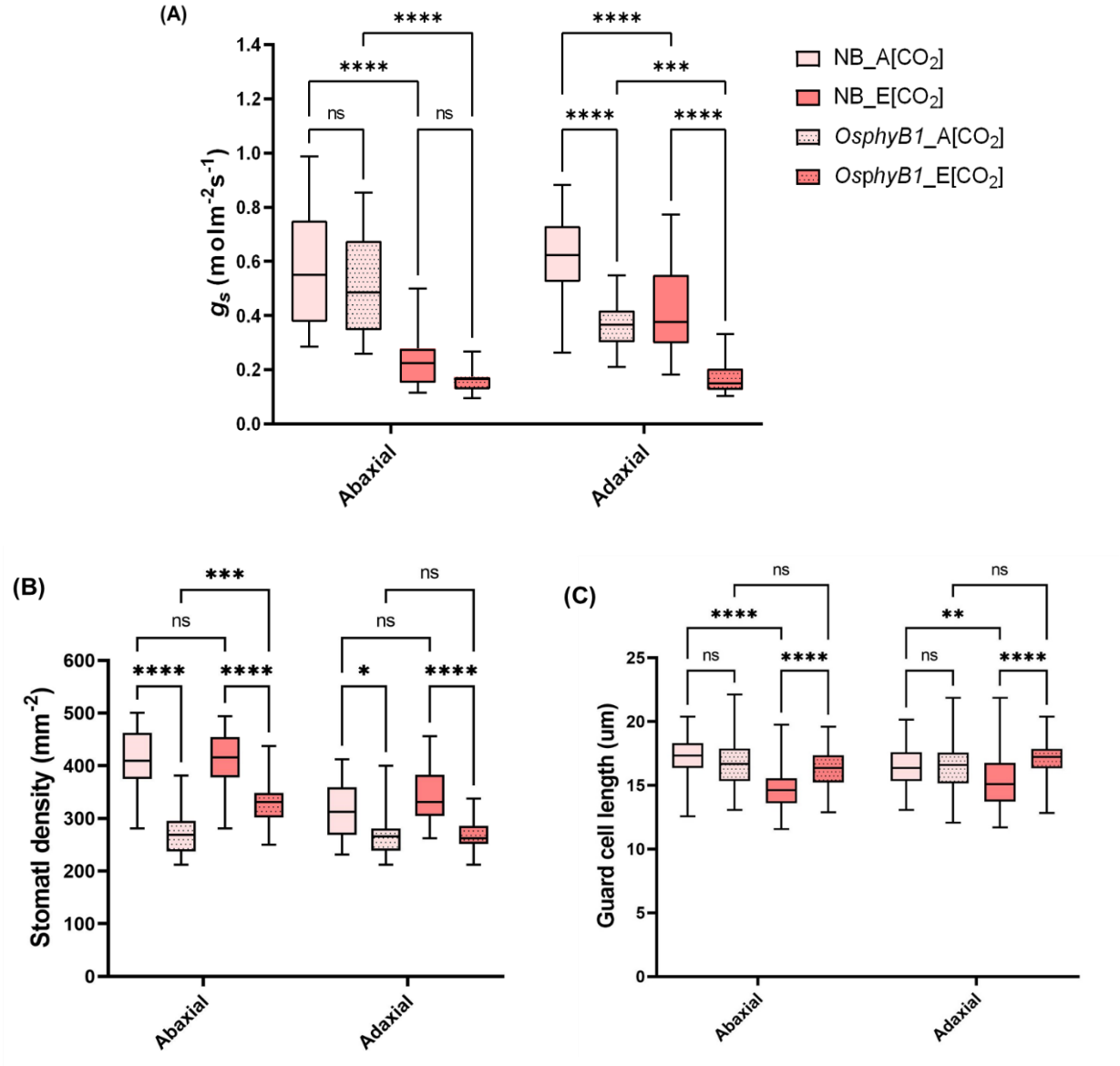

Figure 5.3 g_s and stomatal traits measurement between the flag leaf surfaces of NB and *OsphyB1* grown under A[CO_2] and E[CO_2]. (A) *gs* measurements using a porometer (LI-600 Portable Photosynthesis System) from AB and AD surfaces separately. (B) SD count from AB and AD surfaces was carried out separately. (C) GCL measurements from AB and AD surfaces were conducted separately. Plants were between 55-60 days old post germination where n=6. Comparisons were made between genotypes and [CO_2] treatments. Statistical analysis was conducted using two-way ANOVA with Tukey's multiple comparison tests where the difference between genotypes and [CO_2] treatments were significant with **P < 0.01, ***P < 0.001, ****P < 0.0001, and non-significant (ns) with P ≥ 0.05.

5.5 *OsphyB1* is more water efficient than wild type

Water use efficiency (WUE) is generally a function of water consumption relative to photosynthetic gain i.e. carbon assimilation. Since stomata are the gateway to maintaining water and gas exchange between plant and atmosphere, stomatal function and features can be major determinants of WUE in response to environmental cues. phyB has previously been shown to regulate WUE in Arabidopsis, with *phyB* mutants displaying improved WUE over WT plants (Boccalandro et al. 2009) however, this has not been determined for *phyB* mutants in rice. Therefore, IRGA measurements were taken under cabinet conditions to determine intrinsic water use efficiency measurements (described in section 2.12.2). This data indicated that *OsphyB1* was more water efficient than NB under both A[CO_2] and E[CO_2] growth conditions, similar to what has previously been observed in Arabidopsis. Also, plants (both NB and *OsphyB1*) grown under E[CO_2] showed increased water use efficiency compared to the same genotype under A[CO_2] (Figure 5.4). Similar observation was supported by transpiration (E) measurement as lower transpiration means plants are losing less water (Figure 5.4B).

Carbon isotope discrimination ($\Delta^{13}C$) measures the ratio of ^{12}C and ^{13}C in plant tissue and is used as a proxy for lifetime WUE (Farquhar et al., 1989). This measurement relates to the preference of RuBISCO to fix $^{12}CO_2$ over $^{13}CO_2$ and the relative barrier to gas diffusion presented by stomata. If stomata are more closed and hence present a greater barrier to diffusion, RuBISCO fixes the available $^{12}CO_2$ first before then fixing $^{13}CO_2$ as the [CO_2] in the leaf drops (C_i). Therefore, a lower value of $\Delta^{13}C$ indicates improved WUE (and so is the opposite to iWUE, Figure 5.4A where higher values indicate improved WUE). As with iWUE, the $\Delta^{13}C$ analysis showed higher water efficiency in *OsphyB1* compared to NB under both the [CO_2] growth conditions. However, the trend of having more water efficiency with [CO_2] elevation as observed from iWUE measurements (Figure 5.4A) was not supported suggesting that growth at E[CO_2] resulted in reduced lifetime WUE (Figure 5.4C). Since leaf samples for $\Delta^{13}C$ measurements were collected at a late stage of flag leaves when the panicles were almost filled with grain this might affect the WUE as reported in maize (Cui & Han, 2022). In addition, WUE and $\Delta^{13}C$ are known to vary independently, making it difficult to obtain trends in water use efficiency from $\Delta^{13}C$ data (Seibt et al., 2008).

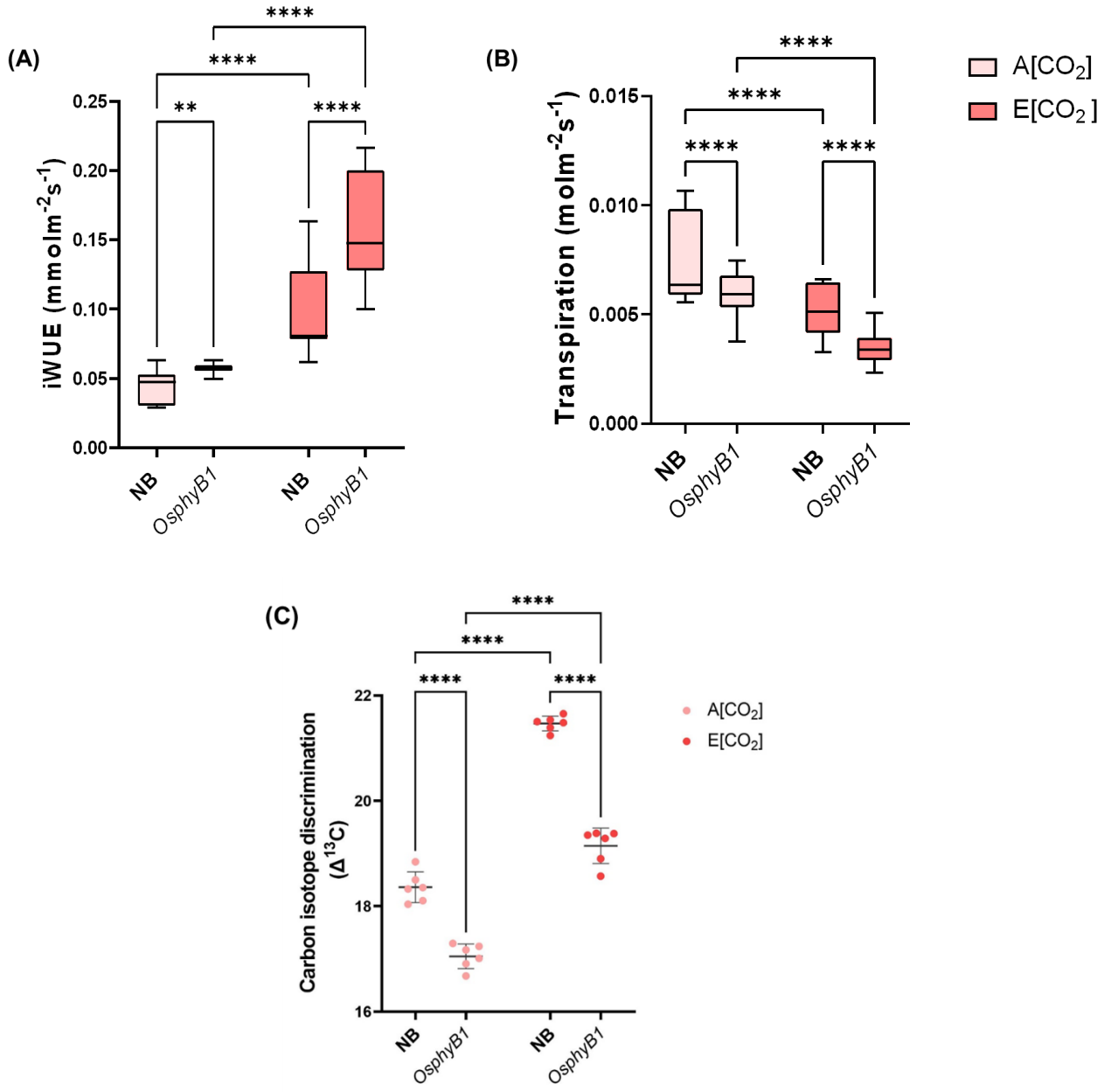

Figure 5.4 WUE measurements from NB and Os*phyB1* flag leaves grown under A[CO_2] and E[CO_2]. **(A)** Intrinsic water uses efficiency (iWUE) measured by dividing A_n by g_s derived from IRGA (LI-6800 Portable Photosynthesis System). **(B)** Transpiration (E) measured from IRGA (LI-6800 Portable Photosynthesis System). **(C)** Carbon isotope discrimination ($\Delta^{13}C$) measurements through IRMS analysis. Plants were between 70-73 days old post germination where n=6. Comparisons were made between genotypes and [CO_2] treatments. Statistical analysis was conducted using two-way ANOVA with Tukey's multiple comparison tests where the difference between genotypes and [CO_2] treatments were significant with **P < 0.01 and ****P < 0.0001.

5.6 Under steady-state conditions photosynthetic parameters are not affected at E[CO_2]

To determine whether OsphyB1 regulates photosynthetic performances, several photosynthetic parameters were measured under the two different [CO_2] growth conditions.

The efficiency of photosystem II (PSII) was measured using a FluorPen (FP100, Photon Systems Instruments) from light and dark-adapted leaves from NB and *OsphyB1* grown under A[CO_2] and E[CO_2] conditions. No significant difference was found between genotypes and between [CO_2] treatments from light-adopted measurements (Fv'/Fm') (Figure 5.5A). However, dark adopted measurements (Fv/Fm) showed a significant difference between NB and *OsphyB1* at both [CO_2] growth conditions though no significant difference was observed with [CO_2] elevation (Figure 5.5B).

Net CO_2 assimilation (A_n) measurements were conducted on flag leaves using an IRGA (LI-6800 Portable Photosynthesis System) to observe any effect of the growing the genotypes at the two different [CO_2]. For these measurements the IRGA light and [CO_2] was set to match the cabinet conditions. No significant difference was found between the [CO_2] conditions in both genotypes. Even the A_n was found similar when compared between the genotypes (Figure 5.5C).

Measurements of total chlorophyll content indicate there is significantly lower chlorophyll in *OsphyB1* compared to NB at both A[CO_2] and E[CO_2] growth conditions. However, no effect of [CO_2] change was observed in total chlorophyll content in the case of both the studied genotypes (Figure 5.5C).

Altogether, different factors to measure photosynthesis efficiency showed no effect of [CO_2] elevation in NB and *OsphyB1*, although *OsphyB1* appeared to be photosynthetically less efficient compared to NB considering Fv/Fm and chlorophyll content data. However, similar net CO_2 assimilation rate under the same light condition between wild rice and *OsphyB1* indicates *OsphyB1* may be more efficient in using light despite having less chlorophyll content.

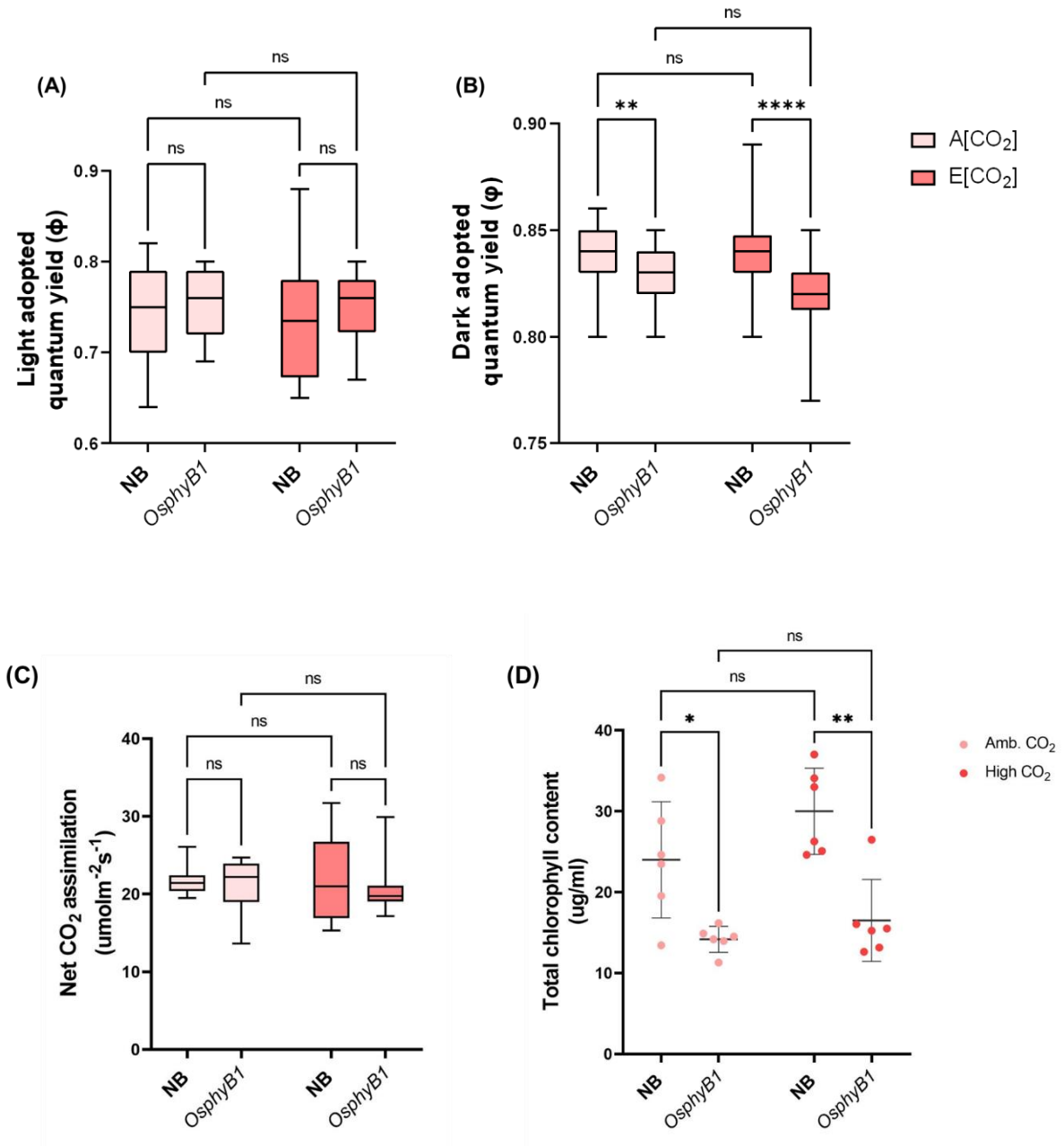

Figure 5.5 Measurements of photosynthetic traits from flag leaves of NB and *OSphyB1* grown under A[CO_2] and E[CO_2]. (A) Light adopted quantum yield measurements and (**B)** Dark adopted quantum yield measurements using FluorPen (FP100, Photon Systems Instruments, Brno, Czech Republic). **(C)** Steady state measurements of net CO_2 assimilation (A_n) from IRGA (LI-6800 Portable Photosynthesis System) after matching the conditions according to the growth chamber conditions. **(D)** Total chlorophyll concentrations measured from flag leaf extraction. Plants were between 70-73 days old post germination where n=6. Comparisons were made between genotypes and [CO_2] treatments. Statistical analysis was conducted using two-way ANOVA with Tukey's multiple comparison tests where the difference between genotypes and [CO_2] treatments were significant with *P < 0.05, **P < 0.01, ****P < 0.0001, and non-significant (ns) with P ≥ 0.05.

5.7 Differential response of E[CO_2] between tillers and flag leaf

To further characterise the response of the two genotypes to growth under different [CO_2], several traits were measured. These included tiller number, initiation of reproductive phase via panicle initiation, flag leaf length, and flag leaf area. Tiller number differs with varieties, environment, and agronomic practices (Mohanan & Mini, 2007). With an elevation of [CO_2], tiller number (vegetative and reproductive tillers) increased significantly in NB but not in *OsphyB1*. At both [CO_2] growth conditions, the number of tillers is always lower in *OsphyB1* than in NB (Figure 5.6A). The reproductive phase started earlier in *OsphyB1* as demonstrated by panicle initiation (days from post-germination of seeds) in comparison to NB at both [CO_2] conditions. This is consistent with previous reports in rice as well as in Arabidopsis phyB mutants (Reed et al., 1993; Takano et al., 2005). However, the effect of E[CO_2] on flowering have demonstrated for the first time here and no effect of [CO_2] treatments on panicle initiation in both genotypes have previously been observed (Figure 5.6A).

Measurements of flag leaf length revealed a significant reduction in length in NB plants grown at E[CO_2], whereas *OsphyB1* flag leaf length did not change under the different [CO_2] (Figure 5.6C). *OsphyB1* flag leaves were shorter than those of NB at A[CO_2] but there was no difference at E[CO_2]. This was reflected in leaf area measurements with NB area reduced at E[CO_2], whilst there was no change in *OsphyB1* (Figure 5.6D).

Therefore, the effect of E[CO_2] was found positive to increase tiller number in NB but negatively impact flag leaf size, whereas these traits did not change in *OsphyB1* under the different growth [CO_2]. Though no reports determine the role of red light to affect tiller number and leaf size in response to CO_2 elevation, but low light is known to impact rice tillering and leaf area (Xiu et al. 2013, Das et al. 2022).

5.8 *OsphyB1* shows a significant reduction in yield compared to wild type

Given the differences in tiller number and flag leaf size and area between NB and *OsphyB1* and that the flag leaf is known to have a significant impact on yield (Li et al.

1998, Yue et al. 2006) the impact of different growth [CO_2] on yield was then determined.

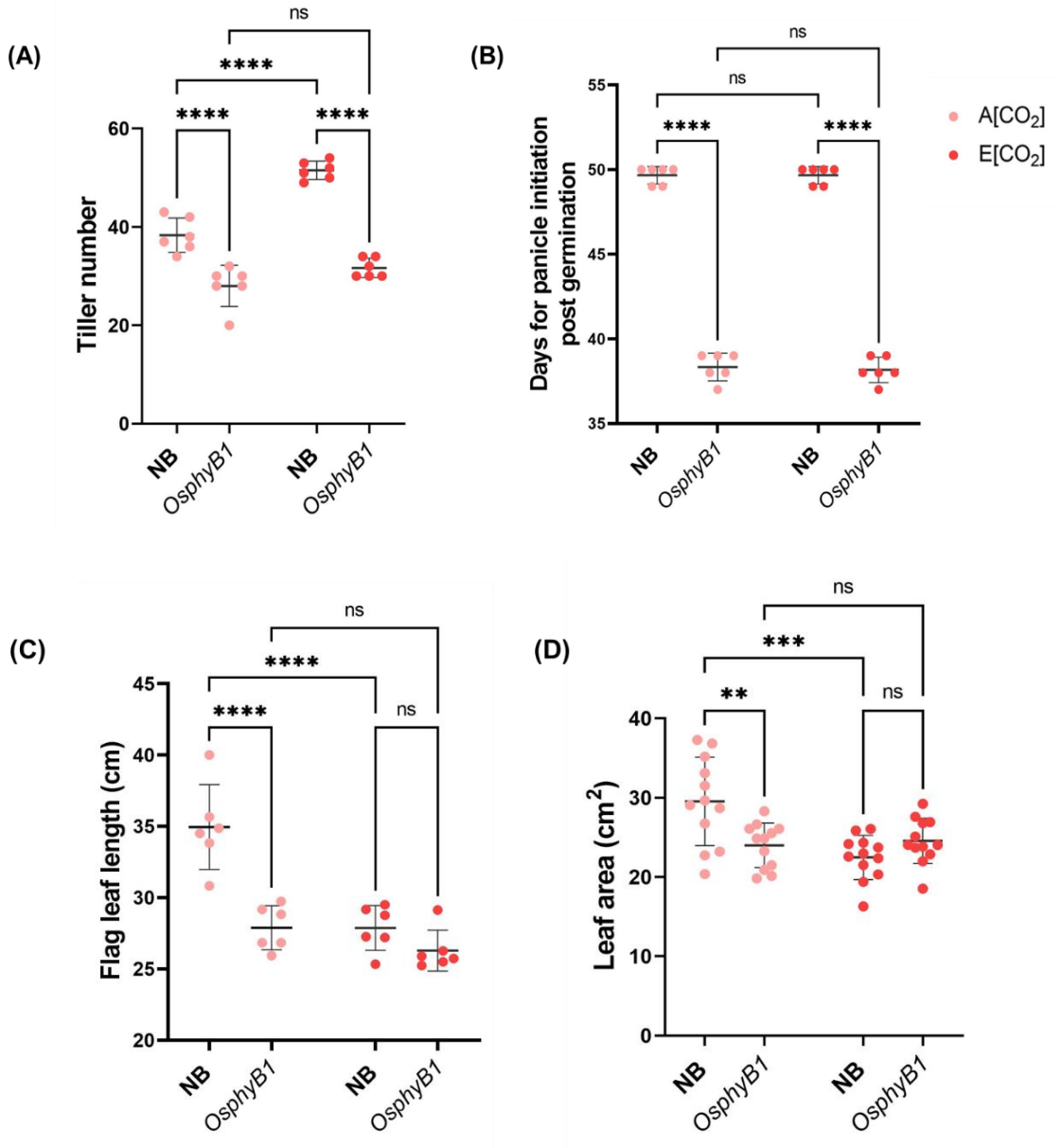

Figure 5.6 Measurements of growth traits from NB and *OsphyB1* grown under A[CO_2] and E[CO_2]. (A) Total tiller number counted when the plants are 66 days old post-germination**. (B)** Time of panicle initiation measured in days post-germination of seeds. **(C)** Measurements of flag leaf length from 60 days old plants. **(D)** Leaf area was measured when the plants were between 63-64 days old post-germination. Biological replicates, n=6. Comparisons were made between genotypes and [CO_2] treatments. Statistical analysis was conducted using two-way ANOVA with Tukey's multiple comparison tests where the difference between genotypes and [CO_2] treatments were significant with **P < 0.01, ***P < 0.001, ****P < 0.0001 and, non-significant (ns) with P ≥ 0.05.

Panicles are important for the rice reproductive phase and yield and total panicle number was lower in NB compared to *OsphyB1* at both [CO_2] growth conditions. Also E[CO_2] did not affect panicle number in NB whereas, *OsphyB1* mutants had significantly more panicles at E[CO_2] (Figure 5.7A). However, when total panicle weight was measured, this was significantly greater in NB compared to *OsphyB1* under both [CO_2] therefore, despite having more panicles *OsphyB1* panicles were significantly lighter (Figure 5.7B). As with panicle number, NB panicle weight did not change under the different [CO_2], whereas *OsphyB1* panicle weight was significantly increased under E[CO_2]. However, it was observed that not all panicles contained seeds and so rather than total panicle weight, the weight of seed bearing, or seedless panicles was then measured (Figure 5.7 C-D). This identified a major difference between NB and *OsphyB1*, which accounts for the reduced weight of *OsphyB1* panicles. NB has significantly more seed-bearing panicles than *OsphyB1* (Figure 5.7C) and conversely, *OsphyB1* had significantly more seedless panicles (Figure 5.7D). The [CO_2] had no effect on the weight of seed bearing panicles in either genotype however, growth at E[CO_2] led to a significant increase in seedless panicles in *OsphyB1* (Figure 5.7D). Therefore, panicles of *OsphyB1* had less developed grains and fewer seeds compared to NB at both [CO_2] conditions (Figure 5.7E).

To determine if this impacted on grain size, filled seeds were removed from panicles and the 100 seed weight was calculated for each genotype and [CO_2] growth treatment. [CO_2] did not appear to effect seed weight in either genotype, though *OsphyB1* seed weight was more variable at E[CO_2]. This may account for why *OsphyB1* seed weight is significantly lower than NB at A[CO_2] (Figure 5.9A).

Collectively, these data indicate that under these growth conditions, [CO_2] has no significant effect on the yield of NB and that *OsphyB* was lower than NB and this was due to a significant increase in seedless panicles.

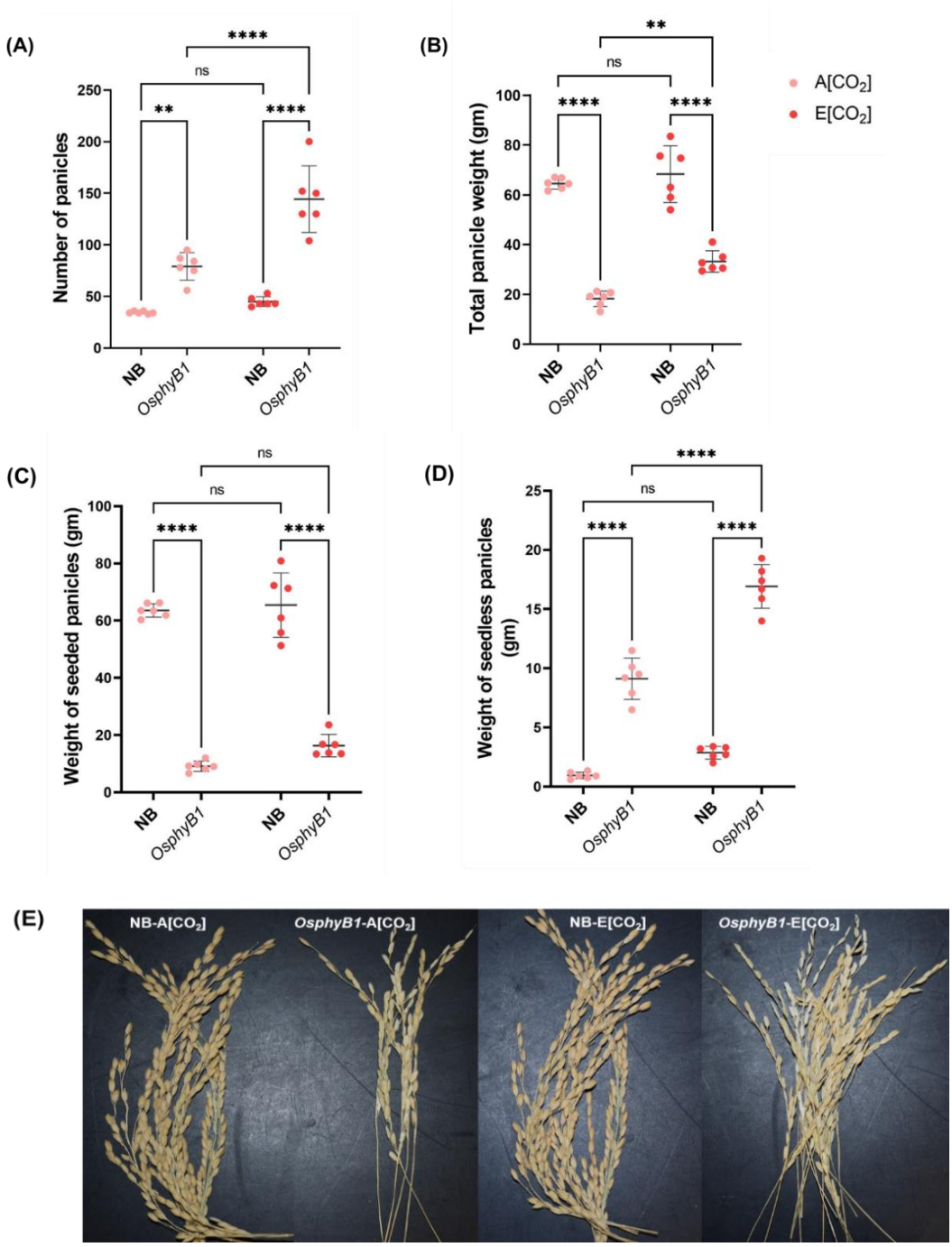

Figure 5.7 Panicle traits observed from NB and *OsphyB1* plants grown A[CO_2] and E[CO_2]. **(A)** Total number of panicles per plant. **(B)** Total panicle weight per plant after harvesting including grain-filled seeds and seedless panicles. **(C)** Weight measured from dried panicles with grain-filled seeds only. **(D)** Weight of panicles that have no grain-filled seeds. **(E)** Representative images of panicles from NB and OsphyB1 grown at A[CO_2] and E[CO_2]. Biological replicates, n=6. Comparisons were made between genotypes and [CO_2] treatments for the above-mentioned measurements**.** Statistical analysis was conducted using two-way ANOVA with Tukey's multiple comparison tests where the difference between genotypes and [CO_2] treatments was significant **P < 0.01, ****P < 0.0001, and non-significant (ns) with P ≥ 0.05.

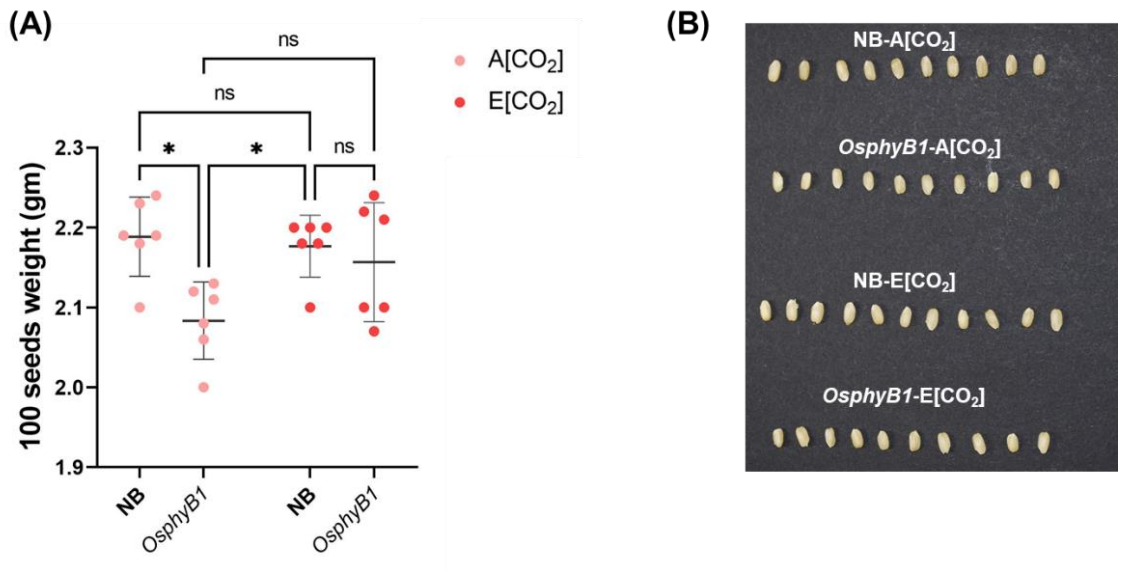

Figure 5.8 Yield from NB and *OsphyB1* plants grown A[CO_2] and E[CO_2]. (A) Weight of 100 seeds from both NB and *OsphyB1*. **(B)** Image of the seed grains from each line grown under different [CO_2] chambers. Biological replicates were n=6. Comparisons were made between genotypes and [CO_2] treatments for the above-mentioned measurements**.** Statistical analysis was conducted using two-way ANOVA with Tukey's multiple comparison tests where the difference between genotypes and [CO_2] treatments were significant **P < 0.01, ****P < 0.0001, and non-significant (ns) with P ≥ 0.05.

5.9 Discussion

Mutants in two different alleles of rice phyB i.e., *OsphyB1* and *OsphyB2* appeared hotter than NB from infra-red thermal images suggesting that they have a reduced stomatal conductance (Section 5.1). In addition, [CO_2] shift within the chamber revealed both the mutants were more responsive in stomatal closure as well as reopening response compared to NB during dynamic [CO_2] changes. This finding indicated a hypersensitive response in rice *phyB* mutant, similar to what was observed in Arabidopsis *phyB-9* as described in section 4.1.

This observation led to the further investigation of the developmental responses of rice *phyB* mutants grown under E[CO_2] and here, considering the importance of flag leaves towards photosynthetic potential and yield, all experiments except for thermal imaging experiments, was carried out using flag leaves (Sicher, 1993; Adachi et al., 2017).

As it was not possible to reliably use the stomatal bioassay system to assess rice stomata to changes in [CO_2], g_s was instead measured using a leaf porometer and infrared gas analyzer. Both methods showed lower g_s in *OSphyB1* compared to NB under both [CO_2] conditions. In addition, E[CO_2] caused a reduction in g_s in both the studied genotypes (section 5.2) agreed with the available literature (Morison, 1987; Drake et al., 1997; De Costa et al., 2003). In addition to functional responses, anatomical traits like SD, GCL, and stomatal patterns are known to affect the determination of g_s (Willmer & Fricker, 1996; Weyers & Lawson, 1997; Hetherington & Woodward, 2003; Casson & Hetherington, 2010; Lawson & Blatt, 2014; Matthews et al., 2018; Faralli et al., 2019). The combined effect of reduced SD and GCL in *OsphyB1* and *OsphyB1* compared to NB was reported to lower the g_s (Liu et al., 2012). However, the present study showed reduced SD as reported but similar GCL in *OsphyB1* compared to NB at A[CO_2]. No reports have shown the effect of E[CO_2] on *OsphyB1* and our work revealed no change in SD and GCL at E[CO_2]. On the contrary, SD and GCL behaved in an opposite manner with [CO_2] elevation in NB (Section 5.2) suggesting the potential involvement of *OsphyB1* in mediating both developmental and functional stomatal response towards E[CO_2].

There are reports on differential stomatal responses on the two leaf surfaces in isobilateral amphistomatous leaves to external stimuli such as light intensity and [CO_2] (Mott & Parkhurst, 1991; Richardson et al., 2017; Wall et al., 2022). Porometer measurements from the present study indicated different g_s from both surfaces of NB and *OsphyB1*. However, with the elevation of [CO_2], the AB surface of both NB and *OsphyB1* showed a greater closure response compared to the AD surface (Figure 5.3A). SD has been reported more on AB surface compared to AD surface in species of rice and we also observed a similar trend in our studied genotypes NB and *OsphyB1* (Ishimaru et al., 2001; Ohsumi et al., 2007; Hubbart et al., 2013; Chatterjee et al., 2020). This might partly suggest the differential response of g_s on both surfaces. However, the lower g_s of AB surface at E[CO_2] could not be explained by changes in SD and/or GCL as the changes appeared to be similar on both surfaces (Figures 5.3B and C). Collectively, this indicates reduction in g_s involved of only functional response with no direct corelation between either the SD or GCL.

In line with lower g_s, *OsphyB1* appeared to be more water efficient than NB from different measurement approaches including IRGA and $\Delta^{13}C$ and is consistent with

existing reports (Boccalandro et al. 2009; Liu et al., 2012). Although at E[CO_2] both the genotypes tended to be more water efficient as determined from iWUE and transpiration measurements from IRGA, $\Delta^{13}C$ showed opposite results with E[CO_2]. $\Delta^{13}C$ is sensitive to the ratio of the chloroplast to ambient CO_2 mole fraction, (Cc /Ca) rather than ratios of intercellular to ambient CO_2 mole fraction (Ci/Ca) and, consequently, to mesophyll conductance (Seibt et al., 2008; Cernusak et al., 2013). It is not possible to determine Cc/Ca from the same gas exchange measurements as the Ci/Ca as mesophyll conductance may differ over time. On the other hand, WUE at the leaf level depends on evaporative demand, which does not directly affect $\Delta^{13}C$. Thus, WUE and $\Delta^{13}C$ vary independently (Seibt et al., 2008) and specifically with changes in atmospheric [CO_2] as evident from the present study.

Though the effect of E[CO_2] was evident from stomatal function responses, anatomy, and WUE between the genotypes, photosynthesis efficiency remained unaffected as measured with A_n, PSII, and chlorophyll content (Section 5.3). No effect of E[CO_2] on A_n was in contrast with existing literature (Allen et al., 1995; Ziska & Teramura, 1995; De Costa et al., 2003). The reasons for such discrepancy might be the difference in [CO_2] from other literature and use of flag leaf in the present study. In addition, use of relatively low light (600 $\mu molm^{-2}s^{-1}$, detailed described in section 2.12.2) instead of high saturating light usually used in IRGA for CO_2 response curve resulted no significant difference. There is also report of unaltered Fv/Fm in wheat with e[CO_2] under well-watered conditions (Conroy et al., 1994). PSII efficiency was found to be stressed in *OsphyB1* compared to NB with less chlorophyll content. However, like A_n, PSII and chlorophyll content remained unaffected with an elevation of [CO_2] in *OsphyB1*.

Though the tiller number increased, flag leaf length and leaf area reduced in NB at E[CO_2] and this is in agreement with existing literature after panicle initiation indicating that the effect of E[CO_2] varied at different growth stages (Kim et al., 2003). Tiller number, flag leaf length, and leaf area remained unchanged in *OsphyB1* with *the* elevation of [CO_2]. A decrease in cell division of the primordial leaf in Os*phyB* was speculated to lower the number of cells in the leaf (Barrôco et al., 2006; Liu et al., 2012) and might play a negative role in tiller number, flag leaf length, and leaf area in *OsphyB1* compared to NB. Also, panicle initiation is earlier in *OsphyB1* similar to *phyB* mutants in Arabidopsis (Dehesh et al., 1991). A similar report has also been published

on rice when grown under LD (long day) conditions (Takano et al., 2009) though plants were grown at ND (neutral day) conditions in the present study. This indicates light signals mediated by phyB delayed flowering at both LD and ND but not at SD (short day) (Takano et al., 2009).

Yield is considerably lower in *OsphyB1* in comparison with NB. Reduced SD observed in *OsphyB1* may act as a CO_2 diffusion barrier that limits CO_2 uptake thereby reducing photosynthesis and ultimately yield. Although, present study reported no difference in A_n between the species but significantly low chlorophyll content and lower Fv/Fm may act as limiting factor to yield. In addition, higher leaf temperature due to reduced SD (Figure 5.1B) seems more likely to reduce spikelet fertility and grain filling in rice (Jagadish et al. 2007; Sreenivasulu et al., 2015; Hu et al. 2022). Interestingly weight of seedless panicles was higher in *OsphyB1* to NB suggesting their enhanced sterility (Sun et al., 2017). A slight decrease in yield at E[CO_2] grown NB correlated with reduced flag leaf length and area since they have a significant influence on rice grain yield (Li et al., 1998; Zhang et al., 2015).

5.9.1 Concluding remarks

1. The physiological functioning of stomata is significantly impacted by E[CO_2], both in the short and long term, while CO_2 assimilation remains unaffected.

2. Adaptations in stomatal behavior in response to E[CO_2] assist in maintaining water balance and ultimately lead to a balanced yield.

3. The role of phyB in mediating responses to E[CO_2] in rice was found to be critical, as evidenced by various measurements conducted in this study.

Chapter 6. General discussion

6.1 Introduction

Stomata are the primary responder controlling the exchange of water vapour and CO_2 between the plant interior and atmosphere depending on the prevailing environmental conditions. As such, they play a major role in regulating plant water relations and carbon gain. The control of plant gas exchange is primarily driven by the regulation of both stomatal aperture and the number of stomata that develop on the leaf surface in response to diverse environmental stimuli to maintain an optimum g_s (Bertolino et al., 2019; Caine et al., 2019; Harrison et al., 2020). Global a[CO_2] is predicted to increase between 730 ppm to 1020 ppm by the 21st century from model simulations (Meehl et al. 2007). The continuing trend for increases in a[CO_2] and warming is predicted to dominate future changes in g_s over other global change factors such as change in precipitation, enhanced nitrogen deposition and ozone pollution (Wang et al., 2012; Liang et al., 2023). Therefore, a better understanding of stomatal aperture regulation in response to high [CO_2] would provide opportunities to manipulate crops for improved yield. This study focused on the interaction of the phytohormones GA and ABA to modulate stomatal closure in response to treatment with E[CO_2]. Additionally, the involvement of light signals via the photoreceptor phyB was determined in this response. Finally, the role of phyB in mediating physiological responses and developmental adaptation in rice under E[CO_2] condition was also investigated.

6.2 E[CO_2]-mediated stomatal closure targets GA metabolism not ABA

A number of studies have identified crosstalk between e[CO_2] and ABA during the promotion of stomatal closure and it has been hypothesised that E[CO_2] can act by sensitising GCs to ABA (reviewed in Engineer et al., 2016). Sensitising a biological system to a signal can be achieved by altering the biosynthesis of the signal or changing the density of receptors. However, there has been contrasting data as to whether [CO_2] regulates the ABA signalling receptors and changes in [CO_2] do not appear to result in any measurable changes in ABA levels (Chater et al., 2015; Hsu et al., 2018; Dittrich et al., 2019; Zhang et al., 2020). An alternative mechanism is to therefore change the concentration of an antagonist to the signals, and this led to the

hypothesis that GAs may modulate GC responses to [CO_2] elevation by countering GC sensitivity to ABA. GA_3 was also found to negate ABA mediated stomatal closure response under [CO_2] free conditions demonstrating its antagonism towards ABA (section 3.4). Application of 100μM of GA_3 or GA_4 was found optimum for the inhibition of E[CO_2]-induced promotion of stomatal closure. Additionally endogenous GA generated in the β-estradiol inducible pUBQ-XVE-GA20ox1-P2A-GA3ox1 line (Rizza et al., 2021) proved to be effective in a similar way (section 3.2). Moreover, GA inhibitors PBZ and DMZ provided support for this hypothesis as they positively mediate [CO_2]-induced stomatal closure (section 3.3). A genetic approach was also used to investigate the role of GA in responses to E[CO_2] by analysing the response to E[CO_2] of mutants in GA metabolism and signalling. A quintuple mutant of GA2ox (*ga2oxq*; deactivate bioactive GAs by 2β-hydroxylation) has previously been shown to have more GA in the system (Rieu et al., 2008). The GC insensitivity of *ga2oxq* towards [CO_2] elevation suggests that a wild type CO_2 response requires GA2ox mediated GA catabolism. (Figures 3.8A and B). Use of other mutants in GA synthesis pathway e.g., GA-deficient mutant *ga3ox1ga3ox2* with very low GA (Mitchum et al., 2006) would provide more insight into the requirements for GA biosynthesis or breakdown in E[CO_2] responses.

As well as the epidermal bioassay system, whole leaf g_s measurements with an IRGA supported a role for GA_3 in inhibiting E[CO_2]-mediated stomatal closure by both inhibiting closure and reducing the rate at which closure occurred. PBZ feeding did results in a reduction in g_s but unlike GA_3 did not significantly alter stomatal closure rate in response to a change in [CO_2] (section 3.7). As PBZ was both sprayed on leaves the night before and then applied by petiole feeding, further analysis may be required to determine whether this method of application significantly altered GA levels over the duration of the experiment.

Since GAs in plants are known to be maintained through feedback and forward regulation of GA metabolism (Hedden & Phillips, 2000; Olszewski et al., 2002) components in GA signalling would help to better understand GA regulation of stomatal responses to E[CO_2]. Stomatal function bioassays with *dellaq* and DELLA stabilized mutant lines 35TAP_RGAΔ17 and 35STAP_GAIΔ17 (Feng et al., 2008; Koini et al., 2009) suggest evidence both for and against DELLA requirements for responses to E[CO_2] (Figures 3.9 and 3.10). This also suggests that stability of the DELLAs rather

than their absence is important for responses to [CO_2]. Not all GA signalling is DELLA-dependent and so it is also feasible that there may be involvement of DELLA-independent pathways, for example via Ca^{2+} dependent signalling as reported in many GA responses (Ishida et al., 2008; Okada et al., 2017).

ROS signalling is known to act as a mediator between ABA and E[CO_2]-mediated stomatal closure (Chater et al., 2015; Ehonen et al., 2019). As expected, ROS levels were seen to increase with increasing [CO_2] as determined by measuring GC fluorescence stained with H_2DCFDA (Figure 3.11A and B). GA treatment did not impact on ROS production in GCs, suggesting that GA is likely not acting via ROS to inhibit E[CO_2] induced promotion of closure. GCs treated with PBZ however, did not appear to generate more ROS with increasing [CO_2], though the levels of ROS were initially higher under F[CO_2] than the control, which does correlate with the reduced apertures of PBZ treated GCs under these conditions. Collectively however, given that GA does not appear to alter ROS production and yet does alter E[CO_2] promotion of closure, it cannot be confidently concluded that GA acts through ROS.

Though not specifically linked to the role of GA in CO_2 responses, mutants in HPCA1, which perceives extracellular ROS to initiate downstream Ca^{2+} signalling, were tested for their response to [CO_2]. As with GA, *hpca1* mutants were found to be involved in regulating E[CO_2]-mediated stomatal closure in the present study (Figure 3.12A and B) in addition to being linked to ABA-mediated stomatal closure (Wu et al. 2020). CO_2 signalling and ROS have only been linked to NADPH respiratory burst oxidase RBOHD and RBOHF (Chater et al. 2015). They generate extracellular ROS so it might be that HPCA1 is perceiving this in the context of GC CO_2 signalling.

Recent studies have found correlations between changes in the expression of GA metabolism genes and GA levels in plants. For example, *GA3ox1* expression was found to correlate with active GA_4 levels at night (Prasetyaningrum et al., 2021). This night-time rise in GA also aligns with circadian control of GA signalling, whereby DELLAs are stabilised during the day and the GID1 receptors are expressed more at night (Arana et al., 2011). In another example of transcriptional control, RVE1 negatively regulates *GA3ox2* expression to control GA levels in seeds, with *rve1* mutants having higher levels of active GA (Jiang et al., 2016). Given these previous studies had shown a link between transcriptional control of GA metabolism genes and

GA levels, it was therefore surprising to find no direct relation to corroborate their involvement (Figure 3.14). A more extensive analysis of GA metabolisms and signalling genes within the Casson lab gave similar findings (data not shown). However, absolute measurement of GAs from two parallel GA biosynthesis pathway showed that active GA_1 from 13-hydroxylation pathway was reduced at E[CO_2] in Col-0 (Figure 3.16). Beyond transcriptional control, post-transcriptional and translational processes expand gene regulatory pathways to shape hormone responses (reviewed in Waadt et al., 2022). Indeed, within GA signalling DELLA stability is regulated post-translationally (reviewed in Blanco-Touriñán et al., 2020). Significantly, measurements of ABA and ABA conjugate from the same samples remained similar with [CO_2] elevation. This provides strong support for the hypothesis that E[CO_2] can promote enhanced sensitivity to ABA by regulating an ABA antagonist, GA. By generating a higher ABA/GA ratio, GC sensitivity to ABA is enhanced and this may regulate the closure response at E[CO_2] (Figure 6.1). Given the lack of a clear transcriptional mechanism the exact molecular mechanism of GA regulation towards E[CO_2]-mediated stomatal closure need to be addressed. However, more widely this data indicates that scenarios in which GA levels are altered may alter GC responses to endogenous ABA; for example, during very early seedling growth when GA levels are high or, as discussed, at night when GA levels are known to peak. It is interesting to note that despite the widely held view that stomata close at night, there is actually a significant level of night-time transpiration due to stomata opening (Fricke, 2019; McAusland et al., 2021).

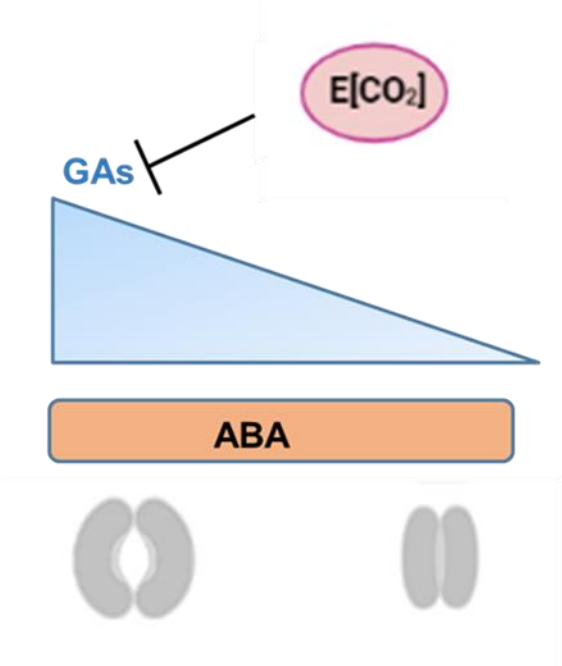

Figure 6.1 GAs has a potential role during E[CO_2]- mediated stomatal closure response. A homeostasis exists between ABA and GA where GA reduces with the elevation of [CO_2], and ABA remains unchanged. Barred line denotes negative regulation.

6.3 phyB mediates E[CO_2]- mediated stomatal closure through ABA and GA homeostasis

Stomatal aperture regulation in response of light and [CO_2] is critical for optimum carbon assimilation (Lawson et al. 2014; Papanatsiou et al. 2019). Despite, the dependence of RL response on photosynthesis no well-defined signalling factor have been reported downstream of the RL perceiving phytochromes that regulate GC responses to [CO_2]. Mutants of the RL photoreceptor phyB (here *phyB-9*) were previously reported to be hypersensitive in their stomatal closure response at E[CO_2] (Brown, 2018). The *phyB-9* allele was recently found to contain a second mutation in the *VENOSA4* gene, which is involved in chloroplast development (Yoshida et al., 2018). This could clearly impact on plant responses to [CO_2] however, by analysing a complementation line in which a PHYB-YFP fusion protein was expressed using the *PHYB* promoter, it appears that the hypersensitivity to E[CO_2] is indeed phyB dependent (Figure 4.3A and B). phyB is reported to regulate ABA and GA either positively or negatively at different stages of plant development (Dong et al., 2008;

Hedden, 2020; Li et al., 2022; Sano & Marion-Poll, 2021). In mature plants, it was shown that *phyB-5* mutants contained more ABA under well-watered conditions and yet, the *phyB* mutant displayed reduced sensitivity to ABA (González et al., 2012). Given the results from present study (chapter 3), where it was shown that E[CO_2] can modulate GA levels and that this may alter ABA sensitivity, attempts were made to explain the hypersensitive closure of *phyB-9* stomata based on ABA and GA metabolism (Figure 4.2). Treatment of *phyB-9* with 100µM GA_3 was able to rescue E[CO_2]-mediated hypersensitive stomatal closure, suggesting that changes in GA and not ABA could account for the hypersensitivity of *phyB* to E[CO_2]. As was the case for Col-0, analysis of the expression of several genes in GA metabolism pathway and their comparison to Col-0 did not provide any clear picture to describe hypersensitive stomatal closure response in *phyB-9* (Figure 4.5). Nonetheless, active GA_4 and its immediate precursor GA_9 from non-13-hydroxylation pathway were reduced with [CO_2] elevation in *phyB-9* in contrast to Col-0 where primarily the 13-hydroxylation pathway was involved. Interestingly, this data could suggest that phyB plays a role in regulating GA_1 and that E[CO_2] inhibits this resulting in the reduced GA_1 levels observed in Col-0 at E[CO_2]. Conversely, in a *phyB* mutant GA_1 levels are already significantly reduced and E[CO_2] now acts to reduce GA_4 levels and it would be interesting to determine if this is mediated by other members of the phytochrome family. Collectively, therefore in a *phyB* mutant both GA_1 and GA_4 levels are reduced at E[CO_2], significantly altering the ABA:GA homeostasis relative to Col-0 and potentially accounting for *phyB* hypersensitivity to E[CO_2]. At the same time no change in ABA was observed, however there were higher levels of ABA-GE in *phyB-9* compared to Col-0 (Section 4.4). Mutation of the ABA biosynthesis genes *NCED3* and *NCED5* rescued *phyB-9* hypersensitivity to Col-0 levels as observed from CO_2 function bioassay with *phyB-9nced3nced5* triple mutant. Interestingly, the triple mutant neither completely abolish the sensitivity to [CO_2] elevation as *nced3nced5* double mutant nor was it hypersensitive as *phyB-9*. This suggests that phyB does not act directly on these ABA biosynthesis to regulate sensitivity to E[CO_2] and that genetically, they act additively (section 4.5), further supporting a role for phyB in regulating GA and not ABA. The involvement of GA metabolism towards *phyB-9* hypersensitivity was checked via circadian clock-related genes, *RVE1* and *RVE2* since they are reported to regulate GA metabolism in a phyB dependent manner during seed dormancy and germination (Finkelstein et al., 2008; Holdsworth et al., 2008; Graeber et al., 2012; Jiang et al.

2016). Partial involvement of RVE1 and RVE2 demonstrated their potential to regulate stomatal closure response towards E[CO_2] (section 4.6). The RVE group of MYB-related (1R-MYB) proteins with RVE1 and RVE2 includes the core components of the circadian clock, CCA1 and LHY (Du et al., 2013). CCA1 and LHY were also found to partially regulate E[CO_2]- mediated stomatal closure response and suggests interplay between circadian clock and high CO_2 response in stomatal aperture regulation (section 4.7); this is particularly interesting given the link between the circadian clock and GA signalling (Arana et al., 2011). Examination of genes defective in GA metabolism by crossing with *phyB-9* background would be a good approach to determine their involvement towards E[CO_2]- mediated stomatal closure response.

6.4 phyB in rice proves critical for E[CO_2]-mediated growth behaviours

Rice *phyB* mutant alleles *OsphyB1* and *OsphyB2* appeared to be hypersensitive in their stomatal closure response to E[CO_2] as was the case for Arabidopsis *phyB-9* (Brown 2018; present study). This potential involvement of phyB at E[CO_2] and considering the importance of stomatal aperture regulation to balance carbon and water utilization (WUE) led to investigate the combined effect of E[CO_2] and phyB on rice growth and physiology. Similar to short term E[CO_2] exposure, both the wild-type control (NB) and *OsphyB1* showed lower g_s under E[CO_2] compared to A[CO_2] grown samples. To determine whether the lower g_s was due to E[CO_2] mediated changes to stomatal anatomical traits like SD and GCL or aperture responses (or a combination), these traits were measured. It was decided to analyse both leaf surfaces as it has demonstrated that abaxial and adaxial surfaces can respond differently (Casson & Hetherington, 2010; Lawson & Blatt, 2014; Richardson et al., 2017; Matthews et al., 2018; Faralli et al., 2019; Wall et al., 2022). Growth under E[CO_2] did result in some genotype and surface specific differences in SD or GCL, however the functional response of changing stomatal aperture appeared to be the key to reduced g_s with [CO_2] elevation (sections 5.3 and 5.4). *OsphyB1* was found to be more WUE than NB in line with existing literatures (Boccalandro et al. 2009; Liu et al., 2012). Though iWUE and transpiration measurements determined positive effect of E[CO_2] towards WUE,

$\Delta^{13}C$ showed no effect (section 5.5). This denotes the discrepancy of using $\Delta^{13}C$ with IRGA to determine WUE (Seibt et al., 2008; Cernusak et al., 2013). For example, the lower g_s with increasing [CO_2] might not change carbon metabolism in later stages of development. Measurements of A_n, PSII and chlorophyll content corroborate this as they remained unaffected with an elevation of [CO_2] in both NB and *OsphyB1* mutant (section 5.6). In this regard, analysis of genes involved in carbon assimilation would provide better understanding. However, several growth traits like tiller number, flag leaf length and area measurements changed in E[CO_2] grown NB compared to A[CO_2] grown samples. In *OsphyB1* mutants these traits were not affected by E[CO_2], despite the hypersensitivity of their stomatal aperture response. The early onset of the reproductive phase with panicle initiation and yield is significantly compromised in *OsphyB1* compared to wild NB (Takano et al., 2005; Takano et al. 2009) but remained unaltered with increasing [CO_2] in both genotypes (Figures 5.6B and 5.8A). Therefore, except for stomatal physiological function being affected by E[CO_2] during both short and long term treatments, E[CO_2] does not appear to promote increases in yield in rice. Altogether, the present study determined that stomatal aperture function is important for improving water use at E[CO_2] and that mutation of phyB improves WUE but conversely, phyB is required for optimum yield irrespective of the growth [CO_2].

6.5 Conclusions and future directions

A model diagram has produced integrating key findings from present study (Figure 6.2). Stomatal aperture regulation in response to increasing [CO_2] was found to be regulated via ABA and GA homeostatic balance in Arabidopsis. E[CO_2]-induced promotion of stomatal closure results from higher ABA to GA ratio where GA is reduced with no alteration in ABA. With existing evidence of interaction between carbon metabolism and GAs synthesis (Paparelli et al., 2013; Prasetyaningrum et al., 2021) and present findings of GA to modulate stomatal aperture to E[CO_2] support a potential avenue to crop engineering under varying [CO_2] conditions. The exact regulatory pathway of GA modulation in stomatal function needs to investigate broadly. RL photoreceptor phyB was also found to regulate E[CO_2]-induced promotion of stomatal closure via ABA and GA homeostasis but with alternative pathways as Col-0. Though, partial involvement of circadian clock genes was found to mediate the response

alongside ABA biosynthesis components; direct involvement of components of GA metabolism needs to be determined. In this regard more mutant lines from GA metabolism pathway alongside use of GA biosensor would be useful tools to investigate this mechanism further. In the model crop rice, phyB was found to be involved in stomatal function regulation in response to E[CO_2] and aid to maintain water balance with optimum yield under E[CO_2] growth condition. Since higher temperature because of increasing [CO_2] is known to affect rice yield (Jagadish et al. 2007; Sreenivasulu et al., 2015; Hu et al. 2022) study the effect of both the factors would be a potential area of future investigation.

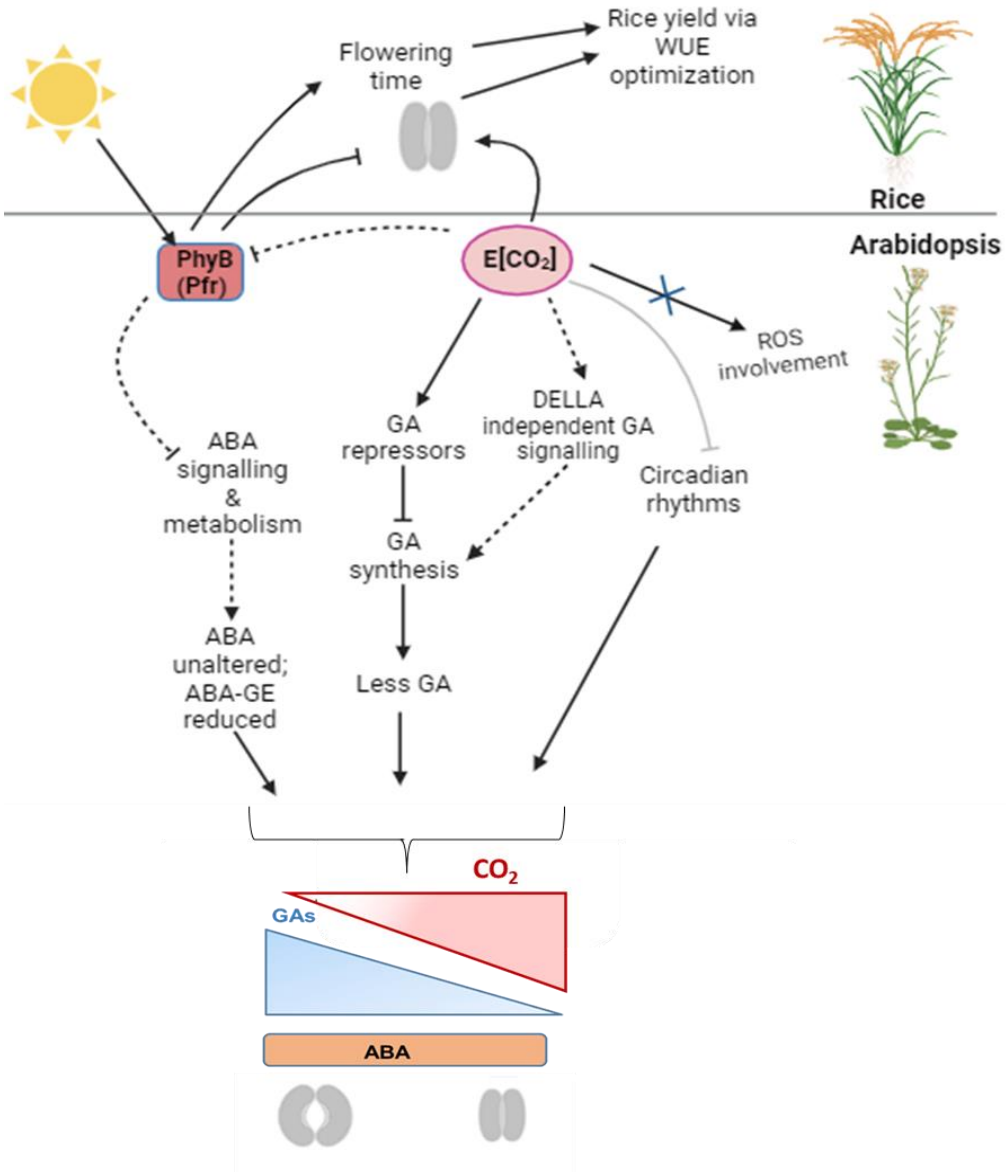

Figure 6.2 Summary model showing the key findings towards E[CO_2]-induced promotion of stomatal in Arabidopsis and rice. In Arabidopsis stomatal closure results from reduction in GA through inactivation of GA synthesis with no alteration in ABA. The experimental evidence does not conclusively demonstrate any role for DELLA or ROS mediated signalling, however it cannot be discounted. Circadian rhythms were found to be partially involved. Red light photoreceptor PhyB was found to sensitize this response via ABA and GA homeostasis. No direct effect of E[CO_2] was examined on Arabidopsis phyB. In rice E[CO_2] and phyB regulates stomatal closure in opposite manner while phyB positively regulates flowering time. Collectively these factors maintain rice yield via WUE optimization Arrow lines for positive regulation, barred line for negative action, dotted arrow for putative positive involvement, dotted bar lines for probable negative effect, gray bar line for partial and negative regulation and blue cross showing no involvement. Image “Created with Biorender.com”.

References

Achard, P., & Genschik, P. (2009). Releasing the brakes of plant growth: How GAs shutdown della proteins. *Journal of Experimental Botany*, *60*(4),1085-1092. https://doi.org/10.1093/jxb/ern301

Achard, P., Liao, L., Jiang, C., Desnos, T., Bartlett, J., Fu, X., & Harberd, N. P. (2007). DELLAs contribute to plant photomorphogenesis. *Plant Physiology*, *143*(3), 1163-1172. https://doi.org/10.1104/pp.106.092254

Achard, P., Renou, J. P., Berthomé, R., Harberd, N. P., & Genschik, P. (2008). Plant DELLAs Restrain Growth and Promote Survival of Adversity by Reducing the Levels of Reactive Oxygen Species. *Current Biology*, *18*(9). https://doi.org/10.1016/j.cub.2008.04.034

Acharya, B. R., & Assmann, S. M. (2009). Hormone interactions in stomatal function. *Plant Molecular Biology*, *69*(4), 451-462. https://doi.org/10.1007/s11103-008-9427-0

Adachi, S., Yoshikawa, K., Yamanouchi, U., Tanabata, T., Sun, J., Ookawa, T., Yamamoto, T., Sage, R. F., Hirasawa, T., & Yonemaru, J. (2017). Fine mapping of Carbon assimilation rate 8, a quantitative trait locus for flag leaf nitrogen content, stomatal conductance and photosynthesis in rice. *Frontiers in Plant Science*, *8*(JAN),60. https://doi.org/10.3389/fpls.2017.00060

Ahmad, S., Ali, H., Ur Rehman, A., Jahan, R., Khan, Z., Ahmad, W., Fatima, Z., Abbas, G., Irfan, M., Ali, H., Khan, M. A., & Hasanuzzaman, M. (2015). Measuring Leaf Area of Winter Cereals by Different Techniques: A Comparison. *Pakistan Journal of Life and Social Sciences*, *13*(2), 117-125. http://www.pjlss.edu.pk

Alabadí, D., Oyama, T., Yanovsky, M. J., Harmon, F. G., Más, P., & Kay, S. A. (2001). Reciprocal regulation between TOC1 and LHY/CCA1 within the Arabidopsis circadian clock. *Science*, *293*(5531). https://doi.org/10.1126/science.1061320

Ali, M. A., Asghar, H. N., Khan, M. Y., Saleem, M., Naveed, M., & Niazi, N. K. (2015). Alleviation of nickel-induced stress in mungbean through application of gibberellic acid. *International Journal of Agriculture and Biology*, *17*(5), 990-994. https://doi.org/10.17957/IJAB/15.0001

Allen, G. J., Kwak, J. M., Chu, S. P., Llopis, J., Tsien, R. Y., Harper, J. F., & Schroeder, J. I. (1999). Cameleon calcium indicator reports cytoplasmic calcium dynamics in Arabidopsis guard cells. *Plant Journal, 19*(6), 735-747. https://doi.org/10.1046/j.1365-313X.1999.00574.x

Allen, J., Guo, K., Zhang, D., Ince, M., & Jammes, F. (2019). ABA-glucose ester hydrolyzing enzyme ATBG1 and PHYB antagonistically regulate stomatal development. *PLoS ONE*, *14*(6). https://doi.org/10.1371/journal.pone.0218605

Allen, L. H. Jr, J. T. Baker, S. L. Albrecht, K. J. Boote, D. Pan, & Vu, J. C. V. (1995). Carbon dioxide and temperature effects of rice. In S. Peng, K. T. Ingram, H.-U. Neue, & L. H. Ziska, (Eds.), *Climate Change and Rice,* (pp. 258-277). Springer-Verlag, Berlin-Heidelberg. doi:10.1007/978-3-642-85193-3_25

Alonso, J. M., Stepanova, A. N., Leisse, T. J., Kim, C. J., Chen, H., Shinn, P., Stevenson, D. K., Zimmerman, J., Barajas, P., Cheuk, R., Gadrinab, C., Heller, C., Jeske, A., Koesema, E., Meyers, C. C., Parker, H., Prednis, L., Ansari, Y., Choy, N., … Ecker, J. R. (2003). Genome-wide insertional mutagenesis of Arabidopsis thaliana. *Science*, 301(5633), 653-657. https://doi.org/10.1126/science.1086391

Ando, E., & Kinoshita, T. (2018). Red Light-Induced Phosphorylation of Plasma Membrane H^+-ATPase in Stomatal Guard Cells. *Plant Physiology*, *178*(2), 838-849. https://doi.org/10.1104/pp.18.00544

Appleford, N. E. J., Evans, D. J., Lenton, J. R., Gaskin, P., Croker, S. J., Devos, K. M., Phillips, A. L., & Hedden, P. (2006). Function and transcript analysis of gibberellin-biosynthetic enzymes in wheat. *Planta*, *223*(3), 568-582. https://doi.org/10.1007/s00425-005-0104-0

Arana, M. V., Marín-De La Rosa, N., Maloof, J. N., Blázqueza, M. A., & Alabadí, D. (2011). Circadian oscillation of gibberellin signaling in Arabidopsis. *Proceedings of the National Academy of Sciences of the United States of America*, *108*(22). https://doi.org/10.1073/pnas.1101050108

Araújo, W. L., Nunes-Nesi, A., Osorio, S., Usadel, B., Fuentes, D., Nagy, R., Balbo, I., Lehmann, M., Studart-Witkowski, C., Tohge, T., Martinoia, E., Jordana, X., DaMatta,

F. M., & Fernie, A. R. (2011). Antisense inhibition of the iron-sulphur subunit of succinate dehydrogenase enhances photosynthesis and growth in tomato via an organic acid-mediated effect on stomatal aperture. *Plant Cell*, *23*(2), 600-627. https://doi.org/10.1105/tpc.110.081224

Ariizumi, T., Murase, K., Sun, T. P., & Steber, C. M. (2008). Proteolysis-independent downregulation of DELLA repression in Arabidopsis by the gibberellin receptor GIBBERELLIN INSENSITIVE DWARF1. *Plant Cell*, *20*(9), 2447-2459. https://doi.org/10.1105/tpc.108.058487

Assmann, S. M. (1993). Signal transduction in guard cells. *Annual Review of Cell Biology*, *9*, 345-375. https://doi.org/10.1146/annurev.cb.09.110193.002021

Assmann, S. M. (2000). Regulation of abscisic acid-induced stomatal closure and anion channels by guard cell AAPK kinase. *Science*, *287* (5451), 300-303. https://doi.org/10.1126/science.287.5451.300

Assmann, S. M., & Shimazaki, K. I. (1999). The multisensory guard cell. Stomatal responses to blue light and abscisic acid. *Plant Physiology*, *119*(3), 809-816. https://doi.org/10.1104/pp.119.3.809

Bae, G., & Choi, G. (2008). Decoding of Light Signals by Plant Phytochromes and Their Interacting Proteins. *Annual Review of Plant Biology*. https://doi.org/10.1146/annurev.arplant.59.032607.092859

Band, L. R., Úbeda-Tomás, S., Dyson, R. J., Middleton, A. M., Hodgman, T. C., Owen, M. R., Jensen, O. E., Bennett, M. J., & King, J. R. (2012). Growth-induced hormone dilution can explain the dynamics of plant root cell elongation. *Proceedings of the National Academy of Sciences of the United States of America*, *109*(19). https://doi.org/10.1073/pnas.1113632109

Baroli, I., Price, G. D., Badger, M. R., & Von Caemmerer, S. (2008). The contribution of photosynthesis to the red light response of stomatal conductance. *Plant Physiology*, *146* (2), 737-747. https://doi.org/10.1104/pp.107.110924

Barrôco, R. M., Peres, A., Droual, A. M., De Veylder, L., Nguyen, L. S. L., De Wolf, J., Mironov, V., Peerbolte, R., Beemster, G. T. S., Inzé, D., Broekaert, W. F., & Frankard, V. (2006). The cyclin-dependent kinase inhibitor Orysa; KRP1 plays an important role in the seed development of rice. *Plant Physiology*, *142*(3), 1053-1064. https://doi.org/10.1104/pp.106.087056

Basu, D., Dehesh, K., Schneider-Poetsch, H. J., Harrington, S. E., McCouch, S. R., & Quail, P. H. (2000). Rice PHYC gene: Structure, expression, map position and evolution. *Plant Molecular Biology*, *44*(1), 27-42. https://doi.org/10.1023/A:1006488119301

Battisti, D. S., & Naylor, R. L. (2009). Historical warnings of future food insecurity with unprecedented seasonal heat. *Science*, *323*(5911), 240-244. https://doi.org/10.1126/science.1164363

Bauer, H., Ache, P., Lautner, S., Fromm, J., Hartung, W., Al-Rasheid, K. A. S., Sonnewald, S., Sonnewald, U., Kneitz, S., Lachmann, N., Mendel, R. R., Bittner, F., Hetherington, A. M., & Hedrich, R. (2013). The stomatal response to reduced relative humidity requires guard cell-autonomous ABA synthesis. *Current Biology*, *23*(1), 53-57. https://doi.org/10.1016/j.cub.2012.11.022

Bent, A. (2006). Arabidopsis thaliana Floral Dip Transformation Method. In K. Wang (Eds.) *Agrobacterium Protocols. Methods in Molecular Biology*, *343*. Humana Press. https://doi.org/10.1385/1-59745-130-4:87

Bertolino, L. T., Caine, R. S., & Gray, J. E. (2019). Impact of stomatal density and morphology on water-use efficiency in a changing world. *Frontiers in Plant Science*,*10* (MAR), 225. https://doi.org/10.3389/fpls.2019.00225

Blanco-Touriñán, N., Serrano-Mislata, A., & Alabadí, D. (2020). Regulation of della Proteins by Post-translational Modifications. *Plant and Cell Physiology*,*61*(11). https://doi.org/10.1093/pcp/pcaa113

Blatt, M. R., & Clint, G. M. (1989). Mechanisms of fusicoccin action: kinetic modification and inactivation of K^+ channels in guard cells. *Planta*, *178*(4), 509-523. https://doi.org/10.1007/BF00963821

Boccalandro, H. E., Rugnone, M. L., Moreno, J. E., Ploschuk, E. L., Serna, L., Yanovsky, M. J., & Casal, J. J. (2009). Phytochrome B enhances photosynthesis at the expense of water-use efficiency in Arabidopsis. *Plant Physiology*, *150*(2), 1083-92. https://doi.org/10.1104/pp.109.135509

Brandt, B., Brodsky, D. E., Xue, S., Negi, J., Iba, K., Kangasjärvi, J., Ghassemian, M., Stephan, A. B., Hu, H., & Schroeder, J. I. (2012). Reconstitution of abscisic acid activation of SLAC1 anion channel by CPK6 and OST1 kinases and branched ABI1 PP2C phosphatase action. *Proceedings of the National Academy of Sciences of the United States of America, 109*(26), 10593-10598. https://doi.org/10.1073/pnas.1116590109

Brown, J. C. (2018). *Photoreceptor regulation of plant responses to light and carbon dioxide*. (March). [Doctoral dissertation, University of Sheffield] White Rose eTheses Online.

Buckley, T. N., Mott, K. A., & Farquhar, G. D. (2003). A hydromechanical and biochemical model of stomatal conductance. *Plant, Cell and Environment*, *26*(10), 1767-1785. https://doi.org/10.1046/j.1365-3040.2003.01094.x

Burden, R. S., Carter, G. A., Clark, T., Cooke, D. T., Croker, S. J., Deas, A. H. B., Hedden, P., James, C. S., & Lenton, J. R. (1987). Comparative activity of the enantiomers of triadimenol and paclobutrazol as inhibitors of fungal growth and plant sterol and gibberellin biosynthesis. *Pesticide Science*, *21*(4),253-267. https://doi.org/10.1002/ps.2780210403

Burla, B., Pfrunder, S., Nagy, R., Francisco, R. M., Lee, Y., & Martinoia, E. (2013). Vacuolar transport of abscisic acid glucosyl ester is mediated by ATP-binding cassette and proton-antiport mechanisms in Arabidopsis. *Plant Physiology*, *163*(3), 1446-1458. https://doi.org/10.1104/pp.113.222547

Caine, R. S., Yin, X., Sloan, J., Harrison, E. L., Mohammed, U., Fulton, T., Biswal, A. K., Dionora, J., Chater, C. C., Coe, R. A., Bandyopadhyay, A., Murchie, E. H., Swarup, R., Quick, W. P., & Gray, J. E. (2019). Rice with reduced stomatal density conserves water

and has improved drought tolerance under future climate conditions. *New Phytologist*, *221*(1), 371-384. https://doi.org/10.1111/nph.15344

Cao, D., Cheng, H., Wu, W., Soo, H. M., & Peng, J. (2006). Gibberellin mobilizes distinct DELLA-dependent transcriptomes to regulate seed germination and floral development in Arabidopsis. *Plant Physiology*, *142*(2), 509-525. https://doi.org/10.1104/pp.106.082289

Casal, J. J., & Sánchez, R. A. (1998). Phytochromes and seed germination. *Seed Science Research*, *8*(3), 317-329. https://doi.org/10.1017/s0960258500004256

Casal, J. J., Candia, A. N., & Sellaro, R. (2014). Light perception and signalling by phytochrome A. In *Journal of Experimental Botany*, *65*(11), 2835–2845. https://doi.org/10.1093/jxb/ert379

Casson, S. A., & Hetherington, A. M. (2010). Environmental regulation of stomatal development. *Current Opinion in Plant Biology*, *13*(1), 90–95. https://doi.org/10.1016/j.pbi.2009.08.005

Casson, S. A., Franklin, K. A., Gray, J. E., Grierson, C. S., Whitelam, G. C., & Hetherington, A. M. (2009). phytochrome B and PIF4 Regulate Stomatal Development in Response to Light Quantity. *Current Biology,* *19*(3), 229-34. https://doi.org/10.1016/j.cub.2008.12.046

Casson, S., & Gray, J. E. (2008). Influence of environmental factors on stomatal development. *New Phytologist*, 178(1), 9–23. https://doi.org/10.1111/j.1469-8137.2007.02351.x

Ceciliato, P. H. O., Zhang, J., Liu, Q., Shen, X., Hu, H., Liu, C., Schäffner, A. R., & Schroeder, J. I. (2019). Intact leaf gas exchange provides a robust method for measuring the kinetics of stomatal conductance responses to abscisic acid and other small molecules in Arabidopsis and grasses. *Plant Methods*, *15*,38. https://doi.org/10.1186/s13007-019-0423-y

Cernusak, L. A., Ubierna, N., Winter, K., Holtum, J. A. M., Marshall, J. D., & Farquhar, G. D. (2013). Environmental and physiological determinants of carbon isotope

discrimination in terrestrial plants. *New Phytologist*, *200*(4),950-965. https://doi.org/10.1111/nph.12423

Chater, C. C. C., Caine, R. S., Fleming, A. J., & Gray, J. E. (2017). Origins and Evolution of Stomatal Development. *Plant Physiology*, *174*(2), 624–638. https://doi.org/10.1104/pp.17.00183

Chater, C., Gray, J. E., & Beerling, D. J. (2013). Early evolutionary acquisition of stomatal control and development gene signalling networks. *Current Opinion in Plant Biology*, *16*(5),638-646. https://doi.org/10.1016/j.pbi.2013.06.013

Chater, C., Peng, K., Movahedi, M., Dunn, J. A., Walker, H. J., Liang, Y. K., McLachlan, D. H., Casson, S., Isner, J. C., Wilson, I., Neill, S. J., Hedrich, R., Gray, J. E., & Hetherington, A. M. (2015). Elevated CO_2-Induced Responses in Stomata Require ABA and ABA Signaling. *Current Biology*, *25*(20), 2709–2716. https://doi.org/10.1016/j.cub.2015.09.013

Chatterjee, J., Thakur, V., Nepomuceno, R., Coe, R. A., Dionora, J., Elmido-Mabilangan, A., Llave, A. D., Reyes, A. M. D., Monroy, A. N., Canicosa, I., Bandyopadhyay, A., Jena, K. K., Brar, D. S., & Quick, W. P. (2020). Natural Diversity in Stomatal Features of Cultivated and Wild Oryza Species. *Rice*, *13*(1). https://doi.org/10.1186/s12284-020-00417-0

Chen, C., Xiao, Y. G., Li, X., & Ni, M. (2012). Light-regulated stomatal aperture in Arabidopsis. *Molecular Plant*, *5*(3), 566-572. https://doi.org/10.1093/mp/sss039

Cheng, H., Qin, L., Lee, S., Fu, X., Richards, D. E., Cao, D., Luo, D., Harberd, N. P., & Peng, J. (2004). Gibberellin regulates Arabidopsis floral development via suppression of DELLA protein function. *Development*, *131*(5), 1055-1064. https://doi.org/10.1242/dev.00992

Choi, H. I., Hong, J. H., Ha, J. O., Kang, J. Y., & Kim, S. Y. (2000). ABFs, a family of ABA-responsive element binding factors. *Journal of Biological Chemistry*, *275*(3), 1723-1730. https://doi.org/10.1074/jbc.275.3.1723

Christie, J. M. (2007). Phototropin blue-light receptors. *Annual Review of Plant Biology, 58*, 21-45. https://doi.org/10.1146/annurev.arplant.58.032806.103951

Cockburn, W. (1983). Stomatal mechanism as the basis of the evolution of CAM and C_4 photosynthesis. *Plant, Cell & Environment*, 6(4), 275-279. https://doi.org/10.1111/1365-3040.ep11611925

Conroy, J., Seneweera, S., Basra, A., Rogers, G., & Nissen-Wooller, B. (1994). Influence of Rising Atmospheric CO_2 Concentrations and Temperature on Growth, Yield and Grain Quality of Cereal Crops. *Functional Plant Biology*, *21*(6), 741. https://doi.org/10.1071/pp9940741

Conti, L., Nelis, S., Zhang, C., Woodcock, A., Swarup, R., Galbiati, M., Tonelli, C., Napier, R., Hedden, P., Bennett, M., & Sadanandom, A. (2014). Small Ubiquitin-like Modifier Protein SUMO Enables Plants to Control Growth Independently of the Phytohormone Gibberellin. *Developmental Cell*, *28*(1), 102-110. https://doi.org/10.1016/j.devcel.2013.12.004

Cornish, K., & Zeevaart, J. A. D. (1986). Abscisic Acid Accumulation by in Situ and Isolated Guard Cells of Pisum sativum L. and Vicia faba L. in Relation to Water Stress. *Plant Physiology*, *81*(4), 1017–1021. https://doi.org/10.1104/pp.81.4.1017

Costa, J. M., Grant, O. M., & Chaves, M. M. (2013). Thermography to explore plant-environment interactions. *Journal of Experimental Botany*, *64*(13), 3937-3949. https://doi.org/10.1093/jxb/ert029

Cramer, M. D., Nagel, O. W., Lips, S. H., & Lambers, H. (1995). Reduction, assimilation and transport of N in normal and gibberellin-deficient tomato plants. *Physiologia Plantarum*, *95*(3), 347-354. https://doi.org/10.1111/j.1399-3054.1995.tb00848.x

Cui, J., & Han, H. (2022). Carbon isotope discrimination and the factors affecting it in a summer maize field under different tillage systems. *PeerJ*, *10*. https://doi.org/10.7717/peerj.12891

Das, D., Pattanaik, D., Panda, D., Dey, P., Baig, M. J., Rout, G. R., Paikray, R. K., Samal, K. C., Panda, R. K., & Gupta, A.K. (2022). Effect of low light stress on plant height,

tiller Number, panicle number, leaf area and yield of long duration rice (*Oryza sativa*. L) varieties. International Journal of Environment and Climate Change. 12(10): 1177-1183. https:// doi.org/10.9734/IJECC/2022/v12i1030914

Daszkowska-Golec, A., & Szarejko, I. (2013). Open or close the gate - Stomata action under the control of phytohormones in drought stress conditions. *Frontiers in Plant Science* ,4(MAY),138. https://doi.org/10.3389/fpls.2013.00138

De Costa, W. A. J. M., Weerakoon, W. M. W., Abeywardena, R. M. I., & Herath, H. M. L. K. (2003). Response of photosynthesis and water relations of rice (*Oryza sativa*) to elevated atmospheric carbon dioxide in the subhumid zone of Sri Lanka. *Journal of Agronomy and Crop Science*, *189*(2), 71-82. https://doi.org/10.1046/j.1439-037X.2003.00012.x

De Datta S. 1981. *Principles and practices of rice production*. New York, NY, USA: Wiley.

De Lucas, M., Davière, J. M., Rodríguez-Falcón, M., Pontin, M., Iglesias-Pedraz, J. M., Lorrain, S., Fankhauser, C., Blázquez, M. A., Titarenko, E., & Prat, S. (2008). A molecular framework for light and gibberellin control of cell elongation. *Nature*, *45*, 480-484. https://doi.org/10.1038/nature06520

Dehesh, K., Tepperman, J., Christensen, A. H., & Quail, P. H. (1991). phyB is evolutionarily conserved and constitutively expressed in rice seedling shoots. *Molecular and General Genetics, 225*(2), 305-13. https://doi.org/10.1007/BF00269863

Dietz, K., Sauter, A., Wichert, K., Messdaghi, D., & Hartung, W. (2000). Extracellular β-glucosidase activity in barley involved in the hydrolysis of ABA glucose conjugate in leaves. *Journal of Experimental Botany*, *51*(346), 937-944. https://doi.org/10.1093/jexbot/51.346.937

Dill, A., & Sun, T. P. (2001). Synergistic derepression of gibberellin signaling by removing RGA and GAI function in Arabidopsis thaliana. *Genetics*, *159*(2), 777-785. https://doi.org/10.1093/genetics/159.2.777

Ding, Z., Doyle, M. R., Amasino, R.M., & Davis, S.J. (2007). A complex genetic interaction between Arabidopsis thaliana TOC1 and CCA1/LHY in driving the circadian clock and in output regulation. *Genetics, 176*(3), 1501-1510. doi: 10.1534/genetics.107.072769.

Dittrich, M., Mueller, H. M., Bauer, H., Peirats-Llobet, M., Rodriguez, P. L., Geilfus, C. M., Carpentier, S. C., Al Rasheid, K. A. S., Kollist, H., Merilo, E., Herrmann, J., Müller, T., Ache, P., Hetherington, A. M., & Hedrich, R. (2019). The role of Arabidopsis ABA receptors from the PYR/PYL/RCAR family in stomatal acclimation and closure signal integration. *Nature Plants*, *5*(9), 1002–1011. https://doi.org/10.1038/s41477-019-0490-0

Doi, M., Kitagawa, Y., & Shimazaki, K. I. (2015). Stomatal blue light response is present in early vascular plants. *Plant Physiology*, *169*(2), 1205-1213. https://doi.org/10.1104/pp.15.00134

Dong, H. K., Yamaguchi, S., Lim, S., Oh, E., Park, J., Hanada, A., Kamiya, Y., & Choi, G. (2008). SOMNUS, a CCCH-type zinc finger protein in Arabidopsis, negatively regulates light-dependent seed germination downstream of PIL5. *Plant Cell*, *20*(5),1260-77. https://doi.org/10.1105/tpc.108.058859

Dong, T., & Hwang, I. (2014). Contribution of ABA UDP-glucosyltransferases in coordination of ABA biosynthesis and catabolism for ABA homeostasis. *Plant Signaling and Behavior, 9*(7), e28888. https://doi.org/10.4161/psb.28888

Dong, T., Xu, Z. Y., Park, Y., Kim, D. H., Lee, Y., & Hwang, I. (2014). Abscisic acid uridine diphosphate glucosyltransferases play a crucial role in abscisic acid homeostasis in Arabidopsis. *Plant Physiology*, *165*(1), 277–289. https://doi.org/10.1104/pp.114.239210

Drake, B. G., Gonzàlez-Meler, M. A., & Long, S. P. (1997). More efficient plants: A Consequence of Rising Atmospheric CO_2? *Annual Review of Plant Biology*, *48*. https://doi.org/10.1146/annurev.arplant.48.1.609

Dreyer, I., Gomez-Porras, J. L., Riaño-Pachón, D. M., Hedrich, R., & Geiger, D. (2012). Molecular evolution of slow and quick anion channels (SLACs and QUACs/ALMTs). *Frontiers in Plant Science*, *3*(NOV), 1-12. https://doi.org/10.3389/fpls.2012.00263

Du, H., Wang, Y. Bin, Xie, Y., Liang, Z., Jiang, S. J., Zhang, S. S., Huang, Y. B., & Tang, Y. X. (2013). Genome-wide identification and evolutionary and expression analyses of MYB-related genes in land plants. *DNA Research*, *20*(5), 437–448. https://doi.org/10.1093/dnares/dst021

Easlon, H. M., & Bloom, A. J. (2013). The effects of rising atmospheric carbon dioxide on shoot-root nitrogen and water signaling. *Frontiers in Plant Science*, *4*(AUG), 1-8. https://doi.org/10.3389/fpls.2013.00304

Edwards, K., Johnstone, C., & Thompson, C. (1991). A simple and rapid method for the preparation of plant genomic DNA for PCR analysis. *Nucleic Acids Research*, *19*(6), 1349. https://doi.org/10.1093/nar/19.6.1349

Ehonen, S., Yarmolinsky, D., Kollist, H., & Kangasjärvi, J. (2019). Reactive Oxygen Species, Photosynthesis, and Environment in the Regulation of Stomata. *Antioxidants and Redox Signaling*, *30*(9), 1220-1237. https://doi.org/10.1089/ars.2017.7455

Engineer, C. B., Hashimoto-Sugimoto, M., Negi, J., Israelsson-Nordström, M., Azoulay-Shemer, T., Rappel, W. J., Iba, K., & Schroeder, J. I. (2016). CO_2 Sensing and CO_2 Regulation of Stomatal Conductance: Advances and Open Questions. *Trends in Plant Science*, *21*(1), 16–30. https://doi.org/10.1016/j.tplants.2015.08.014

Eriksson, S., Böhlenius, H., Moritz, T., & Nilsson, O. (2006). GA_4 is the active gibberellin in the regulation of LEAFY transcription and Arabidopsis floral initiation. *Plant Cell*, *18*(9), 2172-2181. https://doi.org/10.1105/tpc.106.042317

Faralli, M., Cockram, J., Ober, E., Wall, S., Galle, A., Van Rie, J., Raines, C., & Lawson, T. (2019). Genotypic, developmental and environmental effects on the rapidity of g_s in Wheat: Impacts on carbon gain and water-use efficiency. *Frontiers in Plant Science*, *10*, 492. https://doi.org/10.3389/fpls.2019.00492

Farquhar, G., & Wong, S. (1984). An Empirical Model of Stomatal Conductance. Australian Journal of Plant Physiology, *11*(3),191-210. https://doi.org/10.1071/pp9840191

Farquhar, G.D., Hubick, K.T., Condon, A.G., & Richards, R.A. (1989). Carbon Isotope Fractionation and Plant Water-Use Efficiency. In P. W, Rundel, J. R. Ehleringer, & K.

A. Nagy (Eds.) *Stable Isotopes in Ecological Research*. *Ecological Studies, 68*. Springer, New York, NY. https://doi.org/10.1007/978-1-4612-3498-2_2

Fath, A., Bethke, P. C., & Jones, R. L. (2001). Enzymes that scavenge reactive oxygen species are down-regulated prior to gibberellic acid-induced programmed cell death in barley aleurone. *Plant Physiology*, *126*(1),156-166. https://doi.org/10.1104/pp.126.1.156

Feng, S., Martinez, C., Gusmaroli, G., Wang, Y., Zhou, J., Wang, F., Chen, L., Yu, L., Iglesias-Pedraz, J. M., Kircher, S., Schäfer, E., Fu, X., Fan, L. M., & Deng, X. W. (2008). Coordinated regulation of Arabidopsis thaliana development by light and gibberellins. *Nature*, *451*(7177), 475-479. https://doi.org/10.1038/nature06448

Finkelstein, R., Reeves, W., Ariizumi, T., & Steber, C. (2008). Molecular aspects of seed dormancy. *Annual Review of Plant Biology*, *59*, 387-415. https://doi.org/10.1146/annurev.arplant.59.032607.092740

Fischer, G., Lena, V., Goring, H., Koshuchowa, S., & Deckert, C. (1990). Influence of Gibberellic Acid on Stomatal Movement. *Biochemie und Physiologie der Pflanzen*,186(5-6), 367-374. https://doi.org/10.1016/S0015-3796(11)80235-0

Franklin, K. A., & Quail, P. H. (2010). Phytochrome functions in Arabidopsis development. *Journal of Experimental Botany*,61(1),11–24. https://doi.org/10.1093/jxb/erp304

Frey, A., Effroy, D., Lefebvre, V., Seo, M., Perreau, F., Berger, A., Sechet, J., To, A., North, H. M., & Marion-Poll, A. (2012). Epoxycarotenoid cleavage by NCED5 fine-tunes ABA accumulation and affects seed dormancy and drought tolerance with other NCED family members. *Plant Journal*, *70*(3), 501-512. https://doi.org/10.1111/j.1365-313X.2011.04887.x

Fricke, W. (2019). Night-Time Transpiration – Favouring Growth? In *Trends in Plant Science,24*(4). https://doi.org/10.1016/j.tplants.2019.01.007

Fujii, H., & Zhu, J. K. (2009). Arabidopsis mutant deficient in 3 abscisic acid-activated protein kinases reveals critical roles in growth, reproduction, and stress. *Proceedings*

of the National Academy of Sciences of the United States of America, *106* (20), 8380-8385. https://doi.org/10.1073/pnas.0903144106

Fujita, T., Noguchi, K., & Terashima, I. (2013). Apoplastic mesophyll signals induce rapid stomatal responses to CO_2 in *Commelina communis*. *New Phytologist*, *199*(2), 395-406. https://doi.org/10.1111/nph.12261

Fujita, Y., Nakashima, K., Yoshida, T., Katagiri, T., Kidokoro, S., Kanamori, N., Umezawa, T., Fujita, M., Maruyama, K., Ishiyama, K., Kobayashi, M., Nakasone, S., Yamada, K., Ito, T., Shinozaki, K., & Yamaguchi-Shinozaki, K. (2009). Three SnRK2 protein kinases are the main positive regulators of abscisic acid signaling in response to water stress in Arabidopsis. *Plant and Cell Physiology*, *50*(12), 2123-2132. https://doi.org/10.1093/pcp/pcp147

Fukagawa, N. K., & Ziska, L. H. (2019). Rice: Importance for Global Nutrition. *Journal of Nutritional Science and Vitaminology, 65*, S2-S3. https://doi.org/10.3177/jnsv.65.S2

Gamage, D., Thompson, M., Sutherland, M., Hirotsu, N., Makino, A., & Seneweera, S. (2018). New insights into the cellular mechanisms of plant growth at elevated atmospheric carbon dioxide concentrations. *Plant Cell and Environment*, *41*(6),1233-1246. https://doi.org/10.1111/pce.13206

Gangwar, S., Singh, V. P., Srivastava, P. K., & Maurya, J. N. (2011). Modification of chromium (VI) phytotoxicity by exogenous gibberellic acid application in Pisum sativum (L.) seedlings. *Acta Physiologiae Plantarum*, *33*(4), 1385-1397. https://doi.org/10.1007/s11738-010-0672-x

Geiger, D., Scherzer, S., Mumm, P., Marten, I., Ache, P., Matschi, S., Liese, A., Wellmann, C., Al-Rasheid, K. A. S., Grill, E., Romeis, T., & Hedrich, R. (2010). Guard cell anion channel SLAC1 is regulated by CDPK protein kinases with distinct Ca^{2+} affinities. *Proceedings of the National Academy of Sciences of the United States of America*, *107*(17), 8023-8028. https://doi.org/10.1073/pnas.0912030107

Geiger, D., Scherzer, S., Mumm, P., Stange, A., Marten, I., Bauer, H., Ache, P., Matschi, S., Liese, A., Al-Rasheid, K. A. S., Romeis, T., & Hedrich, R. (2009). Activity of guard cell anion channel SLAC1 is controlled by drought-stress signaling kinase-phosphatase

pair. *Proceedings of the National Academy of Sciences of the United States of America*, *106* (50), 21425-21430. https://doi.org/10.1073/pnas.0912021106

Geng, S., Misra, B. B., de Armas, E., Huhman, D. v., Alborn, H. T., Sumner, L. W., & Chen, S. (2016). Jasmonate-mediated stomatal closure under elevated CO_2 revealed by time-resolved metabolomics. *Plant Journal*, *88*(6),947-962. https://doi.org/10.1111/tpj.13296

Goh, C. H., Lee, D. J., & Bae, H. J. (2009). Gibberellic acid of Arabidopsis regulates the abscisic acid-induced inhibition of stomatal opening in response to light. *Plant Science*, *176*(1), 136-142. https://doi.org/10.1016/j.plantsci.2008.10.005

González, C. V., Ibarra, S. E., Piccoli, P. N., Botto, J. F., & Boccalandro, H. E. (2012). Phytochrome B increases drought tolerance by enhancing ABA sensitivity in Arabidopsis thaliana. *Plant, Cell and Environment*, *35*(11), 1958-1968. https://doi.org/10.1111/j.1365-3040.2012.02529.x

Göring, H., Koshuchowa, S., & Deckert, C. (1990). Influence of Gibberellic Acid on Stomatal Movement. *Biochemie Und Physiologie Der Pflanzen*, *186* (5-6), 367-374. https://doi.org/10.1016/s0015-3796(11)80235-80240

Graeber, K., Nakabayashi, K., Miatton, E., Leubner-Metzger, G., & Soppe, W. J. J. (2012). Molecular mechanisms of seed dormancy. *Plant, Cell and Environment*, *35*(10), 1769-1786. https://doi:10.1111/j.1365-3040.2012.02542.x.

Ha, J. H., Kim, J. H., Kim, S. G., Sim, H. J., Lee, G., Halitschke, R., Baldwin, I. T., Kim, J. Il, & Park, C. M. (2018). Shoot phytochrome B modulates reactive oxygen species homeostasis in roots via abscisic acid signaling in Arabidopsis. *Plant Journal*, *94*(5), 790-798. https://doi.org/10.1111/tpj.13902

Harberd, N. P., Belfield, E., & Yasumura, Y. (2009). The angiosperm gibberellin-GID1-DELLA growth regulatory mechanism: How an “inhibitor of an inhibitor” enables flexible response to fluctuating environments. *Plant Cell*, *21*(5), 1328–1339. https://doi.org/10.1105/tpc.109.066969

Harrison, E. L., Arce Cubas, L., Gray, J. E., & Hepworth, C. (2020). The influence of stomatal morphology and distribution on photosynthetic gas exchange. *Plant Journal*,*101(*4),768-779. Blackwell Publishing Ltd. https://doi.org/10.1111/tpj.14560

Hashimoto, M., Negi, J., Young, J., Israelsson, M., Schroeder, J. I., & Iba, K. (2006). Arabidopsis HT1 kinase controls stomatal movements in response to CO_2. *Nature Cell Biology*, *8*, 391-397. https://doi.org/10.1038/ncb1387

Hassidim, M., Dakhiya, Y., Turjeman, A., Hussien, D., Shor, E., Anidjar, A., Goldberg, K., & Green, R. M. (2017). CIRCADIAN CLOCK ASSOCIATED1 (CCA1) and the circadian control of stomatal aperture. *Plant Physiology*, *175*(4), 1864–1877. https://doi.org/10.1104/pp.17.01214

Hauvermale, A. L., Ariizumi, T., & Steber, C. M. (2012). Gibberellin signaling: A theme and variations on DELLA repression. *Plant Physiology*, *160*(1). https://doi.org/10.1104/pp.112.200956

Haworth, M., Scutt, C. P., Douthe, C., Marino, G., Gomes, M. T. G., Loreto, F., Flexas, J., & Centritto, M. (2018). Allocation of the epidermis to stomata relates to stomatal physiological control: Stomatal factors involved in the evolutionary diversification of the angiosperms and development of amphistomaty. *Environmental and Experimental Botany*, *151*, 55-63. https://doi.org/10.1016/j.envexpbot.2018.04.010

Hayashi, M., Inoue, S. I., Takahashi, K., & Kinoshita, T. (2011). Immunohistochemical detection of blue light-induced phosphorylation of the plasma membrane H $^+$-ATPase in stomatal guard cells. *Plant and Cell Physiology*, *52*(7),1238-1248. https://doi.org/10.1093/pcp/pcr072

Hayashi, M., Sugimoto, H., Takahashi, H., Seki, M., Shinozaki, K., Sawasaki, T., Kinoshita, T., & Inoue, S. I. (2020). Raf-like kinases CBC_1 and CBC_2 negatively regulate stomatal opening by negatively regulating plasma membrane H^+-ATPase phosphorylation in Arabidopsis. *Photochemical and Photobiological Sciences*, *19*(1), 88-98. https://doi.org/10.1039/c9pp00329k

He, J., Zhang, R. X., Peng, K., Tagliavia, C., Li, S., Xue, S., Liu, A., Hu, H., Zhang, J., Hubbard, K. E., Held, K., McAinsh, M. R., Gray, J. E., Kudla, J., Schroeder, J. I., Liang,

Y. K., & Hetherington, A. M. (2018). The BIG protein distinguishes the process of CO_2-induced stomatal closure from the inhibition of stomatal opening by CO_2. *New Phytologist*, *218*(1), 232–241. https://doi.org/10.1111/nph.14957

Hedden, P. (1990). The Action of Plant Growth Retardants at the Biochemical Level. In R.P. Pharis & S. B. Rood (Eds.) *Plant Growth Substances* 1988. Springer, Berlin, Heidelberg. https://doi.org/10.1007/978-3-642-74545-4_38

Hedden, P. (2020). The current status of research on gibberellin biosynthesis. *Plant and Cell Physiology*,*61*(11), 1832–1849. Oxford University Press. https://doi.org/10.1093/pcp/pcaa092

Hedden, P., & Graebet, J. E. (1985). Inhibition of Gibberellin Biosynthesis by Paclobutrazol in Cell-free Homogenates of Cucurbita maxima Endosperm and Malus pumila Embryos. *Journal of Plant Growth Regulation*, *4*, 111-122. https://doi.org/10.1007/BF02266949

Hedden, P., & Phillips, A. L. (2000). Gibberellin metabolism: New insights revealed by the genes. *Trends in Plant Science*, *5*(12), 523–530. https://doi.org/10.1016/S1360-1385(00)01790-8

Hedrich, R. (2012). Ion channels in plants. *Physiological Reviews*, *92*(4), 1777-1811. https://doi.org/10.1152/physrev.00038.2011

Helliwell, C. A., Chandler, P. M., Poole, A., Dennis, E. S., & Peacock, W. J. (2001). The CYP88A cytochrome P450, ent-kaurenoic acid oxidase, catalyzes three steps of the gibberellin biosynthesis pathway. *Proceedings of the National Academy of Sciences of the United States of America*, *98*(4), 2065–2070. https://doi.org/10.1073/pnas.98.4.2065

Helliwell, C. A., Sullivan, J. A., Mould, R. M., Gray, J. C., James Peacock, W., & Dennis, E. S. (2001). A plastid envelope location of Arabidopsis ent-kaurene oxidase links the plastid and endoplasmic reticulum steps of the gibberellin biosynthesis pathway. *Plant Journal*, *28*(2), 201-208. https://doi.org/10.1046/j.1365-313X.2001.01150.x

Hennessey, T. L., Freeden, A. L., & Field, C. B. (1993). Environmental effects on circadian rhythms in photosynthesis and stomatal opening. *Planta*, *189*(3), 369–376 https://doi.org/10.1007/BF00194433

Hepworth, C., Doheny-Adams, T., Hunt, L., Cameron, D. D., & Gray, J. E. (2015). Manipulating stomatal density enhances drought tolerance without deleterious effect on nutrient uptake. *New Phytologist*, *208*(2), 336-341. https://doi.org/10.1111/nph.13598

Herrmann, A., & Torii, K. U. (2021). Shouting out loud: Signaling modules in the regulation of stomatal development. *Plant Physiology*, *185*(3), 765-780. https://doi.org/10.1093/PLPHYS/KIAA061

Hetherington, A.M. & Woodward, F.I. (2003). The role of stomata in sensing and driving environmental change. *Nature, 424*(6951), 901-908. https://doi/10.1038/nature01843.

Hirano, K., Ueguchi-Tanaka, M., & Matsuoka, M. (2008). GID1-mediated gibberellin signaling in plants. *Trends in Plant Scienc, 13*(4), 192-199. https://doi.org/10.1016/j.tplants.2008.02.005

Hirayama, T., & Shinozaki, K. (2007). Perception and transduction of abscisic acid signals: keys to the function of the versatile plant hormone ABA. *Trends in Plant Science*, *12*(8), 343-351. https://doi.org/10.1016/j.tplants.2007.06.013

Hiyama, A., Takemiya, A., Munemasa, S., Okuma, E., Sugiyama, N., Tada, Y., Murata, Y., & Shimazaki, K. I. (2017). Blue light and CO_2 signals converge to regulate light-induced stomatal opening. *Nature Communications*, *8*(1), 1–12. https://doi.org/10.1038/s41467-017-01237-5

Holdsworth, M.J., Bentsink, L., & Soppe W.J.J. (2008) Molecular networks regulating Arabidopsis seed maturation, after-ripening, dormancy and germination. *New Phytologist,179*(1),33-54. doi: 10.1111/j.1469-8137.2008.02437.x.

Hõrak, H., Sierla, M., Tõldsepp, K., Wang, C., Wang, Y. S., Nuhkat, M., Valk, E., Pechter, P., Merilo, E., Salojärvi, J., Overmyer, K., Loog, M., Brosché, M., Schroeder, J. I., Kangasjärvi, J., & Kollist, H. (2016). A dominant mutation in the ht1 kinase uncovers

roles of MAP kinases and GHR1 in CO_2-induced stomatal closure. *Plant Cell*, *28*(10), 2493–2509. https://doi.org/10.1105/tpc.16.00131

Horrer, D., Flütsch, S., Pazmino, D., Matthews, J. S. A., Thalmann, M., Nigro, A., Leonhardt, N., Lawson, T., & Santelia, D. (2016). Blue light induces a distinct starch degradation pathway in guard cells for stomatal opening. *Current Biology*, *26*(3), 362-370. https://doi.org/10.1016/j.cub.2015.12.036

Hsu, P., Takahashi, Y., Munemasa, S., Merilo, E., Laanemets, K., Waadt, R., & Pater, D. (2018). Abscisic acid-independent stomatal CO_2 signal transduction pathway and convergence of CO_2 and ABA signaling downstream of OST1 kinase. *Proceedings of the National Academy of Sciences of the United States of America*, *115*(42), 9971–9980. https://doi.org/10.1073/pnas.1809204115

Hu, H., Boisson-Dernier, A., Israelsson-Nordström, M., Böhmer, M., Xue, S., Ries, A., Godoski, J., Kuhn, J. M., & Schroeder, J. I. (2010). Carbonic anhydrases are upstream regulators of CO_2-controlled stomatal movements in guard cells. *Nature Cell Biology*, *12*(1), 87–93. https://doi.org/10.1038/ncb2009

Hu, S., Chen, W., Tong, K., Wang, Y., Jing, L., Wang, Y., & Yang, L. (2022). Response of rice growth and leaf physiology to elevated CO_2 concentrations: A meta-analysis of 20-year FACE studies. *Science of the Total Environment*, *807*(3). https://doi.org/10.1016/j.scitotenv.2021.151017

Hu, Y., Wu, Q., Peng, Z., Sprague, S. A., Wang, W., Park, J., Akhunov, E., Jagadish, K. S. V., Nakata, P. A., Cheng, N., Hirschi, K. D., White, F. F., & Park, S. (2017). Silencing of OsGRXS17 in rice improves drought stress tolerance by modulating ROS accumulation and stomatal closure. *Scientific Reports*, *7*, 15950. https://doi.org/10.1038/s41598-017-16230-7

Hua, D., Wang, C., He, J., Liao, H., Duan, Y., Zhu, Z., Guo, Y., Chen, Z., & Gong, Z. (2012). A plasma membrane receptor kinase, GHR1, mediates abscisic acid- and hydrogen peroxide-regulated stomatal movement in Arabidopsis. *Plant Cell*, 24(6), 2546-2561. https://doi.org/10.1105/tpc.112.100107

Huang, X. Y., Chao, D. Y., Gao, J. P., Zhu, M. Z., Shi, M., & Lin, H. X. (2009). A previously unknown zinc finger protein, DST, regulates drought and salt tolerance in rice via stomatal aperture control. *Genes and Development*, *23*(15), 1805-1817. https://doi.org/10.1101/gad.1812409

Huang, S., Jacoby, R.P., Shingaki-Wells, R.N., Li, L. & Millar, A.H. (2013). Differential induction of mitochondrial machinery by light intensity correlates with changes in respiratory metabolism and photorespiration in rice leaves. *New Phytologist, 198(1),* 103-115. https://doi.org/10.1111/nph.12123

Hubbard, K. E., & Webb, A. A. R. (2011). Circadian rhythms: Flowering locus t extends opening hours. *Current Biology*, 21(16), 636-638. https://doi.org/10.1016/j.cub.2011.06.058

Hubbart, S., Bird, S., Lake, J. A., & Murchie, E. H. (2013). Does growth under elevated CO_2 moderate photoacclimation in rice? *Physiologia Plantarum*, *148*(2), 297–306. https://doi.org/10.1111/j.1399-3054.2012.01702.x

Imes, D., Mumm, P., Böhm, J., Al-Rasheid, K. A. S., Marten, I., Geiger, D., & Hedrich, R. (2013). Open stomata 1 (OST1) kinase controls R-type anion channel QUAC1 in Arabidopsis guard cells. *Plant Journal*, *74*(3), 372-383. https://doi.org/10.1111/tpj.12133

Inoue, S. I., & Kinoshita, T. (2017). Blue light regulation of stomatal opening and the plasma membrane H^+-ATPase. *Plant Physiology*, *174*(2), 531–538. https://doi.org/10.1104/pp.17.00166

IPCC, Climate Change (2023). Synthesis Report. A Report of the Intergovernmental Panel on Climate Change. Contribution of Working Groups I, II and III to the Sixth Assessment Report of the Intergovernmental Panel on Climate Change [Core Writing Team, H. Lee and J. Romero (eds.)]. IPCC, Geneva, Switzerland, (in press) https://www.ipcc.ch/report/ar6/syr/resources/how-to-cite-this-report.

Ishida, S., Yuasa, T., Nakata, M., & Takahashi, Y. (2008). A tobacco calcium-dependent protein kinase, CDPK1, regulates the transcription factor REPRESSION OF SHOOT

GROWTH in response to gibberellins. *Plant Cell*, *20*(12), 3273-3288. https://doi.org/10.1105/tpc.107.057489

Ishimaru, K., Shirota, K., Higa, M., & Kawamitsu, Y. (2001). Identification of quantitative trait loci for adaxial and abaxial stomatal frequencies in *Oryza sativa*. *Plant Physiology and Biochemistry*, *39*(2). https://doi.org/10.1016/S0981-9428(00)01232-8

Israelsson, M., Mellerowicz, E., Chono, M., Gullberg, J., & Moritz, T. (2004). Cloning and overproduction of gibberellin 3-oxidase in hybrid aspen trees. Effects on gibberellin homeostasis and development. *Plant Physiology*, *135*(1), 221-230. https://doi.org/10.1104/pp.104.038935

Israelsson, M., Siegel, R. S., Young, J., Hashimoto, M., Iba, K., & Schroeder, J. I. (2006). Guard cell ABA and CO_2 signaling network updates and Ca^{2+} sensor priming hypothesis. *Current Opinion in Plant Biology*, *9*(6), 654-663. https://doi.org/10.1016/j.pbi.2006.09.006

Ito, T., Ishida, S., Oe, S., Fukazawa, J., & Takahashi, Y. (2017). Autophosphorylation affects substrate-binding affinity of Tobacco Ca2+ -dependent protein kinase. *Plant Physiology*, *174*(4), 2457-2468. https://doi.org/10.1104/pp.17.00515

Ito, T., Nakata, M., Fukazawa, J., Ishida, S., & Takahashi, Y. (2014). Scaffold function of Ca^{2+}-dependent protein Kinase: Tobacco Ca^{2+}-dependent protein kinase1 transfers 14-3-3 to the substrate repression of shoot growth after phosphorylation. *Plant Physiology*, *165*(4), 1737-1750. https://doi.org/10.1104/pp.114.236448

Itoh, H., Ueguchi-Tanaka, M., Sentoku, N., Kitano, H., Matsuoka, M., & Kobayashi, M. (2001). Cloning and functional analysis of two gibberellin 3β-hydroxylase genes that are differently expressed during the growth of rice. *Proceedings of the National Academy of Sciences of the United States of America*, *98*(15), 8909-8914. https://doi.org/10.1073/pnas.141239398

Jagadish S.V., Craufurd, P.Q., & Wheeler, T.R. (2007). High temperature stress and spikelet fertility in rice (*Oryza sativa* L.). *Journal of Experimental Botany, 58*(7), 1627-1635. doi: 10.1093/jxb/erm003.

Jakobson, L., Vaahtera, L., Tõldsepp, K., Nuhkat, M., Wang, C., Wang, Y. S., Hõrak, H., Valk, E., Pechter, P., Sindarovska, Y., Tang, J., Xiao, C., Xu, Y., Gerst Talas, U., García-Sosa, A. T., Kangasjärvi, S., Maran, U., Remm, M., Roelfsema, M. R. G., … Brosché, M. (2016). Natural Variation in Arabidopsis Cvi-0 Accession Reveals an Important Role of MPK12 in Guard Cell CO_2 Signaling. *PLoS Biology*, *14*(12), 1-25. https://doi.org/10.1371/journal.pbio.2000322

Jalakas, P., Merilo, E., Kollist, H., & Brosché, M. (2018). ABA-mediated regulation of stomatal density is OST1-independent. *Plant Direct*, *2*(9), e00082. https://doi.org/10.1002/pld3.82

Jensen, N. B., Ottosen, C. O., & Zhou, R. (2023). Exogenous Melatonin Alters Stomatal Regulation in Tomato Seedlings Subjected to Combined Heat and Drought Stress through Mechanisms Distinct from ABA Signaling. *Plants*, *12*(5), 156. https://doi.org/10.3390/plants12051156

Jezek, M., & Blatt, M. R. (2017). The membrane transport system of the guard cell and its integration for stomatal dynamics. *Plant Physiology*, *174*(2), 487–519. https://doi.org/10.1104/pp.16.01949

Jiang, Z., Xu, G., Jing, Y., Tang, W., & Lin, R. (2016). Phytochrome B and REVEILLE1/2-mediated signalling controls seed dormancy and germination in Arabidopsis. *Nature Communications*, *7*, 1-10. https://doi.org/10.1038/ncomms12377

Jones, H. G. (1999). Use of thermography for quantitative studies of spatial and temporal variation of stomatal conductance over leaf surfaces. *Plant, Cell and Environment*, *22*(9), 1043–1055. https://doi.org/10.1046/j.1365-3040.1999.00468.x

Jung, J. H., Li, Z., Chen, H., Yang, S., Li, D., Priatama, R. A., Kumar, V., & Xuan, Y. H. (2023). Mutation of phytochrome B promotes resistance to sheath blight and saline–alkaline stress via increasing ammonium uptake in rice. *Plant Journal*, *113*(2), 277–290. https://doi.org/10.1111/tpj.16046

Kang, J., Hwang, J. U., Lee, M., Kim, Y. Y., Assmann, S. M., Martinoia, E., & Lee, Y. (2010). PDR-type ABC transporter mediates cellular uptake of the phytohormone abscisic

acid. *Proceedings of the National Academy of Sciences of the United States of America*, *107*(5), 2355-2360. https://doi.org/10.1073/pnas.0909222107

Karlsson, P. E. (1986). Blue light regulation of stomata in wheat seedlings. II. Action spectrum and search for action dichroism. *Physiologia Plantarum*, *66*(2), 207-210. https://doi.org/10.1111/j.1399-3054.1986.tb02410.x

Kay, S. A., Shinozaki, K., & Chua, N. H. (1989). The sequence of the rice phytochrome gene. *Nucleic Acids Research*, 17(7), 2865-2866. https://doi.org/10.1093/nar/17.7.2865

Keenan, T. F., Hollinger, D. Y., Bohrer, G., Dragoni, D., Munger, J. W., Schmid, H. P., & Richardson, A. D. (2013). Increase in forest water-use efficiency as atmospheric carbon dioxide concentrations rise. *Nature*, *499*, 324-327. https://doi.org/10.1038/nature12291

Keller, B. U., Hedrich, R. & Raschke, K. Voltage-dependent anion channels in the plasma membrane of guard cells. *Nature 341*, 450-453 (1989).

Khanna, R., Li, J., Tseng, T. S., Schroeder, J. I., Ehrhardt, D. W., & Briggs, W. R. (2014). COP1 jointly modulates cytoskeletal processes and electrophysiological responses required for stomatal closure. *Molecular Plant*, *7*(9), 1441–1454. https://doi.org/10.1093/mp/ssu065

Kim, H. Y., Lieffering, M., Kobayashi, K., Okada, M., & Miura, S. (2003). Seasonal changes in the effects of elevated CO_2 on rice at three levels of nitrogen supply: A free air CO_2 enrichment (FACE) experiment. *Global Change Biology*, *9*(6). https://doi.org/10.1046/j.1365-2486.2003.00641.x

Kim, S. Y., Ma, J., Perret, P., Li, Z., & Thomas, T. L. (2002). Arabidopsis ABI5 subfamily members have distinct DNA-binding and transcriptional activities. *Plant Physiology*, *130*(2). 688-697. https://doi.org/10.1104/pp.003566

Kim, T. H., Böhmer, M., Hu, H., Nishimura, N., & Schroeder, J. I. (2010). Guard cell signal transduction network: Advances in understanding abscisic acid, CO_2, and Ca^{2+}

signaling. *Annual Review of Plant Biology*, *61*, 561-591. https://doi.org/10.1146/annurev-arplant-042809-112226

King, K. E., Moritz, T., & Harberd, N. P. (2001). Gibberellins are not required for normal stem growth in Arabidopsis thaliana in the absence of GAI and RGA. *Genetics*, *159*(2), 767-776. https://doi.org/10.1093/genetics/159.2.767

Kinoshita, T., Doi, M., Suetsugu, N., Kagawa, T., Wada, M., & Shimazaki, K. I. (2001). phot1 and phot2 mediate blue light regulation of stomatal opening. *Nature*, *414*, 656-660. https://doi.org/10.1038/414656a

Kinoshita, T., Ono, N., Hayashi, Y., Morimoto, S., Nakamura, S., Soda, M., Kato, Y., Ohnishi, M., Nakano, T., Inoue, S. I., & Shimazaki, K. I. (2011). FLOWERING LOCUS T regulates stomatal opening. *Current Biology*, *21*(14), 1232-1238. https://doi.org/10.1016/j.cub.2011.06.025

Kobayashi, M., Sakurai, A., Saka, H., & Takahashi, N. (1989). Quantitative analysis of endogenous gibberellins in normal and dwarf cultivars of rice. *Plant and Cell Physiology*, *30*(7), 963-969. https://doi.org/10.1093/oxfordjournals.pcp.a077841

Kobayashi, Y., Murata, M., Minami, H., Yamamoto, S., Kagaya, Y., Hobo, T., Yamamoto, A., & Hattori, T. (2005). Abscisic acid-activated SNRK2 protein kinases function in the gene-regulation pathway of ABA signal transduction by phosphorylating ABA response element-binding factors. *Plant Journal*, *44*(6), 939-949. https://doi.org/10.1111/j.1365-313X.2005.02583.x

Koini, M. A., Alvey, L., Allen, T., Tilley, C. A., Harberd, N. P., Whitelam, G. C., & Franklin, K. A. (2009). High Temperature-Mediated Adaptations in Plant Architecture Require the bHLH Transcription Factor PIF4. *Current Biology*, *19*(5), 408-413. https://doi.org/10.1016/j.cub.2009.01.046

Kolla, V. A., Vavasseur, A., & Raghavendra, A. S. (2007). Hydrogen peroxide production is an early event during bicarbonate induced stomatal closure in abaxial epidermis of Arabidopsis. *Planta*, *225*(6), 1421–1429. https://doi.org/10.1007/s00425-006-0450-6

Kollist, H., Nuhkat, M., & Roelfsema, M. R. G. (2014). Closing gaps: Linking elements that control stomatal movement. *New Phytologist*, *203*(1), 44-62. https://doi.org/10.1111/nph.12832

Koornneef, M., & van der Veen, J. H. (1980). Induction and analysis of gibberellin sensitive mutants in Arabidopsis thaliana (L.) heynh. *Theoretical and Applied Genetics*, *58*(6), 257-263. https://doi.org/10.1007/BF00265176

Krishnan, P., Swain, D. K., Chandra Bhaskar, B., Nayak, S. K., & Dash, R. N. (2007). Impact of elevated CO_2 and temperature on rice yield and methods of adaptation as evaluated by crop simulation studies. *Agriculture, Ecosystems and Environment*, *122*(2), 233-242. https://doi.org/10.1016/j.agee.2007.01.019

Kucera, B., Cohn, M. A., & Leubner-Metzger, G. (2005). Plant hormone interactions during seed dormancy release and germination. *Seed Science Research*, *15*(4), 281 – 307. https://doi.org/10.1079/ssr2005218

Küpers, J. J., Snoek, B. L., Oskam, L., Pantazopoulou, C. K., Matton, S. E. A., Reinen, E., Liao, C. Y., Eggermont, E. D. C., Weekamp, H., Biddanda-Devaiah, M., Kohlen, W., Weijers, D., & Pierik, R. (2023). Local light signaling at the leaf tip drives remote differential petiole growth through auxin-gibberellin dynamics. *Current Biology*, *33*(1), 75-85. https://doi.org/10.1016/j.cub.2022.11.045

Kurepa, J., & Smalle, J. A. (2022). Auxin/Cytokinin Antagonistic Control of the Shoot/Root Growth Ratio and Its Relevance for Adaptation to Drought and Nutrient Deficiency Stresses. *International Journal of Molecular Sciences*, *23*(4). https://doi.org/10.3390/ijms23041933

Kuromori, T., Miyaji, T., Yabuuchi, H., Shimizu, H., Sugimoto, E., Kamiya, A., Moriyama, Y., & Shinozaki, K. (2010). ABC transporter AtABCG25 is involved in abscisic acid transport and responses. *Proceedings of the National Academy of Sciences of the United States of America*, *107*(5), 2361-2366. https://doi.org/10.1073/pnas.0912516107

Kuromori, T., Sugimoto, E., & Shinozaki, K. (2011). Arabidopsis mutants of AtABCG22, an ABC transporter gene, increase water transpiration and drought susceptibility. *Plant Journal*, *67*(5), 885-894. https://doi.org/10.1111/j.1365-313X.2011.04641.x

Kwak, J. M., Mori, I. C., Pei, Z. M., Leonhard, N., Angel Torres, M., Dangl, J. L., Bloom, R. E., Bodde, S., Jones, J. D. G., & Schroeder, J. I. (2003). NADPH oxidase AtrbohD and AtrbohF genes function in ROS-dependent ABA signaling in Arabidopsis. *The EMBO Journal*, *22*(11),2623-2633. https://doi.org/10.1093/emboj/cdg277

Kwak, J. M., Murata, Y., Baizabal-Aguirre, V. M., Merrill, J., Wang, M., Kemper, A., Hawke, S. D., Tallman, G., & Schroeder, J. I. (2001). Dominant negative guard cell K^+ channel mutants reduce inward-rectifying K+ currents and light-induced stomatal opening in Arabidopsis. *Plant Physiology*, *127*(2), 473-485. https://doi.org/10.1104/pp.010428

Lau, O. S., & Deng, X. W. (2010). Plant hormone signaling lightens up: integrators of light and hormones. *Current Opinion in Plant Biology*, *13*(5), 571-577. https://doi.org/10.1016/j.pbi.2010.07.001

Lau, O. S., & Deng, X. W. (2012). The photomorphogenic repressors COP1 and DET1: 20 years later. *Trends in Plant Science*, *17*(10), 584-93. https://doi.org/10.1016/j.tplants.2012.05.004

Lawrence, S., Pang, Q., Kong, W., & Chen, S. (2018). Stomata tape-peel: An improved method for guard cell sample preparation. *Journal of Visualized Experiments*, *137*, 57422 https://doi.org/10.3791/57422

Lawson, T., & Blatt, M. R. (2014). Stomatal size, speed, and responsiveness impact on photosynthesis and water use efficiency. *Plant Physiology*, *164*(4), 1556-1570. https://doi.org/10.1104/pp.114.237107

Lawson, T., & Morison, J. I. L. (2004). Stomatal function and physiology. In A. R. Hemsley & I. Poole (Eds.), *The Evolution of Plant Physiology: From whole plants to ecosystems* (pp.217-242). Academic press. https://doi.org/10.1016/B978-012339552-8/50013-5

Lawson, T., Lefebvre, S., Baker, N. R., Morison, J. I. L., & Raines, C. A. (2008). Reductions in mesophyll and guard cell photosynthesis impact on the control of stomatal

responses to light and CO_2. *Journal of Experimental Botany*, *59*(13), 3609-3619. https://doi.org/10.1093/jxb/ern211

Lawson, T., Terashima, I., Fujita, T., Wang, Y. (2018). Coordination Between Photosynthesis and Stomatal Behavior. In: W. W. Adams III & I. Terashima (Eds.), *The Leaf: A Platform for Performing Photosynthesis. Advances in Photosynthesis and Respiration*, (pp. 141-161) Springer, Cham. https://doi.org/10.1007/978-3-319-93594-2_6

Lawson, T., von Caemmerer, S., Baroli, I. (2010). Photosynthesis and Stomatal Behaviour. In: U. Lüttge, W. Beyschlag, B. Büdel & D. Francis (Eds.), *Progress in Botany, vol 72*, (pp.265-304) Springer, Berlin, Heidelberg. https://doi.org/10.1007/978-3-642-13145-5_11

Leakey, A. D. B., Ainsworth, E. A., Bernacchi, C. J., Rogers, A., Long, S. P., & Ort, D. R. (2009). Elevated CO_2 effects on plant carbon, nitrogen, and water relations: Six important lessons from FACE. *Journal of Experimental Botany*, *60*(10), 2859-2876. https://doi.org/10.1093/jxb/erp096

Lee, J. S. (2006). Response to Red and Blue Lights by Electrical Currents on the Surface of Intact Leaves. *Journal of Plant Biology*,*49*(2),186-192. https://doi.org/10.1007/BF03031016

Lee, K. P., Piskurewicz, U., Turečková, V., Carat, S., Chappuis, R., Strnad, M., Fankhauser, C., & Lopez-Molina, L. (2012). Spatially and genetically distinct control of seed germination by phytochromes A and B. *Genes and Development, 26*, 1984-1996. https://doi.org/10.1101/gad.194266.112

Lee, S. C., Lan, W., Buchanan, B. B., & Luan, S. (2009). A protein kinase-phosphatase pair interacts with an ion channel to regulate ABA signaling in plant guard cells. *Proceedings of the National Academy of Sciences of the United States of America*, *106*(50), 21419- 21424. https://doi.org/10.1073/pnas.0910601106

Lee, S., Cheng, H., King, K. E., Wang, W., He, Y., Hussain, A., Lo, J., Harberd, N. P., & Peng, J. (2002). Gibberellin regulates Arabidopsis seed germination via RGL2, a

GAI/RGA-like gene whose expression is up-regulated following imbibition. *Genes and Development*, *16*(5), 646-658. https://doi.org/10.1101/gad.969002

Leinonen, I., Grant, O. M., Tagliavia, C. P. P., Chaves, M. M., & Jones, H. G. (2006). Estimating stomatal conductance with thermal imagery. *Plant, Cell and Environment*, *29*(8), 1508–1518. https://doi.org/10.1111/j.1365-3040.2006.01528.x

Lemonnier, P., & Lawson, T. (2023). Calvin cycle and guard cell metabolism impact stomatal function. *Seminars in Cell and Developmental Biology*. *In press.* https://doi.org/10.1016/j.semcdb.2023.03.001

Leymarie, J., Lascève, G., & Vavasseur, A. (1998). Interaction of stomatal responses to ABA and CO_2 in Arabidopsis thaliana. *Australian Journal of Plant Physiology*, *25*(7) 785-791. https://doi.org/10.1071/PP98031

Leymarie, J., Lascève, G., & Vavasseur, A. (1999). Elevated CO_2 enhances stomatal responses to osmotic stress and abscisic acid in Arabidopsis thaliana. *Plant, Cell and Environment*, *22*(3), 301-308. https://doi.org/10.1046/j.1365-3040.1999.00403.x

Leymarie, J., Vavasseur, A., & Lascève, G. (1998). CO_2 sensing in stomata of abi1-1 and abi2-1 mutants of Arabidopsis thaliana. *Plant Physiology and Biochemistry*, *36*(7), 539-543. https://doi.org/10.1016/S0981-9428(98)80180-0

Li Z.K., Pinson, S.R., Stansel J. W., & Paterson, A. H. Genetic dissection of the source-sink relationship affecting fecundity and yield in rice (*Oryza sativa* L.). (1998). *Molecular Breeding, 4,* 419–426. https://doi: 10.1023/A:1009608128785.

Li, C., Zheng, L., Wang, X., Hu, Z., Zheng, Y., Chen, Q., Hao, X., Xiao, X., Wang, X., Wang, G., & Zhang, Y. (2019). Comprehensive expression analysis of Arabidopsis GA2-oxidase genes and their functional insights. *Plant Science*, *285*(April), 1-13. https://doi.org/10.1016/j.plantsci.2019.04.023

Li, J., Li, Y., Yin, Z., Jiang, J., Zhang, M., Guo, X., Ye, Z., Zhao, Y., Xiong, H., Zhang, Z., Shao, Y., Jiang, C., Zhang, H., An, G., Paek, N. C., Ali, J., & Li, Z. (2017). OsASR5 enhances drought tolerance through a stomatal closure pathway associated with ABA

and H_2O_2 signalling in rice. *Plant Biotechnology Journal*, *15*(2), 183–196. https://doi.org/10.1111/pbi.12601

Li, X. M., Zhang, L. H., Li, Y. Y., Ma, L. J., Chen, Q., Wang, L. L., & He, X. Y. (2011). Effects of elevated carbon dioxide and/or ozone on endogenous plant hormones in the leaves of *Ginkgo biloba*. *Acta Physiologiae Plantarum*, *33*(1), 129-136. https://doi.org/10.1007/s11738-010-0528-4

Li, Y. Z., Zhao, Z. Q., Song, D. D., Yuan, Y. X., Sun, H. J., Zhao, J. F., Chen, Y. L., & Zhang, C. G. (2021). SnRK2.6 interacts with phytochrome B and plays a negative role in red light-induced stomatal opening. *Plant Signaling and Behavior*, *16*(6), e1913307. https://doi.org/10.1080/15592324.2021.1913307

Li, Z., Gao, Y., Zhang, Y., Lin, C., Gong, D., Guan, Y., & Hu, J. (2018). Reactive oxygen species and gibberellin acid mutual induction to regulate tobacco seed germination. *Frontiers in Plant Science*, *9*. https://doi.org/10.3389/fpls.2018.01279

Li, Z., Sheerin, D. J., von Roepenack-Lahaye, E., Stahl, M., & Hiltbrunner, A. (2022). The phytochrome interacting proteins ERF55 and ERF58 repress light-induced seed germination in Arabidopsis thaliana. *Nature Communications*, *13*(1). https://doi.org/10.1038/s41467-022-29315-3

Liang, X., Wang, D., Ye, Q., Zhang, J., Liu, M., Liu, H., Yu, K., Wang, Y., Hou, E., Zhong, B., Xu, L., Lv, T., Peng, S., Lu, H., Sicard, P., Anav, A., & Ellsworth, D. S. (2023). Stomatal responses of terrestrial plants to global change. *Nature Communications*, *14*(1), 2188. https://doi.org/10.1038/s41467-023-37934-7

Liu, H., Guo, S., Lu, M., Zhang, Y., Li, J., Wang, W., Wang, P., Zhang, J., Hu, Z., Li, L., Si, L., Zhang, J., Qi, Q., Jiang, X., Botella, J. R., Wang, H., & Song, C. P. (2019). Biosynthesis of DHGA 12 and its roles in Arabidopsis seedling establishment. *Nature Communications*, *10*, 1768. https://doi.org/10.1038/s41467-019-09467-5

Liu, J., Zhang, F., Zhou, J., Chen, F., Wang, B., & Xie, X. (2012). Phytochrome B control of total leaf area and stomatal density affects drought tolerance in rice. *Plant Molecular Biology*, *78*(3), 289-300. https://doi.org/10.1007/s11103-011-9860-3

Liu, T., Carlsson, J., Takeuchi, T., Newton, L., & Farré, E. M. (2013). Direct regulation of abiotic responses by the Arabidopsis circadian clock component PRR7. *Plant Journal*, *76*(1), 101-114. https://doi.org/10.1111/tpj.12276

Liu, T., Ohashi-Ito, K., & Bergmann, D. C. (2009). Orthologs of Arabidopsis thaliana stomatal bHLH genes and regulation of stomatal development in grasses. *Development*, *136*(13), 2265-2276. https://doi.org/10.1242/dev.032938

Liu, X., & Hou, X. (2018). Antagonistic regulation of ABA and GA in metabolism and signaling pathways. *Frontiers in Plant Science*, *9*(FEB), 251. https://doi.org/10.3389/fpls.2018.00251

Liu, Z., Yan, J. P., Li, D. K., Luo, Q., Yan, Q., Liu, Z. Bin, Ye, L. M., Wang, J. M., Li, X. F., & Yang, Y. (2015). UDP-glucosyltransferase71C5, a major glucosyltransferase, mediates abscisic acid homeostasis in Arabidopsis. *Plant Physiology*, *167*(4), 1659–1670. https://doi.org/10.1104/pp.15.00053

Liu, Z., Zhu, X., Liu, W., Qi, K., Xie, Z., Zhang, S., Wu, J., & Wang, P. (2023). Characterization of the REVEILLE family in Rosaceae and role of PbLHY in flowering time regulation. *BMC Genomics*, *24*(1),49. https://doi.org/10.1186/s12864-023-09144-4

Livak, K. J., & Schmittgen, T. D. (2001). Analysis of relative gene expression data using real-time quantitative PCR and the 2-ΔΔCT method. *Methods*, 25(4),402-408. https://doi.org/10.1006/meth.2001.1262

Lo, S. F., Yang, S. Y., Chen, K. T., Hsing, Y. I., Zeevaart, J. A. D., Chen, L. J., & Yu, S. M. (2008). A novel class of gibberellin 2-oxidases control semidwarfism, tillering, and root development in rice. *Plant Cell*, *20*(10), 2603-2618. https://doi.org/10.1105/tpc.108.060913

Locascio, A., Blázquez, M. A., & Alabadí, D. (2013). Genomic analysis of della protein activity. *Plant and Cell Physiology*, *54*(8). https://doi.org/10.1093/pcp/pct082

Long, S. P., & Ort, D. R. (2010). More than taking the heat: Crops and global change. *Current Opinion in Plant Biology*, *13*(3), 240-247. https://doi.org/10.1016/j.pbi.2010.04.008

Long, S. P., Ainsworth, E. A., Rogers, A., & Ort, D. R. (2004). Rising atmospheric atmospheric carbon dioxide: Plants FACE the Future. *Annual Review of Plant Biology*, 55, 591-628. https://doi.org/10.1146/annurev.arplant.55.031903.141610

Long, S. P., Farage, P. K., Bolhár-Nordenkampf, H. R., & Rohrhofer, U. (1989). Separating the contribution of the upper and lower mesophyll to photosynthesis in *Zea mays* L. leaves. *Planta*, *177*(2). https://doi.org/10.1007/BF00392809

Lopez-Molina, L., Mongrand, S., McLachlin, D. T., Chait, B. T., & Chua, N. H. (2002). ABI5 acts downstream of ABI3 to execute an ABA-dependent growth arrest during germination. *Plant Journal*, *32*(3), 317-328. https://doi.org/10.1046/j.1365-313X.2002.01430.x

Lv, C., Huang, Y., Sun, W., Yu, L., & Zhu, J. (2020). Response of rice yield and yield components to elevated [CO_2]: A synthesis of updated data from FACE experiments. *European Journal of Agronomy*, *112*, 12596. https://doi.org/10.1016/j.eja.2019.125961

MacRobbie, E. A. C., & Kurup, S. (2007). Signalling mechanisms in the regulation of vacuolar ion release in guard cells. *New Phytologist*, 175(4), 630-640. https://doi.org/10.1111/j.1469-8137.2007.02131.x

Makowski, D., Marajo-Petitzon, E., Durand, J. L., & Ben-Ari, T. (2020). Quantitative synthesis of temperature, CO_2, rainfall, and adaptation effects on global crop yields. *European Journal of Agronomy*, *115*, 126041. https://doi.org/10.1016/j.eja.2020.126041

Mansfield, T. A., & Heath, O. V. S. (1963). Studies in stomatal behaviour: IX. Photoperiodic effects on rhythmic phenomena in *Xanthium pennsylvanicum*. *Journal of Experimental Botany*, *14*(2), 334-352. https://doi.org/10.1093/jxb/14.2.334

Mansfield, T. A., Hetherington, A. M., & Atkinson, C. J. (1990). Some current aspects of stomatal physiology. *Annual Review of Plant Physiology and Plant Molecular Biology*, *41*(1), 55-75. https://doi.org/10.1146/annurev.pp.41.060190.000415

Mao, J., Zhang, Y. C., Sang, Y., Li, Q. H., & Yang, H. Q. (2005). A role for Arabidopsis cryptochromes and COP1 in the regulation of stomatal opening. *Proceedings of the National Academy of Sciences of the United States of America*, *102*(34), 12270-12275. https://doi.org/10.1073/pnas.0501011102

Masle, J., Gilmore, S. R., & Farquhar, G. D. (2005). The ERECTA gene regulates plant transpiration efficiency in Arabidopsis. *Nature*, *436*, 866-870. https://doi.org/10.1038/nature03835

Matrosova, A., Bogireddi, H., Mateo-Peñas, A., Hashimoto-Sugimoto, M., Iba, K., Schroeder, J. I., & Israelsson-Nordström, M. (2015). The HT1 protein kinase is essential for red light-induced stomatal opening and genetically interacts with OST1 in red light and CO2-induced stomatal movement responses. *New Phytologist*, *208*(4), 1126-1137. https://doi.org/10.1111/nph.13566

Matthews, J. S. A., Vialet-Chabrand, S., & Lawson, T. (2018). Acclimation to fluctuating light impacts the rapidity of response and diurnal rhythm of stomatal conductance. *Plant Physiology*, *176*(3), 1939-1951. https://doi.org/10.1104/pp.17.01809

Matthews, J. S. A., Vialet-Chabrand, S., & Lawson, T. (2020). Role of blue and red light in stomatal dynamic behaviour. *Journal of Experimental Botany,71*(7), 2253–2269. Oxford University Press. https://doi.org/10.1093/jxb/erz563

McAinsh, M. R., Clayton, H., Mansfield, T. A., & Hetherington, A. M. (1996). Changes in stomatal behavior and guard cell cytosolic free calcium in response to oxidative stress. *Plant Physiology*, *111*(4), 1031-1042. https://doi.org/10.1104/pp.111.4.1031

McAusland, L., Smith, K. E., Williams, A., Molero, G., & Murchie, E. H. (2021). Nocturnal stomatal conductance in wheat is growth-stage specific and shows genotypic variation. *New Phytologist*, *232*(1). https://doi.org/10.1111/nph.17563

McAusland, L., Vialet-Chabrand, S., Davey, P., Baker, N. R., Brendel, O., & Lawson, T. (2016). Effects of kinetics of light-induced stomatal responses on photosynthesis and water-use efficiency. *The New Phytologist*, *211*(4). 1209-1220. https://doi.org/10.1111/nph.14000

McClung, C. R. (2014). Wheels within wheels: New transcriptional feedback loops in the Arabidopsis circadian clock. *F1000Prime Reports*,*6*(2). https://doi.org/10.12703/P6-2

McElwain, J. C., & Chaloner, W. G. (1995). Stomatal density and index of fossil plants track atmospheric carbon dioxide in the palaeozoic. *Annals of Botany*, *76*(4), 389-395. https://doi.org/10.1006/anbo.1995.1112

McKown, K. H., & Bergmann, D. C. (2018). Grass stomata. *Current Biology*, *28*(15), 814-816. https://doi.org/10.1016/j.cub.2018.05.074

Meehl, G. A., Covoy C., McAvaney, Latif, M., & Stouffer, R. J. (2005). Overview of the coupled model intercomparison. *Bulletin of the American Meteorological Society, 86*(1), 89-93. http://dx.doi.org/10.1175/BAMS-86-1-89

Meehl, G. A., T. F. Stocker, W.D. Collins, P. Friedlingstein, A.T. Gaye, J. M. Gregory, A. Kitoh, R. Knutti, J. M. Murphy, A. Noda, S. C. B. Raper, I. G. Watterson, A. J. Weaver & Z. C. Zhao. (2007). Global Climate Projections. In S. Solomon, D. Qin, M. Manning, Z. Chen, M. Marquis, K.B. Averyt, M. Tignor & H.L. Miller (Eds.) *Climate Change 2007: The Physical Science Basis. Contribution of Working Group I to the Fourth Assessment Report of the Intergovernmental Panel on Climate Change*. Cambridge University Press, Cambridge, U.K. http://hdl.handle.net/102.100.100/124551?index=1

Mendes, K. R., & Marenco, R. A. (2014). Is stomatal conductance of Central Amazonian saplings influenced by circadian rhythms under natural conditions? *Theoretical and Experimental Plant Physiology*, *26*(2), 115-125. https://doi.org/10.1007/s40626-014-0010-6

Merilo, E., Jalakas, P., Kollist, H., & Brosché, M. (2015). The Role of ABA recycling and transporter proteins in rapid stomatal responses to reduced air humidity, elevated CO_2,

and exogenous ABA. *Molecular Plant*, *8*(4),657-659. https://doi.org/10.1016/j.molp.2015.01.014

Merilo, E., Jõesaar, I., Brosché, M., & Kollist, H. (2014). To open or to close: Species-specific stomatal responses to simultaneously applied opposing environmental factors. *New Phytologist*, *202*(2), 499-508. https://doi.org/10.1111/nph.12667

Merilo, E., Laanemets, K., Hu, H., Xue, S., Jakobson, L., Tulva, I., Gonzalez-Guzman, M., Rodriguez, P. L., Schroeder, J. I., Broschè, M., & Kollist, H. (2013). PYR/RCAR receptors contribute to ozone-, reduced air humidity-, darkness-, and CO_2-induced stomatal regulation. *Plant Physiology*, 162(3):1652-1668. https://doi.org/10.1104/pp.113.220608

Messinger, S. M., Buckley, T. N., & Mott, K. A. (2006). Evidence for involvement of photosynthetic processes in the stomatal response to CO_2. *Plant Physiology*, *140*(2), 771-778. https://doi.org/10.1104/pp.105.073676

Meyer, S., Mumm, P., Imes, D., Endler, A., Weder, B., Al-Rasheid, K. A. S., Geiger, D., Marten, I., Martinoia, E., & Hedrich, R. (2010). AtALMT12 represents an R-type anion channel required for stomatal movement in Arabidopsis guard cells. *Plant Journal*, 63(6), 1054-1062. https://doi.org/10.1111/j.1365-313X.2010.04302.x

Michaud, O., Krahmer, J., Galbier, F., Lagier, M., Galvão, V. C., Ince, Y. Ç., Trevisan, M., Knerova, J., Dickinson, P., Hibberd, J. M., Zeeman, S. C., & Fankhauser, C. (2023). Abscisic acid modulates neighbor proximity-induced leaf hyponasty in Arabidopsis. *Plant Physiology*, *191*(1), 542-55. https://doi.org/10.1093/plphys/kiac447

Mishra, G., Zhang, W., Deng, F., Zhao, J., & Wang, X. (2006). A bifurcating pathway directs abscisic acid effects on stomatal closure and opening in Arabidopsis. *Science*, 312(5771), 264-266. https://doi.org/10.1126/science.1123769

Mitchum, M. G., Yamaguchi, S., Hanada, A., Kuwahara, A., Yoshioka, Y., Kato, T., Tabata, S., Kamiya, Y., & Sun, T. P. (2006). Distinct and overlapping roles of two gibberellin 3-oxidases in Arabidopsis development. *Plant Journal*, *45*(5), 804-818. https://doi.org/10.1111/j.1365-313X.2005.02642.x

Mohanan, K. V., & Mini, C. B. (2007). Relative Contribution of Rice Tillers of Different Status Towards Yield. *International Journal of Plant Breeding and Genetics*, *2*(1). https://doi.org/10.3923/ijpbg.2008.9.12

Mohapatra, P.K., Sahu, B.B. (2022). Importance of Rice as Human Food. *In Panicle Architecture of Rice and its Relationship with Grain Filling* (pp. 1-25). Springer, Cham. https://doi.org/10.1007/978-3-030-67897-5_1

Morison, J. I. L., (1987). Intercellular CO_2 concentration and stomatal response to CO_2. In E. Zeiger, I. R. Cowan & G. D. Farquhar (Eds.) *Stomatal Function* (pp. 229-251). Stanford University Press, Stanford, CA, USA. https://www.jstor.org/stable/4217850

Mott, K. A. (1988). Do Stomata Respond to CO_2 Concentrations Other than Intercellular? *Plant Physiology*,*86*(1),200-203. https://doi.org/10.1104/pp.86.1.200

Mott, K. A. (1990). Sensing of atmospheric CO_2 by plants. *Plant, Cell & Environment*, *13*(7), 731-737. https://doi.org/10.1111/j.1365-3040.1990.tb01087.x

Mott, K. A. (2009). Opinion: Stomatal responses to light and CO_2 depend on the mesophyll. *Plant, Cell and Environment*. 32(11), 1479-1486. https://doi.org/10.1111/j.1365-3040.2009.02022.x

Mott, K. A., & Parkhurst, D. F. (1991). Stomatal responses to humidity in air and helox. *Plant, Cell & Environment*, *14*(5). https://doi.org/10.1111/j.1365-3040.1991.tb01521.x

Mott, K. A., & Peak, D. (2018). Effects of the mesophyll on stomatal responses in amphistomatous leaves. *Plant Cell and Environment*, *41*(12). https://doi.org/10.1111/pce.13411

Mott, K. A., Sibbernsen, E. D., & Shope, J. C. (2008). The role of the mesophyll in stomatal responses to light and CO_2. *Plant, Cell and Environment, 31*, 1299-1306. https://doi.org/10.1111/j.1365-3040.2008.01845.x

Movahedi, M., Zoulias, N., Casson, S. A., Sun, P., Liang, Y. K., Hetherington, A. M., Gray, J. E., & Chater, C. C. C. (2021). Stomatal responses to carbon dioxide and light require

abscisic acid catabolism in Arabidopsis. *Interface Focus*, *11*(2). https://doi.org/10.1098/rsfs.2020.0036

Muehe, E. M., Wang, T., Kerl, C. F., Planer-Friedrich, B., & Fendorf, S. (2019). Rice production threatened by coupled stresses of climate and soil arsenic. *Nature Communications*, *10*(1), 4985. https://doi.org/10.1038/s41467-019-12946-4

Munemasa, S., Hauser, F., Park, J., Waadt, R., Brandt, B., & Schroeder, J. I. (2015). Mechanisms of abscisic acid-mediated control of stomatal aperture. *Current Opinion in Plant Biology*, 28, 154-162. https://doi.org/10.1016/j.pbi.2015.10.010

Murata, Y., Mori, I. C., & Munemasa, S. (2015). Diverse Stomatal Signaling and the Signal Integration Mechanism. *Annual Review of Plant Biology*, *66*,369-392. https://doi.org/10.1146/annurev-arplant-043014-114707

Nagel, D. H., Doherty, C. J., Pruneda-Paz, J. L., Schmitz, R. J., Ecker, J. R., & Kay, S. A. (2015). Genome-wide identification of CCA1 targets uncovers an expanded clock network in Arabidopsis. *Proceedings of the National Academy of Sciences of the United States of America*, *112*(34), E4802-E4810. https://doi.org/10.1073/pnas.1513609112

Nakajima, M., Shimada, A., Takashi, Y., Kim, Y. C., Park, S. H., Ueguchi-Tanaka, M., Suzuki, H., Katoh, E., Iuchi, S., Kobayashi, M., Maeda, T., Matsuoka, M., & Yamaguchi, I. (2006). Identification and characterization of Arabidopsis gibberellin receptors. *Plant Journal*, *46*(5), 880-889. https://doi.org/10.1111/j.1365-313X.2006.02748.x

Nakamichi, N., Kiba, T., Kamioka, M., Suzukie, T., Yamashino, T., Higashiyama, T., Sakakibara, H., & Mizuno, T. (2012). Transcriptional repressor PRR5 directly regulates clock-output pathways. *Proceedings of the National Academy of Sciences of the United States of America*, *109*(42),17123-17128. https://doi.org/10.1073/pnas.1205156109

Negi, J., Matsuda, O., Nagasawa, T., Oba, Y., Takahashi, H., Kawai-Yamada, M., Uchimiya, H., Hashimoto, M., & Iba, K. (2008). CO_2 regulator SLAC1 and its homologues are essential for anion homeostasis in plant cells. *Nature*, *452*(7186). https://doi.org/10.1038/nature06720

Neill, S., Barros, R., Bright, J., Desikan, R., Hancock, J., Harrison, J., Morris, P., Ribeiro, D., & Wilson, I. (2008). Nitric oxide, stomatal closure, and abiotic stress. *Journal of Experimental Botany*, 59(2):165-176. https://doi.org/10.1093/jxb/erm293

Nelson, D. R., Schuler, M. A., Paquette, S. M., Werck-Reichhart, D., & Bak, S. (2004). Comparative genomics of rice and arabidopsis. Analysis of 727 cytochrome P450 genes and pseudogenes from a monocot and a dicot. *Plant Physiology*, *135*(2), 756-772. https://doi.org/10.1104/pp.104.039826

Nemhauser, J. L., Hong, F., & Chory, J. (2006). Different Plant Hormones Regulate Similar Processes through Largely Nonoverlapping Transcriptional Responses. *Cell*,*126*(3), 467-75. https://doi.org/10.1016/j.cell.2006.05.050

Nemhauser, J. L., Mockler, T. C., & Chory, J. (2004). Interdependency of brassinosteroid and auxin signaling in Arabidopsis. *PLoS Biology*, *2*(9). https://doi.org/10.1371/journal.pbio.0020258

Ng, L. M., Melcher, K., Teh, B. T., & Xu, H. E. (2014). Abscisic acid perception and signaling: Structural mechanisms and applications. In *Acta Pharmacologica Sinica*, *35*(5), 567-584. https://doi.org/10.1038/aps.2014.5

Niharika, Singh, N. B., Singh, A., Khare, S., Yadav, V., Bano, C., & Yadav, R. K. (2021). Mitigating Strategies of Gibberellins in Various Environmental Cues and Their Crosstalk with Other Hormonal Pathways in Plants: a Review. *Plant Molecular Biology Reporter*,39(1), 34-49. Springer. https://doi.org/10.1007/s11105-020-01231-0

NOAA, (2022). https://www.climate.gov/news-features/understanding-climate/climate-change-atmospheric-carbon-dioxide

Ogawa, T., Ishikawa, H., Shimada, K., & Shibata, K. (1978). Synergistic action of red and blue light and action spectra for malate formation in guard cells of *Vicia faba* L. *Planta*, 142, 61-65. https://doi.org/10.1007/BF00385121

Oh, E., Yamaguchi, S., Hu, J., Yusuke, J., Jung, B., Paik, I., Lee, H. S., Sun, T. P., Kamiya, Y., & Choi, G. (2007). PIL5, a phytochrome-interacting bHLH protein, regulates gibberellin responsiveness by binding directly to the GAI and RGA promoters in

Arabidopsis seeds. *Plant Cell*, *19*(4), 1192-1208. https://doi.org/10.1105/tpc.107.050153

Ohsumi, A., Kanemura, T., Homma, K., Horie, T., & Shiraiwa, T. (2007). Genotypic variation of stomatal conductance about stomatal density and length in rice (*Oryza sativa* L.). *Plant Production Science*, *10*(3). https://doi.org/10.1626/pps.10.322

Okada, K., Ito, T., Fukazawa, J., & Takahashi, Y. (2017). Gibberellin induces an increase in cytosolic Ca2+via a DELLA-independent signaling pathway. *Plant Physiology*, *175*(4), 1536–1542. https://doi.org/10.1104/pp.17.01433

Okamoto, M., Tanaka, Y., Abrams, S. R., Kamiya, Y., Seki, M., & Nambara, E. (2009). High humidity induces abscisic acid 8′-hydroxylase in stomata and vasculature to regulate local and systemic abscisic acid responses in Arabidopsis. *Plant Physiology*, *149*(2), 825-834. https://doi.org/10.1104/pp.108.130823

Olsen, R. L., Pratt, R. B., Gump, P., Kemper, A., & Tallman, G. (2002). Red light activates a chloroplast-dependent ion uptake mechanism for stomatal opening under reduced CO_2 concentrations in Vicia spp. *New Phytologist*, *153*(3), 497-508. https://doi.org/10.1046/j.0028-646X.2001.00337.x

Olszewski, N., Sun, T. P., & Gubler, F. (2002). Gibberellin signaling: Biosynthesis, catabolism, and response pathways. *Plant Cell*, *14*(SUPPL.), S61-80. https://doi.org/10.1105/tpc.010476

Pandey, S., Wang, R. S., Wilson, L., Li, S., Zhao, Z., Gookin, T. E., Assmann, S. M., & Albert, R. (2010). Boolean modeling of transcriptome data reveals novel modes of heterotrimeric G-protein action. *Molecular Systems Biology*, *6*, 372. https://doi.org/10.1038/msb.2010.28

Pandey, S., Zhang, W., & Assmann, S. M. (2007). Roles of ion channels and transporters in guard cell signal transduction. *FEBS Letters*,581(12), 2325-2336. https://doi.org/10.1016/j.febslet.2007.04.008

Papanatsiou, M., Petersen, J., Henderson, L., Wang, Y., Christie, J.M. & Blatt, M. R. (2019). Optogenetic manipulation of stomatal kinetics improves carbon assimilation

and water use efficiency. *Science* 363, 1456–1459. https://doi.org/10.1126/science.aaw0046

Paparelli, E., Parlanti, S., Gonzali, S., Novi, G., Mariotti, L., Ceccarelli, N., van Dongen, J. T., Kölling, K., Zeeman, S. C., & Perata, P. (2013). Nighttime sugar starvation orchestrates gibberellin biosynthesis and plant growth in Arabidopsis. *Plant Cell*, *25*(10), 3760-3769. https://doi.org/10.1105/tpc.113.115519

Pateli, P., Papafotiou, M., & Chronopoulos, J. (2004). Comparative effects of four plant growth retardants on growth of Epidendrum radicans. *Journal of Horticultural Science and Biotechnology*, *79*(2), 303-307. https://doi.org/10.1080/14620316.2004.11511765

Pei, Z. M., Kuchitsu, K., Ward, J. M., Schwarz, M., & Schroeder, J. I. (1997). Differential abscisic acid regulation of guard cell slow anion channels in arabidopsis wild-type and abi1 and abi2 mutants. *Plant Cell*, 9(3), 409-423. https://doi.org/10.1105/tpc.9.3.409

Pei, Z. M., Murata, Y., Benning, G., Thomine, S., Klüsener, B., Allen, G. J., Grill, E., & Schroeder, J. I. (2000). Calcium channels activated by hydrogen peroxide mediate abscisic acid signalling in guard cells. *Nature, 406*, 731-734. https://doi.org/10.1038/35021067

Peng, S., Huang, J., Sheehy, J. E., Laza, R. C., Visperas, R. M., Zhong, X., Centeno, G. S., Khush, G. S., & Cassman, K. G. (2004). Rice yields decline with higher night temperature from global warming. *Proceedings of the National Academy of Sciences of the United States of America*,*101*(27), 9971-9975. https://doi.org/10.1073/pnas.0403720101

Pham, V. N., Kathare, P. K., & Huq, E. (2018). Phytochromes and Phytochrome Interacting Factors. *Plant Physiology*, *176*(2), 1025-1038. https://doi.org/10.1104/pp.17.01384

Porra, R. J. (2002). The chequered history of the development and use of simultaneous equations for the accurate determination of chlorophylls a and b. *Photosynthesis Research*, 73, (1-3), 149-156. https://doi.org/10.1023/A:1020470224740

Prasetyaningrum, P., Mariotti, L., Valeri, M. C., Novi, G., Dhondt, S., Inzé, D., Perata, P., & van Veen, H. (2021). Nocturnal gibberellin biosynthesis is carbon dependent and

adjusts leaf expansion rates to variable conditions. *Plant Physiology*, *185*(1), 228-239. https://doi.org/10.1093/plphys/kiaa019

Qi, X. F., Wang, X. H., Wang, Q., Li, M., Ma, L. J., Li, Y. Y., Li, X. M., & Wang, L. L. (2021). Photosynthesis, stomatal conductance, endogenous hormones and organic acid synergistic regulation in leaves of rice (*Oryza sativa* L.) under elevated CO_2. *Applied Ecology and Environmental Research*, *19*(5), 3773-3787. https://doi.org/10.15666/aeer/1905_37733787

Rademacher, W. (2000). Growth retardants: Effects on gibberellin biosynthesis and other metabolic pathways. *Annual Review of Plant Biology*, *51*, 501-531. https://doi.org/10.1146/annurev.arplant.51.1.501

Rademacher, W. (2017). Chemical Regulators of Gibberellin Status and Their Application in Plant Production. In P. Hedden & S.G. Thomas (Eds.), *Annual Plant Reviews online* (pp. 359-403). John Wiley & Sons, Ltd. https://doi.org/10.1002/9781119312994.apr0541

Raissig, M. T., Abrash, E., Bettadapur, A., Vogel, J. P., & Bergmann, D. C. (2016). Grasses use an alternatively wired bHLH transcription factor network to establish stomatal identity. *Proceedings of the National Academy of Sciences of the United States of America*, *113*(29), 8326-8331. https://doi.org/10.1073/pnas.1606728113

Raissig, M. T., Matos, J. L., Gil, M. X. A., Kornfeld, A., Bettadapur, A., Abrash, E., Allison, H. R., Badgley, G., Vogel, J. P., Berry, J. A., & Bergmann, D. C. (2017). Mobile MUTE specifies subsidiary cells to build physiologically improved grass stomata. *Science*, *355*(6330), 1215-1218. https://doi.org/10.1126/science.aal3254

Rao, A.N., Wani, S.P., Ramesha, M.S., & Ladha, J.K. (2017). Rice Production Systems. In B. Chauhan, K. Jabran & G. Mahajan (Eds.) *Rice Production Worldwide* (pp. 185-205). Springer, Cham. https://doi.org/10.1007/978-3-319-47516-5_8

Raschke, K. (1975). Simultaneous requirement of carbon dioxide and abscisic acid for stomatal closing in *Xanthium strumarium* L. *Planta*, *125*(3), 243-259. https://doi.org/10.1007/BF00385601

Rausenberger, J., Hussong, A., Kircher, S., Kirchenbauer, D., Timmer, J., Nagy, F., Schäfer, E., & Fleck, C. (2010). An integrative model for phytochrome B mediated photomorphogenesis: From protein dynamics to physiology. *PLoS ONE*, *5*(5). https://doi.org/10.1371/journal.pone.0010721

Reed, J. W., Nagpal, P., Poole, D. S., Furuya, M., & Chory, J. (1993). Mutations in the gene for the red/far-red light receptor phytochrome B alter cell elongation and physiological responses throughout Arabidopsis development. *Plant Cell*, 5(2), 147-157. https://doi.org/10.2307/3869581

Richardson, F., Brodribb, T. J., & Jordan, G. J. (2017). Amphistomatic leaf surfaces independently regulate gas exchange in response to variations in evaporative demand. *Tree Physiology*, *37*(7). https://doi.org/10.1093/treephys/tpx073

Rieu, I., Eriksson, S., Powers, S. J., Gong, F., Griffiths, J., Woolley, L., Benlloch, R., Nilsson, O., Thomas, S. G., Hedden, P., & Phillips, A. L. (2008). Genetic analysis reveals that C19-GA 2-oxidation is a major gibberellin inactivation pathway in Arabidopsis. *Plant Cell*, *20*(9), 2420-2436. https://doi.org/10.1105/tpc.108.058818

Rieu, I., Ruiz-Rivero, O., Fernandez-Garcia, N., Griffiths, J., Powers, S. J., Gong, F., Linhartova, T., Eriksson, S., Nilsson, O., Thomas, S. G., Phillips, A. L., & Hedden, P. (2008). The gibberellin biosynthetic genes AtGA20ox1 and AtGA20ox2 act, partially redundantly, to promote growth and development throughout the Arabidopsis life cycle. *Plant Journal*, *53*(3), 488-504. https://doi.org/10.1111/j.1365-313X.2007.03356.x

Rizza, A., Tang, B., Stanley, C. E., Grossmann, G., Owen, M. R., Band, L. R., & Jones, A. M. (2021). Differential biosynthesis and cellular permeability explain longitudinal gibberellin gradients in growing roots. *Proceedings of the National Academy of Sciences of the United States of America*, *118*(8). https://doi.org/10.1073/pnas.1921960118

Roelfsema, M. R. G., Hanstein, S., Felle, H. H., & Hedrich, R. (2002). CO_2 provides an intermediate link in the red light response of guard cells. *Plant Journal*, *32*(1), 65-75. https://doi.org/10.1046/j.1365-313X.2002.01403.x

Roelfsema, M. R. G., Hedrich, R., & Geiger, D. (2012). Anion channels: Master switches of stress responses. *Trends in Plant Science*, 17(4), 221-229. https://doi.org/10.1016/j.tplants.2012.01.009

Sah, S. K., Reddy, K. R., & Li, J. (2016). Abscisic acid and abiotic stress tolerance in crop plants. *Frontiers in Plant Science*, 7(MAY), 571. https://doi.org/10.3389/fpls.2016.00571

Saleem, M., Asghar, H. N., Khan, M. Y., & Zahir, Z. A. (2015). Gibberellic acid in combination with pressmud enhances the growth of sunflower and stabilizes chromium(VI)-contaminated soil. *Environmental Science and Pollution Research*, *22*(14), 10610-10617. https://doi.org/10.1007/s11356-015-4275-3

Salomé, P. A., Michael, T. P., Kearns, E. V., Fett-Neto, A. G., Sharrock, R. A., & McClung, C. R. (2002). The out of phase 1 mutant defines a role for PHYB in circadian phase control in Arabidopsis. *Plant Physiology*, 129(4), 1674-1685. https://doi.org/10.1104/pp.003418

Sano, N., & Marion-Poll, A. (2021). ABA metabolism and homeostasis in seed dormancy and germination. *International Journal of Molecular Sciences,22*(10), 5069. https://doi.org/10.3390/ijms22105069

Santakumari, M., & Fletcher, R. A. (1987). Reversal of triazole-induced stomatal closure by gibberellic acid and cytokinins in Commelina benghalensis. *Physiologia Plantarum*, *71*(1), 95-99. https://doi.org/10.1111/j.1399-3054.1987.tb04623.x

Santelia, D., & Lawson, T. (2016). Rethinking guard cell metabolism. *Plant Physiology*, *172*(3), 1371-1392. https://doi.org/10.1104/pp.16.00767

Santos, M. G., Davey, P. A., Hofmann, T. A., Borland, A., Hartwell, J., & Lawson, T. (2021). Stomatal Responses to Light, CO_2, and Mesophyll Tissue in *Vicia faba* and *Kalanchoë fedtschenkoi*. *Frontiers in Plant Science*, *12* (Oct), 740534 https://doi.org/10.3389/fpls.2021.740534

Sasaki, T., Mori, I. C., Furuichi, T., Munemasa, S., Toyooka, K., Matsuoka, K., Murata, Y., & Yamamoto, Y. (2010). Closing plant stomata requires a homolog of an aluminum-

activated malate transporter. *Plant and Cell Physiology,51*(3), 354-365 https://doi.org/10.1093/pcp/pcq016

Scherzer, S., Maierhofer, T., Al-Rasheid, K. A. S., Geiger, D., & Hedrich, R. (2012). Multiple calcium-dependent kinases modulate ABA-activated guard cell anion channels. *Molecular Plant*, *5*(6), 1409-1412. https://doi.org/10.1093/mp/sss084

Schmidt, C., Schelle, I., Liao, Y. J., & Schroeder, J. I. (1995). Strong regulation of slow anion channels and abscisic acid signaling in guard cells by phosphorylation and dephosphorylation events. *Proceedings of the National Academy of Sciences of the United States of America,92* (21), 9535-9539 https://doi.org/10.1073/pnas.92.21.9535

Scholl, R. L., May, S. T., & Ware, D. H. (2000). Seed and molecular resources for Arabidopsis. *Plant Physiology*, *124*(4), 1477-1480. https://doi.org/10.1104/pp.124.4.1477

Schomburg, F. M., Bizzell, C. M., Lee, D. J., Zeevaart, J. A. D., & Amasino, R. M. (2003). Overexpression of a novel class of gibberellin 2-oxidases decreases gibberellin levels and creates dwarf plants. *Plant Cell*, *15*(1), 151-163. https://doi.org/10.1105/tpc.005975

Schopfer, P., Plachy, C., & Frahry, G. (2001). Release of reactive oxygen intermediates (superoxide radicals, hydrogen peroxide, and hydroxyl radicals) and peroxidase in germinating radish seeds controlled by light, gibberellin, and abscisic acid. *Plant Physiology*, *125*(4), 1591-1602. https://doi.org/10.1104/pp.125.4.1591

Schroeder, J. I., & Hagiwara, S. (1989). Cytosolic calcium regulates ion channels in the plasma membrane of *Vicia faba* guard cells. *Nature*, *338*(6214). https://doi.org/10.1038/338427a0

Schroeder, J. I., Allen, G. J., Hugouvieux, V., Kwak, J. M., & Waner, D. (2001). Guard cell signal transduction. *Annual Review of Plant Physioogy and Plant Molecular Biology*, *5*,627-658. https://doi.org/10.1146/annurev.arplant.52.1.627

Schwartz, A., & Zeiger, E. (1984). Metabolic energy for stomatal opening. Roles of photophosphorylation and oxidative phosphorylation. *Planta*, *161*(2), 129-136 https://doi.org/10.1007/BF00395472

Seibt, U., Rajabi, A., Griffiths, H., & Berry, J. A. (2008). Carbon isotopes and water use efficiency: Sense and sensitivity. *Oecologia*,*155*(3), 441-454. https://doi.org/10.1007/s00442-007-0932-7

Senthil-Nathan, S. (2021). Effects of elevated CO2 on resistant and susceptible rice cultivar and its primary host, brown planthopper (BPH), Nilaparvata lugens (Stål). *Scientific Reports*, *11*(1), 8905. https://doi.org/10.1038/s41598-021-87992-4

Seo, M., & Koshiba, T. (2002). Complex regulation of ABA biosynthesis in plants. *Trends in Plant Science*, *7*(1), 41-48. https://doi.org/10.1016/S1360-1385(01)02187-2

Seo, M., Hanada, A., Kuwahara, A., Endo, A., Okamoto, M., Yamauchi, Y., North, H., Marion-Poll, A., Sun, T. P., Koshiba, T., Kamiya, Y., Yamaguchi, S., & Nambara, E. (2006). Regulation of hormone metabolism in Arabidopsis seeds: Phytochrome regulation of abscisic acid metabolism and abscisic acid regulation of gibberellin metabolism. *Plant Journal*, *48*(3), 354-366. https://doi.org/10.1111/j.1365-313X.2006.02881.x

Seo, M., Nambara, E., Choi, G., & Yamaguchi, S. (2009). Interaction of light and hormone signals in germinating seeds. *Plant Molecular Biology*, *69*,463-472. https://doi.org/10.1007/s11103-008-9429-y

Sharkey, T. D., & Raschke, K. (1981). Separation and Measurement of Direct and Indirect Effects of Light on Stomata. *Plant Physiology*, *68*(1), 33-40. https://doi.org/10.1104/pp.68.1.33

Sharma, M., Irfan, M., Kumar, A., Kumar, P., & Datta, A. (2022). Recent Insights into Plant Circadian Clock Response Against Abiotic Stress. *Journal of Plant Growth Regulation* ,*41*(8) 3530–3543. https://doi.org/10.1007/s00344-021-10531-y

Sharrock, R. A., & Clack, T. (2002). Patterns of expression and normalized levels of the five Arabidopsis phytochromes. *Plant Physiology*, *130*(1), 442-456. https://doi.org/10.1104/pp.005389

Shimazaki, K., Doi, M., Assmann, S. M., & Kinoshita, T. (2007). Light Regulation of Stomatal Movement. *Annual Review of Plant Biology*, *58*(1), 219-247. https://doi.org/10.1146/annurev.arplant.57.032905.105434

Shu, K., Zhou, W., Chen, F., Luo, X., & Yang, W. (2018). Abscisic acid and gibberellins antagonistically mediate plant development and abiotic stress responses. *Frontiers in Plant Science*, *9*(March), 416. https://doi.org/10.3389/fpls.2018.00416

Sibbernsen, E., & Mott, K. A. (2010). Stomatal responses to flooding of the intercellular air spaces suggest a vapor-phase signal between the mesophyll and the guard cells. *Plant Physiology*, *153*(3), 1435-1442. https://doi.org/10.1104/pp.110.157685

Sicher, R.C. (1993). Assimilate Partitioning within Leaves of Small Grain Cereals. In Y.P. Abrol, P. Mohanty, & Govindjee (Eds.) *Photosynthesis: Photoreactions to Plant Productivity.* Springer, Dordrecht. https://doi.org/10.1007/978-94-011-2708-0_14

Silverstone, A. L., Jung, H. S., Dill, A., Kawaide, H., Kamiya, Y., & Sun, T. P. (2001). Repressing a repressor: Gibberellin-induced rapid reduction of the RGA protein in Arabidopsis. *Plant Cell*, *13*(7). https://doi.org/10.1105/tpc.13.7.1555

Sponsel, V. M., Schmidt, F. W., Porter, S. G., Nakayama, M., Kohlstruk, S., & Estelle, M. (1997). Characterization of new gibberellin-responsive semidwarf mutants of Arabidopsis. *Plant Physiology*, *115*(3),1009-1020. https://doi.org/10.1104/pp.115.3.1009

Spray, C. R., Kobayashi, M., Suzuki, Y., Phinney, B. 0, Gaskint, P., & Macmillant, J. (1996). The dwarf-i (dl) mutant of Zea mays blocks three steps in the gibberellin-biosynthetic pathway. *Proceedings of the National Academy of Sciences of the United States of America, 93* (19), 10515-10518. https://doi.org/10.1073/pnas.93.19.1051

Sreeharsha, R. V., Sekhar, K. M., & Reddy, A. R. (2015). Delayed flowering is associated with lack of photosynthetic acclimation in Pigeon pea (*Cajanus cajan* L.) grown under

elevated CO_2. *Plant Science*, *231*, 82-93. https://doi.org/10.1016/j.plantsci.2014.11.012

Sreenivasulu, N., Butardo, V. M., Jr., Misra, G., Cuevas, R. P., Anacleto, R., & Kavi Kishor, P. B. (2015). Designing climate-resilient rice with ideal grain quality suited for high-temperature stress. *Journal of Experimental Botany, 66* (7), 1737-1748. doi: 10.1093/jxb/eru544

Stout, R. G. (1988). Fusicoccin Activity and Binding in Arabidopsis thaliana. *Plant Physiology*, *88*(4), 999-1001. https://doi.org/10.1104/pp.88.4.999

Sugavanam, B. (1984). Diastereoisomers and enantiomers of paclobutrazol: Their preparation and biological activity. *Pesticide Science*, *15*(3), 296-302. https://doi.org/10.1002/ps.2780150312

Sukiran, N. A., Steel, P. G., & Knight, M. R. (2020). Basal stomatal aperture is regulated by GA-DELLAs in Arabidopsis. *Journal of Plant Physiology*, *250*,153182. https://doi.org/10.1016/j.jplph.2020.153182

Sun, T. P. (2008). Gibberellin Metabolism, Perception and Signaling Pathways in Arabidopsis. *The Arabidopsis Book*, *6*. https://doi.org/10.1199/tab.0103

Sun, T. P. (2010). Gibberellin-GID1-DELLA: A pivotal regulatory module for plant growth and development. *Plant Physiology*, *154*(2), 567-570. https://doi.org/10.1104/pp.110.161554

Sun, T. P. (2011). The molecular mechanism and evolution of the GA-GID1-DELLA signaling module in plants. *Current Biology*,21(9), 338-345. https://doi.org/10.1016/j.cub.2011.02.036

Sun, T. P., & Gubler, F. (2004). Molecular mechanism of gibberellin signaling in plants. *Annual Review of Plant Biology*, *55*, 197-223. https://doi.org/10.1146/annurev.arplant.55.031903.141753

Sun, T. P., & Kamiya, Y. (1994). The arabidopsis GA1 locus encodes the cyclase ent-kaurene synthetase a of gibberellin biosynthesis. *Plant Cell*, *6*(10), 1509-1518. https://doi.org/10.2307/3869986

Sun, T. P., & Kamiya, Y. (1997). Regulation and cellular localization of ent-kaurene synthesis. *Physiologia Plantarum*, *101*(4), 701-708. https://doi.org/10.1034/j.1399-3054.1997.1010405.x

Sun, W., Xu, X. H., Lu, X., Xie, L., Bai, B., Zheng, C., Sun, H., He, Y., & Xie, X. Z. (2017). The Rice Phytochrome Genes, PHYA and PHYB, Have Synergistic Effects on Anther Development and Pollen Viability. *Scientific Reports*, *7*(1). https://doi.org/10.1038/s41598-017-06909-2

Tahir, M., Kanegae, H., &Takano, M. (1998). Phytochrome C (PHYC) gene in rice: isolation and characterization of a complete coding sequence. *Plant Physiology,118*, 1535

Takahashi, Y., Bosmans, K. C., Hsu, P. K., Paul, K., Seitz, C., Yeh, C. Y., Wang, Y. S., Yarmolinsky, D., Sierla, M., Vahisalu, T., McCammon, J. A., Kangasjärvi, J., Zhang, L., Kollist, H., Trac, T., & Schroeder, J. I. (2022). Stomatal CO_2/bicarbonate sensor consists of two interacting protein kinases, Raf-like HT1 and non-kinase-activity activity requiring MPK12/MPK4. *Science Advances*, *8*(49), eabq6161. https://doi.org/10.1126/sciadv.abq6161

Takano, M., Inagaki, N., Xie, X., Kiyota, S., Baba-Kasai, A., Tanabata, T., & Shinomura, T. (2009). Phytochromes are the sole photoreceptors for perceiving red/far-red light in rice. *Proceedings of the National Academy of Sciences of the United States of America, 106* (34), 14705-14710. https://doi.org/10.1073/pnas.090737810

Takano, M., Inagaki, N., Xie, X., Yuzurihara, N., Hihara, F., Ishizuka, T., Yano, M., Nishimura, M., Miyao, A., Hirochika, H., & Shinomura, T. (2005). Distinct and cooperative functions of phytochromes A, B, and C in the control of deetiolation and flowering in rice. *Plant Cell*, *17*(12), 3311-3325. https://doi.org/10.1105/tpc.105.035899

Takemiya, A., Sugiyama, N., Fujimoto, H., Tsutsumi, T., Yamauchi, S., Hiyama, A., Tada, Y., Christie, J. M., & Shimazaki, K. I. (2013). Phosphorylation of BLUS1 kinase by

phototropins is a primary step in stomatal opening. *Nature Communications*, *4*, 2094. https://doi.org/10.1038/ncomms3094Mohapatra

Talon, M., Koornneef, M., & Zeevaart, J. A. D. (1990). Endogenous gibberellins in Arabidopsis thaliana and possible steps blocked in the biosynthetic pathways of the semidwarf ga4 and ga5 mutants. *Proceedings of the National Academy of Sciences of the United States of America*, *87*(20), 7983-7987. https://doi.org/10.1073/pnas.87.20.7983

Tanaka, Y., Sano, T., Tamaoki, M., Nakajima, N., Kondo, N., & Hasezawa, S. (2006). Cytokinin and auxin inhibit abscisic acid-induced stomatal closure by enhancing ethylene production in Arabidopsis. *Journal of Experimental Botany*, *57*(10), 2259-2266. https://doi.org/10.1093/jxb/erj193

Taub, D. (2010). Effects of rising atmospheric concentrations of carbon dioxide on plants. *Nature Education Knowledge*, 3(10), 21. https://www.nature.com/scitable/knowledge/library/effects-of-rising-atmospheric-concentrations-of-carbon-13254108/

Teng, Z., Chen, Y., Meng, S., Duan, M., Zhang, J., & Ye, N. (2023). Environmental Stimuli: A Major Challenge during Grain Filling in Cereals. *International Journal of Molecular Sciences*,*24*(3), 2255. https://doi.org/10.3390/ijms24032255

Thomas, S. G., Phillips, A. L., & Hedden, P. (1999). Molecular cloning and functional expression of gibberellin 2-oxidases, multifunctional enzymes involved in gibberellin deactivation. *Proceedings of the National Academy of Sciences of the United States of America, 96*(8), 4698-4703. https://doi.org/10.1073/pnas.96.8.4698

Tian, W., Hou, C., Ren, Z., Pan, Y., Jia, J., Zhang, H., Bai, F., Zhang, P., Zhu, H., He, Y., Luo, S., Li, L., & Luan, S. (2015). A molecular pathway for CO_2 response In Arabidopsis guard cells. *Nature Communications*, *6*,6057. https://doi.org/10.1038/ncomms7057

Tõldsepp, K., Zhang, J., Takahashi, Y., Sindarovska, Y., Hõrak, H., Ceciliato, P. H. O., Koolmeister, K., Wang, Y. S., Vaahtera, L., Jakobson, L., Yeh, C. Y., Park, J., Brosche, M., Kollist, H., & Schroeder, J. I. (2018). Mitogen-activated protein kinases MPK4 and

MPK12 are key components mediating CO2-induced stomatal movements. *Plant Journal*, *96*(5), 1018-1035. https://doi.org/10.1111/tpj.14087

Tominaga, M., Kinoshita, T., & Shimazaki, K. I. (2001). Guard-cell chloroplasts provide ATP required for H+ pumping in the plasma membrane and stomatal opening. *Plant and Cell Physiology*, *42*(8), 795-802. https://doi.org/10.1093/pcp/pce101

Turečková, V., Novák, O., & Strnad, M. (2009). Profiling ABA metabolites in Nicotiana tabacum L. leaves by ultra-performance liquid chromatography-electrospray tandem mass spectrometry. *Talanta*, *80*(1),390-399. https://doi.org/10.1016/j.talanta.2009.06.027

Tyler, L., Thomas, S. G., Hu, J., Dill, A., Alonso, J. M., Ecker, J. R., & Sun, T. P. (2004). Della proteins and gibberellin-regulated seed germination and floral development in Arabidopsis. *Plant Physiology*, *135*(2), 1008-19 https://doi.org/10.1104/pp.104.039578

Ueguchi-Tanaka, M., Nakajima, M., Motoyuki, A., & Matsuoka, M. (2007). Gibberellin receptor and its role in gibberellin signaling in plants. *Annual Review of Plant Biology*,*58*,183-198. https://doi.org/10.1146/annurev.arplant.58.032806.103830

Ueno, K., Kinoshita, T., Inoue, S. I., Emi, T., & Shimazaki, K. I. (2005). Biochemical characterization of plasma membrane H^+-ATPase activation in guard cell protoplasts of Arabidopsis thaliana in response to blue light. *Plant and Cell Physiology*, *46*(6), 955-963. https://doi.org/10.1093/pcp/pci104

Umezawa, T., Sugiyama, N., Mizoguchi, M., Hayashi, S., Myouga, F., Yamaguchi-Shinozaki, K., Ishihama, Y., Hirayama, T., & Shinozaki, K. (2009). 135(2):1008-19*Proceedings of the National Academy of Sciences of the United States of America*, *106*(41), 1008-1019. https://doi.org/10.1073/pnas.0907095106

UN DESA. (2022). United Nations Department of Economic and Social Affairs, Population Division (2022). World Population Prospects 2022: Summary of Results. *Department of Economic and Social Affairs Population Division*, *3* (UN DESA/POP/2022/TR/NO. 3).

Underwood, W., Melotto, M., & He, S. Y. (2007). Role of plant stomata in bacterial invasion. In *Cellular Microbiology*, *9*(7), 1621-1629. https://doi.org/10.1111/j.1462-5822.2007.00938.x

Urbanová, T., Tarkowská, D., Novák, O., Hedden, P., & Strnad, M. (2013). Analysis of *gibberellins* as free acids by ultra performance liquid chromatography-tandem mass spectrometry. *Talanta*, *112*, 85-94. https://doi.org/10.1016/j.talanta.2013.03.068

Vahisalu, T., Kollist, H., Wang, Y. F., Nishimura, N., Chan, W. Y., Valerio, G., Lamminmäki, A., Brosché, M., Moldau, H., Desikan, R., Schroeder, J. I., & Kangasjärvi, J. (2008). SLAC1 is required for plant guard cell S-type anion channel function in stomatal signalling. *Nature*, *452*,7186. https://doi.org/10.1038/nature06608

Varbanova, M., Yamaguchi, S., Yang, Y., McKelvey, K., Hanada, A., Borochov, R., Yu, F., Jikumaru, Y., Rosa, J., Cortea, D., Choong, J. M., Noel, J. P., Mander, L., Shulaev, V., Kamiya, Y., Rodermel, S., Weiss, D., & Picharsky, E. (2007). Methylation of gibberellins by Arabidopsis GAMT1 and GAMT2. *Plant Cell*, *19*(1), 32-45. https://doi.org/10.1105/tpc.106.044602

Vialet-Chabrand, S., Dreyer, E., & Brendel, O. (2013). Performance of a new dynamic model for predicting diurnal time courses of stomatal conductance at the leaf level. *Plant, Cell and Environment*, *36*(8), 1529-1546. https://doi.org/10.1111/pce.12086

Vishal, B., & Kumar, P. P. (2018). Regulation of Seed Germination and Abiotic Stresses by Gibberellins and Abscisic Acid. *Frontiers in Plant Science*, *9*(JUNE), 838. https://doi.org/10.3389/fpls.2018.00838

Von Caemmerer, S., Lawson, T., Oxborough, K., Baker, N. R., Andrews, T. J., & Raines, C. A. (2004). Stomatal conductance does not correlate with photosynthetic capacity in transgenic tobacco with reduced amounts of Rubisco. *Journal of Experimental Botany*, *55*(400), 1157-1166. https://doi.org/10.1093/jxb/erh128

Waadt, R., Seller, C. A., Hsu, P. K., Takahashi, Y., Munemasa, S., & Schroeder, J. I. (2022). Plant hormone regulation of abiotic stress responses. *Nature Reviews Molecular Cell Biology*,*23*(10). https://doi.org/10.1038/s41580-022-00479-6

Wall, S., Vialet-Chabrand, S., Davey, P., Van Rie, J., Galle, A., Cockram, J., & Lawson, T. (2022). Stomata on the abaxial and adaxial leaf surfaces contribute differently to leaf gas exchange and photosynthesis in wheat. *New Phytologist*, *235*(5), 1743-1756. https://doi.org/10.1111/nph.18257

Wang, C., Hu, H., Qin, X., Zeise, B., Xu, D., Rappel, W. J., Boron, W. F., & Schroeder, J. I. (2015). Reconstitution of CO_2 regulation of SLAC1 anion channel and function of CO_2-permeable PIP2;1 aquaporin as CARBONIC ANHYDRASE4 interactor. *Plant Cell*, *28*(2), 568-582. https://doi.org/10.1105/tpc.15.00637

Wang, D., Heckathorn, S. A., Wang, X., & Philpott, S. M. (2012). A meta-analysis of plant physiological and growth responses to temperature and elevated CO_2. *Oecologia*, *169*(1),1-13. https://doi.org/10.1007/s00442-011-2172-0

Wang, F. F., Lian, H. L., Kang, C. Y., & Yang, H. Q. (2010). Phytochrome B is involved in mediating red light-induced stomatal opening in Arabidopsis thaliana. *Molecular Plant*, *3*(1), 246-259. https://doi.org/10.1093/mp/ssp097

Wang, P., & Song, C. P. (2008). Guard-cell signalling for hydrogen peroxide and abscisic acid. *New Phytologist*, 178 (4). https://doi.org/10.1111/j.1469-8137.2008.02431.x

Wang, X. Q., Ullah, H., Jones, A. M., & Assmann, S. M. (2001). G protein regulation of ion channels and abscisic acid signaling in Arabidopsis guard cells. *Science*, *292*(5524), 2070-2072. https://doi.org/10.1126/science.1059046

Wang, Y. H., Zhang, G., Chen, Y., Gao, J., Sun, Y. R., Sun, M. F., & Chen, J. P. (2019). Exogenous application of gibberellic acid and ascorbic acid improved tolerance of okra seedlings to NaCl stress. *Acta Physiologiae Plantarum*, *41*, 93. https://doi.org/10.1007/s11738-019-2869-y

Wassmann, R., Jagadish, S. V. K., Heuer, S., Ismail, A., Redona, E., Serraj, R., Singh, R. K., Howell, G., Pathak, H., & Sumfleth, K. (2009). Chapter 2 Climate Change Affecting Rice Production. The Physiological and Agronomic Basis for Possible Adaptation Strategies. In D. L. Sparks (Ed.), *Advances in Agronomy*, *101* (pp. 59-111). Academic Press. https://doi.org/10.1016/S0065-2113(08)00802-X

Wassmann, R., Jagadish, S. V. K., Sumfleth, K., Pathak, H., Howell, G., Ismail, A., Serraj, R., Redona, E., Singh, R. K., & Heuer, S. (2009). Chapter 3 Regional Vulnerability of Climate Change Impacts on Asian Rice Production and Scope for Adaptation. In D. L. Sparks (Ed.), *Advances in Agronomy*, *102* (pp. 91-133). https://doi.org/10.1016/S0065-2113(09)01003-7

Webb, A. A. R. (2003). The physiology of circadian rhythms in plants. *New Phytologist, 160*(2), 281–303. https://doi.org/10.1046/j.1469-8137.2003.00895.x

Webb, A. A. R., & Hetherington, A. M. (1997). Convergence of the abscisic acid, CO_2, and extracellular calcium signal transduction pathways in stomatal guard cells. *Plant Physiology*, *114*(4), 1557- 1560. https://doi.org/10.1104/pp.114.4.1557

Webb, A. A. R., McAinsh, M. R., Mansfield, T. A., & Hetherington, A. M. (1996). Carbon dioxide induces increases in guard cell cytosolic free calcium. *Plant Journal*, *9*(3),297-304. https://doi.org/10.1046/j.1365-313X.1996.09030297.x

Weigel, D., & Glazebrook, J. (2006). Transformation of Agrobacterium Using the Freeze-Thaw Method. *Cold Spring Harbor Protocols,7*. https://doi.org/10.1101/pdb.prot4666

Weigel, H. J. (2014). Plant quality declines as CO_2 levels rise. *eLife* (3). https://doi.org/10.7554/eLife.03233

Wen, C. K., & Chang, C. (2002). Arabidopsis RGL1 encodes a negative regulator of gibberellin responses. *Plant Cell*, *14*(1). https://doi.org/10.1105/tpc.010325

Weyers, J. D. B., & Johansen, L. G. (1985). Accurate estimation of stomatal aperture from silicone rubber impressions. *New Phytologist*, *101*(1), 109-115. https://doi.org/10.1111/j.1469-8137.1985.tb02820.x

Weyers, J. D. B., & Lawson, T. (1997). Heterogeneity in Stomatal Characteristics. *Advances in Botanical Research*, *26*, 317-352 https://doi.org/10.1016/S0065-2296(08)60124-X

Willmer, C., & Fricker, M. (1996). Stomata. Dordrecht, the Netherlands, Springer. https://doi.org/10.1007/978-94-011-0579-8

Winter, D., Vinegar, B., Nahal, H., Ammar, R., Wilson, G. V., & Provart, N. J. (2007). An "electronic fluorescent pictograph" Browser for exploring and analyzing large-scale biological data sets. *PLoS ONE*, *2*(8),e718. https://doi.org/10.1371/journal.pone.0000718

Wong, S. C., Cowan, I. R., & Farquhar, G. D. (1979). Stomatal conductance correlates with photosynthetic capacity. *Nature*, *282*(5737). https://doi.org/10.1038/282424a0

Woodward, F. I. (1987). Stomatal numbers are sensitive to increases in CO_2 from pre-industrial levels. *Nature, 327*, 617-618. https://doi.org/10.1038/327617a0

Wroblewitz, S., Hüther, L., Manderscheid, R., Weigel, H. J., Wätzig, H., & Dänicke, S. (2014). Effect of rising atmospheric carbon dioxide concentration on the protein composition of cereal grain. *Journal of Agricultural and Food Chemistry*, *62*(28), 6616-6625. https://doi.org/10.1021/jf501958a

Wu, F., Chi, Y., Jiang, Z., Xu, Y., Xie, L., Huang, F., Wan, D., Ni, J., Yuan, F., Wu, X., Zhang, Y., Wang, L., Ye, R., Byeon, B., Wang, W., Zhang, S., Sima, M., Chen, S., Zhu, M., … Pei, Z. M. (2020). Hydrogen peroxide sensor HPCA1 is an LRR receptor kinase in Arabidopsis. *Nature*, *578*(7796), 577-581. https://doi.org/10.1038/s41586-020-2032-3

Wu, Z., Chen, L., Yu, Q., Zhou, W., Gou, X., Li, J., & Hou, S. (2019). Multiple transcriptional factors control stomata development in rice. *New Phytologist*, *223*(1), 220-232. https://doi.org/10.1111/nph.15766

Xiu, D.Y., Xin J., Zhang, J., Zhou, J.L., Zheng, H.S., & Zhi, Z.Q. (2013). Research progress on the impacts of low light intensity on rice growth and development. Chinese Journal of Eco- Agriculture. 21: 1307-1317. https://doi.org/10.3724/SP.J.1011.2013.30238

Xu, Q., Burgess, P., Xu, J., Meyer, W., & Huang, B. (2016). Osmotic stress- and salt stress-inhibition and gibberellin-mitigation of leaf elongation associated with up-regulation of genes controlling cell expansion. *Environmental and Experimental Botany*, *131*, 101-109. https://doi.org/10.1016/J.ENVEXPBOT.2016.06.001

Xue, S., Hu, H., Ries, A., Merilo, E., Kollist, H., & Schroeder, J. I. (2011). Central functions of bicarbonate in S-type anion channel activation and OST1 protein kinase in CO_2 signal transduction in guard cell. *EMBO Journal*, 30, 1645-1658. https://doi.org/10.1038/emboj.2011.68

Yamaguchi, S. (2008). Gibberellin Metabolism and its Regulation. *Annual Review of Plant Biology, 59*,225-251. https://doi.org/10.1146/annurev.arplant.59.032607.092804

Yang, J., Li, C., Kong, D., Guo, F., & Wei, H. (2020). Light-Mediated Signaling and Metabolic Changes Coordinate Stomatal Opening and Closure. *Frontiers in Plant Science*,*11*, 601478. https://doi.org/10.3389/fpls.2020.601478

Ye, N., Jia, L., & Zhang, J. (2012). ABA signal in rice under stress conditions. *Rice*,*5*,1. https://doi.org/10.1186/1939-8433-5-1

Yoshida, Y., Sarmiento-Mañús, R., Yamori, W., Ponce, M. R., Micol, J. L., & Tsukaya, H. (2018). The arabidopsis phyB-9 mutant has a second-site mutation in the VENOSA4 gene that alters chloroplast size, photosynthetic traits, and leaf growth. *Plant Physiology*,*178*(1), 3-6. https://doi.org/10.1104/pp.18.00764

Young, J. J., Mehta, S., Israelsson, M., Godoski, J., Grill, E., & Schroeder, J. I. (2006). CO_2 signaling in guard cells: Calcium sensitivity response modulation, a Ca^{2+}-independent phase, and CO_2 insensitivity of the gca2 mutant. *Proceedings of the National Academy of Sciences of the United States of America*, *103*(19), 7506-7511. https://doi.org/10.1073/pnas.0602225103

Yu, J., Fan, N., Li, R., Zhuang, L., Xu, Q., & Huang, B. (2019). Proteomic Profiling for Metabolic Pathways Involved in Interactive Effects of Elevated Carbon Dioxide and Nitrogen on Leaf Growth in a Perennial Grass Species. *Journal of Proteome Research*, *18*(6), 2446-2457. https://doi.org/10.1021/acs.jproteome.8b00951

Yuan, S., Linquist, B. A., Wilson, L. T., Cassman, K. G., Stuart, A. M., Pede, V., Miro, B., Saito, K., Agustiani, N., Aristya, V. E., Krisnadi, L. Y., Zanon, A. J., Heinemann, A. B., Carracelas, G., Subash, N., Brahmanand, P. S., Li, T., Peng, S., & Grassini, P. (2021). Sustainable intensification for a larger global rice bowl. *Nature Communications*, *12*(1),7163. https://doi.org/10.1038/s41467-021-27424-z

Yue, B., Xue, W.Y., Luo, L.J., & Xing, Y.Z. (2006). QTL Analysis for flag leaf characteristics and their relationships with yield and yield traits in rice. *Acta Genetica Sinica, 33*, 824–832. https://doi: 10.1016/S0379-4172(06)60116-9.akemiya

Zeiger, E. (1983). The Biology of Stomatal Guard Cells. *Annual Review of Plant Physiology*, *34*(1), 441-475. https://doi.org/10.1146/annurev.pp.34.060183.002301

Zeiger, E., Farquhar, G. D., & Cowan, I. R. (1987). *Stomatal Function.* Stanford, CA: Stanford University Press.

Zhang, B., Ye, W., Ren, D., Tian, P., Peng, Y., Gao, Y., Ruan, B., Wang, L., Zhang, G., Guo, L., Qian, Q., & Gao, Z. (2015). Genetic analysis of flag leaf size and candidate genes determination of a major QTL for flag leaf width in rice. *Rice*, *8*(1). https://doi.org/10.1186/s12284-014-0039-9

Zhang, H., Zhu, H., Pan, Y., Yu, Y., Luan, S., & Li, L. (2014). A DTX/MATE-type transporter facilitates abscisic acid efflux and modulates ABA sensitivity and drought tolerance in Arabidopsis. *Molecular Plant*, *7*(10), 1522-1532. https://doi.org/10.1093/mp/ssu063

Zhang, J., Cao, Y., Tang, J., He, X., Li, M., Li, C., Ren, X., Ding, Y. (2023). Physiology and Application of Gibberellins in Postharvest Horticultural Crops. *Horticulturae, 9(6),* 625. https://doi.org/10.3390/horticulturae9060625

Zhang, J., De-oliveira-Ceciliato, P., Takahashi, Y., Schulze, S., Dubeaux, G., Hauser, F., Azoulay-Shemer, T., Tõldsepp, K., Kollist, H., Rappel, W. J., & Schroeder, J. I. (2018). Insights into the Molecular Mechanisms of CO_2-Mediated Regulation of Stomatal Movements. *Current Biology*, *28*(23), R1356-R1363. https://doi.org/10.1016/j.cub.2018.10.015

Zhang, J., Wang, N., Miao, Y., Hauser, F., McCammon, J. A., Rappel, W. J., & Schroeder, J. I. (2018). Identification of SLAC1 anion channel residues required for CO_2/bicarbonate sensing and regulation of stomatal movements. *Proceedings of the National Academy of Sciences of the United States of America*, *115*(44),11129-11137. https://doi.org/10.1073/pnas.1807624115

Zhang, L., Takahashi, Y., Hsu, P. K., Kollist, H., Merilo, E., Krysan, P. J., & Schroeder, J. I. (2020). FRET kinase sensor development reveals SnRK2/OST1 activation by ABA but not by MeJA and high CO_2 during stomatal closure. *ELife*, *9*, 1-74. https://doi.org/10.7554/eLife.56351

Zhang, X., Chen, Y., Wang, Z. Y., Chen, Z., Gu, H., & Qu, L. J. (2007). Constitutive expression of CIR1 (RVE2) affects several circadian-regulated processes and seed germination in Arabidopsis. *Plant Journal* *51*(3), 512-525. https://doi.org/10.1111/j.1365-313X.2007.03156.x

Zhang, X., Zhang, L., Dong, F., Gao, J., Galbraith, D. W., & Song, C. P. (2001). Hydrogen peroxide is involved in abscisic acid-induced stomatal closure in *Vicia faba*. *Plant Physiology*, *126* (4), 1438–1448. https://doi.org/10.1104/pp.126.4.1438

Zhao, H., Liu, X., Wang, J., Qian, Q. & Zhang, G. (2022). The coordinated regulation mechanism of rice plant architecture and its tolerance to stress. *Frontiers in Plant Science*, 13:1087378. https://doi.org/10.3389/fpls.2022.1087378

Zhao, H., Zhang, Y., & Zheng, Y. (2022). Integration of ABA, GA, and light signaling in seed germination through the regulation of ABI5. *Frontiers in Plant Science*, *13*(Aug), 1000803. Frontiers Media S.A. https://doi.org/10.3389/fpls.2022.1000803

Zhu, C., Kobayashi, K., Loladze, I., Zhu, J., Jiang, Q., Xu, X., Liu, G., Seneweera, S., Ebi, K. L., Drewnowski, A., Fukagawa, N. K., & Ziska, L. H. (2018). Carbon dioxide (CO_2) levels this century will alter the protein, micronutrients, and vitamin content of rice grains with potential health consequences for the poorest rice-dependent countries. *Science Advances, 4*(5), eaaq1012. https://doi:10.1126/sciadv.aaq1012. PMID: 29806023; PMCID: PMC5966189.

Zhu, M., Geng, S., Chakravorty, D., Guan, Q., Chen, S., & Assmann, S. M. (2019). Metabolomics of Red Light-Induced Stomatal Opening in *Arabidopsis thaliana*: Coupling with Abscisic Acid and Jasmonic Acid Metabolism. *Plant Journal*, *101*(6),1331-1348. https://doi.org/10.1111/tpj.14594

Zhu, Y., Nomura, T., Xu, Y., Zhang, Y., Peng, Y., Mao, B., Hanada, A., Zhou, H., Wang, R., Li, P., Zhu, X., Mander, L. N., Kamiya, Y., Yamaguchi, S., & He, Z. (2006).

ELONGATED UPPERMOST INTERNODE encodes a cytochrome P450 monooxygenase that epoxidizes gibberellins in a novel deactivation reaction in rice. *Plant Cell*, *18*(2), 442–456. https://doi.org/10.1105/tpc.105.038455

Ziska, L. H., & Teramura, A. H. (1995). Intraspecific Variation in Growth and Photosynthetic Responses of Rice with Increased Carbon Dioxide. *Climate Change and Rice*. https://doi.org/10.1007/978-3-642-85193-3_23

Zoulias, N., Harrison, E. L., Casson, S. A., & Gray, J. E. (2018). Molecular control of stomatal development. *Biochemical Journal*, *475*(2), 441-454. https://doi.org/10.1042/bcj20170413

Appendix

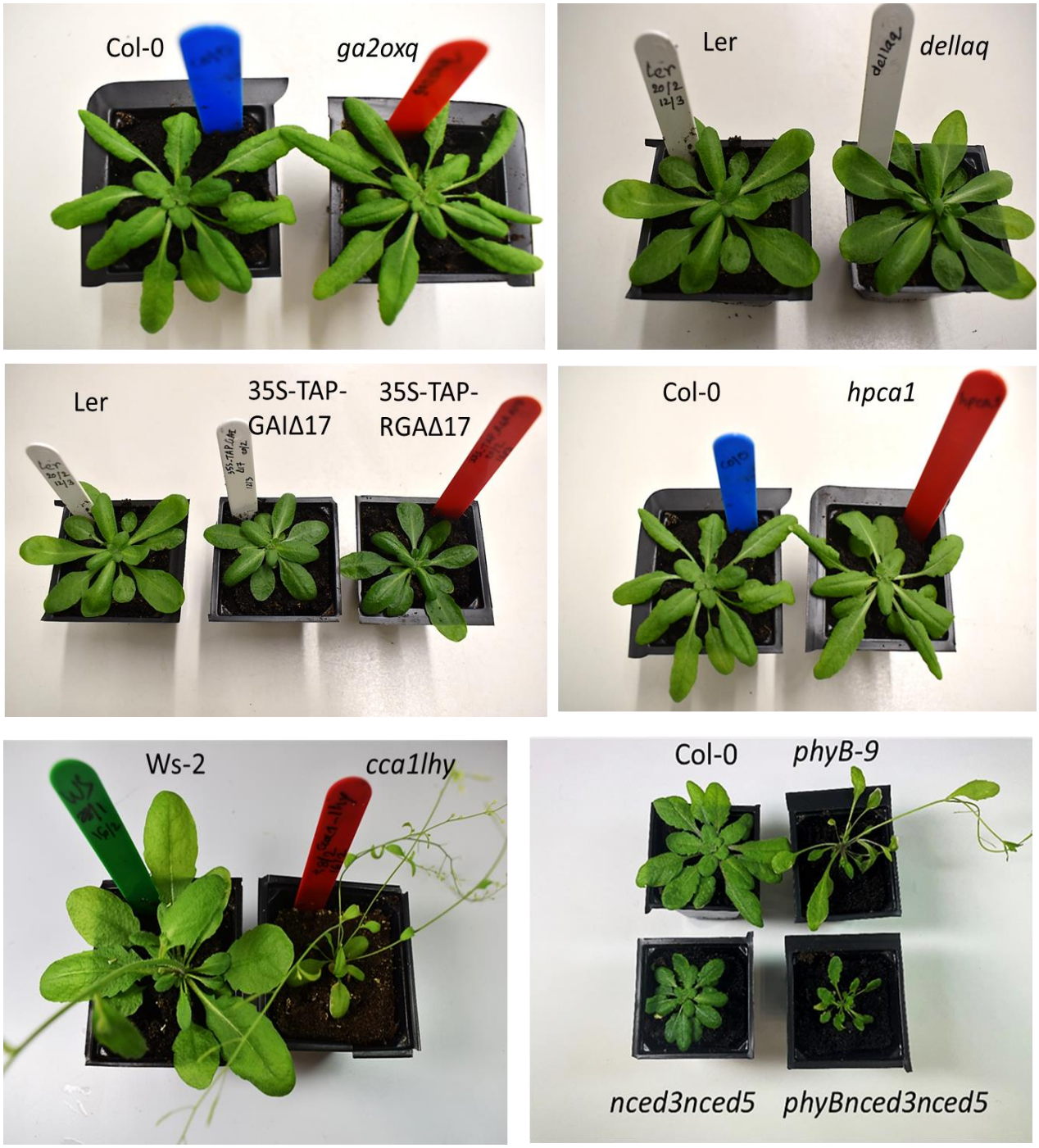

Supplementary 2.1 Images of different Arabidopsis wild and mutant lines used during the present study. Plants were at the age of between 31-36 days post germination. Mutant lines in each of the image has their respective wild background on left hand side of the images.

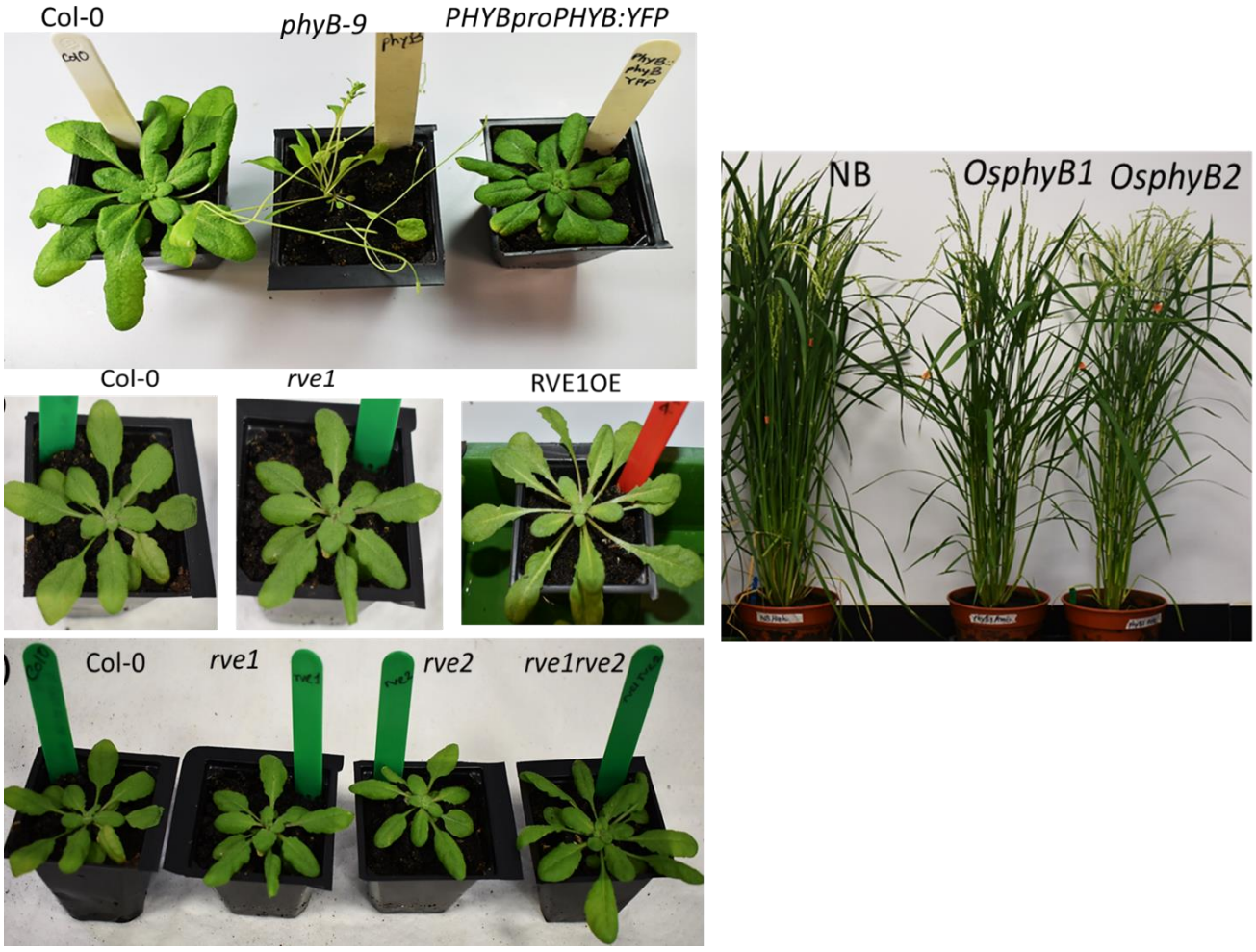

Supplementary 2.2 Images of different Arabidopsis wild and mutant lines (left panel) and rice lines (right panel) used during the present study. Arabidopsis Plants were at the age of between 31-36 days and rice plants were between 65-70 days post germination. Mutant lines in each of the image has their respective wild background on left hand side of the images.

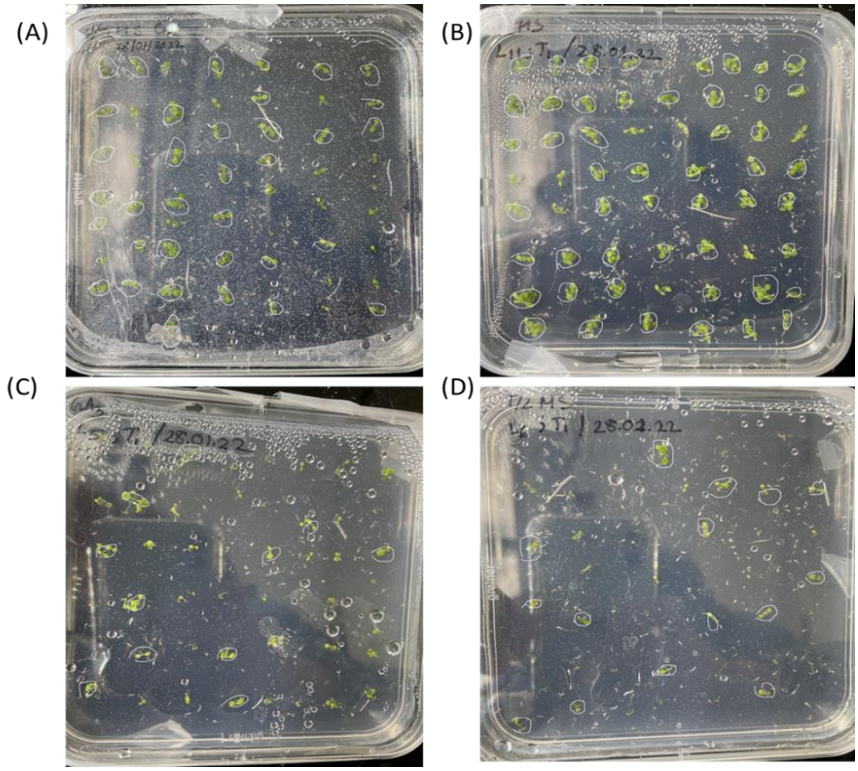

Supplementary 2.3 Germinating seeds to screen putative *RVE1OE* from T1 generation. (A) Col-0 seeds germinated almost completely and without delay. (B) Non *RVE1OE* seeds germinate as Col-0. (C) Seeds of putative *RVE1OE1* line germinated slowly in presence of GA_3 and (D) Delay of germination was more in absence of GA_3 from putative *RVE1OE1* line.

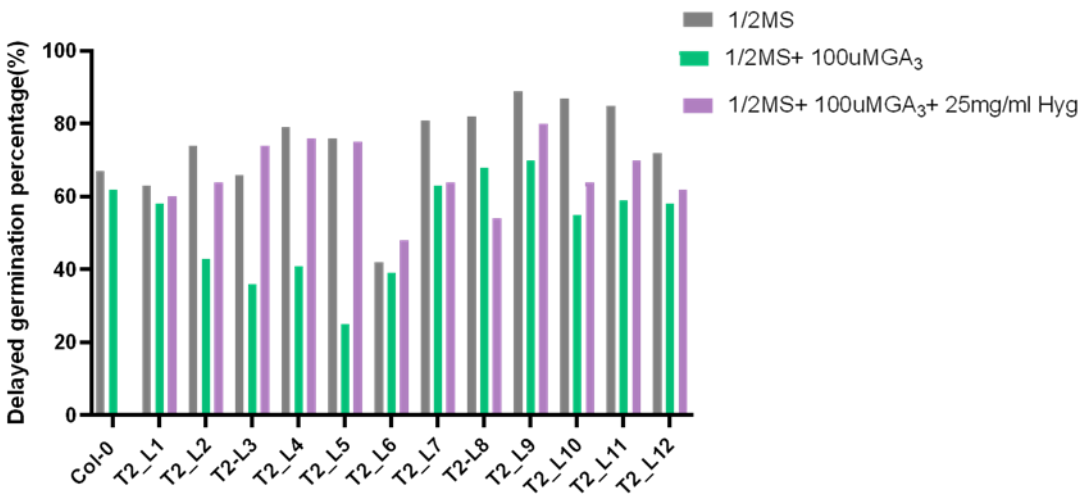

Supplementary 2.4 Percentage of delayed germination of putative *RVE1OE* lines from T2 generation. Number of seeds per plate ranged between 80-60 and three combinations of ½ MS media was used.

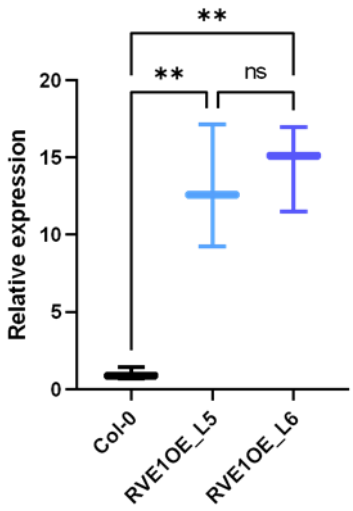

Supplementary 2.5 Confirmation of *RVE1OE* lines. Relative expression of *RVE1* gene in Col-0 and two lines of *RVE1OE*. Statistical analysis was conducted using one-way ANOVA with Tukey's multiple comparison tests where the significant difference between the lines were **P < 0.01 and P ≥ 0.05 non-significant (ns).

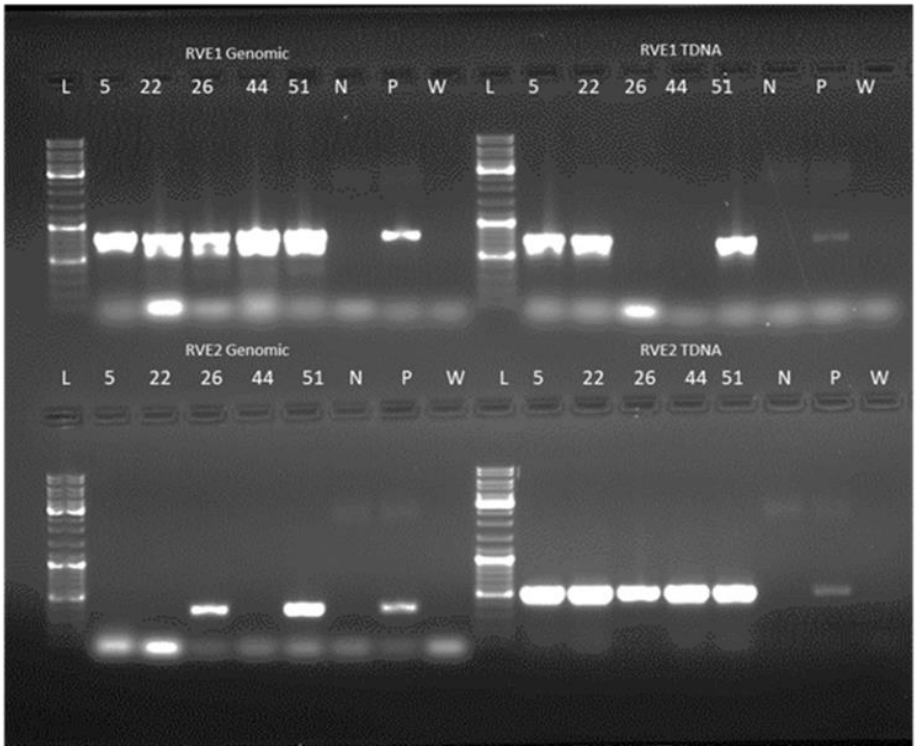

Supplementary 2.6 Confirmation of *RVE1rve1rve2rve2* lines. 1% agarose gel image for the five lines with *RVE1* heterozygous and *rve2* homozygous mutants. Upper left was for *RVE1* genomic and upper right was for T-DNA insertion. Lower one was for *RVE2* genomic and TDNA insertion respectively. L= gene ladder, N=negative, P=positive and W=water control. For genomic PCR, positive control was Col-0 genome and negative control was respective mutant genome. Vice versa for TDNA insertion PCR.

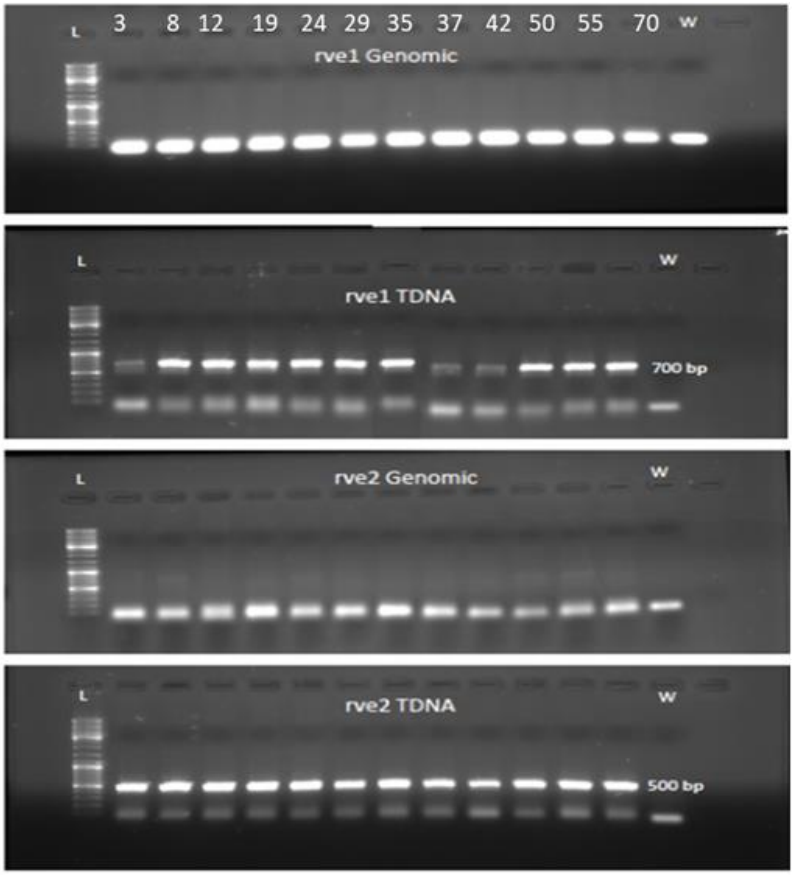

Supplementary 2.7 Confirmation of *rve1rve2* lines. 1% agarose gel image for the twelve *rve1rve2* homozygous double mutants screened from 74 seedlings. Upper two rows were for *RVE1* genomic and T-DNA insertion respectively. Lower two rows were for *RVE2* genomic and TDNA insertion respectively. L= gene ladder and W=water control.

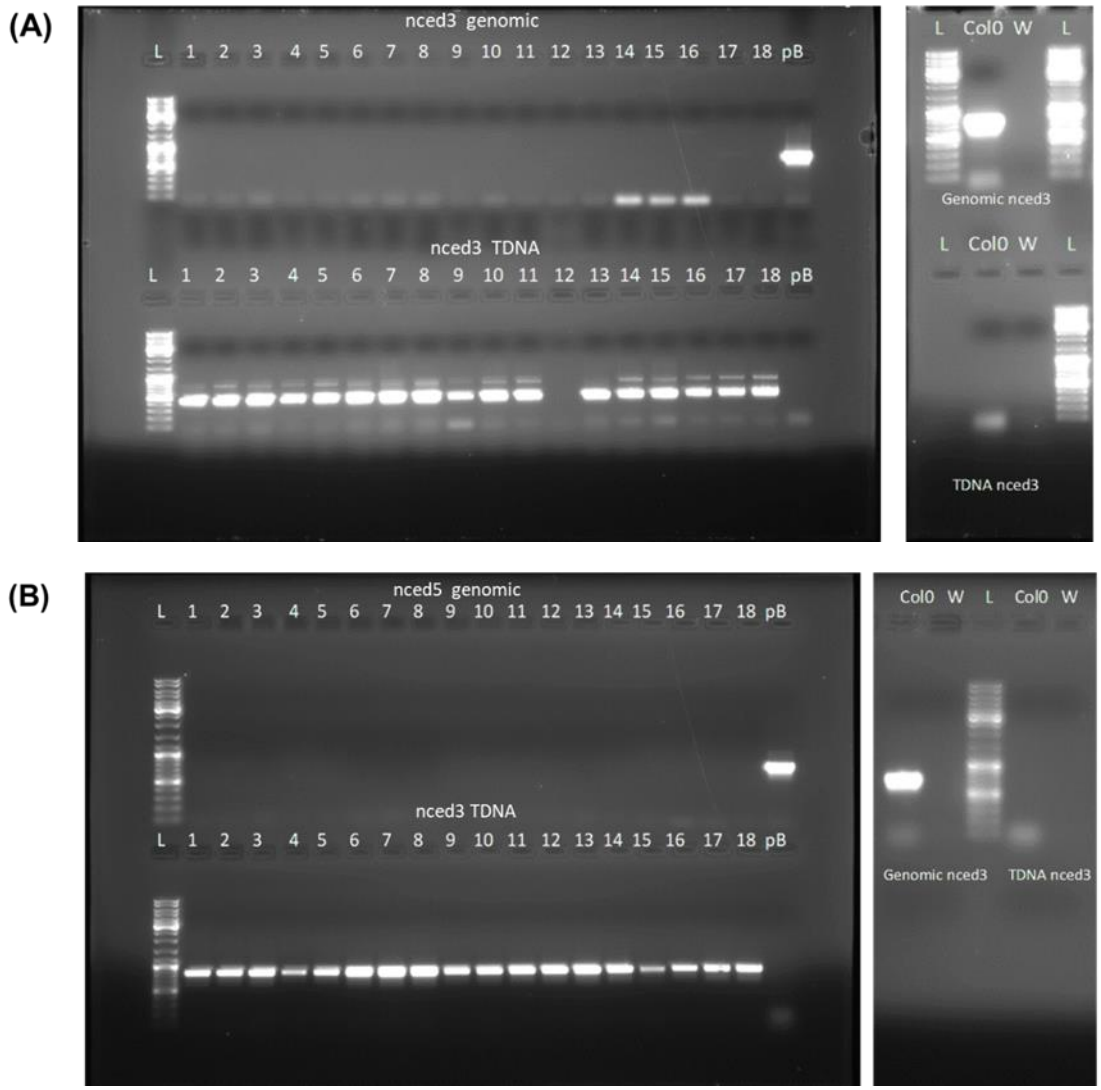

Supplementary 2.8 Confirmation of *nced3nced5* double mutant. 1% agarose gel image for the eighteen putative *phyB-9nced3nced5* triple mutants screened from 74 seedlings. (A) Upper row was for *NCED3* genomic and lower row was for T-DNA insertion respectively. (B) Same as (A) but for *NCED5*. L= gene ladder, W=water control, pB= *phyB-9* and Col0= wild line Col-0.

Figure 2.9 Confirmation of point mutant in *phyB-9* from *phyB-9nced3nced5* triple mutant. Six putative *phyB-9nced3nced5* triple mutant lines sent for sequencing were 1,2, 6,11,15 and 18. Line 19 was *phyB-9* and Genomic was for wild line Col-0. Multiple sequence alignment was conducted using GeneDoc version 2.7.000 and a point mutation of TGA in *phyB-9* instead of TGG as in wild genome was found.

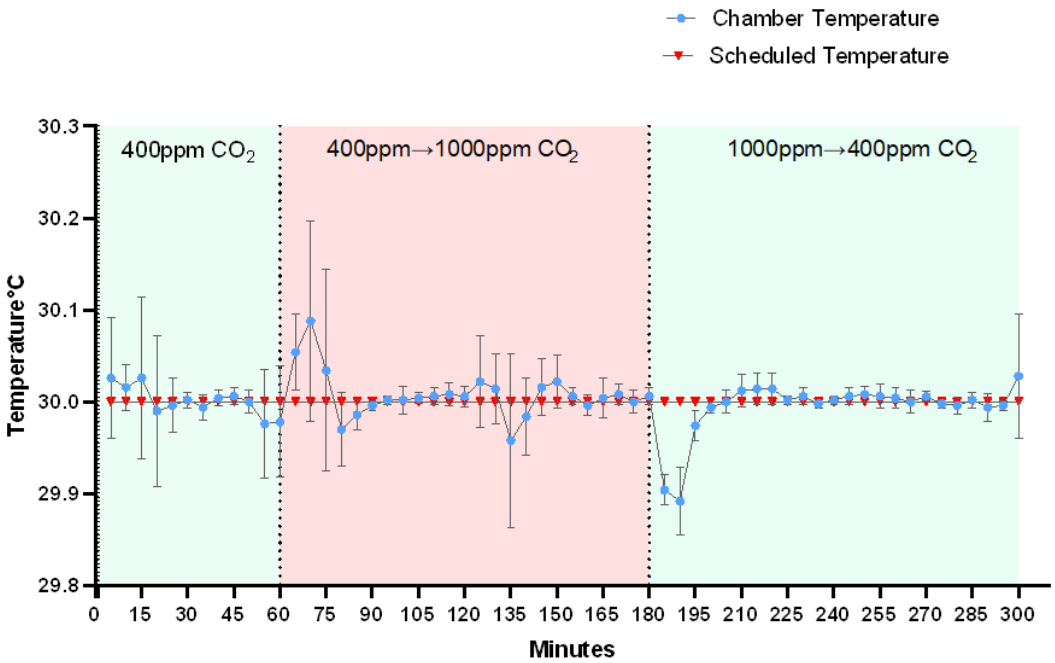

Supplementary 2.10 Matching between running and scheduled temperature from rice growth chambers. Measurements are recorded for 5 subsequent days in line with thermal imaging experiment.

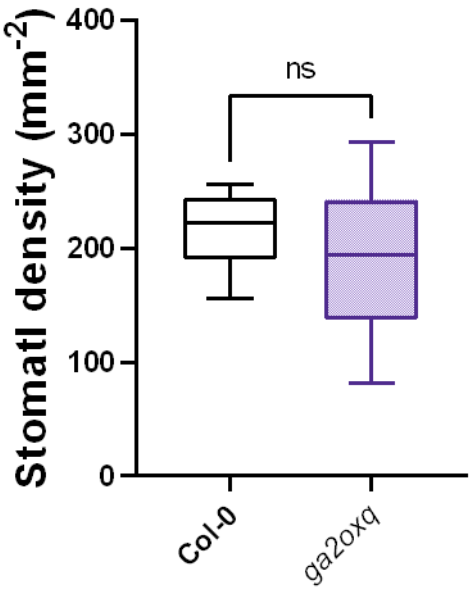

Supplementary 2.11 Measurements of stomatal density from abaxial surface of Col-0 and *ga2oxq*. Mature leaf of same age as bioassay experiment was chosen. The number of replicates/genotypes was 20. Statistical analysis was conducted using unpaired T-test and the difference between the lines was non-significant i.e., P ≥ 0.05.

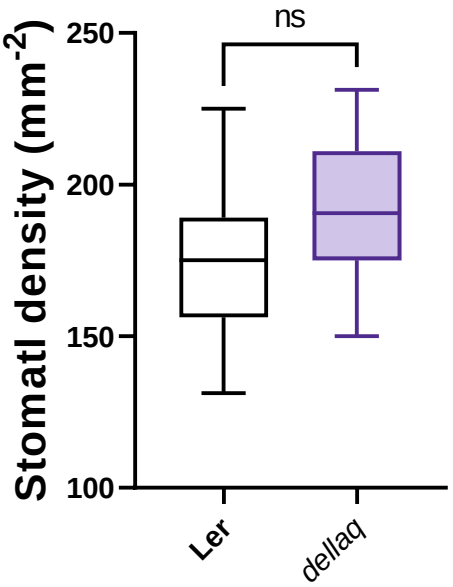

Supplementary 2.12 Measurements of stomatal density from abaxial surface of Ler and *dellaq*. Mature leaf of same age as bioassay experiment was chosen. The number of replicates/genotypes was 20. Statistical analysis was conducted using unpaired T-test and the difference between the lines was non-significant i.e., P ≥ 0.05.

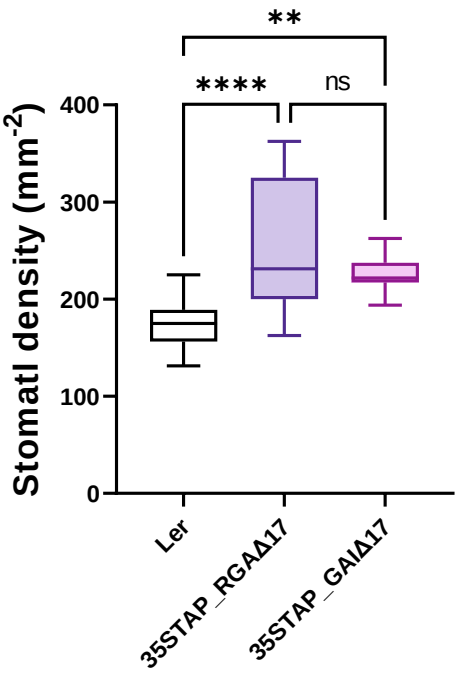

Supplementary 2.13 Measurements of stomatal density from abaxial surface of Col-0, *phyB-9*, *nced3nced5* and *phyB-9nced3nced5*. Mature leaf of same age as bioassay experiment was chosen. The number of replicates/genotypes was 20. Statistical analysis was conducted using one-way ANOVA with Tukey's multiple comparison tests. The adjusted P value among means were **P < 0.01, ****P < 0.0001 and non-significant i.e., P ≥ 0.05.

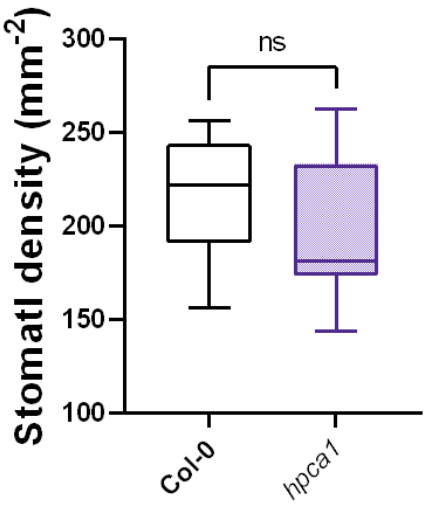

Supplementary 2.14 Measurements of stomatal density from abaxial surface of Col-0 and *hpca1*. Mature leaf of same age as bioassay experiment was chosen. The number of replicates/genotypes was 20. Statistical analysis was conducted using unpaired T-test and the difference between the lines was non-significant i.e., P ≥ 0.05.

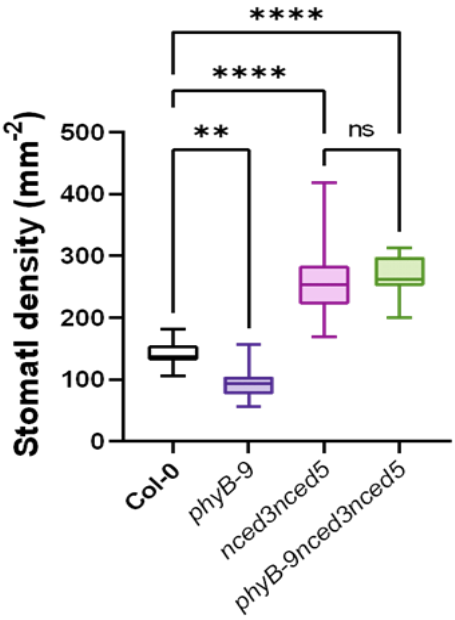

Supplementary 2.15 Measurements of stomatal density from abaxial surface of Col-0, *phyB-9*, *nced3nced5* and *phyB-9nced3nced5*. Mature leaf of same age as bioassay experiment was chosen. The number of replicates/genotypes was 20. Statistical analysis was conducted using one-way ANOVA with Tukey's multiple comparison tests. The adjusted P value among means were **P < 0.01, ****P < 0.0001 and non-significant i.e., P ≥ 0.05.

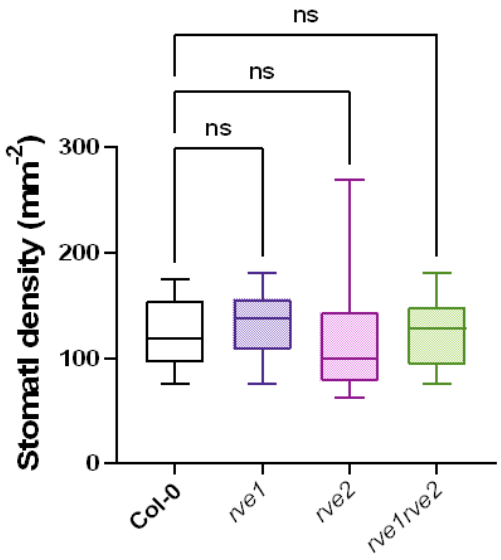

Supplementary 2.16 Measurements of stomatal density from abaxial surface of Col-0, *rve1*, *rve2* and *rve1rve2*. Mature leaf of same age as bioassay experiment was chosen. The number of replicates/genotypes was 20. Statistical analysis was conducted using one-way ANOVA with Tukey's multiple comparison tests. The adjusted P value among means was non-significant i.e., P ≥ 0.05.

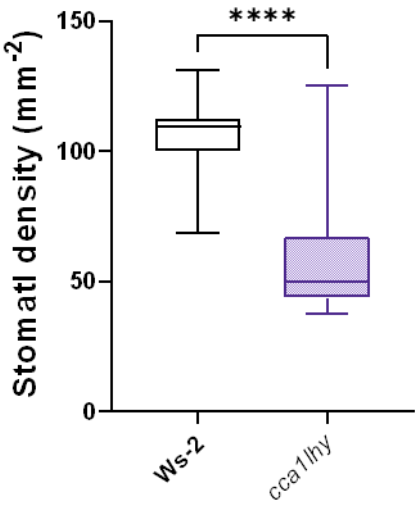

Supplementary 2.17 Measurements of stomatal density from abaxial surface of Ws-2 and *cca1lhy*. Mature leaf of same age as bioassay experiment was chosen. The number of replicates/genotypes was 20. Statistical analysis was conducted using unpaired T-test and with significant difference ****P < 0.0001.